University of Alberta

Characterization of Indicator Minerals and Till Geochemical Dispersal Patterns Associated with the Pine Point Pb-Zn Mississippi Valley-type Deposits, Northwest Territories, Canada

by

Natasha M. Oviatt

A thesis submitted to the Faculty of Graduate Studies and Research
in partial fulfillment of the requirements for the degree of

Master of Science

Earth and Atmospheric Sciences

ABSTRACT

Surficial geological mapping of the Pine Point region records three, possibly four, directions of ice flow. Dispersal of metal-rich till was primarily to the north and west indicating that at least the oldest ice flow trajectory was in contact with mineralized bedrock. This metal-rich till includes indicator minerals (sphalerite, galena, pyrite and smithsonite) and pathfinder elements (Zn, Pb, Fe, Cd, S and Tl). Dispersal of indicator minerals and pathfinder elements are strongest in the direction of the oldest ice flow trajectory immediately down ice of the deposit, and are detectable at the suface within 500 m of the deposit.

Sulphur and Pb isotopes from sphalerite and galena grains in till and bedrock are consistent with a Pine Point provenance.

ACKNOWLEDGEMENTS

Table of Contents

LIST OF TABLES

LIST OF FIGURES

Chapter 1

1.1   Introduction

Exploration for base metal deposits in Canada has recently increased as long-term demand for metals and minerals is expected to grow (Stothart, 2011). Currently, Canada is one of the largest producers of minerals and metals (Stothart, 2011), however the current production of Pb and Zn in Canada attributed to Mississippi Valley-type (MVT) deposits is nil (Sangster, 2002). The landscape of Canada has been shaped by repeated glacial events which have significantly altered the footprint of bedrock-hosted ore deposits. This presents significant hurdles for exploration companies in northern terrain and, as a result, an understanding of glacial deposits and geomorphology is required to execute a successful exploration project. Indicator mineral and till geochemical methods have proven to be successful exploration tools in glaciated terrain for diamond and U deposits (e.g. Dreimanis, 1960; Shilts, 1976; McClenaghan, 2005) but these methods have not been used to explore for MVT deposits and, thus, their applicability for this deposit type is unknown. To improve exploration strategies for MVT deposits in areas that have been glaciated, a till geochemistry and indicator mineral study was carried out on a well studied MVT district. The broad aims of this study were to constrain the chemical and isotopic signature of the ore minerals and track the dispersal of indicator minerals and their geochemical signatures from a single deposit in the Pine Point district, Northwest Territories. The specific goals were to: (1) understand the species, abundance, size distribution, and mineral chemistry of the indicator minerals present as well as their concentrations, grain morphology, and spatial distribution down-ice of the deposit, (2) compare the till matrix geochemistry to that of the ore deposits and the host rocks, and (3) compare the chemistry of the indicator minerals to that of the bedrock. This project will lead to an understanding of the transport and fate of ore minerals during glacial dispersal and will help to improve exploration techniques for these deposit types in glaciated terrain.

1.2   MVT deposits

MVT deposits occur all over the world though primarily in Phanerozoic rocks in the northern hemisphere (Fig. 1-1). They are named after the large district that occurs in the Mississippi Valley, U.S.A. MVT ore deposits are stratabound, epigenetic, carbonate-hosted mineral deposits that usually occur on the margins of sedimentary basins; they are associated with orogenic activity but not igneous activity (e.g. Anderson and Macqueen, 1988; Sverjensky, 1986; Leach and Sangster, 1993). They typically occur in districts that consist of many different deposits (Sangster, 2002). Sphalerite, galena, marcasite, pyrite, dolomite, and calcite are the dominant minerals found in these deposits (Paradis et al., 2007) though some deposits (e.g. in the Mississippi Valley, USA) contain economic concentrations of fluorite and barite (Sverjensky, 1986). Native sulphur, celestite, gypsum, anhydrite, pyrrhotite also occur in some districts (Paradis et al., 2007). The abundance of iron sulphides varies from district to district; some deposits have none (e.g. Daniel's Harbour, Newfoundland) whereas they are abundant in other deposits (Nanisivik, Nunavut); the presence or absence of pyrite can have an effect on the choice of geophysical exploration methods (Leach et al., 1995; St. Marie et al., 2001). The carbonate host rocks are typically subjected to two dolomitizing events with the original limestone being replaced by a fine-grained dolomite that is subsequently replaced by a medium to coarse-grained dolomite (Paradis et al., 2007). It is in this secondary, coarser-grained hydrothermal dolomite that mineralization occurs. These dolomitizing events are crucial to setting the stage for ore mineralization by creating the secondary porosity in form of void space, and by creating large caverns that subsequently collapse creating the collapse breccias associated with the majority of MVT deposits (Rhodes et al., 1984; Qing and Mountjoy, 1994). These collapse features can occur pre-, syn- or post-ore, which is evident by sulphide minerals occurring as brecciated clasts along with dolostone and limestone (Rhodes et al., 1984; Qing and Mountjoy, 1994).
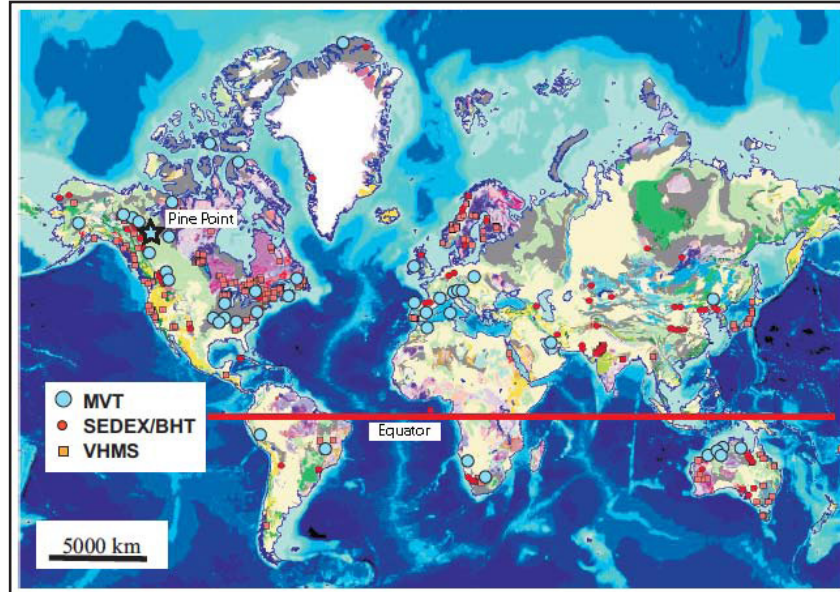
Fig. 1-1: Global distribution of MVT, VMS and SEDEX deposits. The majority of known MVT deposits occur in the northern hemisphere (modified from Paradis et al., 2007).

1.2.1 The geology of the Pine Point district

The Pine Point mining district consists of approximately 100 drill-defined ore bodies that span an area of approximately 1600 km^2 (Hannigan, 2007). The total geologic resource (produced and remaining proven resource) is estimated to be 95.4 Mt of combined Pb and Zn (Hannigan, 2006). The individual deposits range from 100, 000 to 17.5 Mt and have an average grade of 2% Pb and 6.2% Zn (Holroyd et al., 1988) and are concentrated within three distinct trends known as the North, Main and South trends (Fig. 1-2) that are associated with the Great Slave Shear Zone (GSSZ). The GSSZ is an area of highly deformed and sheared rocks that extend for approximately 700 km northeast-southwest from the Northwest Territories into northeastern British Columbia (Eaton and Hope, 2003). The expression of this structure in the Pine Point district is the Hay River-Macdonald Fault Zone (see Pana, 2006).

The Pine Point deposits are hosted in Devonian carbonate units of the Western Canadian Sedimentary Basin (WCSB). The majority of the deposits are hosted by the Presqu'ile barrier which is defined as a reef-like complex (200 m

at its thickest point) that separates the deep marine rocks to the north from the shallow marine rocks to the south (Rhodes et al., 1984; Hannigan, 2007). The lower two-thirds of the Presqu'ile barrier comprises the Upper Keg River Formation. The Upper Keg River Formation consists of flat, lensoidal beds of carbonate sandstones and mudstones. The dolomites of this formation are fine, dense, grey-brown that contain abundant carbonaceous fossils (Skall, 1975; Hannigan, 2007). The overlying Sulphur Point Formation contains the upper third of the Presqu'ile barrier and consists of a build-up of bioherms, bioclastic limestones and carbonate sandstones (Rhodes et al., 1984; Hannigan, 2007). The carbonates of this formation have undergone alteration into a coarse crystalline, vuggy dolomite known as Presqu'ile dolomite which dominantly occurs along the North and Main trends (Skall, 1975; Hannigan, 2007); this dolomite hosts many of the deposits. The majority of deposits contain galena and sphalerite with minor pyrite and marcasite (Rhodes et al., 1984; Hannigan, 2007) within dolomitized host rocks (Rhodes et al., 1984; Qing, 1991). Minor hydrothermal minerals associated with the Pine Point deposits include sulphur (native), pyrrhotite, celestite, barite, gypsum, anhydrite, and fluorite (Hannigan, 2007). Bitumen is also present in the host Paleozoic carbonate rocks and is often associated with the ore.

1.2.2   Orebody morphology and paragenesis

The Pine Point ore deposits occur as either tabular or prismatic bodies. These orebodies have a high-grade core of sphalerite and galena with pyrite and marcasite increasing in abundance toward the periphery of each body (Krebs and Macqueen, 1984; Cumming et al., 1990). Prismatic bodies are more characteristic of the upper barrier (Sulphur Point Formation) with tabular bodies commonly located in the lower barrier (Skall, 1975; Kyle, 1981; Hannigan, 2007; Fig. 1-3).

Eight major paragenetic stages occurring either pre-, syn- or post-ore (summarized in Hannigan, 2007) were identified for Pine Point by observing

4
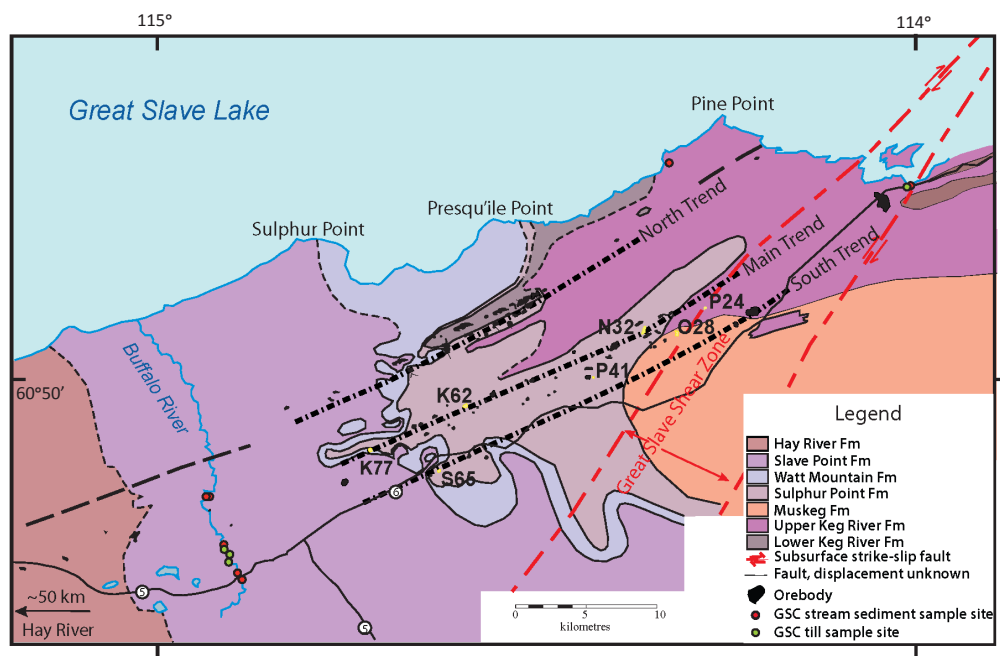
Fig. 1-2: Simplified geology map showing the three trends with respect to the Great Slave Shear Zone and its associated faults. Labelled ore bodies are also locations of till samples. Modified from Hannigan, (2007).

relationships of dissolution and replacement between dolomite and sulphides in open pits, diamond drill core, hand samples and thin sections (Krebs and Macqueen, 1984). During the pre-ore stage, the production of fine and medium–grained crystalline dolomite was prevalent throughout the area as well as the Presqu'ilization, dissolution and karstification of the North and Main trend carbonates (Skall, 1975; Krebs and Macqueen, 1984; Qing, 1991). The fine crystalline dolomites are the most extensive rock type in the area (Skall, 1975; Krebs and Macqueen, 1984; Rhodes et al., 1984) and represent the earliest dolomitizing event (Krebs and Macqueen, 1984; Qing, 1991). They are grey, yellow-grey to brown-grey and have fossils and sedimentary structures that are distinguishable. Medium crystalline dolomites represent a separate dolomitizing event and are buff-brown to grey (Qing, 1998). They occur mainly in the lower barrier and primary fabrics and structures are not preserved in these dolomites (Skall, 1975).

Presqu'ile dolomite occurs primarily on the North and Main trends and hosts the majority of the ore bodies (Krebs and Macqueen, 1984). The contact between this unit and the other dolomite units tends to be sharp and follows bedding planes (Skall, 1975; Krebs and Macqueen, 1984). Saddle dolomite occurs several times in the paragenesis. Saddle dolomite forming an isopachus crust on fine-grained dolomite was cited as evidence for pre-ore deposition while interbedded saddle dolomite and sphalerite crystals were regarded as evidence for syn-deposition (Anderson, 1973; Krebs and Macqueen, 1984). Saddle dolomite also replaced sphalerite in some cases and, therefore, post-dated the ore (Krebs and Macqueen, 1984).
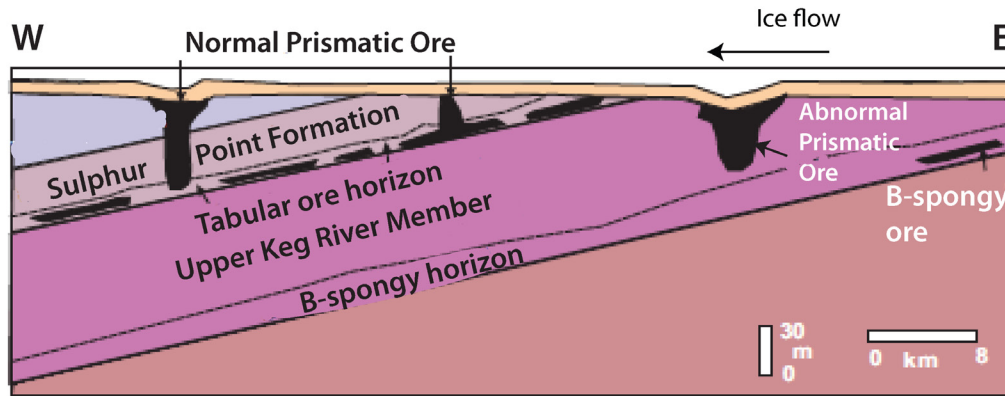
Fig. 1-3: Distribution of ore bodies within the stratigraphy at Pine Point. Prismatic ore bodies are typically located in the upper barrier while tabular ore bodies occur primarily in the lower barrier (from Hannigan, 2007).

Pre-ore dolomitizing events enlarged pre-existing pore space creating large cavities which was integral to the mineralization process (Rhodes et al., 1984). Firstly, iron sulphides were deposited throughout vugs and caverns followed by sphalerite and galena. Studies have shown that sphalerite in the upper barrier is often void filling, colloform and intergrown with galena while sphalerite in the lower barrier is generally crystalline (Campbell, 1966; Krebs and Macqueen, 1984). Sphalerite in the lower barrier also frequently replaces dolomite and limestone (Campbell, 1966; Krebs and Macqueen, 1984). Krebs and Macqueen (1984) observed that near the edges of the orebodies, dark brown sphalerite crystals are intergrown with coarse, crystalline white saddle dolomite. This was interpreted to suggest either co-precipitation of sphalerite and saddle dolomite or replacement of sphalerite with saddle dolomite. Further observations by Krebs and Macqueen (1984) indicate that galena crystals intersect and are irregularly embedded within colloform sphalerite. The authors suggest that either colloform sphalerite or galena were co-precipitated or that galena mineralization post-dated sphalerite in some cases (Krebs and Macqueen, 1984). Cubic galena crystals were precipitated following colloform sphalerite as it usually fills interstitial space between botryoidal sphalerite and/or occurs on the surface of sphalerite.

During this mineralization event, saddle dolomite filled voids, fractures

and veins as well as replaced existing minerals (Krebs and Macqueen, 1984). Solution fracturing and internal filling of sediments are thought to have occurred during mineralization as evidenced by brecciated ores, laminated (alternating with sulphides) sediments and crosscutting dolomite (Krebs and Macqueen, 1984). Calcite crystals precipitated in the remaining pore-space after ore deposition on a regional scale (Krebs and Macqueen, 1984). Sulphur and bitumen also fill remaining pore space indicating that these minerals also precipitated post ore.

1.2.3   Mineralizing fluid characteristics

Fluid inclusions suggest the mineralizing fluids were Ca-Na-Cl brines with temperatures of 50 to 150°C (Macqueen and Powell, 1983; Krebs and Macqueen, 1984; Gleeson & Turner, 2007). A fluid inclusion study by Gleeson and Turner (2007) identified four different fluids associated with Pine Point mineralization events: (1) a Br-rich evaporated seawater, (2) a Br-rich fluid of unknown origin, (3) a Br-poor (Cl-rich) fluid sourced from dissolved halites and (4) a dilute fluid that is likely the Br-rich evaporated seawater that has been diluted by meteoric water. The Br-rich evaporated seawater was determined to be responsible for sulphide mineralization as well as Presqu'ile and saddle dolomites that are associated with the deposits (Gleeson and Gromek, 2006). The dilute fluid was determined to be responsible for the precipitation of late stage calcite as well as native sulphur crystals.

The source of the metals in the deposits is not well known but based on isotopic evidence, the origin for Pb at Pine Point appears to be deep-seated basement rocks (Cumming et al., 1990; Gleeson and Gromek, 2006). Some metals could also have been leached from clastic units along the flow path from the depths of the WCSB to the site of ore deposition (Gleeson and Turner, 2007; Gromek et al., 2012).

1.2.4   Origin and timing of mineralizing fluids

Three possibilities for fluid flow have been proposed for the formation

of MVT deposits. These are: (1) the mixing model, (2) the sulphate reduction model and, (3) the reduced sulphur model. Recent studies (e.g. Adams et al., 2000; Gleeson and Turner, 2007; Gromek et al., 2012) have shown mineralization at Pine Point is likely the result of mixing of at least two fluids at the site of ore deposition. It was suggested the deposits form due to the migration of sedimentary brines into the crystalline basement rocks via structures associated with the GSSZ (Pana, 2006; Gromek et al., 2012). This hypothesis is supported by fluid studies (Gleeson and Turner, 2007; Gromek et al., 2012) that indicate the mineralizing fluids at Pine Point interacted with underlying clastic sediments as well as the crystalline basement rocks.

The timing of mineralization at Pine Point is still poorly constrained but it is generally accepted that it occurred after formation of the barrier (Campbell, 1966; Skall, 1975). Multiple dating methods (radiometric, paleomagnetic, Pb-U, and hydrogeological, among others) have yielded two possible age ranges: Late Devonian to Early Mississipian and Cretaceous to Tertiary (Garven, 1985; Qing, 1991; Qing and Mountjoy, 1992; Nakai et al., 1993; Nesbitt and Muehlenbachs, 1994; among others). These two ages coincide with the Antler (Late Devonian to Early Mississipian) and Laramide orogenies (Cretaceous to Tertiary). Two fluid flow models have been proposed on the basis of these two ages. The first is a gravity-induced fluid flow model in which fluids originating in the Rocky Mountains are focused along aquifers in the WCSB until they reach the site of deposition. The eastward flow is caused by uplift on the western margin of the basin during the Laramide Orogeny (Garven, 1985; Qing and Mountjoy, 1992; among others). The second fluid flow model proposed that hydrothermal circulation is driving fluids along reactivated, rifted back-arc structures during the Antler Orogeny (Nelson et al., 2002). The timing of mineralization at Pine Point is still a matter of contention.

1.3   Mineral exploration in glaciated terrain
1.3.1   Glacial dispersal processes

Glaciers erode, transport and deposit sediment in a manner that reflects

the glacial history of a given region. Glacial deposits (till) are a first-cycle sediment that is composed of freshly crushed bedrock mixed with sediments that have been transported for a few meters up to kilometers (McMartin and McClenaghan, 1999). In an ideal setting, glacial dispersal will form a plume shape with the largest concentration of anomalies (indicator minerals or pathfinder elements) directly overlying the source and continuing down-ice until the anomalies reach the surface (Fig. 1-4; Drake, 1983). The fine sediments (< 2 mm) are produced mainly by the crushing of primary minerals (McMartin and McClenaghan, 2001) and can be isolated into heavy mineral concentrates that contain indicator minerals. Weathering of these fine-grained sediments (sand-sized particles) can concentrate elements in the silt and clay fraction making an ideal medium for determining pathfinder elements.

1.3.2 Indicator minerals

Indicator minerals are a suite of minerals that appear in transported material (stream sediments or glacial till) that indicate the presence of a specific type of mineral deposit, alteration or rock lithology (McClenaghan, 2005). Commonly, indicator minerals have medium to high density, are visually distinctive, are silt or sand sized and robust enough to survive transport and weathering (McClenaghan, 2005). Indicator mineral methods have been in use for thousands of years (Ottensen and Theobald, 1994) and have been used to detect a variety of deposit types such as cassiterite for tin deposits (Ryan et al., 1988), scheelite and wolframite for tungsten deposits (Zantop and Nespereira, 1979; Johansson et al., 1986), and Cr-spinel and Cr-garnet for kimberlites (Gurney, 1984; Fipke et al., 1995). Heavy indicator mineralogy is more sensitive than heavy mineral geochemistry and offers the additional benefit of visual examination of individual grains that can provide information about transport distance and bedrock source (Averill, 2001; McClenaghan, 2005). Indicator mineral methods can also detect dispersal trains/halos that are much larger than the mineralized source; they can also provide information about the source

10

such as nature of the ore, alteration, and proximity to the source (Averill, 2001; McClenaghan, 2005). Another benefit of indicator mineral methods is that they have the sensitivity to detect a few grains in any samples, which is equivalent to a ppb-level detection limit (McClenaghan, 2005).

1.3.3 Till geochemistry

Till geochemical studies are conducted on a reconnaissance, regional or property scale (Levson, 2001). Till geochemical methods are useful as
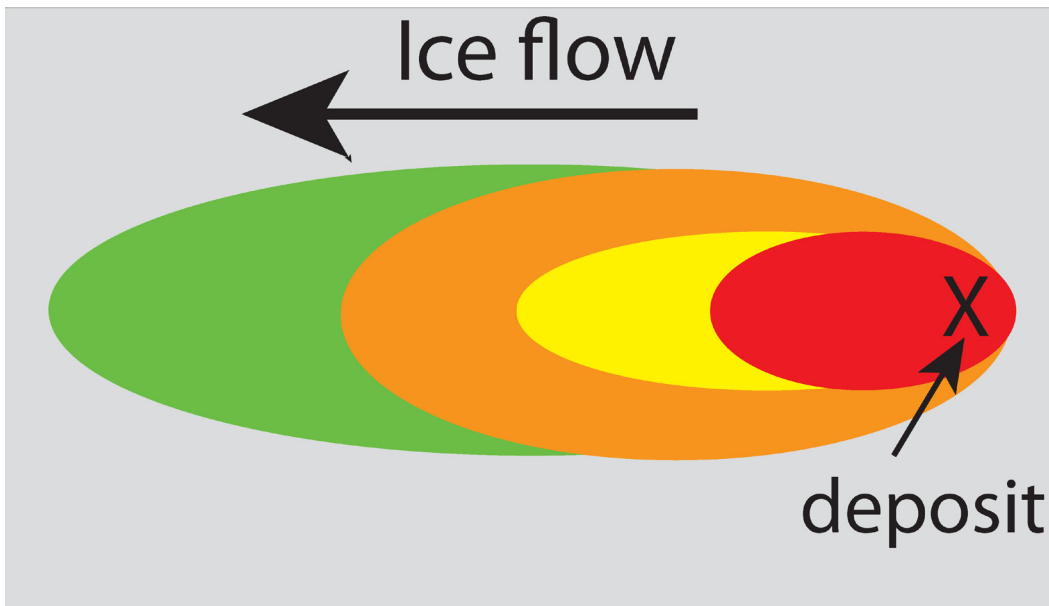
Fig. 1-4: Schematic of ideal dispersal of indicator minerals and pathfinder elements. Ideally, in areas with one ice flow direction and thin till cover, the largest concentrations of indicator minerals and pathfinder elements will be overlying and immediately down ice of the deposit (Drake, 1983; Miller, 1984).

exploration techniques since they too, can detect a much larger geochemically anomalous halo than the source mineralization (e.g. Shilts, 1976; Levson, 2001; McClenaghan and Kjarsgaard, 2001). Prospecting for large anomalous halos (dispersal trains) is a cost-effective mineral exploration method that can help reduce large exploration areas to more specific targets (Shilts, 1976; Levson and Giles, 1995; Levson 2001). Most geochemical surveys begin with reconnaissance scale sampling of stream or esker sediments (e.g. Shilts, 1984; Levson, 2001; McClenaghan and Kjarsgaard, 2001) after which anomalous values can be

followed up with regional and property scale till sampling. These reconnaissance surveys typically consist of the collection of weakly oxidized till 0.5 to 1 m below the natural land surface (McMartin and McClenaghan, 1999). In areas of relatively simple glacial history, dispersal trains tend to rise in a down-ice direction so that the distance between the mineralized source and the tail of the dispersal train tends to increase with increased till thickness (Miller, 1984). Once the tail of the dispersal train has been detected, regional and property scale sampling can occur. In regional and property scale mapping it is important to sample as close to the bedrock/till interface as possible because till composition here will resemble that of the underlying bedrock (McMartin and McClenaghan, 1999). It has been determined that <0.063 mm (silt + clay) and 0.25 - 2 mm fractions of till provide the best contrast between background and anomalous values for pathfinder elements (McClenaghan and Kjarsgaard, 2001). Lodgement till (as opposed to ablation till) is the ideal sample till since minerals in ablation till are near the surface and may have been subjected to more weathering factors than minerals in lodgement till (Shilts, 1976).

1.4   Conclusions

In order to overcome the above stated hurdles for exploration in glaciated terrain, till geochemical and indicator minerals exploration techniques were applied to a well-studied MVT district. Pine Point was chosen for this project because it is a system with simple mineralogy that sub-cropped at the surface allowing glaciers access to mineralized bedrock. There have also been several studies documenting the isotopic signature and ore mineralogy of the deposits. This study applies these techniques to compare the grains recovered from till to those of a single deposit in the district.

In Chapter 2, a 1:50 000 surficial geology map of NTS 85B/15 (Breynat Point) is presented. This map was constructed based on airphoto interpretation and ground-truthing. The accompanying chapter discusses the distribution and characteristics of the surficial deposits in the region. A surficial map was also

produced for the surficial materials overlying deposit O-28.

In Chapter 3, we present data on the paragenesis, Pb and S isotopic composition and geochemistry of the major ore phases from five ore deposits in the Pine Point district. In this chapter ice-flow data and a description of the geochemistry of the till and the morphology, trace element and isotopic composition of the recovered indicator minerals are also presented. Finally, recommendations for drift prospecting for MVT deposits are outlined in this Chapter.

Chapter 4 presents the conclusions of the study and offers suggestions for future work.

1.5   References

Adams, J.J., Rostron, B.J., and Mendoza, C.A., 2000. Evidence for two-fluid mixing at Pine Point, Northwest Territories. Journal of Geochemical Exploration, v. 69-70, p. 103-108.

Anderson, G.M., 1973. The hydrothermal transport and deposition of galena and sphalerite near 100°C. Economic Geology, v. 68, p. 480-492.

Anderson, G.M., and Macqueen, R.W., 1988. Ore deposit models-6. Mississippi Valley-type lead-zinc deposits. *In*: Roberts, R.G., and Sheahan, P.A. (eds) *Ore deposit models*. Geoscience Canada, reprint series 3, p 79-90.

Averill, S.A., 2001. The application of heavy indicator minerals in mineral exploration. *In:* McClenaghan, M.B., Bobrowsky, P.T., Hall, G.E.M., and Cook, S., (eds) *Drift exploration in glaciated terrain*, Geological Society of London, Special Publication 185, p. 69-82.

Campbell, N., 1966. The lead-zinc deposits of Pine Point: Canadian Mining and Metallurgical Bulletin, v. 59, p. 953-960.

Cumming, G.L., Kyle, J.R., and Sangster, D.F., 1990. Pine Point: A case history of lead isotopic homogeneity in a Mississippi Valley-type district. Economic Geology, v. 85, p 133-144.

Drake, L.D., 1983. Ore plumes in till. Journal of Geology, v. 91, p. 707-713.

Dreimanis, A., 1960. Geochemical prospecting for Cu, Pb, and Zn in glaciated areas, eastern Canada. *In*: Marmo, V., Puranen, M. (eds.), Geological Results of Applied Geochemistry and Geophysics, p. 7-19. Report of the 21st International Geological Congress, Part 2, Det Berlingske Bogtrykkeri, Copenhagen.

Eaton, D.W. and Hope, J. 2003. Structure of the crust and upper mantle of the Great Slave Lake shear zone, northwestern Canada, from teleseismic analysis and gravity modelling. Canadian Journal of Earth Sciences, v. 40, p. 1203-1218.

Fipke, C.E., Gurney, J.J., and Moore, R.O., 1995. Diamond exploration techniques emphasizing indicator mineral geochemistry and Canadian examples. Geological Survey of Canada, Bulletin 423.

Garven,, G., 1985. The role of regional fluid flow in the genesis of the Pine Point deposit, Western Canada Sedimentary Basin. Economic Geology, v. 80, p. 307-324.

Gleeson, S.A., and Gromek, P., 2006. Origin of hydrothermal sulphide and dolomite mineralizing fluids in southern Northwest Territories and northern Alberta. *In:* Hannigan, P.K. (ed) *Potential for Carbonate-hosted Lead-zinc*

Mississippi Valley-type Mineralization in Northern Alberta and Southern Northwest Territories. Geoscience Contributions, Targeted Geoscience Initiative, Geological Survey of Canada, Bulletin 591, p. 61-73.

Gleeson, S.A. and Turner, W.A., 2007. Fluid inclusion constraints on the origin of the brines responsible for Pb-Zn mineralization at Pine Point and coarse non-saddle and saddle dolomite formation in southern Northwest Territories. Geofluids v. 7, p 51-68.

Gromek, P., Gleeson, S.A., and Simonetti, A., 2012. A basement-interacted fluid in the N81 deposit, Pine Point Pb-Zn district, Canada: Sr isotopic analyses of single dolomite crystals. Mineralium Deposita, v. 47(7), p. 749-754.

Gurney, J.J., 1984. A correlation between garnets and diamonds in kimberlites. *In*: Kimberlite Occurrence and Origin: a basis for conceptual models in exploration. Geology Department and University Extension, University of Western Australia, Publication Number 8, p. 143-166.

Hannigan, P.K., 2006. Introduction. *In:* Hannigan, P.K. (ed) *Potential for Carbonate-hosted Lead-zinc Mississippi Valley-type Mineralization in Northern Alberta and Southern Northwest Territories.* Geoscience Contributions, Targeted Geoscience Initiative, Geological Survey of Canada, Bulletin 591, p. 9-39.

Hannigan, P., 2007. Metallogeny of the Pine Point Mississippi Valley-Type zinc-lead district, southern Northwest Territories. *In:* Goodfellow, W.D. (ed) *Mineral Deposits of Canada: A Synthesis of Major Deposit-Types, District Metallogeny, the Evolution of Geological Provinces, and Exploration Methods*. Geological Association of Canada, Mineral Deposits Division, Special Publication No. 5, p. 609-632.

Holroyd, R.W., Hodson, T.W., and Carter, K.M., 1988. Unpublished termination report, Pine Point Mines Ltd., June 28, 1988.

Johansson, P., Keinanen, V., and Lehmuspelto, P., 1986. Geochemical exploration of tungsten in glaciogenic deposits in Soretiapulju, western Finnish Lapland. *In*: Prospecting in areas of glaciated terrain-1986, Institute of Mining and Metallurgy, London, p. 61-67.

Krebs, W., and Macqueen, R., 1984. Sequence of diagenetic and mineralization events, Pine Point Lead-Zinc Property, Northwest Territories, Canada. Bulletin of Canadian Petroleum Geology, v. 32, p. 434-464.

Kyle, J.R., 1981. Geology of the Pine Point lead-zinc district. *In:* Wolf, K.H., (ed) *Handbook of strata-bound and stratiform ore deposits.* Elsevier Publishing Company, New York, v. 9, p 643-741.

Leach, D.L, and Sangster, D.F., 1993. Mississippi Valley-type lead-zinc deposits. *In*:

Kirkham, R.V., Sinclair, W.D., Thorpe, R.I., and Duke, J.M. (eds) *Mineral Deposits Modeling.* Geological Association of Canada, Special Paper 40, p 289-314.

Leach, D. L., Viets, J.B., Foley-Ayuso, N., and Klein, D.P., 1995. Mississippi Valley-type Pb-Zn deposits. *In*: DuBray, E.A., (ed) *Preliminary Compilation of Descriptive Geoenvironmental Mineral Deposit Models*, US Government Consulting Group, Open File Report 95-831, p. 234-243.

Levson, V.M., 2001. Regional till geochemical surveys in the Canadian Cordillera: sample media, methods and anomaly evaluation. *In:* McClenaghan, M.B., Bobrowsky, P.T., Hall, G.E.M., and Cook, S., (eds) *Drift exploration in glaciated terrain*, Geological Society of London, Special Publication 185, p. 45-68.

Levson, V.M., and Giles, T.R., 1995. Glacial dispersal patterns of mineralized bedrock: with examples from the Nechako Plateau, central British Columbia. *In*: Bobrowsky, P.T., Sibbick, S.J., Newell, J.M., and Matysek, P.F. (eds) Drift exploration in the Canadian Cordillera. British Columbia Ministry of Energy, Mines and Petroleum Resources Paper 1995-2, p. 67-76.

Macqueen, R.W., and Powell, T.G., 1983. Organic geochemistry of the Pine Point lead-zinc ore field and region, Northwest Territories, Canada. Economic Geology, v. 78, p 1-25.

McClenaghan, M.B. 2005. Indicator mineral methods in exploration. Geochemistry: Exploration, Environment, Analysis, vol. 5, p. 233–245.

McClenaghan, M.B., and Kjarsgaard, B.A., 2001. Indicator mineral and geochemical methods for diamond exploration in glaciated terrain in Canada. *In:* McClenaghan, M.B., Bobrowsky, P.T., Hall, G.E.M., and Cook, S., (eds) *Drift exploration in glaciated terrain*, Geological Society of London, Special Publication 185, p. 83-123.

McMartin, I., and McClenaghan, M.B., 2001. Till geochemistry and sampling techniques in glaciated shield terrain. *In:* McClenaghan, M.B., Bobrowsky, P.T., Hall, G.E.M., and Cook, S., (eds) *Drift exploration in glaciated terrain*, Geological Society of London, Special Publication 185, p. 19-43.

Miller, J.K., 1984. Model for classic indicator trains in till. *In*: Prospecting in Areas of Glaciated Terrain, Institution of Mining and Metallurgy, London, p. 69-77.

Nakai, S., Halliday, A.N., Kesler, S.E., Jones, H.D., Kyle, J.R., and Lane, T.E., 1993. Rb-Sr dating of sphalerites from Mississippi Valley-type (MVT) ore deposits. Geochemica et Cosmochimica Acta, v. 57, p. 417-427.

Nelson, J., Paradis, S., Christensen, J. and Gabites, J. 2002. Canadian Cordilleran Mississippi Valley-type deposits: A case for Devonian-Mississippian back-arc hydrothermal origin. Economic Geology, v. 97, p. 1013–1036.

Nesbitt, B.E., and Muehlenbachs, K., 1994. Paleohydrogeology of the Canadian Rockies and origins of brines, Pb-Zn deposits and dolomitization in the Western Canada Sedimentary Basin. Geology, v. 22, p. 243-246.

Ottensen, R.T., and Theobald, P.K., 1994. Stream sediments in mineral exploration. *In:* Hale, M., and Plant, J.A. (eds) *Drainage geochemistry*. Handbook of Exploration Geochemistry, v.6, p. 147-184.

Pana, D., 2006. Unravelling the structural control of Mississippi Valley-type deposits and prospects in carbonate sequences of the Western Canada Sedimentary Basin. *In:* Hannigan, P.K. (ed.) *Potential for Carbonate-hosted Lead-zinc Mississippi Valley-type Mineralization in Northern Alberta and Southern Northwest Territories: Geoscience Contributions, Targeted Geoscience Initiative*. Geological Survey of Canada, Bulletin 591, p. 255-304.

Paradis, S., Hannigan, P., and Dewing, K., 2007. Mississippi Valley-type lead-zinc deposits, *In:* Goodfellow, W.D. (ed) *Mineral Deposits of Canada: A Synthesis of Major Deposit-Types, District Metallogeny, the Evolution of Geological Provinces, and Exploration Methods*. Geological Association of Canada, Mineral Deposits Division, Special Publication No. 5, p. 609-632.

Qing, H., 1991. Diagenesis of Middle Devonian Presqu'ile dolomite at Pine Point and adjacent subsurface. Unpublished PhD thesis, McGill University.

Qing, H., 1998. Geochemical constraints on the origin and timing of paleofluid flow in the Presqu'ile barrier reef, Western Canada Sedimentary Basin. *In:* Parnell, J. (ed) *Dating of fluid flow and fluid-rock interaction*, Geological Society of London, Special Publication 144, p. 173-187.

Qing, H., and Mountjoy, E., 1992. Large-scale fluid flow in the Middle Devonian Presqu'ile barrier, Western Canada Sedimentary Basin. Geology, v. 20, p. 903-906.

Qing, H., and Mountjoy, E.W., 1994. Origin of dissolution vugs, caverns, and breccias in the Middle Devonian Presqu'ile Barrier, host of Pine Point Mississippi Valley-type deposits. Economic Geology, v. 89, p 858-876.

Rhodes, D., Lantos, E.A., Lantos, J.A., Webb, R.J., Owens, D.C., 1984. Pine Point orebodies and their relationship to the stratigraphy, structure, dolomitization, and karstification of the middle Devonian Barrier complex. Economic Geology, v. 79, p. 991-1055.

Ryan, R.J., Turner, R.G., Stea, R.R., and Rogers, P.J., 1988. Heavy minerals and sediment dispersal as exploration tools for potential tin and gold paleoplacers in Carboniferous rocks, Nova Scotia. *In:* MacDonald, D.R., and Mills, K.A., (eds) *Prospecting in areas of glaciated terrain-1988.* Canadian Institute of Mining and Metallurgy, p. 41-56.

Sangster, D.F., 2002. MVT deposits of the world; database documentation of the World Minerals Geoscience Database Project, http://www.nrcan.gc.ca/gsc/mrd/wmgdb/index_e.php.

Shilts, W.W. 1976. Chapter 15, Drift exploration. *In*: MENZIES, J. (ed.) Past Glacial Environments, Sediments, Forms and Techniques, Butterworth Heinemann, Toronto, p. 411-439.

Skall, H., 1975. The paleoenvironment of the Pine Point lead-zinc district. Economic Geology, v. 70, p. 22-47.

St. Marie, J., Kesler, S.E., and Allen, C.R., 2001. Origin of iron-rich Mississippi Valley-type deposits. Geology, v. 29, p. 59-62.

Stothart, Paul. "The Mining Association of Canada." *2011 Facts and Figures*, accessed 14 October 2012.

Sverjensky, D.A., 1986. Genesis of Mississippi Valley-type lead-zinc deposits. Annual Review, Earth and Planetary Science, v. 14, p. 177-199.

Zantop, H., and Nespereira, J., 1979. Heavy-mineral panning techniques in the exploration for tin and tungsten in NW Spain. *In:* Theobald, P.K. (ed) *Geochemical exploration 1978*, Association of Exploration Geochemists, p. 329-336.

Chapter 2

2.1 Introduction

As part of a Pb-Zn geochemistry and indicator mineral glacial dispersion project undertaken at the Pine Point abandoned mine site, near Hay River, Northwest Territories, a 1:50,000 surficial map of NTS 85B/15 was produced (Appendix A1). In addition, a local scale surficial map was produced at deposit O28, which is the location of the till geochemistry and indicator mineral study. Canadian Geoscience Map 114 (Oviatt and Paulen, 2013) was published by the Geological Survey of Canada and is the focus of this chapter. The objective of this mapping activity was to describe and record the surficial materials in the area and to document their distribution. The construction of the map was completed by interpretation of 1:25,000 airphotos and ground-truthing was carried out over the summer 2011 field season.

The Pine Point district covers an area of approximately 1600 km^2 and consists of 100 drill-defined orebodies that average 2% Pb and 6.2% Zn (Hannigan, 2007). The total geological resource (produced and remaining proven resource) is estimated to be 95.4 Mt (Hannigan, 2007), however the mine site closed in 1988 due to dropping market prices for Pb and Zn and rising mining costs (Hannigan, 2007). Deposit O28 was mined from 1971 to 1975 and produced 1.6 Mt with an average grade of 2% Pb and 3.7% Zn (Holroyd et al., 1988).

The Pine Point area has an extensive Quaternary record. This study has documented evidence of at least three directions of ice flow that were recorded from striae on bedrock surfaces uncovered during past mining activity. A study by Rice et al., (2013) determined there are four visually and characteristically distinctive till units in the Pine Point area. There was no evidence that these till units were from different glacial events but rather that they likely record changes (i.e., provenance) in the western sector of the Laurentide Ice Sheet (LIS) (Rice et al., 2013). It was suggested that the Pine Point area was glaciated throughout the entire Wisconsin and that the margin of the LIS was to the north and west of Pine Point (Rice et al., 2013) as opposed to near the margin of the Canadian Shield

(Dyke et al., 2002) before re-advancing into southern Canada (Dyke and Prest, 1987). This proposition was based on the nature of continuous till sequences mapped at Pine Point, that contained no evidence for ice margin advance or retreat (Rice et al., 2013), however work is currently underway to further develop this hypothesis. During the last glacial maximum, approximately 18 ^{14}C ka BP, the area was covered by ice from the Keewatin Sector of the LIS (Dyke and Prest, 1987; Dyke, 2004). The western margin of the LIS had coalesced with the eastern margin of the Cordilleran Ice Sheet (CIS) covering most of Canada in a sheet of ice (Jackson et al., 1999). Deglaciation began in earnest at approximately 14 ^{14}C ka BP (Dyke and Prest, 1987) beginning with the separation of the CIS and the LIS. Complete separation of these two ice sheets occurred at approximately 12.5 ^{14}C ka and deglaciation began affecting the Pine Point area at approximately 10.5 ^{14}C ka BP (Dyke and Dredge, 1989; Dyke, 2004). Deglaciation of the study area was an easterly retreat of the LIS margin and the formation of glacial Lake McConnell (Lemmen et al., 1994; Dyke, 2004). The geomorphology of the Pine Point region is the result of glaciolacustrine processes associated with glacial Lake McConnell.

2.2   Glacial Lake McConnell

Glacial Lake McConnell was an extensive body of water that occupied the basins of Great Bear, Great Slave and Athabasca lakes. This proglacial lake was one of the largest glacial lakes to exist in Canada (Lemmen et al., 1994) covering approximately 215,000 km^2. The lake existed in three different stages from 11.8 to 8.3 ka BP (Smith, 1994). These stages were named the Hare Indian phase, the Great Bear phase and the Mackenzie phase by Smith (1994). The Mackenzie phase was the most extensive and it directly affected the area of this study (Fig. 2-1). Glacial Lake McConnell formed in the northwestern arm of Great Bear Lake, and extended southwards towards Great Slave Lake when isostatic loading and ice-dams allowed water levels to breach the current 219 m drainage divide between the two basins (Craig, 1965; Smith, 1994; Lemmen et al., 1994). The highest beach ridges in the Pine Point area occur south of Hay River at 295 m

20
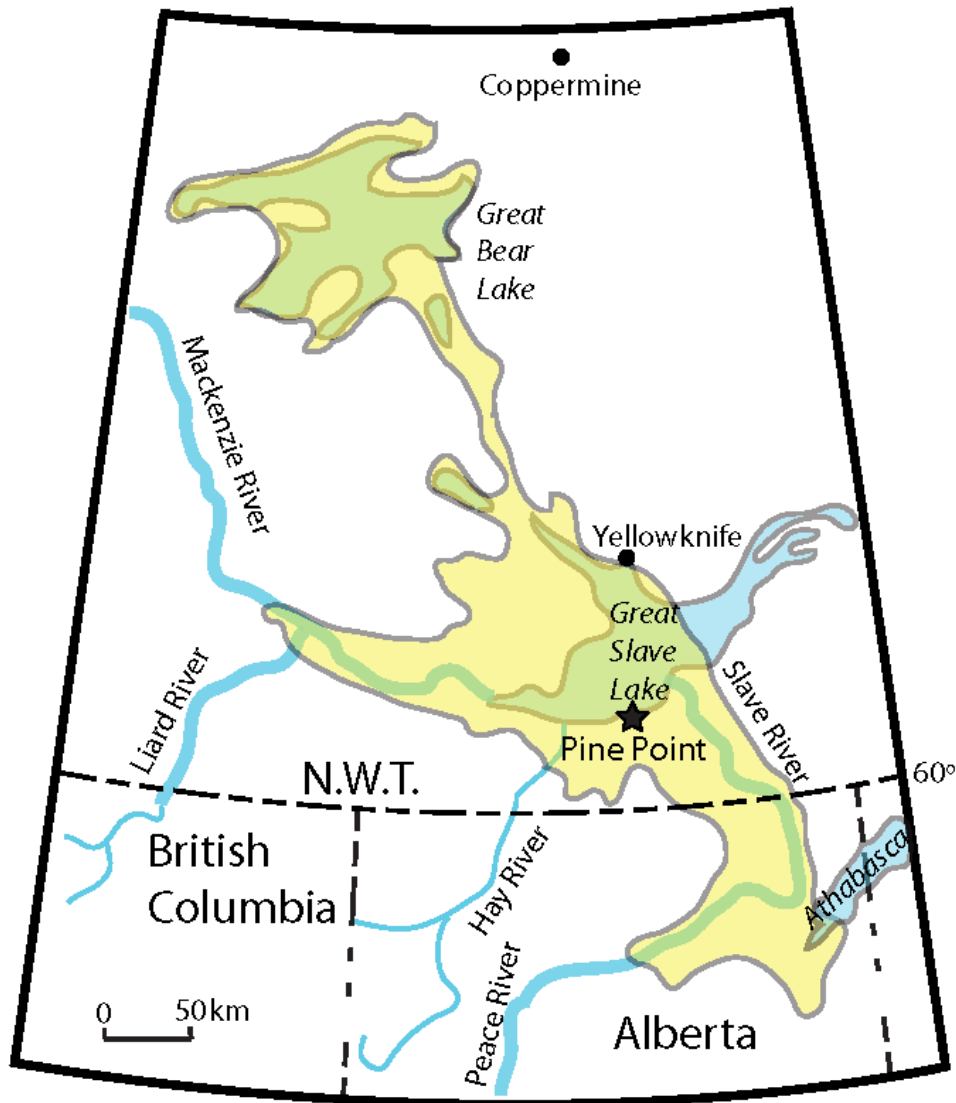
Fig. 2-1: The Mackenzie phase of glacial Lake McConnell in yellow, superimposed on modern drainage basins (modified from Craig (1965) and Lemmen et al., (1994)). The Pine Point region was inundated by this phase. The approximate location of the western margin of the LIS would have been along the eastern edge of glacial Lake McConnell, between Athabasca and Great Slave Lake(Smith, 1994).

a.s.l (Craig, 1965). There are only two known deltas associated with glacial Lake McConnell and therefore, glaciofluvial sediments are generally scarce (Craig, 1965; Smith, 1994; Lemmen et al., 1994).

2.3   Physiography

The Pine Point mining district is located approximately 180 km due south of Yellowknife, Northwest Territories on the south shore of Great Slave Lake (Fig. 2-2). The district lies within the Buffalo Lake topographic map sheet (NTS 85B). The surficial map was produced for NTS 85B/15 (Breynat Point) and contains the western half of the former Pine Point mine. The study area lies within the Great Slave Plain division of the Interior Plains region (Bostock, 1970). The area is poorly drained and characterized by black spruce peatlands with local relief not exceeding 15 m (Lemmen, 1990). The region is pock-marked by thermokarst topography and open pits associated with the relict mine, with most of these
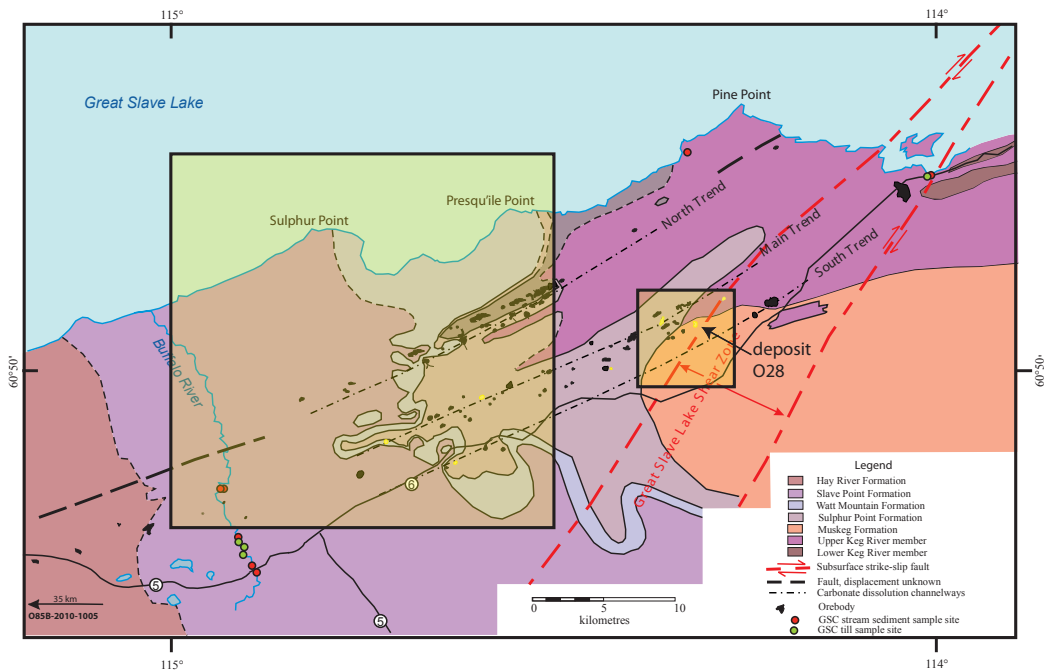
Fig. 2-2: Bedrock geology map of the Pine Point area (modified from Hannigan, 2007) showing the three trends of the orebodies as well as the sample locations for the indicator mineral and till geochemical study. The large yellow box is the outline of NTS 85B/15 (Breynat Point) and the small yellow box is the outline of the local scale surficial map overlying deposit O28 (labelled). Orebodies shown in yellow are locations of regional till samples.

22

features being filled with water.

2.4   Bedrock Geology

The bedrock of the Pine Point area (Fig. 2-2) consists of 350 to 600 m of Ordovician to Devonian units that overlie crystalline basement rocks of the Archean and Proterozoic (Skall, 1975; Kyle, 1977; Rhodes et al., 1984). More specifically, the deposits are hosted by, or proximal to, the Presqu'ile barrier which is a reef-like complex (200 m at its thickest point) that separates the deep marine rocks to the north from the shallow marine rocks to the south (Rhodes et al., 1984; Hannigan, 2007). The Presqu'ile barrier consists of the Upper Keg River and Sulphur Point formations. The Upper Keg River Formation includes the lower two-thirds of the barrier and consists of flat, lensoidal beds of carbonate sandstones and mudstones and fine, dense, grey-brown to buff brown dolomite with abundant carbonaceous fossils (Skall, 1975; Hannigan, 2007). The overlying Sulphur Point Formation consists of a build-up of bioherms, bioclastic limestones and carbonate sandstones (Rhodes et al., 1984; Hannigan, 2007) and has undergone alteration into a coarse crystalline, vuggy dolomite known as Presqu'ile dolomite which is the host of the majority of the ore bodies (Skall, 1975; Hannigan, 2007). Karstification was the primary control for ore deposition in the area (Rhodes et al., 1984; Hannigan, 2007).

2.5   Methods

Initial interpretation of surficial geology was made on 1:25000 scale airphotos (Natural Resources Canada, flight lines A23440-2 to 16, A23368-79 to 88, A23371-52 to 67, A23372-130 to 146, A23373-44 to 59, A23373-170 to 187, and A23374-219 to 233). These areas were then field-checked with till sampling locations, mapping verification sites and at natural and anthropogenic exposures. Access to the northern section of the map-sheet was greatly restricted by extensive fens and wetlands. A total of 133 field stations were recorded and the data from these sites are available in Appendix A2. The final station density across the map-area (excluding Great Slave Lake) was approximately 1 station

23

per 4 km^2. At each station, a hole was dug or a Dutch Auger was inserted to a depth of at least 1 m. A description of the unit(s) present was recorded and photos were taken (Oviatt et al., in press). The final map was produced at a scale of 1:50,000 (Appendix A) and published as Canadian Geoscience Map 114 by the Geological Survey of Canada (Oviatt and Paulen, 2013).

Two sand samples were collected from a large sand dune on the southern edge of the map sheet (E: 625559, N: 6739637, NAD83). The samples were submitted to the Luminescence Dating Laboratory, University of the Fraser Valley (UFV), Abbotsford, British Columbia. The details of the methodologies behind optical dating technology can be found in Lian et al, (2002). The laboratory processes are described in Wintle (1997), Aitken (1998), Huntley and Lian (1999), and Lian and Huntley (2001). The samples were collected from the top of the sand dune (at a depth of 1.5 m from surface) and at the base (approximately 3.5 m from natural land surface). The dates of these samples were determined by exciting sand-sized K-feldspar grains with near-infrared photons. The violet photons that are emitted in response to this excitation are measured. Corrections for environment and anomalous fading are applied before calculation of dates (Wolfe et al., 2004).

2.6   Surficial Geology

The map units in the 85B/15 area are as follows: Bedrock (R), Glacial sediments (T, Tb), Glaciolacustrine sediments (GL, GLr, Gln), Lacustrine sediments (L, Lr, Ln), Alluvial sediments (A, Ap, Af, At), Eolian sediments (E, Er), Organic deposits (O, Owf, Owb), Colluvium (C), and Anthropogenic deposits (H). The most extensive units in the map area are glaciolacustrine sediments deposited by glacial Lake McConnell.

Bedrock (map unit R):

Dolomitized limestone bedrock occurs at the surface at the bottom of a stream bed in the center of the map sheet.

24

Glacial Sediments (map units T, Tv, Tb):

Glacial sediments (till) occur as blanket deposits (Tb) in small patches at slightly higher elevations. These units are typically capped by a boulder or cobble lag produced by glacial Lake McConnell. Glacial sediments (Fig. 2-3) cover approximately 2 % of the surficial map area and typically occur within ridged beach sediment units. The upper contact between till and organic units was usually marked by a thin sand or gravel layer. The upper contact between till and beach ridges were gradational with the silt and clay content of well-sorted sand and gravel increasing towards the contact. Till veneer (generally <2 m thick) occurs in close proximity to the small area of bedrock outcrop, mentioned above. The till at the surface is an unsorted glacial diamicton, with a 10-15 % clast content of mixed lithologies and contains an average of 8 % inorganic carbon and

Fig. 2-3: Sandy-silt till showing fissility. This photo was taken at 1 m depth from the natural land surface.

0.3 % organic carbon (data available in Appendicies B1-3). Till at the surface has a sandy-silt matrix containing an average of 14 % clay, 50 % silt and 36 % sand with an olive-brown color when freshly exposed. Till in the area is predominately light-grey in colour when dry (Table 2-1). Some sandier, light-brown tills were observed.

Joints within fissile till were occasionally iron and manganese stained. Precambrian shield and Paleozoic carbonate clasts were the dominant lithologies in till (Rice et al., 2013) and were generally subrounded to subangular. Clasts

Colour	# of till samples
10YR	50
2.5YR	52
5Y	1

Table 2-1: Munsell colour distribution of till samples. These samples were dry when analyzed.

within the till were usually faceted and striated and ranged in size from granules to large boulders (> 1 m).

Glaciolacustrine Sediments (map units GL, GLr, Gln):

Glaciolacustrine deposits are mapped as beach sediments (GLr), nearshore and littoral deposits (GLn) and undifferentiated (GL). Beach sediments (Fig. 2-4a) occur as ridges throughout the map sheet. Well-developed beach ridges within the 85B/15 map area occur at 190 m and 220 m a.s.l. Beach ridges are characterized by well-sorted, medium grained sand ranging in thickness from 15 cm to over 2 m with a boulder lag. A typical beach ridge consists of: (1) cobble lag, (2) 10-15 cm sand and gravel, (3) ~ 15 cm coarse sand and, (4) and over 40 cm of coarse sand with silt and clay. These ridges contain fragments of clasts that originated on the Canadian Shield indicating that these beaches are remnants of re-worked till. They commonly overlie unmodified till (Fig. 2-4b). Beach sediments cover approximately 40% of the map area and occur in ridges that are sub-parallel to the current shoreline of Great Slave Lake.

Fig. 2-4: (A) Typical example of well-sorted sand occurring within glaciolacustrine beach ridges. The small pink granules were typically Canadian Shield clasts, and (B) photo looking to the southeast of a glaciolacustrine beach ridge overlying till.

Fig. 2-5: Annotated aerial photograph of glacial Lake McConnell beach ridges common throughout the map area (aerial photograph A23373-62, scale 1:25000).

Fig. 2-6: Beach ridge of coarse sand and gravel with a cobble lag that is typical for nearshore and littoral sediments in the Pine Point area.

28

Nearshore and littoral deposits usually occur in close proximity to beach ridges (Fig. 2-5). These deposits are characterized by moderately-sorted open framework sand and gravel that is commonly overlain by a cobble lag (Fig. 2-6). Nearshore and littoral deposits are typically 70 cm to >1 m thick and cover approximately 10 % of the map sheet. Glaciolacustrine deposits are composed mainly of silt and clay and range from 0.1 to 1.2 m in the 85B/15 area. The upper contacts of these deposits were occasionally marked with interbeds of fine sand with silt and clay. These deposits (GL) occur at an elevation of approximately 200 to 215 m a.s.l and cover approximately 5 % of the map sheet.

Lacustrine Sediments (map units L, Lr, Ln):

Lacustrine sediments occur exclusively along the shores of present day Great Slave Lake. Beach sediments (Lr) consist of fine to coarse and gravel. These sediments form ridges along 1 to 1.5 m high. Littoral and nearshore sediments (Ln) occur as fine sand to pebble material with a well-sorted cobble lag. These units occur at elevations between 150 and 160 m a.s.l.

Alluvium Deposits (map units A, Ap, At, and Af):

Alluvium deposits occur along all rivers in the area particularly along the present day Buffalo River. Floodplain (Ap) deposits are described as sorted gravel, sand and silt that occur close to river level forming active floodplains associated with the Buffalo River. Alluvial terrace (At) deposits occur along the banks of the Buffalo River and consist mainly of sand and gravel. Alluvial fan (Af) deposits are poorly sorted sand and gravel and are associated with small creeks and streams that are scattered throughout the map sheet.

Eolian Deposits (map units E, Er):

Eolian deposits occur throughout the map sheet as large (10 m) parabolic dunes (Fig. 2-7A) and as smaller (1-2 m) longitudinal dunes. These dunes are likely produced by the reworking of the beach deposits left by glacial Lake

McConnell. The parabolic dunes are composed of medium to fine-grained sand that contain planar laminations and are rhythmetically bedded. The corrected OSL dates for the sand samples collected at a dune on the south edge of the map sheet were determined to be 11.1 ± 1.1 ka and 10.5 ± 0.9 ka, respectively. These ages were determined by single aliquot regeneration protocol described in Lian et al., (2002).

Organic Deposits (O, Owf, Owb):

Organic deposits are extensive throughout the region. They consist of bogs (Owb) and poorly drained fens (Owf). Bogs are characterized by the presence of black spruce trees and extensive sphagnum moss. Fens are composed of sparsely-treed peatland with numerous ponds. These ponds are often in-filled features associated with thermokarst terrain. Both of these deposits can be locally underlain by shallow permafrost or ground ice. Bogs and fens commonly overlie poorly-drained glacial till or glaciolacustrine sediments and occupy 30 % of the surficial map area. Organic deposits were greater than 2m thick in some places.

Colluvium Deposits (map unit C):

Colluvium deposits consist of deposits created by mass movement of debris along the incised river valley of the Buffalo River. They are characterized by poorly-sorted material that is reflective of the units above the valley.

Anthropogenic Deposits (map unit H):

Anthropogenic deposits occur as mine waste piles, settling ponds and reworked overburden associated with the Pine Point mine operation (1964-1988). There are 17 open pits in the map sheet each with an associated mine waste pile that can exceed 20 m high providing the most extensive topographic relief in the area (Fig. 2-7B).

Fig. 2-7: (A) Parabolic sand dune located on the southern margin of the mapsheet, and (B) Photo looking to the northeast of waste piles from deposits R61 and T58. These wastepiles create the strongest topographic relief in the region
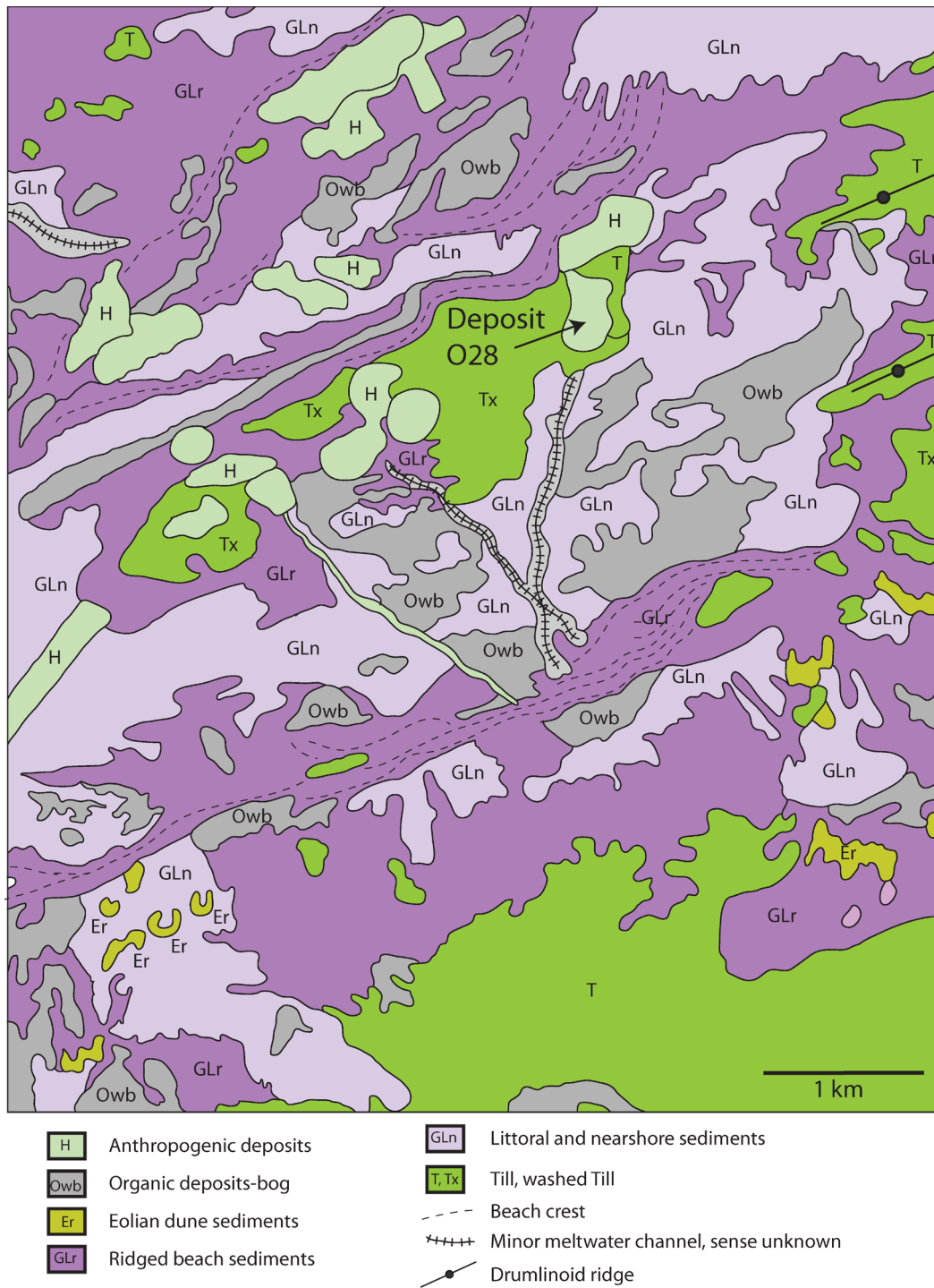
Fig. 2-8: Surficial geology of deposit O28 area. Descriptions of units are available on Canadian Geoscience Map 114 (Oviatt and Paulen, 2013).

32

2.7   Deposit O28

A local-scale map was produced for the deposit O28 area (Fig. 2-8). The construction of the map was completed by interpretation of 1:25,000 aerial photographs (A26302 122-124). The majority of ground control was conducted on the west side of deposit O28 and the final sampling density in the area is 2 sites/km². Three till units were visible on the eastern edge of deposit O28 (Fig. 2-9). The uppermost till (11-MPB-057) has 4 % more clay and less sand than the other two samples in the section (Table 2-2). This unit contains 10% clasts that were observed to be subrounded in nature.

Till occurs at the surface over approximately 15% of the map area. The most significant difference between the deposit O28 area and 85B/15 are the large quantities of till surrounding the deposit O28 area. The southern portion of this map area is covered with a till blanket approximately 6 m thick based on observations of other till units in the area. There are two flutings observed in till units on the eastern margin of the map. These flutings are oriented at
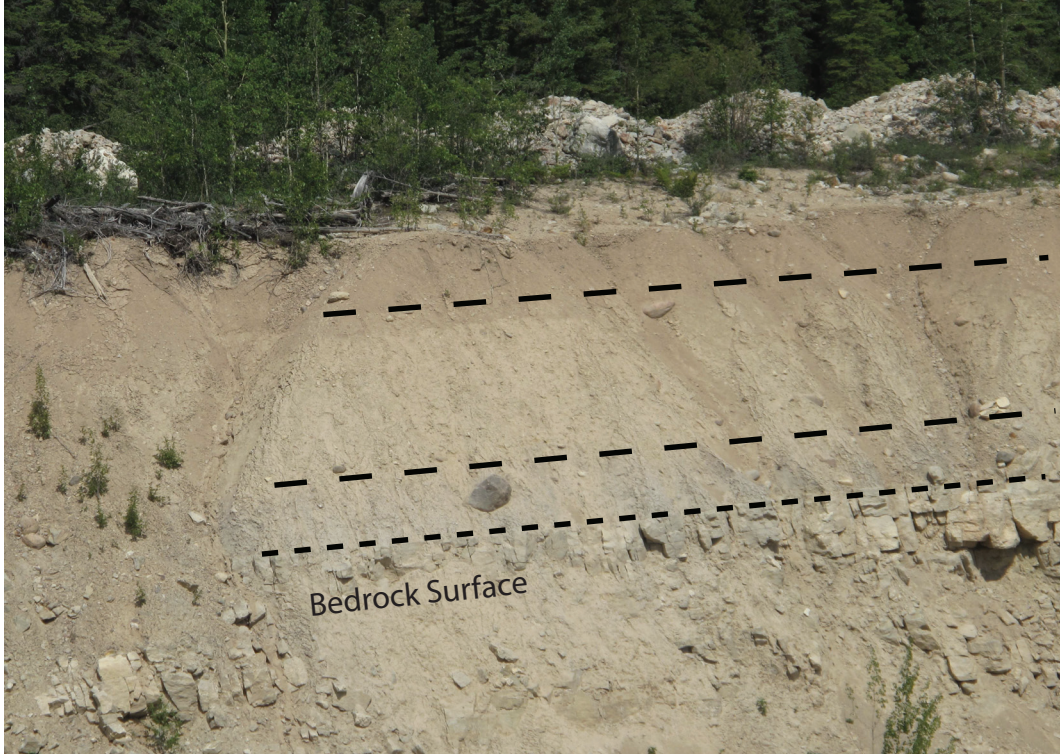
Fig. 2-9: Photo looking towards the northeast wall of deposit O28. Three visually distinctive till units can be seen.

approximately 250°.

Glaciolacustrine beach sediments occur as ridges that have a northeast-southwest trend. These sediments cover approximately 35 % of the map area. Littoral and near-shore sediments deposited by glacial Lake McConnell cover

Sample No.	wt. % Sand-Silt-Clay of <2mm		
	% Sand	% Silt (63-4um)	% Clay (<4um)
11-MPB-055	36.027	41.608	22.365
11-MPB-056	35.933	41.003	23.064
11-MPB-057	31.789	40.917	27.293

Table 2-2: Grain size distribution for 3 till samples on the east wall of deposit O28.

approximately 20 % of the map area. These deposits fill lows between beach ridges.

There is a small dune field of eolian sediments in the southwest corner of the map that consists mainly of parabolic dunes. The eastern margin of the map area contains approximately 3 longitudinal dunes. Eolian sediments cover 5 % of the surficial map area.

Organic deposits cover approximately 15 % of the map area and have similar characteristics to those deposits in 85B/15. Anthropogenic deposits in this area occur as 7 historic open pit mine sites and their associated waste-piles. They cover approximately 10 % of the map area.

2.8   Discussion

The distribution of glacial sediments and subsequent anthropogenic deposits from mining practices are shown on Canadian Geoscience Map 114 (Oviatt and Paulen, 2013). Glaciolacustrine sediments cover the majority of the map area and the nature of these deposits are similar to those documented by Lemmen (1990). The majority of beach ridges occur at elevations of 220 and 190 m a.s.l, which is approximately 50 m lower than the highest reported beach ridge in the area (275 m a.s.l, Craig, 1965; Lemmen, 1990). This beach ridge recorded by Craig (1965) and Lemmen (1990) is located approximately 80 km west and 50

34

km south of the map area. It is likely that these two well-developed beach ridges reflect two minor periods of static lake levels during the history of glacial Lake McConnell.

Lacustrine sediments occur in close proximity to the present day shore of Great Slave Lake. They were observed to occur at elevations between 150 and 160 m a.s.l. which are in agreement with the reported Holocene lake level of 156 m a.s.l at the Slave River delta (Vanderburg and Smith, 1988).

A sand dune located approximately 75 km (Sandy Lake) south of the Pine Point area exhibited similar features (Wolfe et al., 2004) to those observed in the map area. The Sandy Lake dune field has an OSL date of 10.5 ± 0.5 ka (Wolfe et al., 2004). The two OSL dates (11.1 ± 1.1 ka and 10.5 ± 0.9 ka) for the sand samples that were collected from a large dune in the map area are consistent with the Sandy Lake dune field.

The distribution of the surficial materials in the 1:50 000 85B/15 (Breynat Point) map area are consistent with the distribution of sediments for the area as published at a larger scale (1:250 000; Lemmen, 1998 a, b). The detail provided by this smaller scale map is a useful tool for planning drilling programs as well as infrastructure for exploration in the area.

The three visually distinctive till units in the eastern wall of deposit O28 are approximately 6 m thick. The nearby bedrock benches are striated with later phases of ice flow, parallel to the streamlined landforms mapped at surface. Thus, the visually distinguishable till units could possibly correlate to other distinct tills observed in other pits, either preserved from subsequent subglacial erosion and overprinting or the visual differences as well as the slight differences in grain sizes between these three tills could indicate a different and/or weathered bedrock sources and, with abundant sediment supply, were deposited as layered till stratigraphy (cf., Trommelen et al., 2012). A study conducted on a thick till section located in the 85B/15 map sheet was able to indentify 4 distinct till units that they were able to correlate with the three ice flow directions in the region (Rice et al., 2013). Till distinction was identified by comparing/contrasting

35

pebble lithologies, measuring clast fabrics, conducting grain and geochemical analysis as well as documenting any visual differences within the four units. These methods could be applied to the small till section on the eastern wall of deposit O28 to determine the relationship between these tills and the erosional record. This correlation may be difficult to determine as till cover in this area is thin (~5 m) compared to the study conducted on the 85B/15 mapsheet (~22 m) and sediments deposited by earlier ice flows may have been eroded or reworked by subsequent ice flows.

Further consideration could be applied to correlating tills exposed in other open pits across the mine property as well as on a more regional scale by detailed examination of till sections from along the Buffalo and Hay rivers. Additional correlations may be possible by comparison of basic sedimentological properties of each till unit to the tills documented in the siesmic shotholes to the west (Smith, 2011).

2.9　References

Aitken, M.J., 1998. An introduction to Optical dating. Oxford University Press, Oxford, 267 p.

Bostock, H.S., 1970. Physiographic regions of Canada. Geological Survey of Canada, Map 1254A, scale 1:5,000,000.

Craig, B.G., 1965. Glacial Lake McConnell, and the surficial geology of parts of Slave River and Redstone River map-areas, District of Mackenzie. Geological Survey of Canada Bulletin 122, p. 1-33.

Dyke, A.S. 2004. An outline of North American deglaciation with emphasis on central and northern Canada. *In*: J. Ehlers and P.L. Gibbard (eds.), Quaternary Glaciations - Extent and Chronology, Part II. North America. Elsevier B.V., Amsterdam, Development in Quaternary Science Series, Vol. 2: 373-424.

Dyke, A.S., and Dredge, L.A., 1989. Quaternary geology of the northwestern Canadian Shield. *In*: Fulton, R.J., (ed) Quaternary Geology of Canada and Greenland, Geological Survey of Canada, Geology of Canada, no. 1, p. 189-214.

Dyke, A.S., and Prest, V.K., 1987. Late Wisconsin and Holocene history of the Laurentide Ice Sheet. Geographie physique et Quaternaire, v. 41, p. 237-263.

Dyke, A.S., Andrews, J.T., Clark, P.U., England, J.H., Miller, G.H., Shaw, J. and Veillette, J.J. 2002. The Laurentide and Innuitian ice sheets during the Last Glacial Maximum. Quaternary Science Reviews, 21: 9-31.

Hannigan, P., 2007. Metallogeny of the Pine Point Mississippi Valley-Type zinc-lead district, southern Northwest Territories. *In:* Goodfellow, W.D. (ed) *Mineral Deposits of Canada: A Synthesis of Major Deposit-Types, District Metallogeny, the Evolution of Geological Provinces, and Exploration Methods*. Geological Association of Canada, Mineral Deposits Division, Special Publication No. 5, p. 609-632.

Holroyd, R.W., Hodson, T.W., and Carter, K.M., 1988. Unpublished termination report, Pine Point Mines Ltd., June 28, 1988.

Huntley, D.J., and Lian, O.B., 1999. Using optical dating to determine when a mineral grain was last exposed to sunlight. *In:* Lemmen, D.S., and Vance, R.E., (eds) *Holocene Climate and Environmental Change in the Palliser Triangle: A Geoscientific Context for Evaluating the Impacts of Climate Change on the Southern Canadian Prairies.* Geological Survey of Canada, Bulletin 534, p. 211-222.

Jackson, L.E., Jr., Phillips, F.M. and Little, E.C. 1999. Cosmogenic [36]Cl dating of the maximum limit of the Laurentide Ice Sheet in southwestern Alberta. Canadian

Journal of Earth Sciences, 36: 1347-1356.

Kyle, J.R., 1977. Development of sulphide hosting structures and mineralization, Pine Point, Northwest Territories. Ph.D. thesis, University of Western Ontario, 226 p.

Lemmen, D.S., 1990. Surficial materials associated with glacial Lake McConnell, southern District of Mackenzie. *In:* Current Research, Part D, Geological Survey of Canada, Paper 90-1D, p. 79-83.

Lemmen, D.S., 1998a. Surficial geology, Klewi River, District of Mackenzie; Northwest Territories. Geological Survey of Canada, "A" Series Map, 1905, scale 1:250 000.

Lemmen, D.S., 1998b. Surficial geology, Buffalo Lake, District of Mackenzie; Northwest Territories. Geological Survey of Canada, "A" Series Map, 1906, scale 1:250 000.

Lemmen, D.S., Duk-Rodkin, A., and Bednarski, J.M., 1994. Late glacial drainage systems along the northwestern margin of the Laurentide Ice Sheet. Quaternary Science Reviews, v. 13, p. 805-828.

Lian, O.B., and Huntley, D.J., 2001. Luminescence dating. *In:* Last, W.M., and Smol, J.P. (eds) *Tracking environmental change using lake sediments, v. 1: Basin analysis, coring, and chronological techniques*, p. 261-282.

Lian, O.B., Huntley, D.J., and Wolfe, S.A., 2002. Optical dating of eaolian dune sand from the Canadian prairies. Geographie physique et Quaternaire, v. 56, p. 191-202.

Oviatt, N.M. and Paulen, R.C. 2013. Surficial geology, Breynat Point, NTS 85-B/15, Northwest Territories. Geological Survey of Canada, Canadian Geoscience Map 114 (preliminary), scale 1:50,000.

Oviatt, N.M., Paulen, R.C. and Rufiange, E.C. In press. Surficial geology field observations and photographs for the Breynat Point map area (NTS 85B/15), Northwest Territories. Geological Survey of Canada, Open File.

Rhodes, D., Lantos, E.A., Lantos, J.A., Webb, R.J., Owens, D.C., 1984. Pine Point orebodies and their relationship to the stratigraphy, structure, dolomitization, and karstification of the middle Devonian Barrier complex. Economic Geology, v. 79, p. 991-1055.

Rice, J.M., Paulen, R.C., Menzies, J.M., McClenaghan, M.B. and Oviatt, N.M., 2013. Glacial stratigraphy of the Pine Point Pb-Zn mine site, Northwest Territories. Geological Survey of Canada, Current Research Paper 2013-5, 17 p.

Skall, H., 1975. The paleoenvironment of the Pine Point lead-zinc district. Economic Geology, v. 70, p. 22-47.

Smith, D.G. 1994. Glacial Lake McConnell: paleogeography, age, duration and associated river deltas, Mackenzie River basin, western Canada. Quaternary Science Reviews, v. 13, p. 829-843.

Smith, I.R., 2011. The seismic shothole drillers' log database and GIS for Northwest Territories and norther Yukon: an archive of near-surface lithostratigraphic surficial and bedrock geology data. Geological Survey of Canada Open File 6833, 1 DVD, doi:10.4095/288754.

Trommelen, M.S., Ross, M., and Campbell, J.E., 2012. Inherited clast dispersal patterns: Implications for palaeoglaciology of the SE Keewatin Sector of the Laurentide Ice Sheet. Boreas, 10.1111/j.1502-3885.2012.00308.

Vanderburg, S. and Smith, D.G., 1988. Slave River delta: geomorphology, sedimentology, and Holocene reconstruction. Canadian Journal of Earth Sciences, v. 25 p. 1990-2004.

Wintle, A.G., 1997. Luminescene dating: Laboratory procedures and protocols. Radiation measurements, v. 27, p. 769-817.

Wolfe, S.A., Huntley, D.J., and Ollerhead, J., 2004. Relict late Wisconsinan dune fields of the northern Great Plains, Canada. Geographie physique et Quaternaire, v. 58, p. 323-336.

Chapter 3

3.1   Introduction

During the extensive history of Canada's repeated glaciations, most of the landscape was covered with ice. As a result glacial deposits cover much of Canada's surface and present significant hurdles for exploration companies in these terrains. Therefore, an understanding of glacial deposits and geomorphology is necessary to execute a successful exploration project. Indicator mineral and till geochemical methods have proven to be successful exploration tools in glaciated terrain (e.g. Dreimanis, 1960; Shilts, 1996; McClenaghan, 2005) however, there are few published studies using these methodologies for base metal exploration, particularly for the carbonate hosted Pb and Zn deposits known as Mississippi Valley-type (MVT) deposits.

The Pine point district in the Northwest Territories, Canada is a reasonably well- characterized MVT system. It was mined between 1964 and 1988 and produced 70.8 Mt of ore (Holroyd et al., 1988). The ore mineralogy and the Pb and S isotopic compositions of the ore phases have been previously studied (e.g. Sasaki and Krouse, 1969; Kyle, 1977; 1981) and some of the individual deposits subcropped and were exposed to glacial erosion. The purpose of this study, therefore, was to constrain the till geochemical signature and the nature of the indicator minerals associated with a single Pb-Zn deposit (O28) in the Pine Point MVT district. The aims of this project were; 1) to conduct the first comparison of Pb and S isotopic signatures of individual galena and sphalerite grains in a MVT deposit and till immediately down ice; 2) to document the indicator minerals of MVT deposits that can be recovered from till and 3) to compare the indicator mineral signatures of a MVT deposit to the till geochemical signatures associated with the same deposit.

The primary objective was to help improve exploration for MVT deposits in glaciated terrains by documenting and characterizing the ore minerals in till.

3.2   Location and physiography

The Pine Point MVT district is located approximately 180 km south of Yellowknife on the south shore of Great Slave Lake (Fig. 3-1), Northwest Territories. The district lies in the Great Slave Plain physiographic region of the Western Interior Plains (Bostock, 1970). The region is relatively flat with local relief not exceeding 15 m (Lemmen et al., 1994). Black spruce bogs are the most prominent vegetation in the area. Access to the historic mine site and open pits can be accessed via Highways 5 and 6 and mine roads by truck or all-terrain vehicle in the summer.
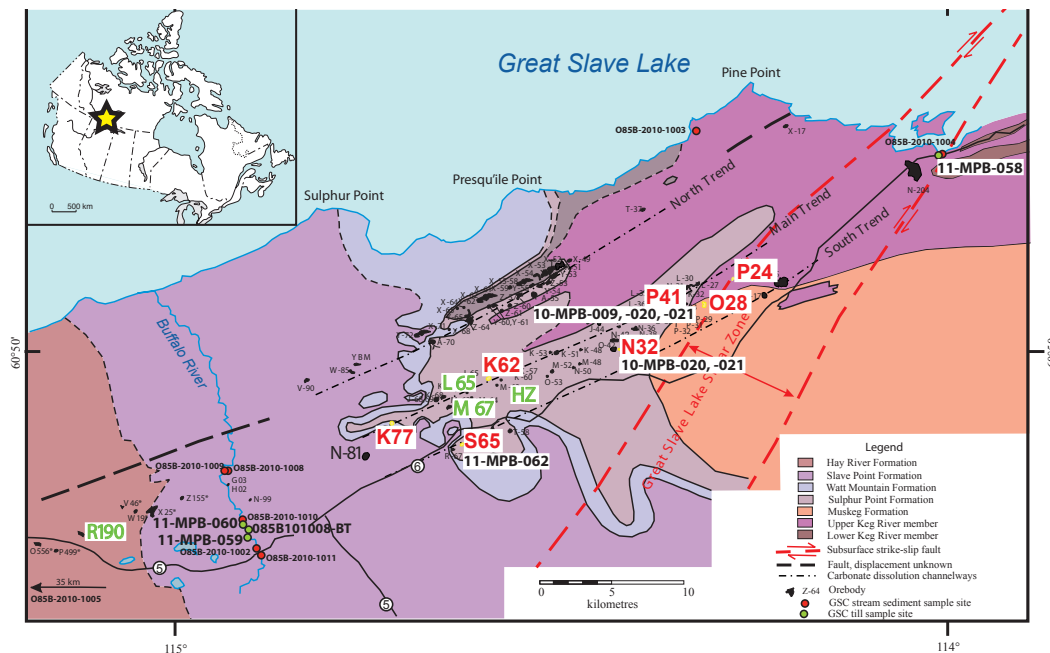
Fig. 3-1: Location map of study area (modified from Hannigan, 2007). Deposits in red are locations of regional till samples, green are locations of bedrock samples. A detailed study was conducted on deposit O28.

3.3   Regional geology

The Pine Point district is located near the erosional edge of the Western Canadian Sedimentary Basin (WCSB) and the Canadian Shield. The underlying crystalline basement is considered to be of Archean and Proterozoic age (Skall, 1975; Kyle, 1981; Rhodes et al., 1984; Okulitch, 2006; Hannigan, 2007). The Great Slave Shear Zone (GSSZ) is considered to be a boundary between the

Churchill and Slave cratonic provinces (Morrow et al., 2006) that extends for approximately 700 km from Northwest Territories into northeastern British Columbia (Eaton and Hope, 2003). The GSSZ occurs as a span of highly deformed and sheared rocks that are bounded by large-scale lateral strike slip faults (Eaton and Hope, 2003).

The orebodies are concentrated within 3 NE-SW trending zones referred to as the North trend, Main trend and South trend (Fig. 3-1). The McDonald Fault, a component of the GSSZ, cuts through the basement rocks immediately below and sub-parallel to these three trends (Skall, 1975; Kyle, 1981; Pana, 2006). It has been interpreted that tectonic activity associated with the McDonald fault may have created these trends (Pana, 2006).

Mineralization is hosted in Givetian age rocks of the Middle Devonian, specifically, the Keg River, Pine Point, Sulphur Point, and Watt Mountain Formations (Fig. 3-2). The Muskeg Formation, to the south of the district, occurs coevally with the Pine Point Formation. The bedrock geology of the Pine Point area is described in great detail by Skall (1975) and Rhodes et al., (1984).

3.4   Pine Point MVT district

Individual orebodies in the Pine Point district range from 100,000 to 17.5 million tonnes and have an average grade of 2% Pb and 6.2% Zn (Hannigan, 2007). The ore field consists of 100 drill-defined orebodies (Hannigan, 2007) that are dispersed over an area of approximately 1600 km^2. The total geological resource (produced and remaining proven resource) is estimated to be 95.4 Mt (Hannigan, 2007).

The majority of known deposits in the district occur within the Presqu'ile barrier which is a coarsely dolomitized reef-like complex (Rhodes et al., 1984; Hannigan, 2007). The lower two thirds of the Presqu'ile barrier are composed Upper Keg River Formation. The Sulphur Point Formation comprises the upper third of the barrier.

Ore deposits at Pine Point are classified as either tabular or prismatic

Slave Point Formation: The Slave Point Formation conformably overlies the Watt Mountain Formation and can be divided into four distinct members. These members are composed of sediments associated with tidal flat, shallow platform and deep platform environments. The Amco shale is a 3.1 m thick, blue-grey argillaceous limestone. Detailed descriptions of the Fort Vermilion, Caribou, and Needle Lake members can be found in Skall, 1975.

Watt Mountain Formation: The Watt Mountain Formation is regionally extensive as it extends north of the barrier complex as well as to the south where it disconformably overlies the Sulphur Point Formation (Rhodes et al., 1984; Lantos, 1983). This formation is 30 m thick to the north of the barrier complex and thins to approximately 10 m overlying the barrier (Lantos, 1983).

Windy Point Formation: The Windy Point Formation is a thin wedge of carbonates that conformably overlies the Buffalo River Formation. This unit thickens from 20 m on the south shore of Great Slave Lake to 50 m on the west shore (Rhodes et al., 1984).

Buffalo River Formation: The Buffalo River Formation is a green-grey shale that thickens to 60 m to the north of the barrier complex. This formation comformably overlies the Pine Point Formation to the north of the barrier complex and disconformably overlies the Sulphur Point Formation to the south of the barrier complex (Skall, 1975; Rhodes et al., 1984).

Muskeg Formation: Grey to buff-grey, fine, dense dolomites intercalated with gypsum and anhydrite beds are the main characteristics of the Muskeg Formation. This unit is time equivalent to the Pine Point formation with some overlap of the Sulphur Point Formation. The contact between the Muskeg and Sulphur Point Formations is gradual with beds of the former extending northward into the Sulphur Point Formation (Rhodes et al., 1984). This formation has a maximum thickness of 150 m south of the barrier complex to essentially 0 m overlying the barrier complex.

Sulphur Point Formation: The Sulphur Point formation is composed of light cream to white limestones that are visually distinctive from the dolomites of the Keg River and Pine Point Formations. These limestones have been dolomitized to form the coarse crystalline saddle dolomite referred to as Presqu'ile dolomite. This formation conformably overlies the Pine Point formation in the vicinity of the barrier complex and overlies the Muskeg Formation (described below) to the south of the barrier. This unit is 65 m thick over the barrier complex and thins to approximately 9 m in the south.

Pine Point Formation: The Pine Point formation conformably overlies the Keg River formation and consists mainly of dolomitized limestones with varying amounts of argillaceous material. Skall (1975) divided this unit into two distinct facies based on the concentration of argillaceous material. Dolomitized limestones are mainly sucrosic and vary in colour depending on the amount of impurities such as bitumen and clay particles. The Pine Point formation is approximately 175 m thick and contains a unit called the B-spongy Member at its base (Rhodes et al., 1984). This member is composed of floatstones containing stromatoporids, corals and brachiopods and is regionally extensive to the south into the Elk Point basin.

Keg River Formation: The Keg River formation is a laterally continuous and regionally extensive unit. This formation is composed of grey-brown to buff-brown, fine-grained, sucrosic dolomite. Argillaceous and carbonaceous wisps are common throughout unit (Skall, 1975). The Keg River formation maintains a constant thickness of approximately 65 m (± 10 m) over the Pine Point mine area thickening up to 90 m to the south. Approximately 50 m above the base of this dolomite are 1 to 3 fossiliferous shale marker beds (E-marker shales, Campbell, 1966). These shale marker beds provide a great time-stratigraphic unit for the area as most drillholes in the Pine Point area were drilled until they reached these marker beds (Rhodes et al., 1984).

Fig. 3-2: Stratigraphic column of units associated with Pine Point mineralization (modified from Hannigan, 2007).

43

(Kyle, 1981; Rhodes et al., 1984). Prismatic orebodies are characteristic of the upper barrier while tabular orebodies occur mainly in the lower barrier (Skall, 1975; Kyle, 1981). Deposit O28, which is the focus of this paper, is a tabular ore body that contained an average grade of 2.0 % Pb and 3.7 % Zn. From 1971 to 1975 a total of 1.6 Mt was mined from this deposit (Holroyd et al., 1988).

3.5   Paragenesis

There are eight major paragenetic stages that occur either pre-, syn- or post-ore identified for Pine Point (Krebs and Macqueen, 1984). Prior to mineralization carbonate host rocks are typically subjected to two dolomitizing events (Paradis et al., 2007). The original limestone is usually first replaced by the fine-grained dolomite that is subsequently replaced by a medium to coarse-grained dolomite (Paradis et al., 2007). These dolomitizing events create the secondary porosity in the form of vugs and caverns that is conducive to MVT mineralization (Rhodes et al., 1984; Qing and Mountjoy, 1994). Sulphide minerals associated with the deposits include galena and sphalerite with minor pyrite (Skall, 1975; Kyle, 1981; Hannigan, 2007). Brecciated ores, laminated (alternating with sulphides) sediments and cross-cutting dolomites are evidence for solution collapse and internal filling of sediments that occurred during mineralization (Krebs and Macqueen, 1984). Coarse-grained calcite, native sulphur and bitumen filled the remaining pore-space post mineralization.

3.6   Genetic models

There have been several models presented for MVT genesis (e.g. Jackson and Beales, 1967; Cathles and Smith, 1983; Garven and Freeze, 1984; Morrow et al., 1990; among others). Recent work suggests there were four different fluids responsible for mineralization at Pine Point (Gleeson and Gromek, 2006; Gleeson and Turner, 2007; Gromek et al., 2012) and that possibly some of these fluids were derived from the basement and focused along faults associated with the GSSZ (Morrow et al., 2006; Pana, 2006; Gromek et al., 2012). Mineralization occurs where the metal-bearing fluids mix with sulfide-rich fluids (Adams et al.,

2000; Gleeson and Turner, 2007).

3.7 Surficial geology

The Keewatin sector of the Laurentide Ice Sheet (LIS) is the source of glacial sediments in the region (Dyke and Prest, 1987; Lemmen, 1990; Dyke, 2004). These sediments overlie relatively flat bedrock topography resulting in low-relief geomorphology that is characteristic of the Pine Point area.

Glacial sediments (till) increase in thickness from east to west across the district. Historic drill hole data indicates that till is locally thicker in karst collapse features (Lemmen, 1990). Till at the surface in the area has a silt to fine sand matrix with very little clay (Lemmen, 1998b). Four visually distinctive till units have been identified in the area (Rice et al., in press). It was suggested that these till units likely record variations in the western margin of the LIS rather than separate glacial events (Rice et al., in press).

The landscape surrounding the Pine Point mine site has glacially streamlined features such as flutings that mostly reflect the last ice flow trajectory (Lemmen, 1990).

The Pine Point region was deglaciated between 10.0 and 9.6 ^{14}C ka BP (Dyke, 2004) and was inundated by glacial Lake McConnell (Smith, 1994). Most of the till surfaces are winnowed, and there was extensive reworking of the till into glaciolacustrine littoral sediments over much of the area (Lemmen, 1990). Glaciolacustrine deposits occur as shorelines and beach ridges, some of which have been reworked into eolian dunes. At approximately 7.8 ^{14}C ka BP, it was speculated that basin uplift in the region had restored Great Slave Lake to its current position (Dyke and Prest, 1987; Dyke, 2004).

3.8 Glacial Lake McConnell

Glacial Lake McConnell, one of the largest glacial lakes to exist in Canada (Lemmen et al., 1994), occupied the basins of Great Bear, Great Slave and Athabasca Lakes. The lake existed in three stages known as the Hare Indian Phase, the Great Bear phase and the Mackenzie phase from 11.8 to 8.3 ka bp

(Smith, 1994). The Pine Point region was covered by glaciolacustrine sediments in the form of beach ridges and littoral and near shore sediments that were likely deposited by the Mackenzie phase, which was the most extensive and directly affected the region. The highest beach ridges (295 a.s.l.) in the Pine Point area occur south of Hay River near Enterprise (Craig, 1965).

3.9   Methods
3.9.1   Field methods

Following a reconnaissance of 30 open pits at the former Pine Point mine, a total of 96 till and 76 bedrock samples were collected over the course of two field seasons (2010 and 2011). Striation measurements were recorded at 12 sites throughout the region. Approximately 18-22 kg of till was collected for heavy mineral analysis and 3 kg for till matrix geochemistry. The majority of the till samples (n= 83) were collected in the vicinity of deposit O28 on the east side of the property (Fig. 3-3). Deposit O28 was chosen for detailed till sampling because: a) mineralization sub-cropped giving glaciers access to mineralized bedrock, b) detailed ice flow information was preserved on the pit shoulder in the form of striated outcrops, c) till was of moderate thickness (~6m) which provided the opportunity to sample vertical sections, d) the land surface was relatively undisturbed for sampling both up and down ice, e) no known sub-cropping ore bodies occurred directly up-ice (east) of deposit O-28, and f) it was one of the few pits in the region where till is exposed at surface that was not extensively reworked by glacial Lake McConnell.

To document the dispersal of pathfinder elements and indicator minerals in the vicinity of a known orebody (O28), till samples were collected up-ice, overlying and down-ice of the ore zone. These samples were collected with respect to sub-cropping mineralization and taking into account possible dispersal from all 3 ice flow trajectories. Up-ice till samples were collected on the east side of the ore zone as well as at Paulette Creek (~15 km east of the eastern most deposit) to establish background concentrations.

Additional till samples were collected in 2011 to complement the results

obtained from the samples collected in 2010. In order to determine any vertical variations in the till, samples were collected from excavated pits at 1, 2, and 3 m depth from the natural land surface. Four sections were also sampled from the upper west wall of deposit O28 in this manner (A-D in Fig. 3-3).

Regional till samples (Fig. 3-1) were collected from deposits N32 (10-MPB-020, -021), P41 (10-MPB-009, -017 and -018), K62 (11-PTA-037, -042), S65 (11-MPB-062), and K77 (11-MPB-061). These samples were collected to document any differences in till matrix geochemistry as well as size and morphology of the indicator minerals from different deposits. To establish regional down-ice concentrations of indicator minerals and pathfinder elements, 3 till samples were collected along the banks of the Buffalo River (11-MPB-059, -060, 085B101008BT; Fig. 3-1).

3.9.2 Ice flow patterns

Since natural exposures of outcrop in the region are scarce, initial assessment of glacial history within the study area included the observation of the orientation of large-scale glacially streamlined landforms (flutings). Past mining activities around the open pits included the removal of overburden exposing underlying bedrock. Small-scale erosional ice-flow indicators on bedrock such as glacial striae, grooves and outcrop sculpting were observed on these exposed surfaces. Striations were measured on essentially flat outcrop surfaces and relative ages of striated surfaces were determined where possible (Fig. 3-4). Relative ages of striated surfaces were determined by evaluating their relative positions on the outcrop according to the criteria defined by Lundqvist (1990) and McMartin and Paulen (2009).

3.9.3 Bedrock sampling

A total of 77 bedrock samples were collected from five different deposits in the Pine Point district to determine the characteristics of the sulphide minerals present (Fig. 3-1). Bedrock samples were collected from newly available diamond drill core from M67, L65, HZ, and R190 and waste rock piles from O28. These

47

Fig. 3-3: Locations of samples in the O28 area (A) and surrounding the deposit (B). Samples collected in 2010 are labelled as 10-MPB-series (in black) and samples collected in 2011 are labelled as 11-MPB-series. Striation measurements are marked with arrows from the oldest (1) to the youngest (3).

48
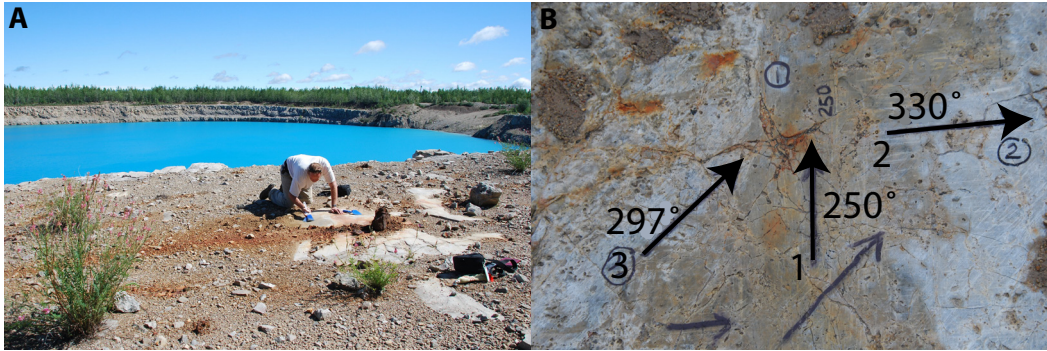
Fig. 3-4: (A) Typical striation site on bedrock outcrop cleared by mining practices, and (B) cross-cutting striations showing 3 phases of ice flow.

samples were collected based on visual inspection as well as assay data in some cases. Fifteen of these samples were sent to Overburden Drilling Management Limited (ODM), Ottawa, for recovery of the heavy mineral fraction and picking of mineral grains. An additional 47 bedrock samples were made into polished thin section (PTS) at Vancouver Petrographics, Langley for microscope observations and electron microprobe analysis (EPMA).

3.9.4 Geological Survey of Canada Sedimentology lab

Before being submitted to a commercial lab for geochemical analysis, grain size analysis was completed at the GSC Sedimentology Lab in Ottawa. The >0.063 mm size fraction was separated using a stack of wet sieves while grain sizes <0.063 mm were determined using a Lecotrac LT-100 Particle Size Analyser. Carbonate content of the till matrix was determined using the LECO Cr 412 Method. The LECO method as well as a complete account of GSC Sedimentology lab procedures are described in detail by Girard et al., (2004) and Spirito et al., (2011).

3.9.5 Indicator mineral recovery

A total of 15 bedrock samples were submitted to ODM for disaggregation and production of heavy mineral concentrate (HMC). Bedrock samples were described and logged by an ODM geologist before disaggregation in an electric pulse disaggregator. Results from bedrock HMC were normalized to 1 kg processing weight before presentation of results. Magmatic massive sulphide

indicator minerals (MMSIMs®) were recovered from the bulk 18 to 22 kg till samples. Gold grains and kimberlite indicator minerals were also examined. Results from MMSIMs® were normalized to a 10 kg processing weight prior to presentation of results. A detailed description of ODM processes for heavy mineral concentrates in till samples is available in Appendix B1.

3.9.6 Till matrix geochemical analysis

The <0.063 mm fraction of till was analyzed by ACME Analytical Laboratories in Vancouver. Base and precious metals concentrations were determined using a 30 g split that was digested in aqua regia and analyzed using ICP-MS. Major oxides and several minor elements (Ba, Ni, Sr, Zr, Y, Nb and Sc) were also determined on a 0.2 g split by lithium metaborate fusion/ICP-MS followed by nitric acid digestion. A complete data set and detailed description of analytical techniques can be found in Appendix B2 (Open File 7320).

3.9.7 Microprobe analysis

Selected sulphide minerals in polished thin section and 100 indicator mineral grains recovered from till samples were analyzed using the CAMECA SX100 and the JEOL 8900 Electron Probe Microanalyzers (EPMA). The CAMECA SX100 was operated with 20 kV accelerating voltage, 20 nA probe current with a 1 micron beam diameter. The JEOL 8900 was operated with the same conditions. Manganese, S, Zn, Fe, Pb, Ag, As, Sb, Se, Hg, Ge, and Cu were analysed. Table 3-1 provides a list of the standards used for calibration. Only analyses with total concentrations of 100 +/- 2 % were used in calculations of statistics and data plotting. Concentrations for elements that were below three standard deviations from the total background counts were not included in calculations of statistics or for plotting.

3.9.8 Isotope analysis

Sulphur isotope analysis was conducted on sphalerite grains from 16 bedrock samples and 54 grains recovered from 6 till samples at the University of

Table 3-1: Data for standards used in EPMA analysis for bedrock and till samples.

Element	Standard Name	Wt. (%)
Cd	Cd_metal	100
Ge	Ge_metal	100
Ag	AgMetal	100
Sb	Sb_metal	100
Fe	pyrite	46.55
In	In_metal	100
As	arsenopyrite	45.21
S	sphalerite	33.02
Hg	cinnabar	86.22
Mn	Mn_2O_3	69.60
Se	umangite	44.89
Pb	PbS	86.6
Zn	sphalerite	66.8
Cu	Cu_metal	100

Calgary's Isotope Science Lab. Samples were analyzed by the Continuous Flow-Isotope Ratio Mass Spectrometry (CF-EA-IRMS) method using a Carlo Erba NA 1500 elemental analyzer connected to a VG PRISM II mass spectrometer. Samples were loaded into tin cups and flash combusted on a quartz tube combustion reactor that has a temperature maintained at 1020°C. Liberated gases (SO_2, CO_2, and NO_x) are separated by a GC column then leaked into the mass spectrometer (http://www.ucalgary.ca/uofcisl/techniques). Analytical precision for these samples was ±0.3 ‰ and all raw $\delta^{34}S$ values were normalized to international reference materials (IAEA S1, IAEA S2 and IAEA S3).

Lead isotope analysis was conducted on galena grains from 9 bedrock samples as well as on 57 grains recovered from 6 till samples at the University of Alberta's Radiogenic Isotope Facility (RIF). The analysis procedure at the RIF is to first dissolve galena grains in a 2N HCl solution. Samples are then gently heated to 50°C causing the fractional crystallization of $PbCl_2$ which are then washed with 4N HCl and ultrapure water. Lead is separated from the residual crystals by dissolving them in 1 ml of ultrapure 2% HNO_3 that has been diluted by a factor of 5000. The Pb isotopic composition is measured on a Nu Plasma Multi-Collector ICP Mass Spectrometer. Ratios were corrected using the NIST Standard Reference Material SRM981. Absolute Pb isotope ratios for SRM981 are $^{206}Pb/^{204}Pb$= 16.9373 ± 0.0027, $^{207}Pb/^{204}Pb$= 15.4901 ± 0.0022, and $^{208}Pb/^{204}Pb$= 36.6921±0.0061 (Todt et al., 1996).

3.10   Results
3.10.1 Ice flow data

Striation measurements indicate that there were at least 3 (possibly 4) ice flow trajectories in the Pine Point region (Fig. 3-4). Relative ages of these measurements suggest that the earliest ice flow direction was to the southwest (~230°), followed by an intermediate phase to the northwest (~300°), and the last phase to the west southwest (~250°). Large-scale streamlined glacial landforms (flutings) are also oriented in the direction of this last ice flow trajectory. Evidence of a fourth, short-lived, intermediate phase of ice flow exists on the

bedrock surface at deposit X15. Striation measurements indicated that this phase was to the northwest (~330°) and has cross-cutting relationships that suggest the timing of this event to be before the northwest (~300°) intermediate event and after the oldest the southwest (~250°) event.

Till deposits at the eastern margin of the former mine district range from <1 m to 3 m thick, and gradually thicken westward to >25 m at the western pits. Till in the Pine Point area has a sandy-silt matrix containing an average of 14% clay, 50% silt and 36% sand (Fig. 3-5). The till matrix contains an average of 8 % inorganic carbon and 0.3 % organic carbon as determined by the LECO method.

3.10.2 Ore mineralogy of bedrock samples

Sphalerite, galena and pyrite/marcasite were identified in polished thin section along with the gangue minerals dolomite, calcite, and native sulphur.

Paragenetic sequences were constructed for each of the five ore bodies studied; the minerals observed have been classified into pre-, syn-, and post-ore paragenetic stages (Fig. 3-6). The first step in the pre-ore stage was the replacement of the original limestone with fine and medium-grained dolomite.
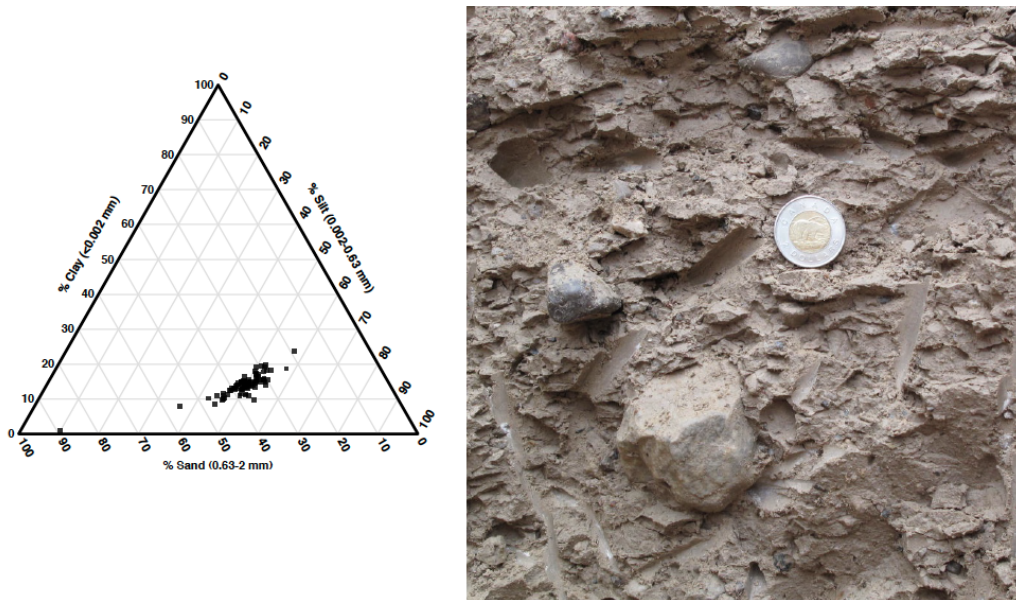
Fig. 3-5: (A) Ternary plot of the clay, silt and sand compositions in the till matrix (n=85) and, (B) Fissile till collected from sample 11-MPB-013 containing subangular, faceted clasts (Canadian two-dollar coin, 28 mm diameter, for scale).

This fine-grained dolomite was followed by the development of the Presqu'ile dolomite (500- 1000 μm; Fig. 3-7) in each of the deposits excluding deposit O28. Some deposits (O28, M67, and L65) contain pre-ore saddle dolomite.

The sulphide minerals precipitated in the ore stage are pyrite, galena (cubic and skeletal), and sphalerite (colloform, cleiophane, honey-brown, and blackjack). Pyrite is typically the first mineral to precipitate in each deposit (Kyle, 1977; Krebs and Macqueen, 1984) but in the R190, O28, and L65 deposits, pyrite and cubic galena co-precipitate in the early stages of mineralization. Pyrite in bedrock samples occurred as cubes, botryoidal fans, needles as well as fine-grained masses (Fig. 3-8a-d) however the paragenetic order of these phases were difficult to determine.

Galena occurred as the cubic and skeletal variety in all deposits with the exception of deposit O28 which was void of skeletal galena. The different textures of galena observed were dendritic, fracture and vug filling and banded galena (Fig. 3-9 a-f). Cubic galena grains ranged from 50 to 5000 μm and skeletal grain dimensions typically ranged from 50 to 1500 μm. Cubic galena typically occurred cogenentically with sphalerite however there was also evidence of pre- and post-sphalerite deposition (Fig. 3-10a-c). Skeletal galena occurred exclusively cogenetically within cleiophane and colloform sphalerite.

Sphalerite occurs as four distinct varieties; honey-brown, blackjack, colloform and cleiophane. The different textures of sphalerite that were observed are: snow-on-roof, banded, dendritic and ascicular (Fig. 3-11a-f). Sphalerite crystals in thin section ranged from 100 to 500 μm and individual bands in colloform sphalerite ranged from 50 to 1500 μm in thickness. Colloform and cleiophane sphalerite were paragenetically earlier than blackjack sphalerite. Blackjack sphalerite typically formed an isopachus crust on colloform sphalerite (M67 and L65) or as isolated crystal patches (HZ). Samples from deposits O28 and R190 did not contain blackjack sphalerite. Honey-brown sphalerite is cogenetic with colloform sphalerite or paragenetically late as in deposits M67 and HZ. Galena filled vugs and fractures (HZ) which marked the end of the ore stage.
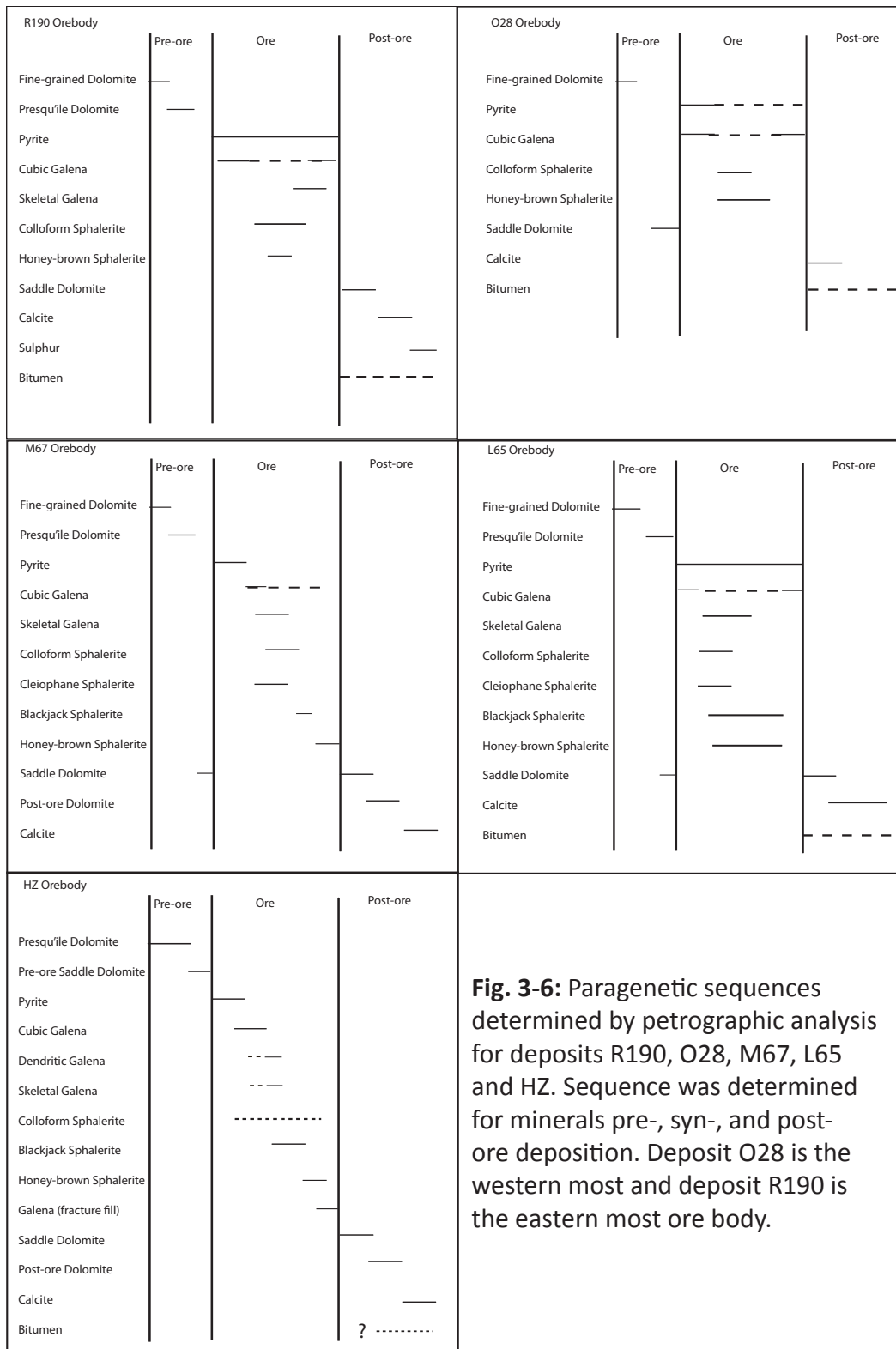
Fig. 3-6: Paragenetic sequences determined by petrographic analysis for deposits R190, O28, M67, L65 and HZ. Sequence was determined for minerals pre-, syn-, and post-ore deposition. Deposit O28 is the western most and deposit R190 is the eastern most ore body.

The post-ore stage is characterized by the precipitation of saddle dolomite, calcite and in some cases native sulphur (R190; Fig. 3-11a). Bitumen was present in samples from all deposits excluding M67. It was difficult to determine when bitumen formed, however, in most cases it is coeval with calcite. Saddle dolomite crystals were typically 2 to 5 mm in size and were characterized by sweeping extinction and curved crystal faces. Calcite was typically clear and colourless, sometimes exhibiting clear twinning.

3.10.3 Nature and distribution of the recovered indicator minerals

This section will focus on the 0.25-0.5 mm fraction when discussing till unless otherwise noted, because this fraction best shows the distribution of these indicator minerals. Appendix C contains data for bedrock and till grain
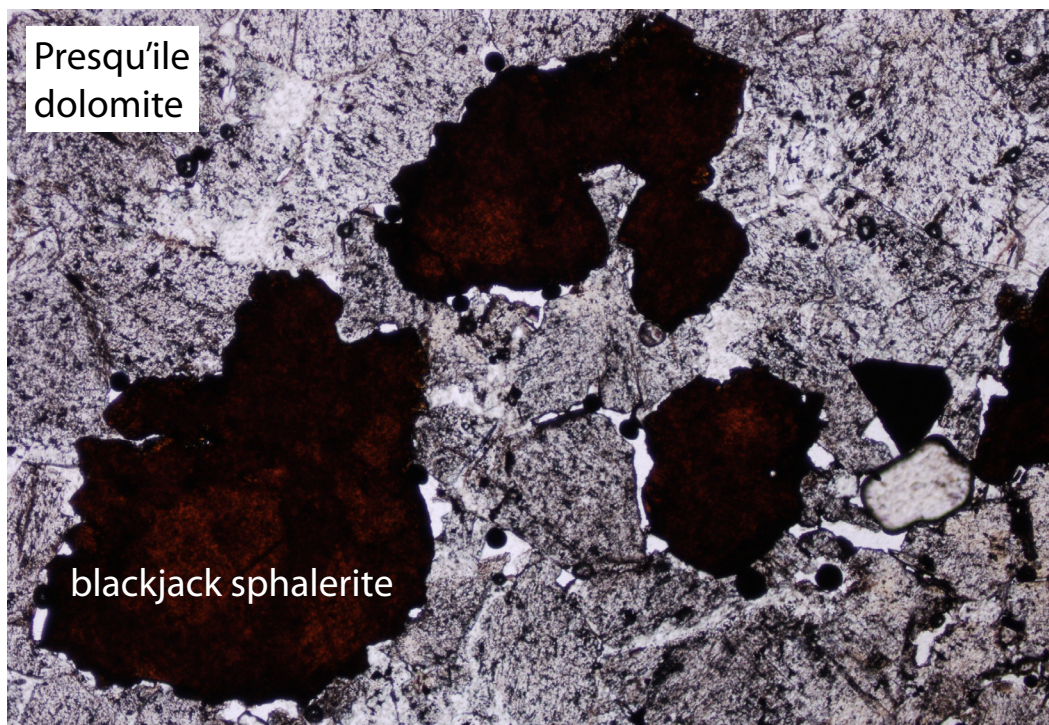
Fig. 3-7: Blackjack sphalerite in Presqu'ile dolomite host from sample 10-MPB-R75. Field of view is 4 mm.
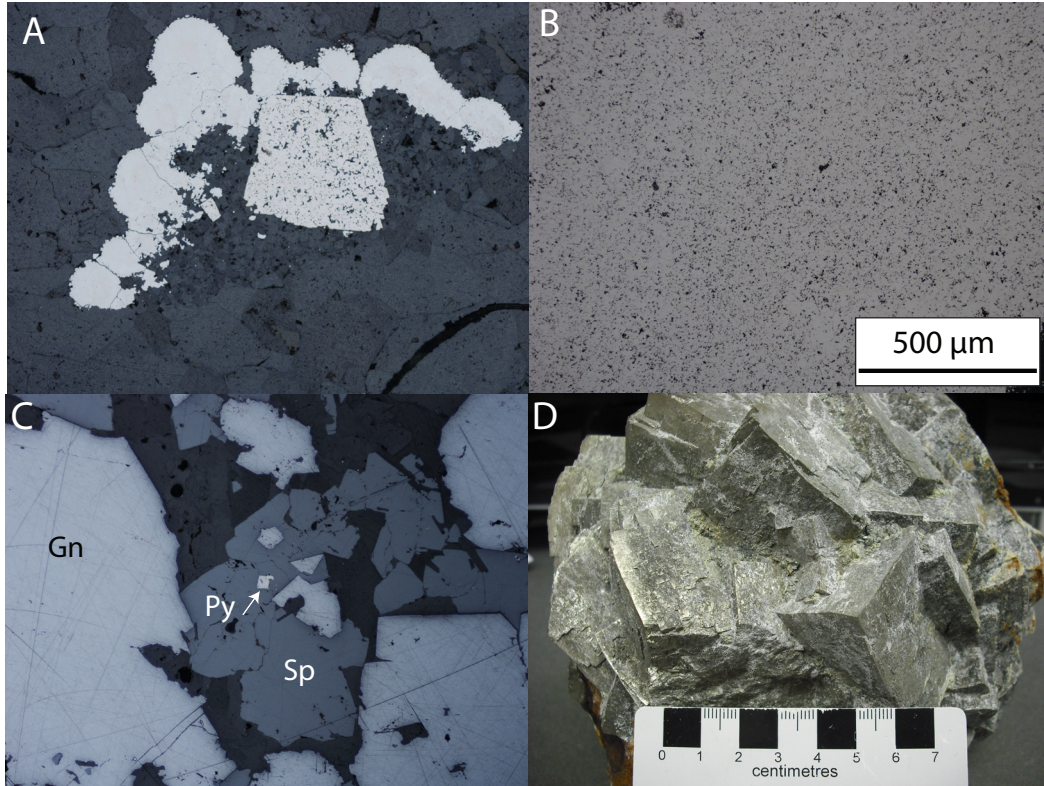
Fig. 3-8: Pyrite in thin section and hand sample(A) botroydial pyrite in dolomite host, (B) massive pyrite, (C) inclusion pyrite and, (D) massive, 3 cm, cubic pyrite from deposit S65.
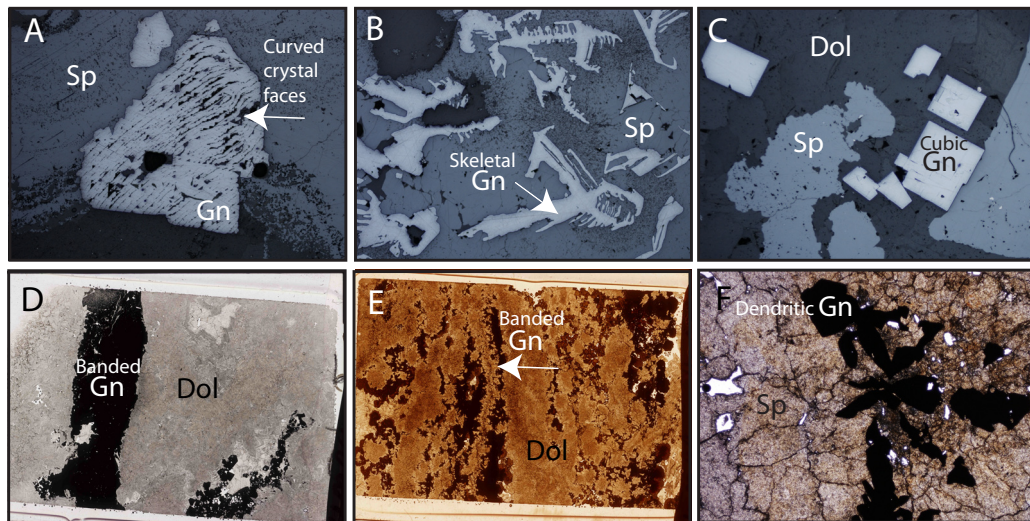
Fig. 3-9: Galena textures and varities in thin section: (A) Galena crystal showing evidence of diagenesis in the form of curved crystal faces, (B) skeletal galena in colloform sphalerite, (C) cubic galena, (D, E) banded galena and (F) dendritic galena.
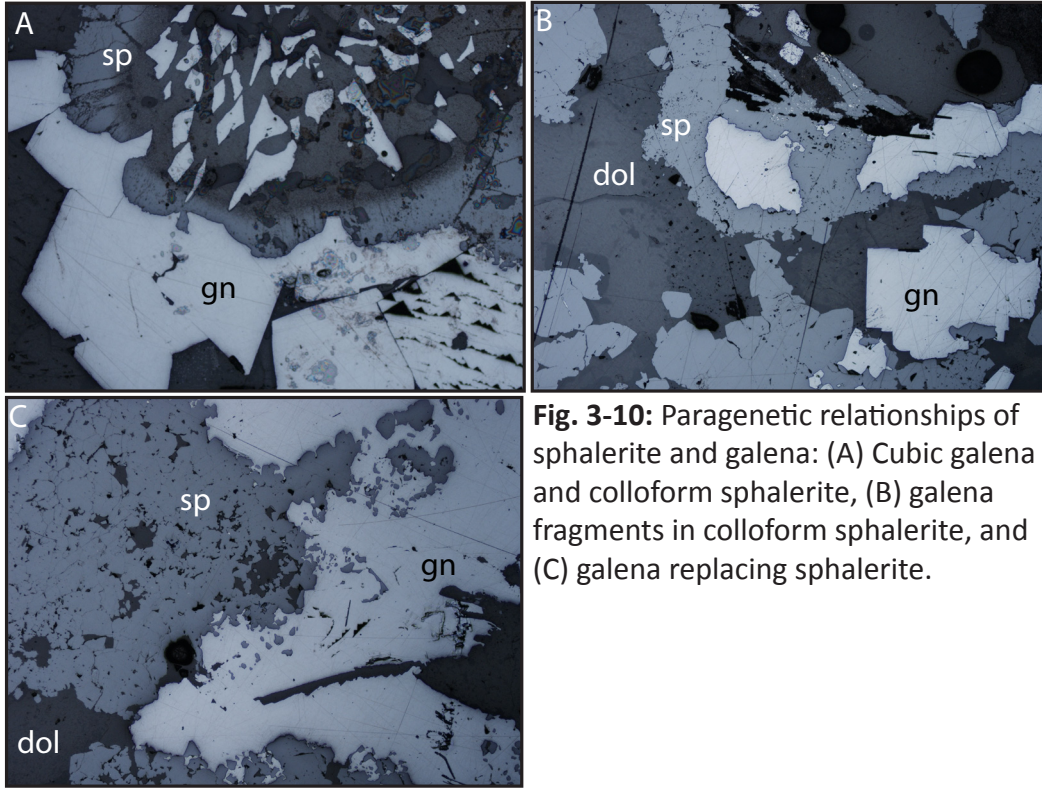
Fig. 3-10: Paragenetic relationships of sphalerite and galena: (A) Cubic galena and colloform sphalerite, (B) galena fragments in colloform sphalerite, and (C) galena replacing sphalerite.

EPMA as well as grain counts for heavy mineral concentrates. Till geochemistry data are available in Appendix D1 and D2 as well as Geological Survey of Canada Open File 7320.

Grains of sphalerite, galena, pyrite, and smithsonite were recovered from the tills. Smithsonite was only recovered from three samples in the vicinity of the ore zone at deposit O28 therefore, this paper will focus on the characteristics of sphalerite, galena and pyrite, which are the common ore minerals.

The majority of sphalerite grains recovered from till ranged from 0.25 to 1.0 mm, though few samples contained sphalerite grains in the pan concentrate (~25 μm). The most abundant size fraction was 0.25 to 0.5 mm, however, samples in close proximity to the deposit contained the majority of sphalerite grains in the 1.0 to 2.0 mm fraction. Figure 3-12 shows the distribution of sphalerite grains recovered from the 0.25 to 0.5 mm fraction of till.

Galena grains recovered from till samples range from 25 μm to 2 mm in size. The majority of galena grains were recovered from the 25 μm to 0.5 mm
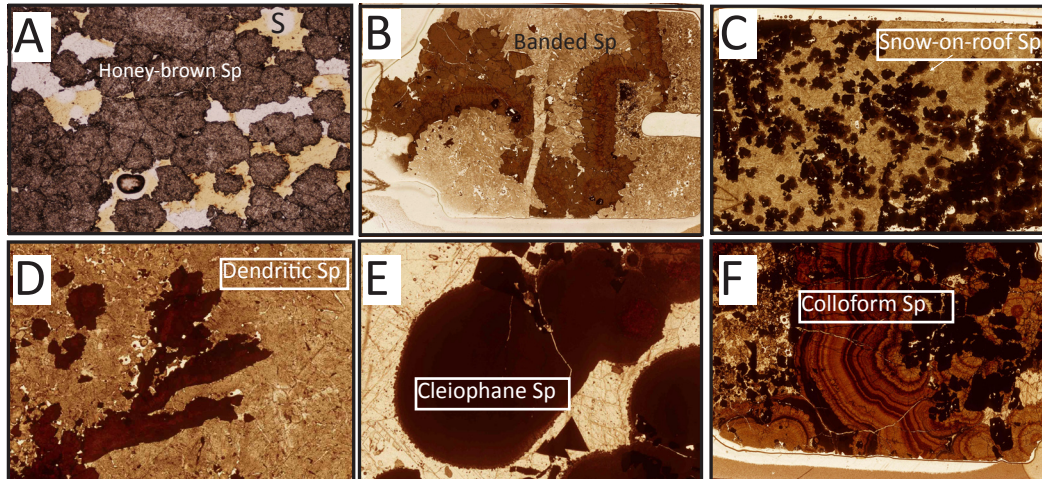
Fig. 3-11: Different textures and varieties of sphalerite: (A) honey-brown sphalerite with native sulphur filling interstitial space, (B) banded sphalerite, (C) snow-on-roof sphalerite, (D) dendritic sphalerite, (E) cleiophane sphalerite, and (F) colloform sphalerite.

size fraction, however, galena grains occurred in all size fractions in 27 % of all till samples. Background concentration for galena is 0 grains/10 kg and was determined in the same fashion as background concentrations of sphalerite grains. Galena grains recovered from till samples are typically cubic, however some grains had a discontinuous coating of anglesite that gave the grains a more rounded appearance. Samples 10-MPB-004, -005 and -028 contain 53097, 2419 and 8065 grains/10 kg respectively, and all three samples are immediately down-ice of the ore zone at O28 (Fig. 3-13).

Pyrite grains recovered from till samples were 25 µm to 0.5 mm in size. Sample 10-MPB-004, -030 and -005 contain 26549, 7576 and 3226 grains of pyrite. These samples were again located down-ice of the ore zone on the bedrock bench surrounding deposit O28. There was no EPMA analysis conducted on pyrite grains recovered from till samples.

3.10.4 Microprobe analyses of bedrock and indicator minerals

EPMA was conducted on 80 to 85 sphalerite grains of each textural variety recovered from bedrock samples (Table 3-2). Zinc concentrations in sphalerite ranged from 43.95 to 67.48 wt % and S concentrations ranged from 32.03 to 39.19 wt %. Spatial variations in Fe concentrations (0.02 to 16.94 wt
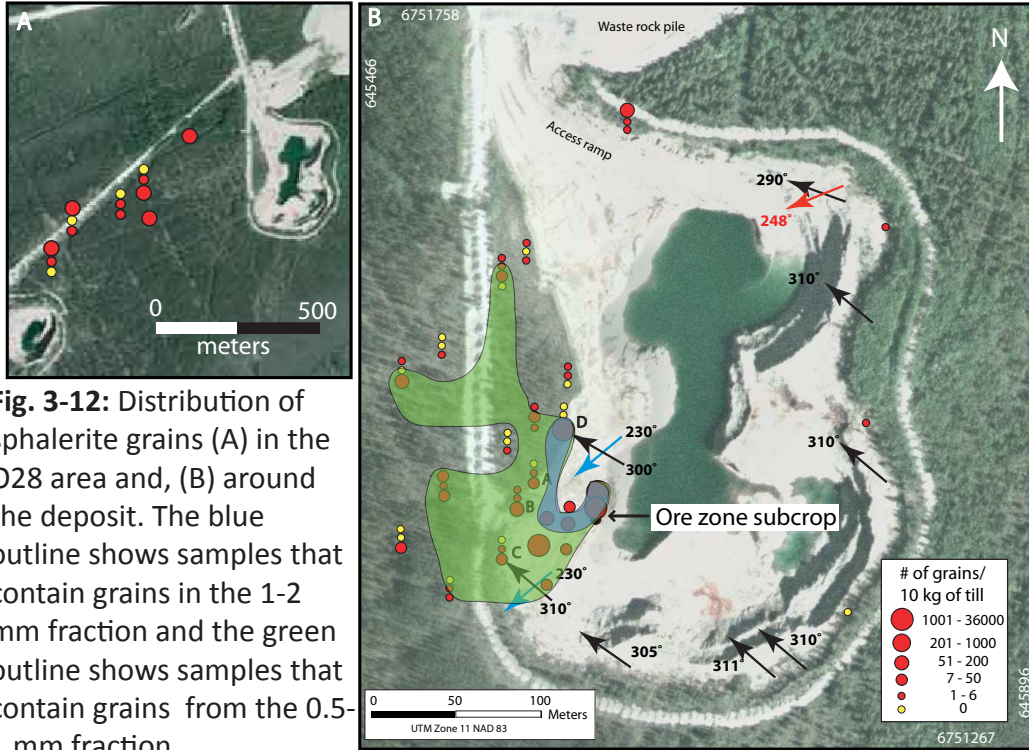
Fig. 3-12: Distribution of sphalerite grains (A) in the O28 area and, (B) around the deposit. The blue outline shows samples that contain grains in the 1-2 mm fraction and the green outline shows samples that contain grains from the 0.5-1 mm fraction.
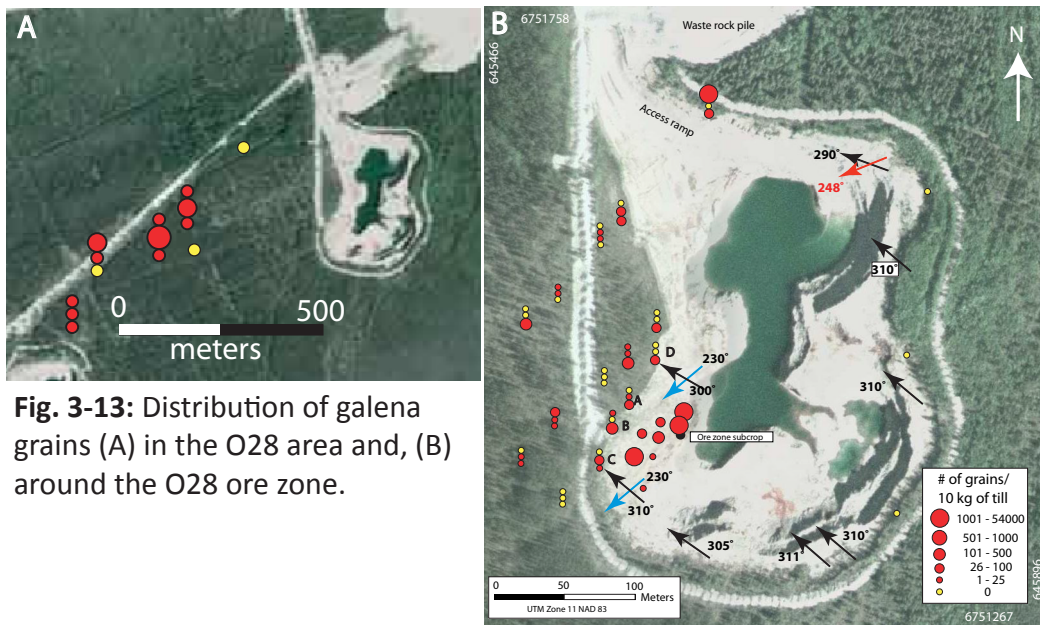
Fig. 3-13: Distribution of galena grains (A) in the O28 area and, (B) around the O28 ore zone.

%) were detected with a general decrease from east to west across the district with the highest concentrations in deposit O28 and the lowest in deposit R190 (Fig. 3-14). Cadmium concentrations ranged from <0.01 to 0.51 wt %. Deposit M67 was the most geochemically distinct of the five deposits in this study. This deposit had low concentrations (below detection limits) of Ge, Ag, In, Sb, Pb, Cu and Hg unlike the other deposits (Fig. 3-15a). Deposit R190 had higher concentrations of Sb, Cu and Hg than the other deposits (Table 3-2). Germanium was most abundant in deposit L65.

Iron concentrations of sphalerite within a single deposit varied with the texture of sphalerite; they were highest in blackjack sphalerite and lowest in honey-brown sphalerite. Concentrations of Pb ranged from 0.02 to 16.94 wt % with cleiophane and colloform sphalerite typically containing the highest concentrations on average (Fig. 3-15b). Honey-brown sphalerite had higher concentrations of Cd than blackjack sphalerite which contained concentrations
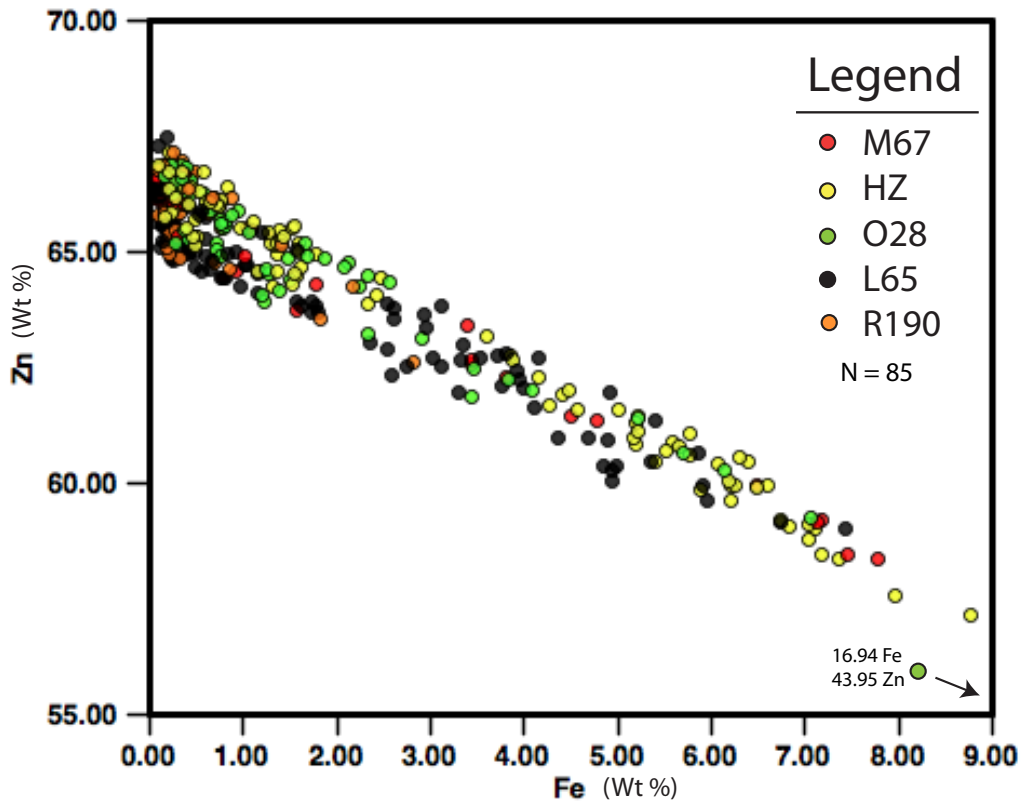
Fig. 3-14: Zinc versus Fe concentrations for sphalerite grains by deposit. Deposit O28 (east) contains the highest concentrations of Fe while deposit R190 (west) contains the lowest concentrations.

below detection limit. Dendritic sphalerite contained the highest concentrations of Ge (Table 3-2).

Major and trace element analyses indicated that sphalerite grains from till have similar concentrations to those recovered from bedrock samples (Table 3-2; Fig. 3-15c). Zinc concentration ranged from 64.06 to 67.27 wt % while S concentration ranged from 32.24 to 34.13wt % i.e. within the compositional range of the bedrock sphalerite. Similarly, the concentrations of Mn, Fe, Ge and Se in sphalerite recovered from the till were similar to bedrock sphalerite grains but those of As, Ag, Cd, In, Sb, Pb, Cu, and Hg were on average lower.

EPMA was conducted on 58 bedrock grains of both skeletal and cubic galena grains as well as each texture (Table 3-3).

Sulphur concentrations in galena grains appeared to have a bimodal distribution (Fig. 3-16a) with lower S concentrations ranging from 12.5 to 13.25 wt % and higher S concentrations range from 13.75 to 14.00 wt %. The total range for S concentration was from bedrock samples ranged from 12.53 to 13.93 wt %. Galena from deposits R190 and M67 had S concentrations in the latter range. Cubic and skeletal galenas had essentially the same geochemistry except that Zn concentrations were slightly higher in skeletal galena (Fig. 3-16b). There was no detectable Ag in any of the galenas analysed in this study (Table 3-3).

Concentrations of Pb, S and Se were similar in galena grains recovered from till samples compared to those in bedrock samples. Galena grains recovered from till samples had lower concentrations of Fe, Zn, Ge, As, In, Sb, Cu and Hg than bedrock galena. Cadmium concentrations ranged from 0.008 to 0.093 wt % in galena grains recovered from till samples which was higher than that determined for bedrock grains (Table 3-3).

Iron concentrations in pyrite grains from bedrock samples ranged from 41.98 to 47.25 wt % and S concentrations ranged from 51.70 to 54.37 wt %. Selenium (0.012 – 0.07 wt %) was detected in all five deposits excluding R190. Pyrite from deposit O28 contained detectable Ge, In, Sb, Pb and Hg while data from the other four deposits were below the detection limits (Fig. 3-17a). All

Table 3-2: Summary statistics (in wt. %) for EPMA data on sphalerite grains recovered from till and bedrock (b.d is below detection limit).Detection limits and total concentrations for analyses can be found in Appendix C.

Summary statistics		S	Mn	Fe	Zn	Ge	As	Ag	Cd	In	Sb	Pb	Cu	Hg	Se
HZ deposit	max	33.99	0.04	8.78	67.13	0.15	0.10	0.09	0.32	0.06	0.04	0.77	0.04	0.15	0.10
(N=30)	min	32.13	0.01	0.10	57.15	0.02	0.02	0.02	0.03	0.02	0.02	0.06	0.01	0.02	0.02
	median	33.17	0.02	1.59	64.50	0.04	0.05	0.04	0.24	0.03	0.03	0.20	0.02	0.07	0.04
	mean	33.17	0.02	3.11	63.24	0.05	0.05	0.04	0.21	0.03	0.03	0.25	0.02	0.07	0.04
	σ	0.42	0.01	2.61	2.78	0.03	0.02	0.02	0.10	0.01	0.01	0.16	0.01	0.04	0.02
L65 deposit	max	34.01	0.03	7.87	67.48	0.12	0.14	0.09	0.43	0.05	0.03	0.87	0.03	0.17	0.10
(N=21)	min	32.06	0.01	0.05	56.88	0.02	0.02	0.02	0.03	0.02	0.02	0.03	0.01	0.03	0.01
	median	33.10	0.02	0.61	64.90	0.07	0.06	0.05	0.23	0.02	0.02	0.41	0.01	0.08	0.04
	mean	33.02	0.02	1.68	64.16	0.07	0.06	0.05	0.24	0.03	0.02	0.40	0.02	0.08	0.05
	σ	0.39	0.01	1.93	1.97	0.04	0.03	0.02	0.09	0.01	0.00	0.22	0.01	0.04	0.02
M67 deposit	max	33.80	0.03	7.77	66.83	b.d	0.08	b.d	0.51	b.d	b.d	b.d	b.d	b.d	0.06
(N=6)	min	32.68	0.03	0.09	58.36	b.d	0.07	b.d	0.18	b.d	b.d	b.d	b.d	b.d	0.06
	median	33.12	0.03	0.71	65.32	N/A	0.07	N/A	0.25	N/A	N/A	N/A	N/A	N/A	0.06
	mean	33.15	0.03	1.75	64.46	N/A	0.07	N/A	0.27	N/A	N/A	N/A	N/A	N/A	0.06
	σ	0.26	N/A	2.35	2.46	N/A	0.01	N/A	0.09	N/A	N/A	N/A	N/A	N/A	N/A
O28 deposit	max	39.19	0.03	16.94	66.90	0.03	0.14	0.08	0.43	0.06	0.05	0.76	0.03	0.15	0.10
(N=14)	min	32.06	0.01	0.16	43.95	0.02	0.02	0.02	0.03	0.02	0.02	0.05	0.01	0.02	0.01
	median	33.07	0.01	1.22	64.95	0.03	0.06	0.03	0.19	0.03	0.02	0.19	0.02	0.07	0.04
	mean	33.12	0.01	1.95	64.36	0.03	0.06	0.04	0.19	0.03	0.03	0.24	0.02	0.08	0.04
	σ	0.81	0.01	2.48	3.10	0.01	0.03	0.02	0.12	0.02	0.01	0.16	0.01	0.04	0.02
R190 deposit	max	33.60	0.03	4.68	67.14	0.05	0.10	0.03	0.36	0.04	0.05	0.86	0.12	0.17	0.08
(N=14)	min	32.03	0.02	0.04	60.47	0.02	0.02	0.03	0.18	0.02	0.05	0.14	0.01	0.03	0.02
	median	33.16	0.02	0.41	66.08	0.03	0.06	0.03	0.21	0.02	0.05	0.29	0.05	0.10	0.06
	mean	33.06	0.02	0.71	65.77	0.03	0.06	0.03	0.22	0.03	0.05	0.34	0.07	0.10	0.05
	σ	0.34	0.00	0.85	1.24	0.01	0.02	0.00	0.06	0.01	0.01	0.19	0.05	0.05	0.02

Summary statistics		S	Mn	Fe	Zn	Ge	As	Ag	Cd	In	Sb	Pb	Cu	Hg	Se
Honey-brown sphalerite	max	33.77	0.03	2.95	67.14	0.12	0.14	0.09	0.51	0.06	0.05	0.87	0.12	0.17	0.10
(N=198)	min	32.06	0.01	0.05	62.90	0.02	0.02	0.02	0.03	0.02	0.02	0.03	0.01	0.02	0.01
	med	33.09	0.01	0.42	65.73	0.05	0.06	0.04	0.24	0.03	0.02	0.18	0.01	0.07	0.04
	mean	32.98	0.01	0.72	65.61	0.05	0.06	0.04	0.24	0.03	0.03	0.24	0.03	0.08	0.04
	σ	0.37	0.01	0.68	0.90	0.03	0.03	0.02	0.11	0.02	0.01	0.18	0.03	0.04	0.02
Cleiophane sphalerite	max	33.75	0.03	5.41	67.48	0.07	0.08	0.05	0.33	b.d	b.d	0.79	0.03	0.09	0.03
(N=47)	min	32.39	0.02	0.09	60.37	0.07	0.03	0.05	0.11	b.d	b.d	0.25	0.03	0.03	0.02
	med	33.02	0.02	0.60	64.95	0.07	0.04	0.05	0.19	N/A	N/A	0.50	0.03	0.08	0.02
	mean	33.02	0.02	1.46	64.46	0.07	0.05	0.05	0.20	N/A	N/A	0.50	0.03	0.07	0.02
	σ	0.25	0.01	1.59	1.69	N/A	0.02	N/A	0.06	N/A	N/A	0.16	N/A	0.03	0.01
Colloform sphalerite	max	33.74	0.03	6.73	66.17	0.06	0.14	0.09	0.35	0.04	0.05	0.77	b.d	0.11	0.07
(N=29)	min	32.21	0.01	0.06	59.17	0.02	0.02	0.02	0.03	0.02	0.05	0.13	b.d	0.02	0.01
	med	32.90	0.02	1.37	65.07	0.04	0.06	0.03	0.18	0.03	0.05	0.47	N/A	0.07	0.04
	mean	32.96	0.02	2.13	64.07	0.04	0.06	0.04	0.20	0.03	0.05	0.44	N/A	0.06	0.04
	σ	0.32	0.01	1.96	1.94	0.02	0.03	0.03	0.09	0.01	N/A	0.19	N/A	0.03	0.02
Blackjack sphalerite	max	39.19	0.04	16.94	65.53	0.07	0.10	0.09	b.d	0.05	0.03	0.77	0.02	0.15	0.10
(N=74)	min	32.40	0.01	1.04	43.95	0.02	0.03	0.02	b.d	0.02	0.02	0.08	0.01	0.02	0.02
	med	33.36	0.02	5.21	60.81	0.03	0.06	0.04	N/A	0.03	0.03	0.22	0.01	0.07	0.06
	mean	33.42	0.02	5.34	60.73	0.04	0.06	0.04	N/A	0.03	0.02	0.25	0.02	0.08	0.05
	σ	33.42	0.02	5.34	60.73	0.04	0.06	0.04	N/A	0.03	0.02	0.25	0.02	0.08	0.05
Acicular texture	max	33.36	b.d	2.60	64.76	b.d	0.08	b.d	0.40	b.d	b.d	b.d	b.d	b.d	b.d
(N=6)	min	32.82	b.d	0.71	63.35	b.d	0.08	b.d	0.34	b.d	b.d	b.d	b.d	b.d	b.d
	med	33.07	N/A	1.50	64.42	N/A	0.08	N/A	0.37	N/A	N/A	N/A	N/A	N/A	N/A
	mean	33.11	N/A	1.49	64.31	N/A	0.08	N/A	0.37	N/A	N/A	N/A	N/A	N/A	N/A
	σ	0.20	N/A	0.70	0.52	N/A	N/A	N/A	0.04	N/A	N/A	N/A	N/A	N/A	N/A
Dendritic texture	max	33.97	0.03	7.62	62.01	0.15	0.06	0.04	b.d	0.05	0.04	0.37	0.02	0.15	0.06
(N=18)	min	32.81	0.01	4.55	58.54	0.02	0.02	0.04	b.d	0.04	0.04	0.11	0.01	0.03	0.02
	med	33.49	0.02	5.81	60.48	0.08	0.05	0.04	N/A	0.04	0.04	0.23	0.01	0.07	0.03
	mean	33.43	0.02	5.83	60.32	0.07	0.05	0.04	N/A	0.04	0.04	0.24	0.01	0.08	0.03
	σ	0.40	0.01	0.90	1.05	0.05	0.02	N/A	N/A	0.00	N/A	0.08	0.00	0.05	0.01
Snow on roof texture	max	33.35	0.03	1.53	66.41	b.d	0.06	0.04	0.06	0.05	0.03	0.74	0.02	0.15	0.10
(N=11)	min	32.82	0.01	0.25	64.63	b.d	0.02	0.04	0.06	0.02	0.03	0.16	0.02	0.04	0.02
	med	33.13	0.02	0.76	65.42	N/A	0.04	0.04	0.06	0.02	0.03	0.35	0.02	0.06	0.06
	mean	33.12	0.02	0.73	65.52	N/A	0.04	0.04	0.06	0.03	0.03	0.39	0.02	0.08	0.06
	σ	0.17	0.01	0.40	0.57	N/A	0.02	N/A	N/A	0.02	N/A	0.21	N/A	0.04	0.03
Banded texture	max	33.02	0.02	4.74	66.06	b.d	0.10	0.08	b.d	0.04	0.04	0.23	0.03	0.10	0.06
(N=8)	min	32.74	0.01	0.47	61.80	b.d	0.03	0.02	b.d	0.02	0.03	0.08	0.03	0.06	0.02
	med	32.85	0.01	1.98	64.67	N/A	0.06	0.06	N/A	0.02	0.03	0.14	0.03	0.07	0.03
	mean	32.86	0.01	2.30	64.30	N/A	0.07	0.05	N/A	0.03	0.03	0.15	0.03	0.08	0.04
	σ	0.11	0.00	1.58	1.59	N/A	0.03	0.03	N/A	0.01	0.01	0.06	N/A	0.02	0.02
Indicator minerals	max	34.13	0.03	3.04	67.27	0.03	0.07	0.03	0.44	0.02	0.01	0.40	b.d	0.17	0.10
(N=70)	min	32.24	0.005	0.167	64.06	0.03	0.01	0.01	0.02	0.01	0.01	0.01	b.d	0.01	0.01
	med	33.19	0.014	0.7915	66.47	0.03	0.04	0.02	0.12	0.02	0.01	0.10	N/A	0.05	0.04
	mean	33.23	0.01	0.93	66.25	0.03	0.04	0.02	0.13	0.02	0.01	0.12	N/A	0.06	0.04
	σ	0.35	0.01	0.58	0.72	N/A	0.02	0.01	0.11	0.01	0.00	0.08	N/A	0.04	0.02

Table 3-3: Summary statistics of EPMA data from galena grains recovered from bedrock and till samples (b.d is below detection limit).

Summary statistics		S	Mn	Fe	Zn	Ge	As	Ag	Cd	In	Sb	Pb	Cu	Hg	Se
HZ deposit	max	13.91	0.04	0.07	3.32	0.12	0.09	b.d	b.d	0.07	0.05	89.27	0.03	0.06	0.10
(N=80)	min	12.61	0.01	0.04	0.01	0.02	0.01	b.d	b.d	0.02	0.05	83.87	0.01	0.02	0.01
	median	13.05	0.02	0.04	0.07	0.04	0.05	N/A	N/A	0.03	0.05	86.42	0.02	0.04	0.04
	mean	13.20	0.02	0.05	0.25	0.05	0.05	N/A	N/A	0.04	0.05	86.52	0.02	0.04	0.04
	σ	0.40	0.01	0.01	0.55	0.03	0.02	N/A	N/A	0.01	N/A	0.99	0.01	0.02	0.02
L65 deposit	max	13.92	0.02	1.33	0.98	0.11	0.08	b.d	b.d	0.03	b.d	88.94	0.01	0.02	0.07
(N=37)	min	12.59	0.01	0.04	0.01	0.02	0.02	b.d	b.d	0.02	b.d	85.21	0.01	0.02	0.02
	median	13.63	0.01	0.06	0.10	0.08	0.05	N/A	N/A	0.02	N/A	86.84	0.01	0.02	0.05
	mean	13.34	0.01	0.23	0.29	0.08	0.05	N/A	N/A	0.02	N/A	86.90	0.01	0.02	0.04
	σ	0.44	0.00	0.48	0.34	0.03	0.02	N/A	N/A	0.01	N/A	1.21	0.00	N/A	0.02
M67 deposit	max	13.79	b.d	0.05	0.45	b.d	b.d	b.d	b.d	b.d	b.d	88.63	b.d	b.d	0.06
(N=7)	min	13.57	b.d	0.04	0.05	b.d	b.d	b.d	b.d	b.d	b.d	86.77	b.d	b.d	0.06
	median	13.66	N/A	0.04	0.24	N/A	N/A	N/A	N/A	N/A	N/A	87.49	N/A	N/A	0.06
	mean	13.66	N/A	0.04	0.25	N/A	N/A	N/A	N/A	N/A	N/A	87.58	N/A	N/A	0.06
	σ	0.07	N/A	0.00	0.18	N/A	N/A	N/A	N/A	N/A	N/A	0.71	N/A	N/A	N/A
O28 deposit	max	13.82	0.05	0.47	2.12	0.12	0.10	b.d	b.d	0.07	0.04	88.22	0.02	0.10	0.10
(N=76)	min	12.73	0.01	0.05	0.02	0.01	0.02	b.d	b.d	0.02	0.02	84.96	0.01	0.03	0.01
	median	12.95	0.02	0.17	0.03	0.06	0.06	N/A	N/A	0.03	0.03	85.87	0.02	0.04	0.04
	mean	13.07	0.02	0.22	0.27	0.06	0.05	N/A	N/A	0.03	0.03	86.10	0.02	0.05	0.04
	σ	0.30	0.01	0.20	0.59	0.03	0.02	N/A	N/A	0.02	0.01	0.73	0.00	0.03	0.02
R190 deposit	max	13.89	b.d	0.05	0.99	0.12	0.06	b.d	b.d	b.d	b.d	89.18	b.d	b.d	0.08
(N=31)	min	13.45	b.d	0.04	0.06	0.06	0.06	b.d	b.d	b.d	b.d	86.69	b.d	b.d	0.05
	median	13.65	N/A	0.05	0.22	0.09	0.06	N/A	N/A	N/A	N/A	87.93	N/A	N/A	0.06
	mean	13.65	N/A	0.04	0.34	0.09	0.06	N/A	N/A	N/A	N/A	87.87	N/A	N/A	0.07
	σ	0.12	N/A	0.00	0.33	0.01	0.00	N/A	N/A	N/A	N/A	0.61	N/A	N/A	0.01

Summary statistics		S	Mn	Fe	Zn	Ge	As	Ag	Cd	In	Sb	Pb	Cu	Hg	Se
Cubic galena	max	13.84	0.05	0.05	2.12	0.12	0.10	b.d	b.d	0.07	0.04	89.18	0.02	0.10	0.10
(N=135)	min	12.69	0.01	0.04	0.01	0.01	0.02	b.d	b.d	0.02	0.02	84.96	0.01	0.02	0.01
	median	13.48	0.02	0.04	0.04	0.07	0.05	N/A	N/A	0.03	0.03	86.63	0.01	0.04	0.05
	mean	13.30	0.02	0.05	0.23	0.07	0.05	N/A	N/A	0.04	0.03	86.68	0.02	0.05	0.05
	σ	0.38	0.01	0.00	0.50	0.03	0.02	N/A	N/A	0.02	0.01	1.03	0.00	0.03	0.02
Skeletal galena	max	13.92	0.03	0.06	0.91	0.11	0.09	b.d	b.d	0.04	b.d	88.63	0.03	b.d	0.08
(N=25)	min	12.68	0.01	0.04	0.02	0.02	0.03	b.d	b.d	0.02	b.d	85.28	0.01	b.d	0.02
	median	13.01	0.02	0.05	0.30	0.07	0.04	N/A	N/A	0.03	N/A	86.47	0.02	N/A	0.03
	mean	13.24	0.02	0.05	0.37	0.06	0.05	N/A	N/A	0.03	N/A	86.60	0.02	N/A	0.04
	σ	0.41	0.01	0.01	0.30	0.03	0.02	N/A	N/A	0.01	N/A	1.01	0.01	N/A	0.02
Dendritic texture	max	13.69	0.04	b.d	0.07	0.07	0.09	b.d	b.d	0.04	0.05	89.27	0.03	0.06	0.10
(N=22)	min	12.67	0.01	b.d	0.01	0.02	0.02	b.d	b.d	0.03	0.05	85.11	0.02	0.02	0.01
	median	13.02	0.02	N/A	0.03	0.03	0.04	N/A	N/A	0.04	0.05	86.31	0.02	0.04	0.03
	mean	13.03	0.02	N/A	0.04	0.04	0.05	N/A	N/A	0.03	0.05	86.49	0.02	0.04	0.04
	σ	0.28	0.01	N/A	0.02	0.01	0.02	N/A	N/A	0.01	N/A	1.03	0.01	0.03	0.02
Fracture fill texture	max	13.91	0.04	0.06	3.32	0.10	0.06	b.d	b.d	0.03	b.d	88.06	0.02	0.06	0.08
(N=18)	min	12.61	0.01	0.04	0.03	0.02	0.01	b.d	b.d	0.03	b.d	83.87	0.02	0.06	0.02
	median	13.47	0.02	0.05	0.21	0.08	0.04	N/A	N/A	0.03	N/A	86.94	0.02	0.06	0.05
	mean	13.29	0.02	0.05	0.44	0.07	0.04	N/A	N/A	0.03	N/A	86.70	0.02	0.06	0.05
	σ	0.49	0.01	0.01	0.88	0.03	0.02	N/A	N/A	N/A	N/A	1.20	0.00	N/A	0.02
Banded texture	max	13.87	0.05	0.47	0.99	0.09	0.10	b.d	b.d	b.d	b.d	88.87	0.02	0.04	0.07
(N=16)	min	12.73	0.01	0.04	0.02	0.03	0.04	b.d	b.d	b.d	b.d	85.11	0.02	0.04	0.01
	median	12.93	0.02	0.05	0.03	0.04	0.07	N/A	N/A	N/A	N/A	85.81	0.02	0.04	0.04
	mean	13.20	0.02	0.18	0.17	0.05	0.07	N/A	N/A	N/A	N/A	86.76	0.02	0.04	0.04
	σ	0.44	0.01	0.19	0.36	0.02	0.02	N/A	N/A	N/A	N/A	1.50	N/A	N/A	0.02
Indicator Minerals	max	13.78	0.06	0.03	0.05	0.06	0.05	b.d	0.09	b.d	b.d	88.29	0.00	0.11	0.08
(N=61)	min	13.14	0.01	0.01	0.01	0.01	0.01	b.d	0.01	b.d	b.d	85.73	0.00	0.01	0.01
	median	13.40	0.02	0.01	0.01	0.02	0.04	N/A	0.03	N/A	N/A	86.63	N/A	0.02	0.03
	mean	13.40	0.02	0.01	0.02	0.03	0.03	N/A	0.03	N/A	N/A	86.80	N/A	0.04	0.04
	σ	0.13	0.01	0.01	0.01	0.01	0.01	N/A	0.02	N/A	N/A	0.61	N/A	0.04	0.02

Fig. 3-15: Median values for EPMA analysis on sphalerite grains from (A) all 5 deposits, (B) four different varieties and, (C) data from sphalerite grains recovered from till samples compared to those from bedrock at deposit O28.

Fig. 3-16: Distribution of (A) Pb vs S and, (B) EPMA data for different varieties of galena grains.
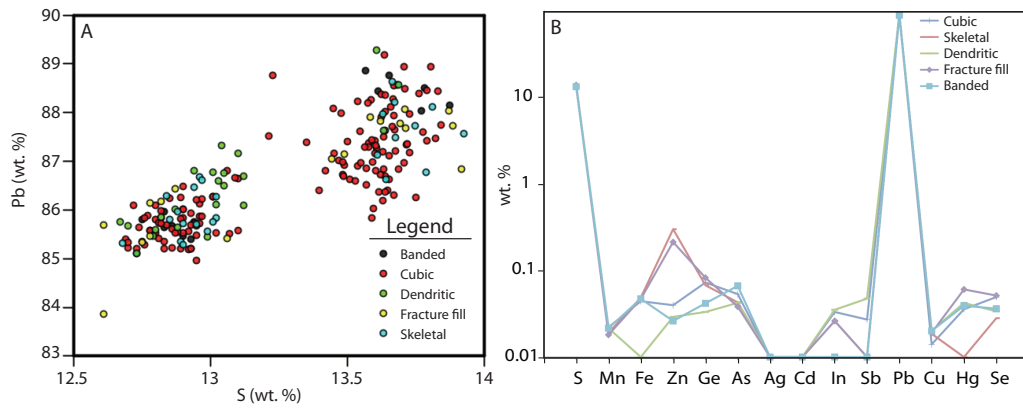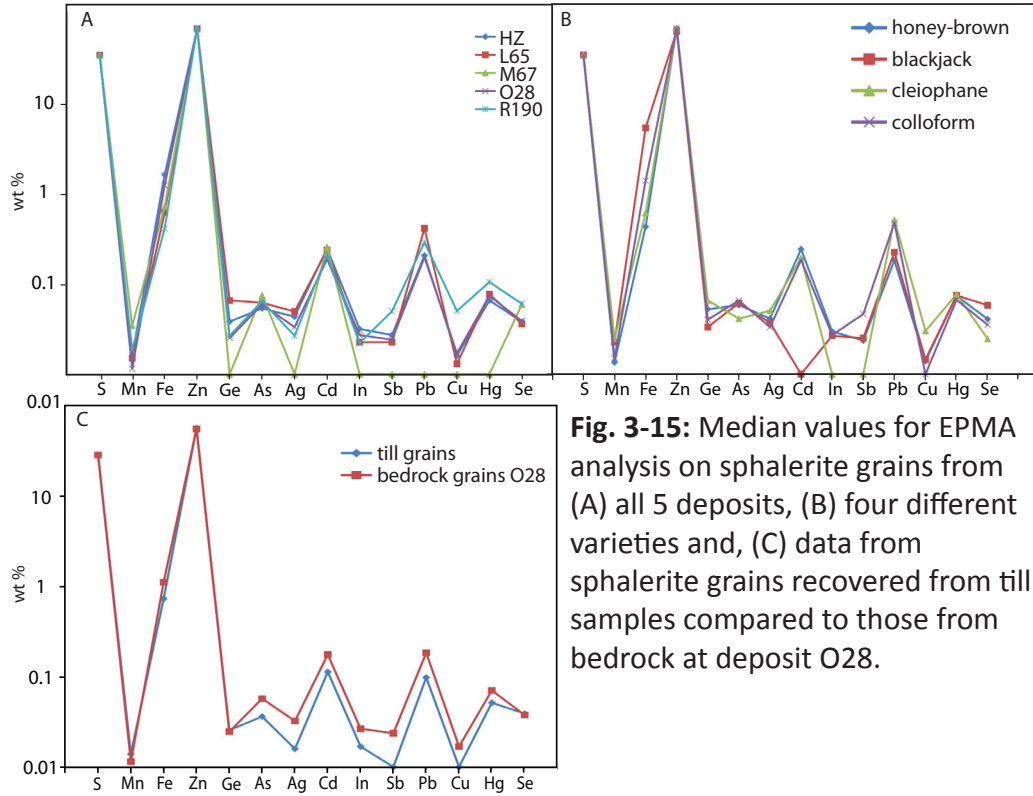
elements analyzed had near identical concentrations in inclusions and botryoidal pyrite excluding Mn and As (Fig. 3-17b). Botryoidal pyrite contained 0.03-0.24 wt % Mn and inclusion pyrite contained higher concentrations of As (0.05-0.22 wt %).

3.10.5 Sulphur Isotopic composition of bedrock and indicator minerals

Sphalerite from bedrock samples had a range in $\delta^{34}S$ values between 20.6 and 24.2 ‰ and sphalerite grains recovered from till had $\delta^{34}S$ values between −5.3 and 24.4 ‰ (Table 3-4). There was no distinguishable difference between the different varieties of sphalerite analyzed.
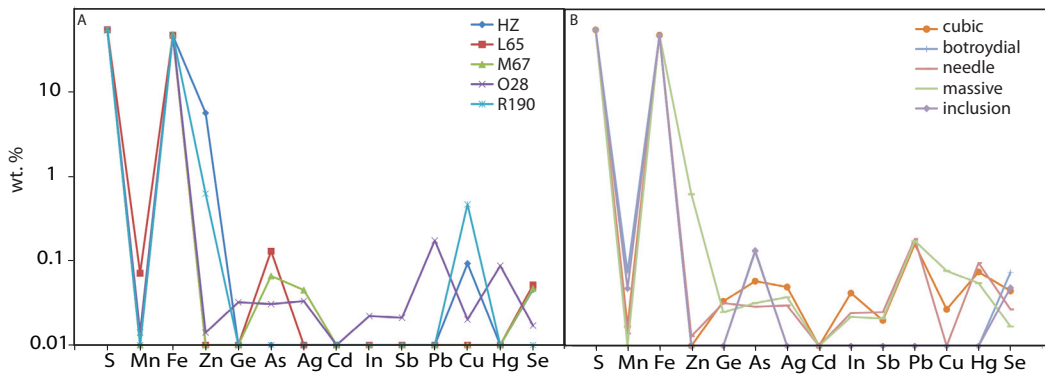
Fig. 3-17: Spider diagrams for EPMA analysis on pyrite grains by (A) deposit, and (B) grain type.

The majority of sphalerite grains from till samples fell within the range of bedrock values with the exception of two grains. These two grains had isotope values of 7.8 and −5.3 ‰ (Fig. 3-18). Till sample (10-MPB-030) which contained the grain with the $\delta^{34}S$ of −5.3 ‰ was collected on the bedrock bench immediately down-ice of the ore zone at deposit O28 (Fig. 3-3). Till sample 11-MPB-029, which contained the grain with a $\delta^{34}S$ value of 7.8 ‰, is located approximately 100 m down-ice of the ore zone at the bottom of an excavated trench nearly 3 m above the bedrock/till interface.

Galena crystals liberated from bedrock samples and those isolated from till samples have homogeneous $^{208}Pb/^{204}Pb$, $^{207}Pb/^{204}Pb$ and $^{206}Pb/^{204}Pb$ values (Table 3-5).

3.10.6 Till geochemistry

A detailed report of the till geochemistry associated with deposit O28 at the Pine Point mining district can be found in GSC Open File 7320 (Appendix B2; Oviatt et al., 2013). Aqua regia digestion/ICP-MS of the <0.063 mm fraction of
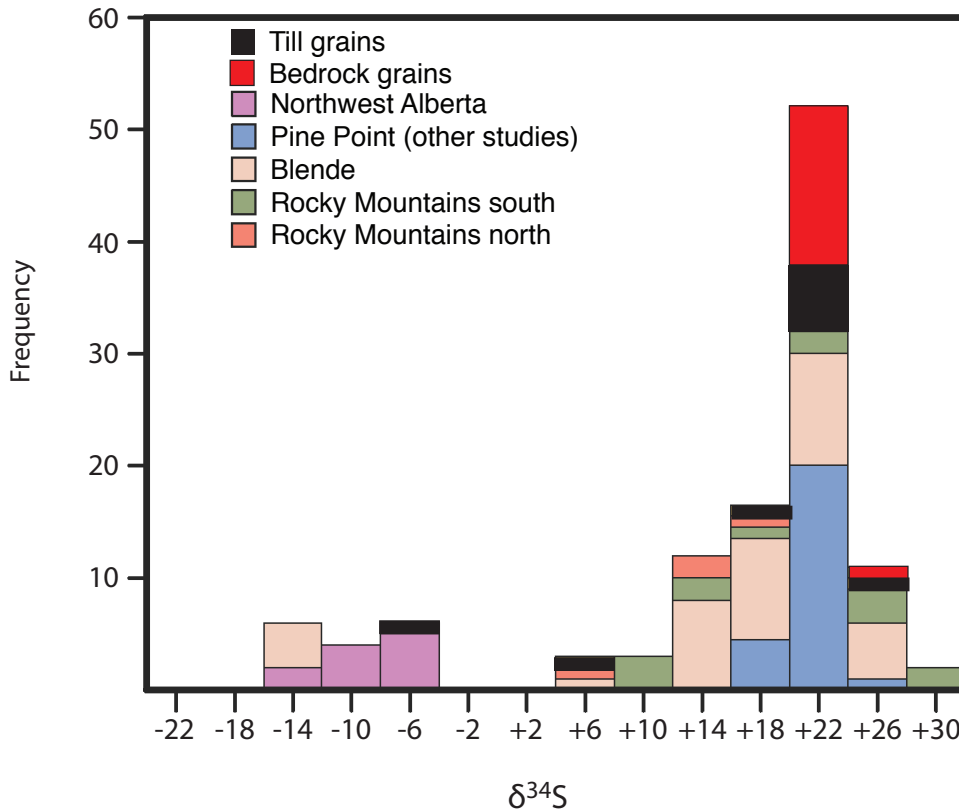
Fig. 3-18: Histogram of $\delta^{34}S$ values for sphalerite grains recovered from bedrock and till from this study compared to $\delta^{34}S$ values for sphalerite grains in bedrock samples from previous studies (Evans et al., 1968; Sasaki and Krouse, 1969) as well as from other MVT deposits in the Canada (Paradis et al., 2006). Sphalerite grains recovered from till samples collected in northwestern Alberta are also included for comparison (Paulen et al., 2011).

till identified Zn, Pb, Cd, Fe, Tl, S and Se as the pathfinder elements associated with deposit O28. Above background concentrations of these elements were detectable for at least 500 m down ice (Table 3-6). Zinc concentrations in till ranged from 1 to 3497 ppm. Samples 10-MPB-004, -030 and -031 contained the highest concentrations of zinc and were located overlying and immediately

Table 3-4: Results for sulphur isotope analysis on sphalerite grains from bedrock and till samples.

Sample #	Till/Bedrock?	δ³⁴S (‰)
10-MPB-R66	Bedrock	23.8
10-MPB-R27	Bedrock	23.8
10-MPB-R27	Bedrock	24.2
10-MPB-R02	Bedrock	22.0
10-MPB-R67	Bedrock	22.5
10-MPB-R68	Bedrock	23.8
10-MPB-R42	Bedrock	21.6
10-MPB-R74	Bedrock	23.1
10-MPB-R75	Bedrock	23.2
10-MPB-R75	Bedrock	23.3
10-MPB-R76	Bedrock	23.3
10-MPB-R46A	Bedrock	21.1
10-MPB-R50	Bedrock	20.6
10-MPB-R55	Bedrock	20.9
10-MPB-004	Till	24.4
10-MPB-026	Till	20.9
11-MPB-029	Till	7.8
11-MPB-054	Till	20.5
11-MPB-055	Till	19.1
11-MPB-060	Till	21.8
10-MPB-030	Till	-5.3

Table 3-5: Results for Pb isotope analysis on galena grains recovered from till and bedrock samples. The 2-sigma error is reported for each measurement.

Sample		²⁰⁸Pb/²⁰⁴Pb	2-sig	²⁰⁷Pb/²⁰⁴Pb	2-sig	²⁰⁶Pb/²⁰⁴Pb	2 -sig
10-MPB-R02	total replacement	38.132	0.004	15.570	0.002	18.177	0.001
10-MPB-R19	cubic galena	38.137	0.004	15.571	0.002	18.171	0.002
10-MPB-R30	skeletal galena	38.150	0.005	15.575	0.002	18.172	0.002
10-MPB-R65	cubic galena	38.138	0.005	15.571	0.002	18.172	0.002
10-MPB-R67	early galena	38.146	0.005	15.573	0.002	18.172	0.002
10-MPB-R67	dendritic	38.135	0.005	15.569	0.002	18.169	0.002
10-MPB-R68	dendritic	38.136	0.005	15.570	0.002	18.166	0.002
10-MPB-R46A	skeletal galena	38.132	0.003	15.567	0.001	18.166	0.001
10-MPB-R46B	late galena	38.136	0.005	15.570	0.002	18.166	0.002
10-MPB-R50	banded	38.152	0.004	15.575	0.001	18.170	0.001
10-MPB-R55	banded	38.141	0.006	15.572	0.002	18.166	0.002
10-MPB-OO4	till	38.135	0.004	15.573	0.002	18.174	0.001
10-MPB-O26	till	38.135	0.003	15.574	0.001	18.179	0.001
11-MPB-O29	till	38.130	0.005	15.576	0.002	18.166	0.002
11-MPB-O53	till	38.141	0.004	15.576	0.001	18.175	0.001
11-MPB-O55	till	38.141	0.005	15.576	0.002	18.180	0.002
11-MPB-O60	till	38.136	0.007	15.574	0.002	18.175	0.003

down-ice of the ore zone. Concentrations of Pb in the till matrix ranged from 15 to 2015 ppm and were highest in samples overlying (10-MPB-004) and immediately down ice (10-MPB-026) of the orezone. Cadmium concentrations in till samples varied between 0.11 and 11.37 ppm and were highest in till samples overlying (10-MPB-004) and down-ice of the deposit (Fig.3-3; 10-MPB-005, -026, -028, -030 and -031). Concentrations of Fe in the till matrix ranged from 0.70 to 1.71 %. The highest concentrations were from samples on the bedrock bench surrounding deposit O28 as well as in up-ice sample 11-MPB-058. Iron had a background concentration of <1.04 %. Sulphur concentrations ranged from 0.2 to 0.33 % and the background concentration was <0.01 %. Concentrations of Se varied between 0.05 and 6.2 ppm. The background concentration for this element was <0.14 %. Thallium concentrations ranged from 0.01 to 0.42 % with a background concentration of <0.13 %. The highest concentrations of S, Se and Tl occurred on the bedrock bench surrounding deposit O28. Thallium also had elevated concentrations in samples collected 1 m below the natural land surface mainly in the direction of the second ice flow trajectory.

3.11   Discussion

The sand content of the till at Pine Point is moderate but it is still useful for indicator mineral studies. The high inorganic carbon content of the till matrix is a reflection of the underlying Paleozoic carbonate rocks. Sphalerite, galena and pyrite typically weather quickly once exposed to the atmosphere and are not preserved as indicator minerals in other types of massive sulphide deposits. At

Table 3-6: Summary table of pathfinder elements and their distance down ice from the ore zone.

Element	Background	m down-ice			
		<10	10-50	50-250	500
Pb (ppm)	28	2015	270	75	48
Zn (ppm)	82	3497	604	211	160
Fe (%)	1.04	1.15	0.97	0.86	0.81
Cd (ppm)	0.2	11.4	1.3	0.5	0.4
Tl (ppm)	0.13	0.15	0.13	0.13	0.11
S (%)	0.01	0.27	0.03	0.01	0.02
Se (ppm)	0.14	0.30	0.20	0.14	0.19

Pine Point, however, the carbonate content of the till matrix helps to preserve the sulphide minerals as indicator minerals (Stu Averill, pers. comm).

Before this study only one direction of ice flow was known for the region (Lemmen, 1998a, b), possibly due to the limited exposure of unweathered bedrock outcrop. The availability of striae on bedrock surfaces exposed during past mining practices indicate the possibility of 3, possibly 4, directions of ice flow for the region. These striae on the bedrock surface near the open pit indicate that glaciers were in contact with the surface and, therefore, eroded the orezone. These three different ice flow trajectories likely reflect changing conditions on the western margin of the LIS during the Wisconsin as opposed to separate glaciations based on the thickness of the continuous till sequences and the lack of evidence (intertill sediments, oxidized horizons) for the latter (Rice et al., 2013).

3.11.1 Bedrock variability

The Pine Point district is approximately 1600 km^2 with many deposits. At the time it was mined the company only assayed for Pb, Zn, Fe, Mn and Na (unpublished memo, Skall 1970). Previous studies at Pine Point suggested that there are no consistent variations of the trace element concentrations in sphalerite, galena or pyrite either across the district or within the paragenesis (Kyle, 1977). The small sample set presented here, suggests, however, that there are some spatial and temporal variations in major and trace element contents of sphalerite, galena and pyrite. These variations are evident in different deposits at Pine Point as well as within the different varieties and textures of minerals.

The crystal structure of sphalerite can contain a variety of minor/trace elements (Doelter, 1912; Stoiber, 1940). In some MVT districts these elements are economically retrievable (e.g. 4700 ppm Cd in the deposits of the Tri-State district; Hagni, 1983) and in some cases they cause environmental concerns for mining practices (Schwartz, 1997; Schwartz, 2000). Trace elements can occur in sphalerite by simple substitution (Fe^{2+}, Cu^{2+}, Cd^{2+}, Mn^{2+} and Hg^{2+}; Cook et al.,

2009) into the lattice, coupled substitution (Cu^++In^{3+}; Johan, 1988) or as micro-inclusions of other minerals that contain these elements (e.g. Stoiber, 1940; Warren and Thompson, 1945; Cook et al., 2009; Pfaff et al., 2011).

A recent study by Pfaff et al., (2011) on the Wiesloch MVT deposit in Germany showed that trace element concentrations of Cd, Cu, and Ag occur in higher concentrations in crystalline sphalerite while As and Pb concentrations are higher in colloform sphalerite. The results of the Wiesloch study are mostly consistent with the results seen in this study, in that Cu, and Ag preferentially occur in crystalline sphalerite while As and Pb concentrations are found in colloform sphalerite (Fig. 3-15b) with the exception of Cd. Cadmium concentrations at Pine Point are high in the crystalline honey-brown sphalerite but are below detection limits in the crystalline blackjack sphalerite. The lack of Cd in blackjack sphalerite at Pine Point could be the result of the lack of cation sites available due to Fe occupying these sites as these two cations substitute in the same location (Kostov and Minceva-Stefanova, 1982). This would also explain why the highest Cd concentrations and the lowest Fe concentrations are found in honey-brown sphalerite. Cadmium concentrations for sphalerite grains determined in this study are slightly higher (0.17 wt % higher) than those reported in previous literature for Pine Point (Kyle, 1977; Jonasson and Sangster, 1978). The larger sample set in this study (n=418) versus the previous study (n=69) could explain this difference.

The concentrations of Pb in cleiophane and colloform sphalerite are higher than those in the other varieties. It is not known if these values pertain to Pb in the mineral lattice, or come from micro-inclusions in the sphalerite. Germanium is commonly partitioned into low-Fe sphalerite (Johan, 1988). This is consistent with the low Ge concentrations in blackjack sphalerite, which has much higher Fe concentrations than the other minerals. There are no correlations with other elements to determine whether Ge substitution is by simple substitution of Zn^{2+} by Ge^{2+} or by coupled substitution of tetravalent Ge with another monovalent element (as suggested by Johan 1988). As with Cd,

Ge is also typically present in MVT districts in economic concentrations (Hagni, 1983).

There is a slight decrease in Fe concentrations in sphalerite from deposits in the east (1.22 wt %, deposit O28) to those in the west (0.41 wt %, deposit R190) of the district. The amount of Fe that is incorporated into the sphalerite crystal structure is influenced by the fugacity of reduced S as well as the temperature and pressure of the fluid (Barton and Toulmin, 1966; Anderson, 1973; Scott, 1973; Hutchinson and Scott, 1983). Iron content of sphalerite (in equilibrium with pyrite) increases with decreasing temperature and pressure (Barton and Toulmin, 1966; Scott, 1973) which could indicate that the ore forming fluids were cooling and/or depressurizing as they migrated to the east. These studies were conducted at higher temperatures and pressures than at Pine Point so further investigation would be required to determine the cause of this trend at Pine Point.

Sphalerite grains from deposit M67 contain lower concentrations of Ge, Ag, In, Sb, Pb, Cu, and Hg than other deposits. This may suggest that these fluids had a fundamentally different chemistry (i.e. were derived from a different source area), or that precipitation elsewhere had already depleted the fluids in these elements. Deposits M67 and HZ appear to be different in trace element geochemistry than the other deposits in this study. Further work is required to determine whether these trends do exist or if they are artefacts of sampling.

Silver and Bi are common trace elements found in galena formed in many different geological settings (Foord and Shawe, 1989). However, the very low Ag concentrations found in this study are consistent with the literature for Pine Point (Kyle, 1977) and low Ag concentrations are characteristic of galena from MVT deposits (Hagni, 1983). Iron concentrations were also generally higher and Cu concentrations were generally lower in galena grains from this study compared to previous studies (Kyle, 1981). This is likely due to the larger sample set of this study compared to previous studies.

Most studies have concluded that trace elements associated with galena

are most likely the result of micro-inclusions (Edwards, 1954; Nesterova, 1958; Foord and Shawe, 1989). The varying concentrations of Fe, Zn, and Ge may be attributed to micro-inclusions of sphalerite. The trace elements Sb and Hg can substitute for Pb in the galena structure. The higher Sb concentrations in the two eastern most deposits, and the bimodal distribution of S (low and high) in galena grains in bedrock as determined by EPMA could be indicative of changing ore fluid compositions.

Data from EPMA analysis show some differences in the Mn, Zn, As, Ag and Cu trace element contents of pyrite by deposit. There were no differences in the pyrite trace element concentrations determined for this study compared to those of previous studies (Kyle, 1981). Zinc, As and Cu concentrations may be elevated in pyrite grains that contain micro-inclusions of sphalerite, arsenopyrite and chalcopyrite, respectively (Fleischer, 1959). Manganese can substitute for Fe in the pyrite crystal structure (Auger, 1941; Fleischer, 1959), and the elevated contents of this element in deposit L65 likely indicates the composition of the fluid that deposited these pyrites differed from those of the other deposits. There is no trend in Fe concentrations from east to west as there is in sphalerite. Pyrite is paragenetically earlier than sphalerite and may have precipitated under different physiochemical conditions.

The method of analysis used here, EPMA, is not conducive to analysing very low concentrations of trace elements and there is a need for laser ablation ICP-MS studies to further explore the variations of the sulphide chemistry temporally and spatially.

3.11.2 Bedrock isotopes:

The Pb isotope data from the bedrock and galena recovered from till samples are comparable with those reported in the literature for Pine Point (e.g. Sasaki and Krouse, 1969; Cumming and Robertson; 1969; Cumming et al., 1990) as well as others along the GSSZ (e.g. Paradis et al., 2006; Paulen et al., 2011). These lead isotope data have been plotted with respect to the 'shale curve'

(Fig. 3-19) of Godwin and Sinclair (1982) that also contains data from studies conducted on other MVT districts in the Canadian Cordillera as well as the WCSB. All 17 samples from both bedrock and till lie within the Pine Point MVT cluster indicating that those samples that were recovered from till likely have a Pine Point origin.

The Pb isotope values at Pine Point have a characteristic and unusually narrow range in compositions; this has been attributed to either a homogenous source or to thorough mixing during extraction, transport and subsequent sulfide deposition (Cumming and Robertson, 1969; Cumming et al., 1990). The Pb isotope signature is indicative of Pb sourced from a depleted lower crustal source such as the underlying basement rocks (Nelson et al., 2002; Paradis et al., 2006). Equally the δ^{34}S values determined for bedrock samples in this study are comparable with the data from previous studies at Pine Point (e.g. Evans et al., 1968; Sasaki and Krouse, 1969) as well as the Blende and Rocky Mountain
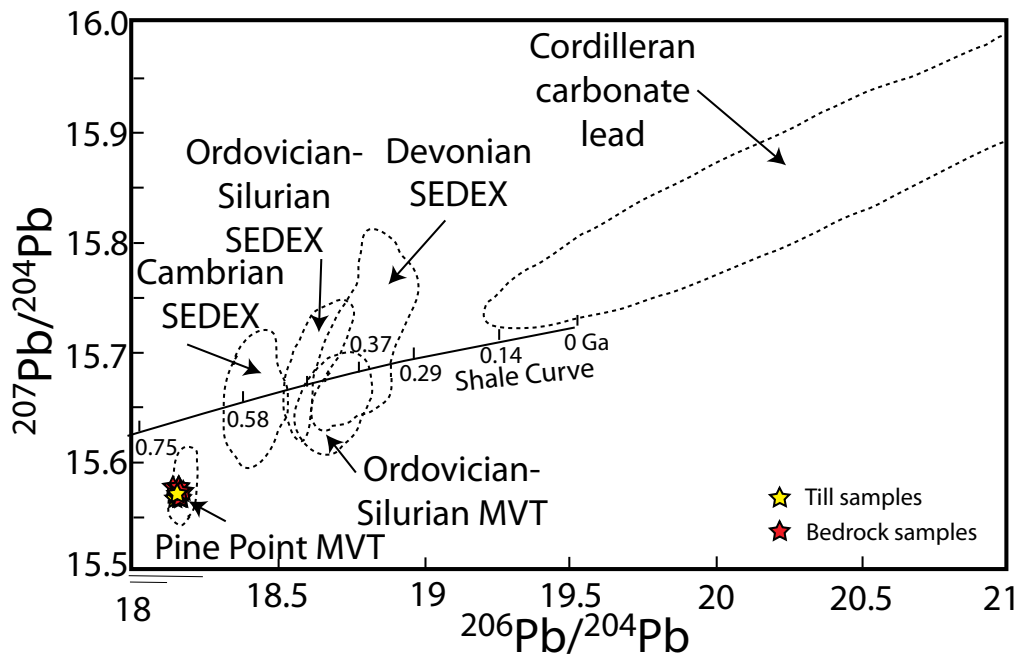
Fig. 3-19: Lead isotope values for till and bedrock samples plotted on the 'shale curve' (Godwin and Sinclair, 1982). Both till and bedrock samples from this study plot within the narrow range defined for Pine Point. Categories for this plot are defined from data from Godwin et al., (1982), Morrow and Cumming, (1982), Nelson et al., (2002) and Paradis et al., (2006).

76

deposits (Fig. 3-16). The majority of sphalerite grains recovered from till samples had similar δ^{34}S values to the bedrock samples as well as other MVT districts (Paradis et al., 2006) in British Columbia and Alberta. The bulk of our data fall within the narrow range of δ^{34}S values of 20.1 ‰ ± 2.6 defined by Sasaki and Krouse (1969) for the Pine Point District. The isotopic composition of the S in these deposits is too enriched in ^{34}S to be from a magmatic source (Evans et al., 1968) and instead are likely to be derived from Devonian seawater which had δ^{34}S values of approximately +20 ‰ during Givetian time (Claypool et al., 1980). Previous studies attribute the relatively small range of δ^{34}S values to sulfate reduction by biogenic activity followed by homogenization before emplacement as sulfides (Sasaki and Krouse, 1969). Other studies of the sulphur isotopic composition of the bitumen at Pine Point suggest that the incorporation of heavy sulphur into bitumen may have resulted in the thermochemical reduction of sulphate that produced the sulphide which caused the precipitation of the Pine Point ores (Macqueen and Powell, 1983; Powell and Maqueen, 1984; Fowler et al., 1993)

There were two till grains that had significantly different signatures. The sphalerite grain that yielded a -5.3 ‰ value appears to be coated by some material, possibly bitumen, which could alter the isotopic composition. The δ^{34}S values for bitumen were determined to range from +3 ‰ to +12.4 ‰ (Sasaki and Krouse, 1969; Powell and Macqueen, 1984). It is also possible that this grain contains micro-inclusions of other minerals that may also alter the isotopic signature. The other outlying sample, 11-MPB-029, which has δ^{34}S values of +7.8 ‰, is visually indistinguishable from the other grains. This sample is located approximately 20 m down-ice of the ore zone at deposit O28. The close proximity of this sample to the ore zone likely indicates that this sphalerite grain is from Pine Point and not some other source.

The δ^{34}S value of +7.8 ‰ can also be derived from the reduction of seawater sulphate (Claypool et al., 1980). The proximity of the sample to the O28 deposit suggests that the sample set (n=118) of Sasaki and Krouse (1969)

77

may not have captured the total isotopic variability in the Pine Point district and the true range of $\delta^{34}S$ values may be larger. In any case, the S and Pb isotopic signatures of the indicator grains do seem to reflect those of the deposit source and are a useful tool in an indicator mineral study.

3.11.3 Relationship between till geochemistry of the <0.063 mm fraction of till and indicator minerals

In till samples on the bedrock bench surrounding deposit O28, the geochemical signature is dispersed strongly in the direction of the first ice flow trend. The elements Cd, Fe, and Se all have diminished concentrations within 40 m of the ore zone while S has below background concentrations within 24 m of the ore zone. Samples that are farther away (>250 m) from the ore zone have concentrations that are higher at the tops of sections, though these are not as high as those samples on the bedrock bench. This likely a net effect of all 3 ice flow trajectories in the area. These results indicate that the dispersal of mineralized debris experiences a relatively low angle of climb. Regional samples also contain above background concentrations for all pathfinder elements indicating these elements are detectable on a regional scale.

Till samples that had high concentrations of Zn in the silt + clay fraction (<0.063 mm) did not necessarily have large quantities of sphalerite grains in the sand sized fraction of till and vice versa. Till samples approximately 30 m from the orezone contain above background concentrations of sphalerite grains in the sand sized fraction, however they do not contain anomalous values in the silt + clay fraction. The sphalerite grains in the till closer to the deposit typically remained in the sand sized fraction. Till samples that were located further down ice from the orezone had higher concentrations of Zn in the till matrix and lower counts of sphalerite grains in the sand sized fraction. These further till samples were typically located at the tops of 3 m vertical sections and would have been subjected to all three phases of ice-flow.

Galena grains recovered from till tend to have a stronger correlation with Pb concentrations in the silt and clay fraction. This is likely because galena is a

softer mineral (hardness: 2.5) than sphalerite (hardness: 3.5-4) and therefore would be more susceptible to glacial comminution than sphalerite. Samples that contain large quantities of galena grains and have high Pb concentrations in the till matrix could be due to the break-up of larger, massive galena grains that exist in the bedrock.

Galena grains coated in anglesite ($PbSO_4$) were recovered from till samples that were considered to contain low to medium levels of oxidation. Oxidation levels of till samples were determined based on field observations. The coating on these grains is patchy and SEM images indicate that the majority of anglesite occurs in depressions within the grain, which suggests that this mineral may have formed prior to glacial entrainment. Anglesite may have entirely coated these grains which was then removed during glacial transport. There was no anglesite identified in the bedrock samples.

3.11.4 Glacial transport

Sphalerite, galena and pyrite as well as elevated concentrations of all pathfinder elements were detected in till down-ice of the O28 deposit at the surface at least 500 m from the deposit and in regional samples at Buffalo River approximately 10 km down ice from the closest known ore body (deposit N81; Fig. 3-1). It is unknown whether or not this ore body sub-cropped at the surface so it is possible that these elements and indicator minerals are not locally derived. The coarsest sphalerite and galena grains were recovered from samples within 50 m of the O28 ore-body indicating that indicator mineral grain size can indicate proximity to deposit.

Most of the indicator mineral dispersal appears to be in the direction of the first two ice flow trajectories indicating that the deforming bed of the glacier (e.g., Alley et al., 1986; van der Meer et al., 2003), at the time of the third ice flow trajectory, did not have access to bedrock or the ore zone. The absence of striations in the direction of the last ice flow trajectory (250°) on the west side of deposit O28 supports this hypothesis. This area was likely till covered following

79

the intermediate ice flow phase.

3.12   Implications for exploration

Galena and sphalerite are preserved as indicator minerals in carbonate-hosted deposits. In other base metal deposits these minerals would be easily weathered in a surficial environment and would be ineffective indicator minerals.

In this study, surface till sampling was able to detect MVT deposits that were buried under approximately 3 m of till up to 500 m from a known deposit. Till geochemical anomalies were detected in regional samples indicating that regional sampling will be able to detect the presence of the district but not necessarily individual deposits. While surface sampling was able to detect deposit O28, in areas of thicker cover, samples from depth will also be needed.

Based on the results of this study some recommendations of exploration techniques for MVT deposits in glaciated terrain can be made. First and foremost it is important to obtain detailed, up to date ice flow information. In areas with multiple ice flow trajectories, a sampling strategy should be in place to capture possible dispersal in the direction of the net effect of each trajectory. To ensure that any data collected is of significance it is important to follow QA/QC procedures for till sampling, which are described in great detail by Spirito et al., (2011).

The <0.063 mm fraction of till (matrix) should be analyzed for base and precious metals by aqua regia/ICP-MS. It is beneficial to analyze for precious metals as some MVT deposits have economical quantities of Ag (i.e. Nanisivik). In addition to matrix analyses, indicator minerals should be recovered from the pan concentrate, 0.25-0.5 mm, 0.5-1.0 mm, and 1.0-2.0 mm non-ferromagnetic heavy mineral fractions. The two coarsest fractions can be used to determine proximity to the ore body. Finally, analyzing galena and sphalerite grains for their Pb and S isotopic signature can help characterize the bedrock source. Before submitting samples for Pb and S isotopic analysis, it is important to image sphalerite and galena grains with a SEM to check for any impurities that may alter the signal or

give null values.

3.13   Conclusions

There are now three, possibly four, phases of ice flow known for the Pine Point area. The west-northwest dispersal of metal-rich till in the O28 area indicates that at least the oldest ice flow trajectory had contact with mineralization. The pathfinder elements Zn, Pb, Fe, Cd, S, and Tl as well as indicator minerals sphalerite and galena are detectable at the surface near the deposit. EPMA may have identified trace element variations between different deposits though further work is required to follow up on this.

Sulphur and Pb isotopes were successful in determining provenance of sphalerite and galena grains recovered from till samples. The isotope results indicate that these grains likely originated at Pine Point.

Based on EPMA data collected in this study there may be possible trace element variations among the different varieties of sphalerite, galena and pyrite as well as across the different deposits however further investigation is required to quantify and validate these findings.

An exploration program consisting of till matrix geochemistry, characterization of indicator minerals and S isotopes are the ideal combination for determining the presence of deposits associated with MVT districts in glaciated terrain.

3.14   References

Alley, R.B., Blankenship, D.D., Bentley, C.R. and Rooney, S.T. 1986. Deformation of till beneath ice stream B, West Antarctica. Nature, v. 322, p. 57-59.

Adams, J.J., Rostron, B.J., and Mendoza, C.A., 2000. Evidence for two-fluid mixing at Pine Point, Northwest Territories. Journal of Geochemical Exploration, v. 69-70, p. 103-108.

Anderson, G.M., 1973. The hydrothermal transport and deposition of galena and sphalerite near 100°C. Economic Geology, v. 68, p. 480-492.

Anderson, G.M., and Macqueen, R.W., 1988. Ore deposit models-6. Mississippi Valley-type lead-zinc deposits. *In*: Roberts, R.G., and Sheahan, P.A. (eds) *Ore deposit models*. Geoscience Canada, reprint series 3, p 79-90.

Arne, D.C., Curtis, L.W., and Kissin, S.A., 1990. Internal zonation in a carbonate-hosted Zn-Pb-Ag deposit, Nanisivik, Baffin Island, Canada. Economic Geology, v. 86, p. 699-717.

Auger, P.E., 1941. Zoning and district variations of the minor elements in pyrite of Canadian gold deposits. Economic Geology, v. 36, p. 401-423.

Barton, P.B. Jr., and Toulmin, P., 1966. Phase relations involving sphalerite in the Fe-Zn-S system. Economic Geology, v. 61, p. 815-849.

Bostock, H.S., 1970. Physiographic regions of Canada. Geological Survey of Canada, Map 1254A, scale 1:5,000,000.

Cathles, L.M., and Smith, A.T., 1983. Thermal constraints on the formation of Mississippi Valley-type lead-zinc deposits and their implications for episodic basin dewatering and deposit genesis. Economic Geology, v. 78, p 983-1002.

Claypool, G.E., Holser, W.T., Kaplan, I.R., Sakaiand, H., and Zak, I., 1980. The age curves of sulfur and oxygen isotopes in marine sulfate and their mutual interpretation. Chemical Geology, v. 28, p. 199-260.

Cook, N.J., Ciobanu, C.L., Pring, A., Skinner, W., Danyushevsky, L., Shimizu, M., Saini-Eidukat, B., and Melcher, F., 2009. Trace and minor elements in sphalerite: a LA-ICP-MS study. Geochemica et Cosmochimica Acta, v. 73, 4761-4791.

Craig, B.G., 1965. Glacial Lake McConnell, and the surficial geology of parts of Slave River and Redstone River map-areas, District of Mackenzie. Geological Survey of Canada Bulletin 122, p. 1-33.

Cumming, G.L., and Robertson, D.K., 1969. Isotopic composition of lead from the Pine Point deposit. Economic Geology, v. 64, p 731-732.

Cumming, G.L., Kyle, J.R., and Sangster, D.F., 1990. Pine Point: A case history of lead isotopic homogeneity in a Mississippi Valley-type district. Economic Geology, v. 85, p 133-144.

Doelter, C., 1912. Handbuch der Mineralchemie. Part 1, p. 307-313.

Dreimanis, A., 1960. Geochemical prospecting for Cu, Pb, and Zn in glaciated areas, eastern Canada. *In*: Marmo, V., Puranen, M. (eds.), Geological Results of Applied Geochemistry and Geophysics, p. 7-19. Report of the 21st International Geological Congress, Part 2, Det Berlingske Bogtrykkeri, Copenhagen.

Dyke, A.S. 2004. An outline of North American deglaciation with emphasis on central and northern Canada. In: J. Ehlers and P.L. Gibbard (eds.), Quaternary Glaciations - Extent and Chronology, Part II. North America. Elsevier B.V., Amsterdam, Development in Quaternary Science Series, Vol. 2: 373-424.

Dyke, A.S., and Prest, V.K., 1987. Late Wisconsin and Holocene history of the Laurentide Ice Sheet. Geographie physique et Quaternaire, v. 41, p. 237-263.

Eaton, D.W. and Hope, J. 2003. Structure of the crust and upper mantle of the Great Slave Lake shear zone, northwestern Canada, from teleseismic analysis and gravity modelling. Canadian Journal of Earth Sciences, v. 40, p. 1203-1218.

Edwards, A.B., 1954. Textures of the ore minerals and their significance. Australasian Institute of Mining and Metallurgy, 2nd edition, p. 1-242.

Evans, C.R., Campbell, F.A., and Krouse, H.R., 1968. A reconnaissance study of some western Canadian lead-zinc deposits. Economic Geology, v. 64, p 349-359.

Fleischer, M., 1959. Minor elements in some sulfide minerals. Economic Geology, 50th Anniversary Volume, p. 970-1024.

Foord, E.E., and Shawe, D.R., 1989. The Pb-Bi-Ag-Cu-(Hg) chemistry of galena and some associated sulfosalts: a review and some new data from Colorado, California and Pennsylvania. Canadian Mineralogist, v. 27, p. 363-382.

Fowler, M.G., Kirste, D.M., Goodarzi, F., and Macqueen, R.W., 1993. Optical and geochemical classification of Pine Point bitumens and evidence for their origin from two separate source rocks. Energy Sources, v. 15(2), p. 315-337.

Garven, G., and Freeze, R.A., 1984. Theoretical-analysis of the role of groundwater-flow in the genesis of stratabound ore-deposits.2. Quantitative results, American Journal of Science, v. 284 (10), p. 1125-1174.

Girard, I., Klassen, R.A., and Laframboise. 2004. Sedimentology laboratory manual. Terrain Sciences Division, Geological Survey of Canada, Open file 4823.

Gleeson, S.A. and Turner, W.A., 2007. Fluid inclusion constraints on the origin of the brines responsible for Pb-Zn mineralization at Pine Point and coarse non-saddle and saddle dolomite formation in southern Northwest Territories. Geofluids v. 7, p 51-68.

Godwin, C.J., and Sinclair, A.J., 1982. Average lead isotope growth curves for shale-hosted zinc-lead deposits, Canadian Cordillera. Economic Geology, v., 77, p. 675-690.

Hagni, R.D., 1983. Minor elements in Mississippi Valley-type ore deposits. *In:* Shanks, W.C. (ed) *Cameron Volume on Unconventional Mineral Deposits*. Society of Economic Geologists, 246 p.

Hannigan, P., 2007. Metallogeny of the Pine Point Mississippi Valley-Type zinc-lead district, southern Northwest Territories. *In:* Goodfellow, W.D. (ed) *Mineral Deposits of Canada: A Synthesis of Major Deposit-Types, District Metallogeny, the Evolution of Geological Provinces, and Exploration Methods*. Geological Association of Canada, Mineral Deposits Division, Special Publication No. 5, p. 609-632.

Holroyd, R.W., Hodson, T.W., and Carter, K.M., 1988. Unpublished termination report, Pine Point Mines Ltd., June 28, 1988.

Hutchinson, M.N., and Scott, S.D., 1983. Experimental calibration of the sphalerite cosmobarometer. Geochemica et Cosmochemica Acta 47, p. 101-108.

Jackson, S.A., and Beales, F.W., 1967. An aspect of sedimentary basin evolution: the concentration of Mississippi Valley-type ores during late stages of diagensis. Canadian Petroleum Geology Bulletin, v. 15, p 383-433.

Johan, Z., 1988. Indium and germanium in the structure of sphalerite: an example of coupled substitution with copper. Mineralogy and Petrology, v. 39, p. 211-229.

Jonasson, I.R., and Sangster, D.F., 1978. Zn:Cd ratios for sphalerites separated from some Canadian sulphide ore samples. Geological Survey of Canada, Scientific and Technical Notes, Current Research Paper 78-1B. p. 195-201.

Kostov, I., and Minceva-Stefanova, J., 1982. Sulphide minerals, Crystal chemistry, parageneses and systematics. Academic Publishing House, Pensoft. 415 p.

Krebs, W., and Macqueen, R., 1984. Sequence of diagenetic and mineralization events, Pine Point Lead-Zinc Property, Northwest Territories, Canada. Bulletin of Canadian Petroleum Geology, v. 32, p. 434-464.

Kyle, J.R., 1977. Development of sulphide hosting structures and mineralization, Pine Point, Northwest Territories. Ph.D. thesis, University of Western Ontario, 226 p.

Kyle, J.R., 1981. Geology of the Pine Point lead-zinc district. *In:* Wolf, K.H., (ed) *Handbook of strata-bound and stratiform ore deposits.* Elsevier Publishing Company, New York, v. 9, p 643-741.

Leach, D.L, and Sangster, D.F., 1993. Mississippi Valley-type lead-zinc deposits. *In*: Kirkham, R.V., Sinclair, W.D., Thorpe, R.I., and Duke, J.M. (eds) *Mineral Deposits Modeling.* Geological Association of Canada, Special Paper 40, p 289-314.

Lemmen, D.S., 1990. Surficial materials associated with glacial Lake McConnell, southern District of Mackenzie. *In:* Current Research, Part D, Geological Survey of Canada, Paper 90-1D, p. 79-83.

Lemmen, D.S., 1998a. Surficial geology, Buffalo Lake, District of Mackenzie; Northwest Territories. Geological Survey of Canada, "A" Series Map 1906, scale 1:250 000.

Lemmen, D.S., 1998b. Surficial geology, Klewi River, District of Mackenzie; Northwest Territories. Geological Survey of Canada, "A" Series Map 1905, scale 1: 250 000.

Lemmen, D.S., Duk-Rodkin, A., and Bednarski, J.M., 1994. Late glacial drainage systems along the northwestern margin of the Laurentide Ice Sheet. Quaternary Science Reviews, v. 13, p. 805-828.

Lundqvist, J., 1990. Glacial morphology as an indicator of the direction of glacial transport, *In:* Kujansuu, R., and Saarnisto, M. (eds) Glacial Indicator Tracing, A.A. Balkema, p. 61-70.

Macqueen, R.W., and Powell, T.G., 1983. Organic geochemistry of the Pine Point lead-zinc ore field and region, Northwest Territories, Canada. Economic Geology, v. 78, p 1-25.

Marshall, R.R., and Joensuu, O., 1961. Crystal habit and trace element content of some galenas. Economic Geology, v. 56, p. 758-771.

McClenaghan, M.B. 2005. Indicator mineral methods in exploration. Geochemistry: Exploration, Environment, Analysis, vol. 5, p. 233–245.

McMartin, I. and Paulen, R.C. 2009. Ice-flow indicators and the importance of ice-flow mapping for drift prospecting. *In:* R.C. Paulen and I. McMartin (eds.), *Application of Till and Stream Sediment Heavy Mineral and Geochemical Methods to Mineral Exploration in Western and Northern Canada*. Geological Association of Canada, Short Course Notes 18, p. 15-34.

Morrow, D.W., 1998. Regional subsurface dolomitization; Models and constraints. Geoscience Canada, v. 25, p. 57-70.

Morrow, D.W., Cumming, G.L., and Aulstead, K.L., 1990. The gas-bearing Devonian Manetoe Facies, Yukon and Northwest Territories. Geological Survey of Canada, Bulletin 400, P. 1-54.

Morrow, D.W., MacLean, B.C., Miles, W.F., Tzeng, P. and Pana, D. 2006. Subsurface structures in southern Northwest Territories and northern Alberta: implications for mineral and petroleum potential. *In:* Hannigan, P.K. (ed.) Potential for Carbonate-hosted Lead-zinc Mississippi Valley-type Mineralization in Northern Alberta and Southern Northwest Territories: Geoscience Contributions, Targeted Geoscience Initiative. Geological Survey of Canada, Bulletin 591, p. 41-59.

Nelson, J., Paradis, S., Christensen, J. and Gabites, J. 2002. Canadian Cordilleran Mississippi Valley-type deposits: A case for Devonian-Mississippian back-arc hydrothermal origin. Economic Geology, v. 97, p. 1013–1036.

Nesterova, Y.S., 1958. On the question about the chemical composition of galena. Geokhimiya, v. 7 p. 667-677 (in Russian).

Okulitch, A.V. (compiler) 2006. Phanerozoic bedrock geology, Slave River, District of Mackenzie, Northwest Territories. Geological Survey of Canada, Open File 5281, scale 1:1,000,000.

Olson, R.A., 1977. Geology and genesis of zinc-lead deposits within a late Proterozoic dolomite, northern Baffin Island, N.W.T. Unpublished PhD thesis, University of British Columbia, 371 p.

Oviatt, N.M., McClenaghan, M.B., Paulen, R.C., and Gleeson, S.A., 2013. Till geochemical signatures of the Pine Point Mississippi Valley-type district, Northwest Territories. Geological Survey of Canada Open File 7320, 18 p.

Pana, D., 2006. Unravelling the structural control of Mississippi Valley-type deposits and prospects in carbonate sequences of the Western Canada Sedimentary Basin. *In:* Hannigan, P.K. (ed.) *Potential for Carbonate-hosted Lead-zinc Mississippi Valley-type Mineralization in Northern Alberta and Southern Northwest Territories: Geoscience Contributions, Targeted Geoscience Initiative*. Geological Survey of Canada, Bulletin 591, p. 255-304.

Paradis, S., Turner, W.A., Coniglio, M., Wilson, N. and Nelson, J.L. 2006. Stable and radiogenic isotopic signatures of mineralized Devonian carbonate rocks of the northern Rocky Mountains and the Western Canada Sedimentary Basin. In: P.K. Hannigan (ed.), Potential for Carbonate-hosted Lead-zinc Mississippi Valley-type Mineralization in Northern Alberta and Southern Northwest Territories: Geoscience Contributions, Targeted Geoscience Initiative, Geological Survey of

Canada, Bulletin 591, p. 75-103.

Paradis, S., Hannigan, P., and Dewing, K., 2007. Mississippi Valley-type lead-zinc deposits, *In:* Goodfellow, W.D. (ed) *Mineral Deposits of Canada: A Synthesis of Major Deposit-Types, District Metallogeny, the Evolution of Geological Provinces, and Exploration Methods*. Geological Association of Canada, Mineral Deposits Division, Special Publication No. 5, p. 609-632.

Paulen, R.C., Paradis, S., Plouffe, A., and Smith, I.R., 2011. Pb and S isotopic composition of indicator minerals in glacial sediments from NW Alberta, Canada: implications for Zn-Pb base metal exploration. Geochemistry: Exploration, Environment, Analysis, v. 11, p. 309-320.

Pfaff, K., Koenig, A., Wenzel, T., Ridley, I., Hildebrandt, L.H., Leach, D.L., and Markl, G., 2011. Trace and minor element variations and sulfur isotopes in crystalline and colloform ZnS: Incorporation mechanisms and implications for their genesis. Chemical Geology, v. 286, p. 118-134.

Plouffe, A., Paulen, R.C., and Smith, I.R., 2006. Indicator mineral content and geochemistry of glacial sediments from northwest Alberta (NTS 84L, M): new opportunities for mineral exploration. Geological Survey of Canada, Open File 5121.

Powell, T.G., and Macqueen, R.W., 1984. Precipitation of sulfide ores and organic matter: Sulfate reactions at Pine Point, Canada. Science, v. 224, p 63-66.

Qing, H., and Mountjoy, E.W., 1994. Origin of dissolution vugs, caverns, and breccias in the Middle Devonian Presqu'ile Barrier, host of Pine Point Mississippi Valley-type deposits. Economic Geology, v. 89, p 858-876.

Rhodes, D., Lantos, E.A., Lantos, J.A., Webb, R.J., Owens, D.C., 1984. Pine Point orebodies and their relationship to the stratigraphy, structure, dolomitization, and karstification of the middle Devonian Barrier complex. Economic Geology, v. 79, p. 991-1055.

Rice, J.M., Paulen, R.C., Menzies, J.M., McClenaghan, M.B. and Oviatt, N.M., in press. Glacial stratigraphy of the Pine Point Pb-Zn mine site, Northwest Territories. Geological Survey of Canada, Current Research Paper.

Sasaki, A., and Krouse, H.R., 1969. Sulfur isotopes and the Pine Point lead-zinc mineralization. Economic Geology, v. 64, p. 718-730.

Schwartz, M.O., 1997. Mercury in zinc deposits: economic geology of a polluting element. International Geology Review, v. 39, p. 905-923.

Schwartz, M.O., 2000. Cadmium in zinc deposits: economic geology of a polluting element. International Geology Review, v. 42 (5), p. 445-469.

Scott, S.D., 1973. Experimental calibration of the sphalerite geobarometer. Economic Geology, v. 68, p. 466-474.

Shilts, W.W. 1996. Chapter 15, Drift exploration. *In*: MENZIES, J. (ed.) Past Glacial Environments, Sediments, Forms and Techniques, Butterworth Heinemann, Toronto, p. 411-439.

Skall, H., 1975. The paleoenvironment of the Pine Point lead-zinc district. Economic Geology, v. 70, p. 22-47.

Skall, H., 1977. The geology of the Pine Point barrier reef complex. *In:* McIlreath, I.A., and Harrison, R.D. (eds) *The geology of selected carbonate oil, gas and lead-zinc reservoirs in western Canada.* Canadian Society of Petroleum Geologists, Core Conference, no. 5, p 19-38.

Smith, D.G. 1994. Glacial Lake McConnell: paleogeography, age, duration and associated river deltas, Mackenzie River basin, western Canada. Quaternary Science Reviews, v. 13, p. 829-843.

Spirito, W.A., McClenaghan, M.B., Plouffe, A., McMartin, I., Campbell, J.E., Paulen, R.C., Garrett, R.G. and Hall, G.E.M. 2011. Till sampling and analytical protocols for GEM projects: from field to archive. Geological Survey of Canada, Open File 6850, 1 CD-ROM.

Stoiber, R.E., 1940. Minor elements in sphalerite. Economic Geology, v. 35, p. 501-519.

Todt, W., Cliff, R.A., Hanser, A., and Hoffman, A.W., 1996. Evaluation of 202Pb-205Pb double spike for high-precision lead isotope analysis. *In:* Basu, A.I., and Hart, S.R., (eds) *Geophysical Monograph.* v. 95 p. 429-437.

van der Meer, J.J.M., Menzies, J. and Rose, J. 2003. Subglacial till: the deforming glacier bed. Quaternary Science Reviews, v. 22, p. 1659-1685.

Warren, H.V., and Thompson, R.M., 1945. Sphalerites from Western Canada. Economic Geology, v. 40., p. 309-335.

Chapter 4

4.1   Conclusions

The glaciated terrain of northern Canada presents many hurdles to exploration geologists. The till geochemical signature and indicator minerals associated with a well-studied MVT deposit were documented to improve exploration techniques for these deposits in glaciated areas.

1. The work outlined in Chapter 2 indicates that the most prominent surficial deposit in the region is glaciolacustrine littoral and nearshore sediments caused by extensive reworking of glacial till by wave action from glacial Lake McConnell. The surficial deposits on the eastern margin of the district are slightly different than those on the western side. The work outlined in Chapter 3 documents that there are 3, possibly 4, different ice flow trajectories that affected the region where there was previously only 1 known ice flow trajectory. This indicates that the Quaternary history of the area may be more complex than previously reported.

2. Obtaining up-to-date ice flow information is integral to any exploration program. Failure to do so could result in a sampling program that could miss potential targets. In areas with more than one ice flow trajectory it is important to execute a sampling strategy that captures the possible dispersal of indicator minerals and till geochemical signatures that are the result of the net effect of each ice flow trajectory.

3. This work has shown that the pathfinder elements associated with the Pine Point deposits are Zn, Pb, Cd, Fe, Tl, S and Se and the associated indicator minerals are sphalerite, galena, and pyrite. Smithsonite and cerussite also occur to a much lesser degree. MVT deposits are hosted in carbonate rocks which is an important factor in the survival of these grains in glacial sediments. In areas with less carbonate content these minerals would be easily weathered and, therefore, are not valuable indicator minerals.

4. The isotopic work conducted in Chapter 3 confirms that galena grains recovered from till are identical to galena grains recovered from bedrock

samples. This indicates that the galena grains in till likely originated at Pine Point. Chapter 3 also shows that the $\delta^{34}S$ values for the majority sphalerite grains recovered from till samples were consistent with those recovered from bedrock grains with the exception of two grains. These grains may indicate that the range of $\delta^{34}S$ values determined for Pine Point in the past is actually larger than reported.

5. The research conducted in this M.Sc. project reveals exploration strategies that can be applied to MVT deposits occurring in glaciated terrain. These strategies include; obtaining up-to-date ice flow information, analyzing the <0.063 mm fraction of till for base and precious metals, recovering and characterizing indicator minerals related to the deposit, and analyzing the Pb and S isotopes of galena and sphalerite grains to determine the bedrock provenance of grains in till. Perhaps the most significant result is that surface till sampling can detect these deposits under approximately 3-5 m of till on a regional and local scale.

4.2   Future work

This study has uncovered some possible geochemical signatures that may be unique to the five different deposits as well as the different varieties of sphalerite, galena and pyrite examined in this study. Further investigation using LA-ICPMS techniques would be beneficial to quantify and further define these trace element variations. If there are variations between different deposits within a MVT district then understanding these variations would be valuable to any exploration program. For instance, if a till sample has a different geochemical signature than other till samples in the area, this could indicate the presence of an undiscovered deposit.

Additionally, there is potential at the (O28) deposit to instigate a sampling program that could document the angle of climb of the till geochemical signature and indicator minerals from the ore zone to the surface. This information would be beneficial in determining the dispersal train for deposit O28. In order to do this, a series of trenches from the surface to the bedrock would need to be excavated at varying distances down-ice from O28. Then samples would need to be collected at regular intervals from bedrock to the surface.

Finally, additional studies re-examining the ice flow history of the region would be beneficial to our understanding of the advance/retreat of the

Laurentide Ice Sheet. Mining processes uncovered numerous bedrock outcrops that were previously covered by thick deposits of glacial sediments making a study like this more feasible. The construction of open pit mines in the region also made thick sequences of till observable providing an opportunity to study till stratigraphy and other features that may expand our knowledge base of the glacial history of the region.

In conclusion, the pathfinder elements and characterization of the indicator minerals associated with the Pine Point MVT district have been documented. A surficial map documenting the distribution of sediments on the west side of the Pine Point mine property has been produced and exploration strategies have been suggested that should help overcome some of the hurdles encountered when working in glaciated terrain.

Appendix A1. Canadian Geoscience Map 114: Surficial geology of Breynat Point (NTS 85B/15)

REFERENCES

Craig, B.G., 1965. Glacial Lake McConnell, and the surficial geology of parts of Slave River and Redstone River map areas, District of Mackenzie; Geological Survey of Canada, Bulletin 122, 33 p.

Dyke, A.S. and Prest, V.K., 1987. Late Wisconsin and Holocene history of the Laurentide Ice Sheet; Geographie physique et Quaternaire, 41, 26 p.

Dyke, A.S., Andrews, J.T., Clark, P.U., England, J.H., Miller, G.H., Shaw, J. and Veillette, J.J. 2002. The Laurentide and Innuitian ice sheets during the Last Glacial Maximum. Quaternary Science Reviews, 21, 22 p.

Lemmen, D.S., 1990. Surficial materials associated with glacial Lake McConnell, southern District of Mackenzie; Geological Survey of Canada, Current Research 1990-1D, 5 p.

Lemmen, D.S., 1998a. Surficial geology, Klewi River, District of Mackenzie, Northwest Territories; Geological Survey of Canada, "A" Series Map 1905, scale 1: 250 000.

Lemmen, D.S., 1998b. Surficial geology, Buffalo Lake, District of Mackenzie, Northwest Territories; Geological Survey of Canada, "A" Series Map 1906, scale 1:250 000.

Lemmen, D.S., Duk-Rodkin, A. and Bednarski, J.M., 1994. Late glacial drainage systems along the northwestern margin of the Laurentide Ice Sheet; Quaternary Science Reviews, 13, 23 p.

Mathews, W.H., 1980. Retreat of the last ice sheets in northeastern British Columbia and adjacent Alberta; Geological Survey of Canada, Bulletin 331, 27 p.

Rice, J.M., Paulen, R.C., Menzies, J.M., McClenaghan, M.B., and Oviatt, N.M., In Press. Glacial stratigraphy of the Pine Point Pb-Zn Mine Site; Northwest Territories; Geological Survey of Canada, Current Research, X p.

Smith, D.G., 1994. Glacial Lake McConnell: Paleogeography, age, duration, and associated river deltas, Mackenzie River Basin, western Canada; Quaternary Science Reviews, 13, 14 p.

ACKNOWLEDGMENTS

Surficial mapping was undertaken under the Geomapping for Energy and Minerals (GEM) Program in conjunction with Tamerlane Ventures Incorporated and Teck Resources Limited as partial requirement for a M.Sc. thesis and the Geomapping for Energy. J. Rice (Brock University), M.B. McClenaghan (GSC Ottawa) and S. Gleeson (University of Alberta) are thanked for their enthusiastic support and assistance in the field. T. Lynds (GSC Atlantic) is thanked for providing digital topographic and satellite imagery.

Abstract

The Pine Point region is of very low relief and characterized by black spruce bogs with local relief not exceeding 20 m. During Wisconsin time, the Breynat Point map sheet was actively and continuously glaciated by the Laurentide Ice Sheet which was generally flowing to the west. Multiple till units were observed in the open pits, however only the uppermost unit was mapped at surface. The map area was completely inundated by proglacial Lake McConnell which formed during deglaciation, glaciolacustrine sediments are the dominant materials that occur as beach ridges and littoral sediments. Reworked beach ridges form eolian dunes up to 15 m high. Raised strandlines formed by earlier phases of Great Slave Lake mark the former isostatic rebound of the land surface. Organic deposits are extensive within mature peatlands and fens which are underlain by discontinuous permafrost with active thermokarst. Abandoned open pits and waste piles pockmark the former Pine Point mining district.

Résumé

La région de la mine Pine Point, au relief très peu élevé, est caractérisée par des tourbières à épinettes noires avec, par endroits, un relief qui ne dépasse pas 20 m. Au cours du Wisconsinien, la région de la carte Breynat Point était recouverte de façon active et continue par les glaces de l'Inlandsis laurentidien. De nombreuses unités de till ont été observées dans les mines à ciel ouvert; toutefois, seule l'unité supérieure a été cartographiée à la surface. Pendant la déglaciation, le lac proglaciaire McConnell a entièrement submergé la région de la carte, où les sédiments glaciolacustres sont les matériaux prédominants sous forme de crêtes de plage et de sédiments littoraux. Des crêtes de plage remaniées prennent la forme de dunes éoliennes atteignant jusqu'à 15 m de hauteur. Des anciennes lignes de rivage soulevées, formées par les phases précoce ou Grand lac des Esclaves, indiquent l'ancien relèvement isostatique de la région. Les dépôts organiques très étendus, comportant des tourbières et des marais matures, reposent sur un pergélisol discontinu avec un modèle de thermokarst actif. Des mines à ciel ouvert et des amas de stériles abandonnés ponctuent le paysage de l'ancien district minier de Pine Point.

National Topographic System reference

Cover illustration
Photo of an expansive black spruce peatland developed on low-relief Glacial Lake McConnell sediments, looking to the northeast from top of the waste pile at PX 5-65. Waste piles from PX R-61 and T-58 rise above the peatland terrain in the background. 85-B/15 (60° 46' 53.436"N/114° 37' 17.814" W). Northwest Territories. Photograph by Roger C. Paulen 2013-002
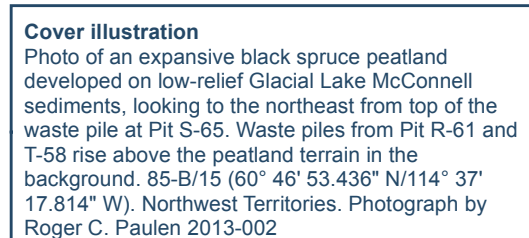
Catalogue No. M183-1/114-2013E-PDF
ISBN 978-1-100-21746-8
doi:10.4095/292247

© Her Majesty the Queen in Right of Canada 2013

Natural Resources Canada | Ressources naturelles du Canada

CANADIAN GEOSCIENCE MAP 114
SURFICIAL GEOLOGY
BREYNAT POINT
Northwest Territories
NTS 85-B/15
1:50 000

ess.nrcan.gc.ca

Canadian Geoscience Maps

Canada

SURFICIAL GEOLOGY
BREYNAT POINT
Northwest Territories
NTS 85-B/15
1:50 000

0 1 2 3 4 km

The Geological Survey of Canada welcomes corrections or additional information from users.

This publication is available for free download through GEOSCAN (http://geoscan.ess.nrcan.gc.ca/).

Preliminary publications in this series have not been scientifically edited.

Recommended citation
Oviatt, N.M. and Paulen, R.C., 2013. Surficial Geology, BREYNAT POINT, NTS 85-B/15, Northwest Territories; Geological Survey of Canada, Canadian Geoscience Map 114 (preliminary), scale 1:50 000. doi:10.4095/292247

CANADIAN GEOSCIENCE MAP 114
SURFICIAL GEOLOGY
BREYNAT POINT
Northwest Territories
NTS 85-B/15

LEGEND

QUATERNARY

SURFICIAL DEPOSITS

POST LAST GLACIATION

NONGLACIAL ENVIRONMENT

H — Anthropogenic deposits: culturally-made or modified geological materials such that their physical properties have been drastically altered, generally >2 m thick, and includes open pit mines, mine tailings, waste piles and settling ponds and reworked overburden associated with the Pine Point mine operation and former town site (1964-1988).

C — Colluvial deposits, undifferentiated: mass wasting debris; poorly sorted; massive to stratified debris, variable thickness, deposited by direct, gravity-induced movement; composition is dependant on source material.

ORGANIC DEPOSITS: peat and muck; 1 to 4 m thick on average; formed by the accumulation of plant material in various stages of decomposition; generally occurs as low relief, wet terrain (swamps, bogs and muskeg) over poorly drained substrates.

Owb — Organic deposits-bog: sphagnum or forest peat formed in an ombrotrophic environment; wet terrain; may be treed with black spruce or treeless; area may be locally underlain by ground ice or shallow permafrost conditions, with thermokarst terrain related to melting ground ice.

Owf — Organic deposits-fen: derived from sedged and partially decayed shrubs in a eutrophic environment; forms relatively open peatlands with a mineral-rich water table that persists seasonally near the surface; generally covered with low shrubs and an occasionally sparsely treed with larch (tamarack).

O — Organic deposits, undifferentiated: undifferentiated bog and fen deposits; area may be locally underlain by ground ice or shallow permafrost; often associated with minor channels established for surface drainage and impacted by beaver activity.

EOLIAN SEDIMENTS: medium to fine sand wind-deposited; derived from glaciolacustrine deposits; in some areas eolian sediments are thin or absent between dune ridges.

Er — Eolian dune sediments: generally >2 m thick, forming parabolic and longitudinal dune ridges.

E — Eolian sediments, undifferentiated:

ALLUVIAL SEDIMENTS: sorted gravel, sand, silt and organic detritus; commonly stratified, variable thickness; deposited by streams.

Ap — Floodplain sediments: gravel, sand silt and organic detritus, sorted, >1 m thick; forming active floodplains close to river level with meander channels and scroll bars.

At — Alluvial terrace sediments: >2 m thick, inactive terraces above modern floodplain.

Af — Alluvial fan sediments: gravel, sand, silt and organic detritus, poorly sorted, >1 m thick.

A — Alluvial sediments, undifferentiated:

LACUSTRINE SEDIMENTS: cobble to pebble gravel, sand, silt and minor clay; >1 m thick, consisting of beach and storm deposits, ice-rafted debris and also formed from recent fluctuations in lake levels, deposited along the shoreline of Great Slave Lake.

Lr — Lacustrine beach sediments: fine sand to coarse cobble gravel; forming beach ridges of gravel up to 2 m high, sediments deposited adjacent to Great Slave Lake.

Ln — Littoral and nearshore sediments: fine to coarse sand beaches with minor gravel and ice-rafted debris, relief is typically <1 m, sediments formed in the nearshore environment of Great Slave Lake.

POSTGLACIAL OR LATE WISCONSIN

PROGLACIAL AND GLACIAL ENVIRONMENTS

GLr — GLACIOLACUSTRINE SEDIMENTS: coarse gravel, sand, silt and minor clay; commonly massive to poorly stratified; >1 m thick; derived from winnowing of till in relatively shallow water; formed in proglacial Lake McConnell.

GLr — Ridged beach sediments: pebbly to granular sand; well-sorted, formed from glaciolacustrine sedimentation during isostatic rebound and/or lowering of proglacial Lake McConnell; commonly forms laterally extensive ridges; relief is typically 0.5 to 2.0 m.

GLn — Littoral and nearshore sediments: sand and gravel grading up from a fine silty-sand sediment; moderately sorted, commonly overlain by an open framework cobble lag <1 m thick.

GL — Glaciolacustrine sediments, undifferentiated: sand, silt and minor clay deposits; commonly overlain by organic deposits, low relief terrain.

GLACIAL SEDIMENTS (TILL): diamicton, carbonaceous sandy to silty matrix with striated and faceted clasts of various lithologies; clast content varies from 10 to 15%; thickness ranges from 1 to >30 m thick; till ridges have typically been exposed to varying degrees of washing and winnowing from proglacial Lake McConnell; generally increasing in thickness to the west; deposited directly by the Laurentide Ice Sheet.

Tv — Till veneer: diamicton, <2 m thick; unit includes local patches of outcrop and till blanket.

Tb — Till blanket: diamicton, >2 m thick, continuous till cover forming undulating topography that locally obscures underlying units.

PRE-QUATERNARY

BEDROCK, PALEOZOIC

R — Bedrock, undifferentiated: sedimentary bedrock; Devonian dolomitized carbonate rocks of the Presqu'ile barrier, consisting of the Upper Keg River and Sulphur Point formations.

Mine waste rock.

Winnowed sediments with lag deposits.

Geological contact, defined.

Buried drumlinoid ridge.

Drumlinoid ridge.

Minor meltwater channel, sense known.

Minor meltwater channel, sense unknown.

Beach crest.

Terrace scarp.

Corrected age of 11.1 ± 1.1 ka 11-PTA-105A

GREAT SLAVE LAKE

Presqu'ile Cove

Sulphur Point

Breynat Bight

Appendix A2. Mapping field data

site number	Pit	easting	northing	Elevation	Surficial Unit	Comments
11-MPB-M001		630377	6746042	211	beach sediments	loose sand and gravel, moderately sorted beach sand, grades into coarse sand with some silt
11-MPB-M002		630245	6746448	200	beach sediments	down slope from last site, series of ridges
11-MPB-M003		630149	6746585	206	GLv/T	
11-MPB-M004		629705	6747383	194	GL	
11-MPB-M005		624768	6747306	184	Of	
11-MPB-M006		626944	6748049	179	GL	silt and clay from 15cm to 1m
11-MPB-M007		627133	6748263	187	O	1.5m of O overlying GL
11-MPB-M008	64N	628657	6749555	181	A	anthropogenic all around this pit
11-MPB-M009		630808	6750162	184	GL	15cm of O
11-MPB-M010	N-61	630305	6750561	189		not on topo, there is till here . Area is in middle of fen.
11-MPB-M011	X-56	632395	6752157	180	?	Pit surrounded by bog and fen
11-MPB-M012	M-52	634775	6746263	226	S/G	1 m of sand and gravel on NW side of pit. Surrounding pit is till ~30 m thick (even more in Karst collapsed zones) 2 types of till, grey and sandy brown
11-MPB-M013	K-53	634319	6747777	219	Tb	Drained pit, Tb all around this pit, drained even more. Bedrock exposed. Very thin ~30 cm gravel layers below organics on NE, next to ramp. Some sections have 1 m and organics
11-MPB-M014	K-57	632139	6746844	211	?	S side of pit has 1 m+ of sand and gravel possibly stratified. Some white, uniform, clast-free material on NW side .
11-MPB-M015	J-69	626657	6743847	211	?	Lake sediments first 30 cm overlying till, need to work around this pit.
11-MPB-M016	k-77	623557	6742049	203	?	
11-MPB-M017	N-81	621616	6740117	214	?	anthropogenics all to North
11-MPB-M018		632772	6747482	205		15 cm of well sorted sand overlying sand and gravel to 1 m. Surficial unit, beach sediments, very rounded pebbles on lee-side of beach ridge. Well sorted gravel at top of ridge closer to road
11-MPB-M019		632655	6747655	203		~ 10 cm of glacial lacustrian overyling till. At bottom of ridges, area flattens out briefly
11-MPB-M020		632968	6747728	203		~10 cm lake sediments overlying till. Cmoe down off the ridge ground is wetter here. Vegetation change. .

11-MPB-M021		633108	6747601	214	~50 cm fo sand and gravel (loose) we are next to road. ~ 85 cm of sand and gravel well sorted then very moist till. Beach ridge over till
11-MPB-M022	Y-54	633669	6752634	180	in fen
11-MPB-M023		635664	6750274	194	~85 cm of GL overlying till It had fissility but very clast poor
11-MPB-M024		631846	6746164	233	loose sand with sub-rounded pebbles to 70 cm. Boulder horizon, after boulder horizon we get into really coarse sand, moderatly sorted, site is located in low point in series of ridges, top of ridges had cobble. Large pebble lag. Top of ridges has large boulder lag at 10-15 cm
11-MPB-M025		632278	6745281	222	at the surface there is ~ 10 cm of very well sorted pebbles, overlying a well sorted sand (coarse). Interbeds of this occur for 1 m getting coarrser at 1 m mark.
11-MPB-M026		631322	6743343	226	~65 cm of poorly sorted sand and gravel. Underlying ~15 cm of sand at 85 cm mark very poorly sorted sand, Pebbles were faceted and striated.
11-MPB-M027		632166	6743686	225	~ 15 - 20 cm of Organic, then cobble log for about 10 cm moderatley sorted, heavily oxidized sand to a poorly sorted fine sand and silt with pebbles from ~65 cm to 1m
11-MPB-M028		632696	6743922	226	till at surface up to 1 m sandy to silt matrix, photo of auger and site
11-MPB-M029		634999	6745055	234	1.5 m of bog overlying till. Photos looking NW
11-MPB-M030		636033	6745640	237	~1.8 m of organic overlying sand
11-MPB-M031		634645	6744654	236	moderatley sorded sand. Photo looking east. From 0.1 m to 1 m all same material. In lows between ridges poorly sorted bobbles, pebbles and silt ~ 70 cm into washed till
11-MPB-M032		634957	6743942	235	poorly sorted sand and gravel well rounded, loosley packed. Beach sediments on low point next to ridge features. Ridge has a moderatley sorted sand (mostly) with some gravel core overlain by cobble lag.
11-MPB-M033		634977	6744092	235	~10 cm of well sorted sand below ~10 cm of organic both over washed till to ~90cm
11-MPB-M034		633696	6743073	229	well sorted sand to depth of 1 m, few pebbles
11-MPB-M035		633725	6741979	228	bog, with washed till underneath
11-MPB-M036		633704	6742336	230	poorly sorted sand and gravel with silt skins. Tw
11-MPB-M037		625099	6744917	193	1 m of very fine sand silt and clay. Next to large sand dune
11-MPB-M038		625485	6744958	205	~15 cm of washed clast poor sllit and very fine sand (Tw) overlying 85 cm of till
11-MPB-M039		625639	6745114	201	~15 cm of sand overlying till... Well sorted sand ~50 cm to 1 m of sand
11-MPB-M040		626369	6745071	208	~75 cm of well sorted sand overlying 15 cm of washed till into till. Heavily washed, it was very clast poor, (there was a lag of pebbes and coarse sand ~ 1m) or GL
11-MPB-M041		626695	6745268	207	well sorted sand cap for 30 cm then 70 cm of sand (coarse gravel)

ID		Easting	Northing	Value	Description
11-MPB-M042		626557	6745137	208	15 cm organic overlying sand and cobbles
11-MPB-M043		626581	6743937	201	lake seds are ~1.2 m from natural land surface. Sharp contact with till, consistent around pit J-69
11-MPB-M044		627771	6743588	214	~ 70 cm of fine to medium grain well sorted samd. At 75 cm medium sand and pebbles with cobble lag.
11-MPB-M045		629721	6743401	218	~20 cm of well sorted sand and till. Maybe a lag of sand and pebble. Very sandy till, highest sand content in area. Tx
11-MPB-M046		632025	6742139	238	~ 3.4 m of loose sand and gravel. Ridge cuts through pit at ~225
11-MPB-M047		628399	6745133	238	Bog Owb
11-MPB-M048		628833	6741051	223	15 cm of organics, 15 cm of loose sand and gravel, sharp contact with till.
11-MPB-M049		618913	6737404	227	~ 30 cm of cobbles and large pebbles grading to ~ 70 cm of moderately sorted sub-rounded pebbles and sand. Pebbles have silt skin on them. Large cobbles with sand and pebble unit
11-MPB-M050		618854	6737486	225	15 cm of organics, cobble lag, sand (coarse) with cobbles for 50 cm then till to 1 m
11-MPB-M051		619307	6737460	228	~15 cm organic, then sand with occasional cobble and pebble. Then ~15 cm of coarse sand and gravel then ~ 20 cm of Overlying 50 cm of very wet sand with pebbles, some silt. Could be Till, clasts are sub-rounded and faceted many resemble shield lithogies
11-MPB-M052		617979	6737883	226	till at surface here
11-MPB-M053		617302	6736977	225	till at surface augered into ditch..
11-MPB-M054		620006	6738397	226	sand dune here.. Sand for 1 m at E 620268 N 6738602 and ele 228
11-MPB-M055		621287	6739261	226	1 m of sand grading into Tx sand was well sorted medium grained.
11-MPB-M056		622579	6739795	221	~ 30 cm of sand over till.
11-MPB-M057		623978	6740452	222	~ 30 cm organic then ~ 15 cm lake sediments (silt and clay few to no cobbles) then till
11-MPB-M058		625524	6741309	215	~ 15 cm of organic. ~ 10 cm of lake seds. Then till unit until 1 m GLv/T
11-MPB-M059		628358	6742181	225	1.5 m below natural surface at ~ 1 m- 50 cm of mod sorted coarse sand and pebbles. Pebbles are sub-rounded possible till rip-ups.
11-MPB-M060		630252	6745782	210	
11-MPB-M061	M-52	634733	6746223	230	some beach seds. 10 cm of organics overlying 50 cm of poorly sorted snad and gravel with boulders, then till. Bouder horizon at 1.5 m from surface. Below sand and gravel, non– continous around pit
11-MPB-M062		634553	6746913	214	large ridge feature cuts across road at top of features we had 70 cm of moderatley sorted sand 70- 1 m thick of poorly sorted sand and gravel further down slope where it flattens out we have till at surface (under 10 cm of organic)
11-MPB-M063		632515	6746532	220	
11-MPB-M064		629515	6744135	215	1 m of oragnic over till

Sample ID		Easting	Northing	Elev.	Code	Description
11-MPB-M065	1-65	629031	6745596	198		GL on west side under 65 cm of organics. Till everywhere else thin lag of sand and gravel on top under organics
11-MPB-M066		631408	6744779	221		Owb and 2+ m
11-MPB-M067		627971	6741735	231		Ridges are ~ 2.5 m hight. 60 cm is layered fine, well sorted sand, interbedded with coarse pea gravel. ~70 cm there is a cobble layer. Then what appeared to be reworked till to 1.2 m slight a cobble lag overlies the poorly sorted material. This feature extends accross the road at a trend of 255
11-MPB-M068		626138	6740034	242		large cobble pile next to gravel put just down road from ast site. Gravel pit is ~4.5 m deep
11-MPB-M069		621570	6740043	214		area around pit is completely disturbed.
11-MPB-M070		610874	6738294	202	GL	from surface to 1 m is v.f sand to silt to clay, no clasts, we are close to beach ridges,
11-MPB-M071		611000	6737750	190		till in forest,
11-MPB-M072		611078	6737720	198	T	
11-MPB-M073		611500	6737098	190		very dense clay, silt and sand. clasts at 70 cm
11-MPB-M074		612683	6739430	202		clay rich till
11-MPB-M075		611861	6738684	198	GLr	well sorted sand, 75cm more coarse sand
11-MPB-M076		611754	6738139	201	GLr	1 m of well sorted sand.
11-MPB-M077		623602	6738328	234	Tx	silt and clay mostly gone, Just south of ridge feature
11-MPB-M078		623557	6738330	228	GLr	on south flank of ridge, moderately sorted sand and gravel with cobble lag (at 15cm) at 80 cm is washed till.
11-MPB-M079		623508	6738517	227	Tx	
11-MPB-M080		623457	6738729	233	GLr	no cobbles on road.
11-MPB-M081		621687	6739575	213		~ 40 cm of fine grain well sorted sand. Overlying ~ 70 cm of sandy lake seds (silt, clay and sand, no clasts) overlying ~ 10 cm well sorted laminated oxidized med grain sand overlying till
11-MPB-M082		620127	6746523	188		Till at surface
11-MPB-M083		619756	6747055	190	T	till at surface here
11-MPB-M084		619812	6746938	190	GLn	Upper 30 cm is moderately sorted sand and gravel with silt skins. 30 cm of pea gravel then back into moderately sorted and and gravel to 1 m.
11-MPB-M085		619749	6746330	191	T	till at surface
11-MPB-M086		619082	6746669	187	Tx	~ 70- 80 cm of moderately sorted sand and gravel over Tx (poorly sorted sand and gravel, no fines) large cobbley-ridge just to south of site
11-MPB-M087		618048	6746622	188	GL	1 m of GL at surface
11-MPB-M088		618213	6746310	193	T	1 m of till here
11-MPB-M089		617445	6745952	197	GLr	1 m of moderately to well sorted sand at 1 m started to hit large cobbles
11-MPB-M090		617421	6745570	196	T	1 m of till in bog

11-MPB-M091		618244	6743985	191		top 60 cm is poorly sorted sand and gravel. 60 cm - 1 m washed till. ~ 270 m up road is gravel pit with at least 1.5 m of moderately sorted sand gravel
11-MPB-M092		618472	6743736	199	T	Till from surface, 15 cm of Organic
11-MPB-M093		618670	6743609	202		~ 60 cm of coarse grain well sorted sand . Cobble lag overlying 10 cm of washed till overlying till to depth 1 m
11-MPB-M094		618829	6743145	205	T	30 cm organic large boulder lag into till up to 1 m.
11-MPB-M095		618898	6742972	209		10 cm organic, boulder lag. 10 cm of well-sorted sand into lightly washed till from ~ 50 cm to 60 cm highly oxidized sandy till 60-100 cm very dense dry till.Orientation ~ 243
11-MPB-M096		619102	6742683	204		20 cm organics over Gl 20 cm into Till
11-MPB-M097		620867	6743144	199		1 m of sand and clay overyling till
11-MPB-M098		620912	6742807	208		1 m of well sorted sand.
11-MPB-M099		620740	6743078	199		lags of boulders at surface into till to depth
11-MPB-M100		619967	6742915	205		1 m of O over till (grey till)
11-MPB-M101		619608	6742586	215		Same sort of material as 11-MPB-M094 10 cm of O, overlying 20 cm of very loosely pached sand and gravel. Large boulders throughout . At 60 cm we get to pebble cobble material with silt skins. At 1 m we have very lightly washed till
11-MPB-M102		619485	6742195	222		~ 50 cm of washed till (very similar to 11-MPB-M101), over till
11-MPB-M103		615904	6743834	197	T	till at surface here 182 m to E we have 70 cm of washed till over till
11-MPB-M104		616911	6744695	181		~ 20 cm of well sorted fine grained sand overlying till
11-MPB-M105		617287	6744524	190		~ 50 cm of washed till (poorly sorted sand and gravel) overlying till.
11-MPB-M106		619810	6741303	224		30 cm of med sand with boulders overlying 70 cm of poorly sorted sand and gravel. GLn on very top of ridge feature
11-MPB-M107		620290	6741069	216		50 cm of poorly-sorted sand and gravel (Tx) overlying 50 cm up till
11-MPB-M108		621082	6739507	221		50 cm of well sorted sand over till.
11-MPB-M109		631940	6741880	237	Tx	2 m of poorly sorted matierlal mostly open framework sand and gravel some fissility is observed throughout the section, on South. wall of pit ~ 80 cm of poorly sorted sand and gravel. No structure overlying 2 m of well-sorted, fine grained sand with ripples over-lying highly oxidized sand and gravel (moderately sorted)
11-MPB-M110		626280	6742864	212		70 cm of poorly- sorted sand and gravel overlying classic till
11-MPB-M111		624802	6742626	215		1 m of sand and clay with some find sand in places
11-MPB-M112	K-77	623481	6742043	207		15 cm of organic material overlying ~ 30 cm of laminated silt sand clay and gravel material overlying ~ 30 cm of fine sand with pebbles with till rip up clasts. All overlying till with sand lenses
11-MPB-M113		622782	6741380	211		sand and clay at surface here to 1 m
11-MPB-M114		622751	6739349	221		All sand here, well sorted medium grained, up to 1 m

ID	Easting	Northing			Description
11-MPB-M115	622952	6739053	222		~ 1m of poorly sorted sand and gravel material. Likely washed till, lots of cobbles throughout it.
11-MPB-M116	620279	6736785	229		~ 50 cm of clean sand overlying 50 cm of sand and cobbles
11-MPB-M117	620501	6737304	228		till at surface
11-MPB-M118	621086	6737467	229		1 m of poorly-sorted open framework sand and gravel more cobbly at 70 cm
11-MPB-M119	621530	6737826	233		1.5 m of organic overlying well- sorted sand (50 cm)
11-MPB-M120	625736	6739180	227		south of very large sand dunes, poorly sorted sand and gravel with most fines removed. Fine sand to cobbles
11-MPB-M121	627509	6740987	238		Very rounded cobbles on surface on other side of highway as well but not as thick
11-MPB-M122	639611	6743404	223		silt and clay no sand at all from surface
11-MPB-M123	628154	6741996	230		90 cm of poorly-sorted loosely packed sand and gravel with cobbles. 10 cm of well sorted sand into coarse grained moderately sorted sand. At E 628900 N 6742100 we have till and sand and gravel, likely disturbed
11-MPB-M124	629190	6742076	232		On south side of hwy, 1 m of well-sorted sand. Last 10 cm (90-100) pebble content increases.
11-MPB-M125	630401	6742408	232		on N side of Highway ridge like feature on one side of road only. Dug 1 m into back (N) side of it. 1 m of poorly-sorted sand, pebbles and cobbles. Just to N of this site at dugout shows till at surface
11-MPB-M126	623521	6743450	202	T	Till at surface, very sandy, more clay rich at 90 cm
11-MPB-M127	624871	6744475	203	T	Till at surface
11-MPB-M128	624633	6744590	207	GL	Lake seds at surface, silt and clay some fine sand layers
11-MPB-M129	624434	6744218	200	Tx	30 cm of poorly sorted sand, pebbles and cobbles (Tx) overlyin till to 1 m
11-MPB-M130	624152	6743850	200	T	90 cm of poorly-sorted coarse sand, cobbles and pebbles (till classic at 1 m)
11-MPB-M131	623945	6743716	202		1 m of well sorted sand with few pebbles
11-MPB-M132	633635	6743939	238	T	
11-MPB-M133	625091	6739505	233	Tx	

Appendix B1. Geological Survey of Canada Open File

Indicator minerals in till and bedrock samples from the Pine Point Mississippi Valley-Type (MVT) district, Northwest Territories

Natasha M. Oviatt[1], M. Beth McClenaghan[2], Roger C. Paulen[2], Sarah A. Gleeson[1], S.A. Averill[4], and Suzanne Paradis[3]

(1) University of Alberta, Department of Earth and Atmospheric Sciences, Edmonton, Alberta, T6G 2E3

(2) Geological Survey of Canada, 601 Booth Street, Ottawa, Ontario, K1A 0E8

(3) Geological Survey of Canada, 9860 West Saanich Road, P.O. Box 6000, Sidney, British Columbia, V8L 4B2

(4) Overburden Drilling Management, Unit 107, 15 Capella Court, Ottawa, Ontario, K2E 7X1

Table of Contents

List of Tables

List of Figures

105

List of Plates

ABSTRACT

An indicator mineral study was conducted at the Pine Point Mississippi Valley-Type (MVT) district in northern Canada to document the abundance, morphology, size and chemistry of the indicator minerals present in the deposits and in till down-ice. Till and bedrock samples for this study were collected in 2010 and, based on results from these samples, additional till samples were collected in 2011. Heavy mineral concentrates (specific gravity 3.2) were isolated from till samples and indicator minerals were picked from this fraction. Indicator minerals identified for the Pine Point MVT deposits include sphalerite, galena, smithsonite and pyrite. Sphalerite and galena are the most useful indicator minerals because they are the most abundant in ore and till samples down ice and they are sufficiently physically that they survive glacial transport.

1.   INTRODUCTION

As long-term demand for metals and minerals is expected to grow (Stothart, 2011) base metal deposits have become a major exploration target in Canada. As indicator mineral and till geochemical methods have proven to be successful exploration tools in glaciated terrain (e.g. Averill, 2001; McClenaghan, 2005) focus has shifted to apply these exploration methods to Mississippi Valley-Type (MVT) deposits. Canada is one of the most mineral resource-rich countries in the world and one of the largest producers of minerals and metals (Stothart, 2011). Prior to 2002, the production of Pb and Zn in Canada from MVT deposits was 30%, however, current Canadian production is nil (Sangster, 2002). To improve Pb and Zn exploration in glaciated areas, the Geological Survey of Canada (GSC), in collaboration with the University of Alberta, Tamerlane Ventures Incorporated and Teck Resources Limited have initiated a study of the till geochemistry and indicator mineral signature of the Pine Point MVT district, Northwest Territories. Till geochemistry data from this study are presented in GSC Open File 7320 (Oviatt et al., 2013) while the focus of this report is to present indicator mineral data.

2.   LOCATION AND PHYSIOGRAPHY

The Pine Point mining district is on the south shore of Great Slave Lake, Northwest Territories, on the eastern margin of the Western Canada Sedimentary Basin (WCSB; Fig. 1). The district is approximately 180 km due south of Yellowknife, in the Buffalo Lake topographic map sheet (NTS 85B) and approximately 50 km east of the town of Hay River. The Buffalo River flows north into Great Slave Lake on the western side of the study area. Black spruce bogs characterize the area and local relief does not exceed 15 m (Lemmen et al., 1994). The Pine Point mine site and open pits can be accessed via Highway 6 and mine roads by truck or ATV in the summer.
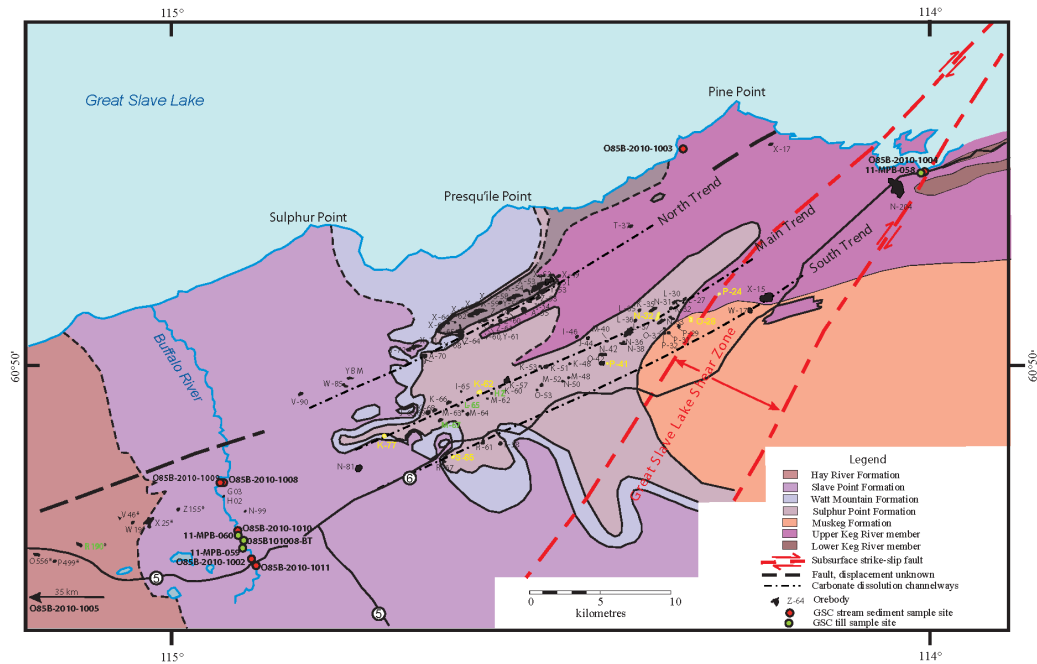
Fig. 1: Regional bedrock geology map (modified from Hannigan, 2007) with the three trends (North, Main and South) and their orebodies in the Pine Point mining district, Northwest Territories. Till samples were collected from open pits labelled in yellow and at yellow dots, bedrock samples were collected from deposits labelled in red, stream sediments were collected from locations indicated by green dots.

3. Exploration History

The Pine Point mining district was discovered by prospectors heading north during the Klondike gold rush (1896-1898) who staked claims on a gossanous outcrop at Sulphur Point on the shore of Great Slave Lake. Little work was conducted on these claims until 1929 when the Northern Lead Zinc Company was formed, which included Cominco Limited (Campbell, 1966). The focus of Northern Lead Zinc Company's 1929-1930 exploration program was to determine if the known ore bodies were connected beneath the surface and to define the ore grade of the sub-cropping mineralization. The occurrence of the Great Depression in the early 1930s halted all exploration in the area. Between 1940 and 1947, Cominco Limited directed a drilling program to delineate ore bodies associated with basement faulting (Campbell, 1966). In 1963, an induced polarization geophysical survey was conducted in the area, which led to the

discovery of ore bodies that did not subcrop (Hannigan, 2006). The Pine Point mines opened in 1964 and were one of Canada's most profitable Pb-Zn mining districts until 1987 when they were shut down. Between 1975 and 1981, Westmin Resources conducted drilling programs approximately 25 km west of Cominco's open pits and discovered nine additional deposits (Hannigan, 2007). None of these western deposits have been mined.

Soil surveys have been conducted in the area to characterize Zn-rich shales that occur in the region and determine whether or not they are a source for the Zn metal in the Pine Point deposits. The high concentrations of Zn that still remain in these shales indicate that they were likely not the source for mineralization at Pine Point (Macqueen and Ghent, 1975; Brabec, 1983).

Tamerlane Ventures Incorporated optioned the unmined Westmin Resources deposits at Pine Point in 2008 and are currently exploring and assessing the feasibility of several deposits (Hannon et al., 2012).

4.   Bedrock Geology

The Pine Point region is underlain by rocks of the eastern margin of the Western Canada Sedimentary Basin. The bedrock of the Pine Point area is consists of 350 to 600 m thick Ordovician to Devonian rocks that overlie crystalline basement rocks of the Archean and Proterozoic (Skall, 1975; Kyle, 1981; Rhodes et al., 1984; Okulitch, 2006; Hannigan, 2007). More specifically, the deposits are hosted by, or proximal to, the Presqu'ile barrier which is a reef-like complex (200 m at its thickest point) that separates the deep marine rocks to the north from the shallow marine rocks to the south (Rhodes et al., 1984; Hannigan, 2007). The Presqu'ile barrier consists of the Upper Keg River and Sulphur Point formations. The Upper Keg River Formation includes the lower two-thirds of the barrier and consists of flat, lensoidal beds of carbonate sandstones and mudstones and fine, dense, grey-brown to buff brown dolomite with abundant carbonaceous fossils (Skall, 1975; Hannigan, 2007). The overlying Sulphur

112

Point Formation consists of a build-up of bioherms, bioclastic limestones and carbonate sandstones (Rhodes et al., 1984; Hannigan, 2007) and has undergone alteration into a coarse crystalline, vuggy dolomite known as Presqu'ile dolomite which is the host of the majority of the ore bodies (Skall, 1975; Hannigan, 2007). Karstification was the primary control for ore deposition in the area (Rhodes et al., 1984; Hannigan, 2007).

The Great Slave Lake Shear Zone (GSLSZ) is an area of highly deformed and sheared rocks that extends for approximately 700 km from Northwest Territories down into northeastern British Columbia (Eaton and Hope, 2003). It is considered to be a boundary between the Churchill and Slave cratonic provinces (Morrow et al., 2006). Lead isotopic studies (Nelson et al., 2002; Paradis et al., 2006) indicate that mineralizing fluids likely originated in the basement using faults using the GSLSZ as a conduit. This event would likely have occurred in the Phanerozoic when the fault zone was reactivated during the Laramide orogeny (Morrow et al., 2006). The orebodies are concentrated within 3 NE-SW trending zones referred to as the North trend, Main trend and South trend (Fig. 1). The McDonald Fault, a component of the GSLSZ, cuts through the basement rocks immediately below and sub-parallel to these three trends (Skall, 1975; and Kyle, 1981). It has been interpreted that tectonic activity associated with the MacDonald fault may have had a part in creating these trends (Skall, 1977).

The ore field consists of 100 drill-defined orebodies (Hannigan, 2007) that span an area of approximately 1600 km^2. The orebodies range from 100,000 to 17.5 million tonnes and have an average grade of 2% Pb and 6.2% Zn (Hannigan, 2007). The total geological resource (produced and remaining proven resource) is estimated to be 95.4 Mt (Hannigan, 2007). The mine site closed in 1988 due to dropping market prices for Pb and Zn and due to rising mining costs.

The deposits consist of galena and sphalerite with minor pyrite and marcasite (Hannigan, 2007). Galena occurs as isolated crystals or as massive patches and, as the skeletal variety within colloform sphalerite (Plate 1).

Sphalerite is present as very fine-crystalline colloform textures or occurs as isolated crystals (from 1 mm to 5 mm). Sphalerite crystals range from a dark Fe-rich variety to a light honey-brown type. Sphalerite, galena, and pyrite also occur as brecciated clasts in some instances (Plate 2). Minor hydrothermal minerals associated with the Pine Point deposits include marcasite, pyrite, sulphur, pyrrhotite, celestite, barite, gypsum, anhydrite, and fluorite (Hannigan, 2007). Bitumen is also present in the host Paleozoic carbonate rocks. Table 1 provides a summary for the ore minerals associated with Pine Point.

Table 1: Summary of the ore minerals in the Pine Point MVT district summarized from Hannigan (2007) and the size range of each mineral as seen in polished thin section, bedrock and till heavy mineral concentrates in this study.

Mineral	Formula	Found in PTS in this Study	Found in Bedrock HMC in this Study	Found in Till in this Study
Major and minor minerals in the ore:				
Sphalerite	(Zn,Fe)S	0.1-1.5 mm	0.05-2 mm	0.075-2mm
Galena	PbS	0.05-5 mm	0.025-2 mm	0.025-2 mm
Pyrite	FeS2	0.01-0.5 mm	0.025-0.5 mm	0.025-0.5 mm
Marcasite	FeS2	No	0.025-0.5 mm	0.025-0.5 mm
Trace and Rare Minerals in the ore:				
Zn-bearing minerals				
Smithsonite	ZnCO3	No	No	0.25-2 mm
Pb-bearing minerals				
Cerussite	PbCO3	No	No	0.25-1 mm
Cu-bearing minerals				
chalcopyrite	CuFeS2	No	No	0.25-0.5 mm
Ba-bearing minerals				
Barite	BaSO4	No	No	0.25-0.5 mm

5.   Surficial Geology

The low-relief geomorphology of the Pine Point area is the result of the relatively flat bedrock topography overlain by glacial sediments formed and deposited by the Keewatin sector of the Laurentide Ice Sheet. Till cover occurs as a continuous blanket that generally increases in thickness from east to west across the Pine Point mine district. Till deposits at the eastern margin of the former mine district range from <1 m to 3 m thick, and gradually thicken westward to >25 m at the western pits. Till is locally thicker where karst collapse structures have created depressions in the bedrock surface. Historic drill hole data indicates that till is up 100 m thick in places (Lemmen, 1990). Commonly, till in the area has a silt to fine sand matrix with very little clay (Lemmen, 1998b). The landscape surrounding the Pine Point mine site has glacially streamlined features such as flutings that mostly reflect the last ice flow trajectory. The

The Pine Point region was deglaciated sometime between 10.0 and 9.6 ^{14}C ka BP (Dyke, 2004) and was inundated by glacial Lake McConnell (Smith, 1994). Most of the till surfaces are winnowed, and there was extensive reworking of the till into glaciolacustrine littoral sediments over much of the area (Lemmen, 1990). Glaciolacustrine deposits occur as shorelines and beach ridges, some of which have been reworked into eolian dunes. At approximately 7.8 ^{14}C ka BP, it was speculated that basin uplift in the region had restored Great Slave Lake to its current position (Dyke and Prest, 1987; Dyke, 2004).

Surficial mapping was carried out in the Pine Point area by the GSC from 1989 to 1994, mainly to expand the knowledge of Glacial Lake McConnell and associated deposits (Lemmen 1998a, 1998b). Surficial geology maps were published for Buffalo Lake (NTS 85B) and Klewi River (NTS 85A) and a single phase of ice flow to the west was identified (Lemmen, 1990). There is very little published information on the ice flow history of the region and southern Great Slave Lake in general (Prest et al., 1968; Paulen et al., 2009). Additional research on Glacial Lake McConnell was conducted east of the area by Smith (1994).

115

6. METHODS

6.1. Field sampling

Till and bedrock sampling were conducted in the summers of 2010 and 2011. Field data including till/bedrock sample location and depth are reported in Appendicies E1 and E2. A detailed description of field sampling methods are reported in GSC Open file 7320 (Oviatt et al., 2013).

6.2. Bedrock sampling

A total of 75 bedrock samples were collected from diamond drill core and waste rock piles adjacent to open pits. One mineralized grab sample (10-MPB-035) was collected from the natural land surface approximately 100 m from near deposit O28. Based on availability of relatively fresh drill core, five orebodies were sampled: R190, M67, L65, HZ and O28 (Fig. 1). These bedrock samples were collected to determine the characteristics of the sulphide minerals present at Pine Point. Fifteen bedrock samples were sent to Overburden Drilling Management Limited (ODM), Ottawa, for recovery of the heavy mineral fraction and picking of indicator minerals. Forty-seven of the bedrock samples were made into polished thin sections (PTS) at Vancouver Petrographics, Langley for petrography and electron microprobe analysis (EMP). Field collection data for bedrock samples are listed in Appendix E1. Photographs of bedrock samples, including a polished slab and PTS, as well as hand sample and PTS descriptions are included in Appendix E2.

6.3. Till sampling

A total of 15 till samples were collected across the Pine Point district at a regional scale and 64 (excluding field duplicates) till samples were collected proximal to deposit O28. Field collection data for till samples are listed in Appendix E3. Deposit O28 was chosen for detailed till sampling because: 1) mineralization sub-cropped and thus was eroded by glaciers, 2) no known sub-cropping ore bodies occur directly up-ice (east) of deposit O28 thus east should

reflect background, 3) multiple striated outcrops on the pit shoulders provide detailed ice flow information, 4) till is of moderate thickness (~6m) providing the opportunity to sample till in the third dimension, and 5) the natural land surface is relatively undisturbed for sampling both up and down ice.

Till samples were collected up-ice, overlying and down-ice of the ore zone at deposit O28 with respect to three prominent ice-flow trajectories preserved in striations on the pit shoulders (Fig. 2). Up-ice till samples (10-MPB-023, -024, -025) were collected on the east side of the pit at the till/bedrock interface and were used to establish background concentrations. Eight till samples (10-MPB-004, -005, -026 to -028, -030, -031, 11-MPB-008) were collected overlying and just down ice of the O28 ore zone on the stripped bedrock surface exposed on the west side of the open pit.

Three vertical sections of till (A, B, and C in Fig. 2) were sampled in the upper west wall of the pit to collect till samples 50 m down ice. Three till samples were collected from each section at ~1, 3 and 5 m depths below the natural land surface (Plate 3). Based on the indicator mineral results for these 2010 till samples (10-MPB-032 to 034, -036 to 041), additional till samples were collected in 2011 in a pattern that widens westward (Fig. 2) from the ore zone (11-MPB-002 to 007, -009 to 014, -017 to 033, -035 to 044, -046 to 054). These till samples were collected from 3 m trenches (Plate 4) to document vertical patterns in the till composition. An additional section of till was sampled in the upper west wall of the pit (D, Fig. 2). This section was sampled in the same manner as sections A, B, and C. Two field duplicate samples were collected 11-MPB-034 is a duplicate of 11-MPB-033 and 11-MPB-016 is a duplicate of 11-MPB-009 to assess field variabililty. Field data for all till samples in this study are listed in Appendix E1.

Regional till samples (Fig. 1) were collected at deposits P24 (10-MPB-013, -014), N32 (10-MPB-020, -021), and P41 (10-MPB-009, -017 and -018) to document any variance in the geochemistry and indicator mineral size and morphology in till around different orebodies. Till sample 11-MPB-058 was

Fig. 2: Locations of till samples collected at deposit O28. Samples collected in 2010 (10-MPB-series) are shown in black and samples collected in 2011 (11-MPB-series) are shown in pink. Three vertical samples were collected from excavated pits at ~1, 2, and 3 m below the natural land surface. A,B,C, and D indicate locations of vertical sections in the western pit wall sampled in 2010 and referred to in text.

collected from Paulette Creek 15 km up-ice of the eastern most Pb-Zn deposit to determine "background" concentrations of indicator minerals. Seven till samples were collected from deposits K62 (11-PTA-037, -042), S65 (11-MPB-062), K77 (11-MPB-061), and sections along the Buffalo River (11-MPB-059, -060, 085B101008BT) to establish down ice indicator mineral concentrations in till.

6.4. Sample processing and indicator mineral picking

Fifteen bedrock samples were submitted to Overburden Drilling Management Limited (ODM), Ottawa for disaggregation and production of heavy mineral concentrates (HMC). Before disaggregation, each bedrock sample was described by ODM geologists and these descriptions are reported in McClenaghan et al., (2012). Polished thin sections (PTS) for 57 bedrock samples were described by the senior author and are reported in Appendix E2. Sample processing and indicator mineral picking procedures used by ODM, as well as the weights of all fractions produced and indicator mineral abundances for bedrock samples are reported in McClenaghan et al., (2012). Sphalerite, galena and other minerals indicative of the Pine Point MVT deposits were counted in each bedrock sample. Indicator mineral data from bedrock samples were normalized to 1 kg weight because processing weights varied from 41.0 to 274.7 g. Normalized indicator mineral data from bedrock samples are listed in Appendix F1.

Bulk till samples were also processed at ODM to recover the heavy mineral fraction. Sphalerite, galena and other minerals indicative of the Pine Point MVT deposits as well as other routine indicator mineral suites (magmatic massive sulphide indicator minerals (MMSIMs®), kimberlite indicator minerals, gold grains) were counted in each till sample. Sample processing and indicator mineral picking procedures used by ODM, as well as the weights of all fractions produced and indicator mineral abundances for till samples are reported in McClenaghan et al., (2012). Indicator mineral data from till samples were normalized to 10 kg because till sample weights collected and processed varied between 5.5 and 15 kg. Normalized indicator mineral data from till samples are

119

listed in Appendix F2 and are discussed in the results section of this paper.

6.5. Electron microprobe analysis

Selected sulphide minerals in PTS were analyzed at the University of Alberta using the CAMECA SX100 and the JEOL 8900 Electron Probe Microanalyzers (EPMA). Selected indicator mineral grains from till samples were mounted in a 25 mm epoxy puck prior to EPMA. A map of this puck is included in Appendix C. Elements determined are: Mn, S, Zn, Fe, Pb, Ag, As, Sb, Se, Hg, Ge, and Cu. Operating conditions for EPMA analysis are listed in Appendix G. The detection limits are reported as three standard deviations from the total background counts. Values that were below detection limit were removed before calculations and plotting. EPMA data for bedrock grains and till grains are listed in Appendix C.

7. RESULTS

The results and discussion will focus on the 0.25-0.5 mm fraction of till and bedrock unless otherwise noted.

7.1. Quality control/quality assurance

Table 2 is a summary of the unnormalized grain counts recovered from quartz blanks submitted with the bedrock samples. Most quartz blanks contained no sulphide grains in the 0.25 to 0.5 mm fraction with the exception of three blank samples: 10-MPB-R30blk, 10-MPB-R58blk and 10-MPB-R57blk. Sample 10-MPB-R30blk contains 2 sphalerite grains and was processed after bedrock sample 10-MPB-R30, which contains approximately 80% massive colloform sphalerite. The pan concentrate for this bedrock sample contains approximately 500 grains of sphalerite, 500 grains galena and 50 grains of pyrite.

Blank sample 10-MPB-R58blk contains 1 grain of sphalerite and 1 grain of galena in the 0.25 to 0.5 mm fraction. Bedrock sample 10-MPB-R58 was processed before this blank and it contains the highest abundance of sphalerite

and galena grains of all bedrock samples processed. The pan fraction for sample 10-MPB-R58blk contains approximately 150 grains sphalerite, 250 grains galena and 30 grains of pyrite.

Blank sample 10-MPB-R57blk contains 2 grains of galena and was processed after bedrock sample 10-MPB-R57, which contains approximately 80% galena. The pan concentrate for sample 10-MPB-R57blk contains approximately 100 grains sphalerite, 2500 grains galena and 2 grains of pyrite.

In summary, significant contamination was detected in the pan concentrate fraction of every blank sample that was processed except for the very first blank sample at the beginning of the batch. Processing a quartz blank after each bedrock sample allows carryover from the previous sulphide-bearing sample to be "caught" by the blank, thus limiting carry over to the next real bedrock sample. This significant level of contamination between samples indicates that in future, the EPD equipment at ODM should be totally dismantled and thoroughly cleaned after disaggradation of any sulphide-rich sample.

7.2. Field duplicates

Table 3 shows a comparison of indicator minerals recovered from duplicate field samples. There are some discrepancies between the samples particularly in the pan concentrate of galena. Till sample 11-MPB-009 contains 76923 grains of galena in the pan concentrate while its field duplicate, 11-MPB-016 contains 23 grains. Sample 11-MPB-009 contains 2308 grains of sphalerite and 615 grains of pyrite in the 0.25 – 0.5 mm fraction of till while sample 11-MPB-016 contains 2 grains of sphalerite and pyrite in the same fraction.

The grain counts for 11-MPB-034 and its duplicate 11-MPB-033 are consistent in sphalerite, pyrite and smithsonite. The greatest discrepancy occurs in the pan concentrate of galena. Sample 11-MPB-034 contains 159 galena grains in the pan concentrate while its duplicate contains 41 grains.

7.3. Sphalerite

7.3.1. Sphalerite in bedrock

Sphalerite in PTS occurs as: 1) honey-brown, 2) blackjack (Fe-rich), 3) colloform and 4) cleiophane varieties. Different textures that occur are: 1) snow-on-roof, 2) banded sphalerite, 3) dendritic, and 4) ascicular (Plate 5). All sphalerite varieties occur as brecciated fragments in some samples. Honey-brown and blackjack varieties occur as isolated crystals or as patches. Colloform sphalerite is evident in most bedrock samples. The bands of colloform sphalerite range from 50 to 1500 µm in thickness, while the individual botryoids range in size from 100 µm to up to 3 cm or more. The size range of sphalerite crystals in PTS was 100 to 1500 µm, though some crystals up to 0.5 cm were observed in hand sample. Very fine, powdery yellow sphalerite (cleiophane) occurs in some bedrock samples and usually has skeletal galena radiating outwards from the middle of the grain.

In bedrock heavy mineral concentrates (HMC), sphalerite grains were primarily recovered from the 0.25 to 0.5 mm fraction. The largest concentration of grains was recovered from sample 10-MPB-R21, which is a bedrock sample that contains approximately 60 % sphalerite and 20 % galena in hand sample. Grains were also recovered from every bedrock sample in pan concentrate fractions. The size range of sphalerite grains recovered ranges from 25 µm to 2 mm. Data for indicator minerals recovered from bedrock are reported in Table 4.

EPMA of each of the four varieties of sphalerite was conducted on 80 to 85 grains randomly selected from PTS. Care was taken obtain data points from each grain variety as well as each different texture. The concentration of Zn in sphalerite in bedrock samples in this study ranges from 43.95 to 67.48 wt %. Iron concentrations in sphalerite grains range from 0.02 to 16.94 wt % and that of S ranges from 32.03 to 39.19 wt %. Minor elements Cd and Pb have concentrations

Table 2: Summary of sphalerite, galena, and pyrite abundance in the 0.25-0.5 mm heavy mineral and pan concentrate fractions of bedrock samples and in quartz blanks that were processed prior to and after each bedrock sample at Overburden Drilling Management Limited.

Sample number	Sphalerite 0.25-0.5 mm	Galena 0.25-0.5 mm	Pyrite 0.25-0.5 mm	Additional grains 0.25-0.5 mm	Pan Concentrate grains
10-MPB-QBlk5	0	0	0	0	1 pyrite grain
10-MPB-R25	10,000	15	0	0	~200 grains marcasite, ~2000 grains galena, ~5000 grains sphalerite
10-MPB-QBlkR25	0	0	0	0	1 grain pyrite, 1 grain galena
10_MPB-R32	20000	150	2	0	~25000 grains galena, 1% sphalerite
10-MPB-QBlkR32	0	0	0	0	5 grains pyrite, ~15 grains galena
10-MPB-R37	0	0	35000	0	90% pyrite
10-MPB-QBlkR37	0	0	0	1 hornblende grain and 2 metal turnings	~500 grains pyrite, 9 grains galena
10-MPB-R38	0	0	30000	0	60% pyrite, 10% marcasite, ~25 grains galena
10-MPB-QBlkR38	0	0	0	0	~200 grains pyrite
10-MPB-R43	60000	1200	1	0	2% galena, 60% sphalerite
10-MPB-QBlkR43	0	0	0	0	~100 grains pyrite, ~30 grains galena, ~40 grains sphalerite
10-MPB-R21	70000	8000	0	0	20% galena, 70% sphalerite
10-MPB-QBlkR21	0	0	0	0	~20 grains pyrite, ~150 grains galena, ~40 grains sphalerite
10-MPB-R30	120000	400	0	0	~100 grains pyrite, 2% galena, 80% sphalerite
10-MPB-QBlkR30	2	0	0	1 hornblende grain	~50 grains pyrite, ~500 grains galena, ~500 grains sphalerite

10-MPB-R17	20000	1500	30000	0	70% pyrite, 2% galena, 10% sphalerite
10-MPB-QBlkR17	0	0	0	2 metal turnings	~200 grains pyrite, ~50 grains galena, ~30 grains sphalerite
10-MPB-R59	70000	12000	0	0	~200 grains pyrite, 80% galena, 5% sphalerite
10-MPB-QBlkR59	0	0	0	0	~30 grains pyrite, ~700 grains galena, ~200 grains sphalerite
10-MPB-R12	7000	5000	0	0	70% marcasite, 5% galena, 10% sphalerite
10-MPB-QBlkR12	0	0	0	0	~200 grains marcasite, ~500 grains galena, ~50 grains sphalerite
10-MPB-R15	55000	60000	6000	0	40% marcasite, 10% galena, 20% sphalerite
10-MPB-QBlkR15	0	0	0	2 metal turnings	~100 grains pyrite, ~350 grains galena, ~40 grains sphalerite
10-MPB-R05	35000	100000	35000	0	50% pyrite, 10% galena, 25% sphalerite
10-MPB-QBlkR05	0	0	0	0	~150 grains pyrite, ~500 grains galena, ~30 grains sphalerite
10-MPB-R58	200000	200000	0	0	20% galena, 70% sphalerite
10-MPB-QBlkR58	1	1	0	2 metal turnings	~30 grains pyrite, ~250 grains galena, ~150 grains sphalerite
10-MPB-R34	150000	180000	0	0	30% galena, 40% sphalerite
10-MPB-QBlkR34	0	0	0	0	~15 grains pyrite, ~1000 grains galena, ~40 grains sphalerite
10-MPB-R57	100000	300000	0	0	80% galena, 20% sphalerite
10-MPB-QBlkR57	0	2	0	1 metal turning	2 grains pyrite, ~2500 grains galena, ~100 grains sphalerite

Table 3: Comparison of indicator mineral counts recovered from the pan concentrate, 0.25 – 0.5 mm, 0.5 – 1.0 mm and 1.0 – 2.0 mm size fractions of field duplicate till samples. These indicator mineral counts have been normalized to 10 kg.

Sample	Sphalerite				Galena				Pyrite				Smithsonite			
	No. grains pan	No. grains 0.25-0.5 mm	No. grains 0.5-1.0 mm	No. grains 1.0-2.0 mm	No. grains pan	No. grains 0.25-0.5 mm	No. grains 0.5-1.0 mm	No. grains 1.0-2.0 mm	No. grains pan	No. grains 0.25-0.5 mm	No. grains 0.5-1.0 mm	No. grains 1.0-2.0 mm	No. grains pan	No. grains 0.25-0.5 mm	No. grains 0.5-1.0 mm	No. grains 1.0-2.0 mm
11-MPB-009	0	2308	46	1	76923	62	15	0	385	615	0	0	0	0	0	0
11-MPB-016	0	2	0	0	23	1	0	0	153	2	0	0	0	0	0	0
11-MPB-034	0	0	0	0	159	4	3	0	16	1	0	0	0	0	0	0
11-MPB-033	0	3	2	0	41	0	0	0	25	41	0	0	0	0	0	0

ranging from 0.18-0.51 wt % and 0-0.87 wt % respectively. Trace elements In, Cu, Sb, and Ge have concentrations that range from 0.01 to 0.03, 0.55, 0.07, and 0.09 wt %, respectively. Zinc concentrations are highest in grains from deposits R190 and O28 while cleiophane sphalerite has the highest concentration of Zn (Fig. 3a). Grains with the highest concentrations of Zn have the lowest concentrations of Fe. Thus, cleiophane sphalerite has the lowest concentrations of Fe (0.094 to 5.4 wt %) and blackjack sphalerite has the highest concentrations of Fe (1.03 to 16.94 wt %)(Fig. 3b). Sphalerite in bedrock samples from the M67 deposit have the most diverse trace element geochemistry. This deposit contains below detection limit concentrations of Ge, Ag, In, Sb, Pb, Cu and Hg in comparison to the other orebodies in this study (Fig. 4). Deposit HZ has higher concentrations of Sb, Cu and Hg (0.016-0.036 wt %, 0.011-0.035 wt %, and 0.024-0.154 wt % respectively) in sphalerite as compared to the other deposits studied. Honey-brown (0.03-0.51 wt %), colloform (0.03-0.35 wt %) and cleiophane (0.11-0.33 wt %) varieties of sphalerite have the highest concentrations of Cd while blackjack sphalerite has below detection limit concentrations (Fig. 5). Lead concentrations vary between all the varieties of sphalerite but are more often the highest in cleiophane (0.25-0.79 wt %) and colloform sphalerite (0.13-0.77 wt %).
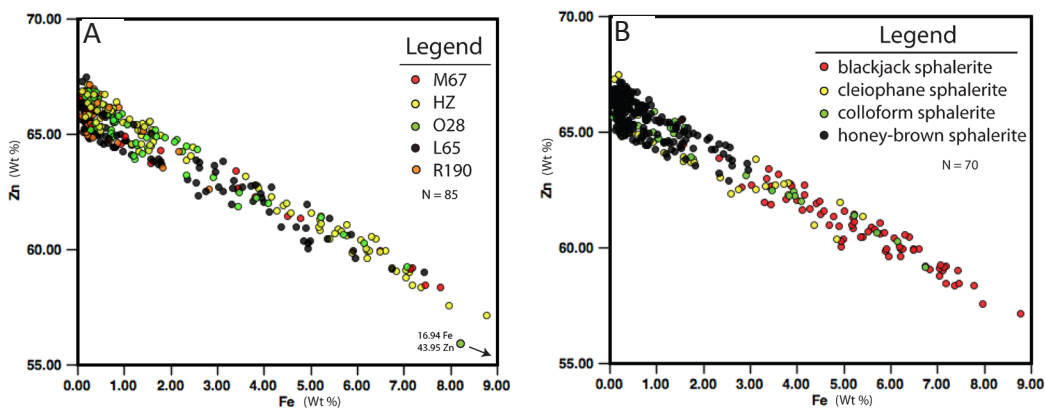
Fig. 3: Relationship of Zn versus Fe content for sphalerite in the (A) five different deposits considered in this study in the Pine Point MVT district, and (B) different varieties in all five deposits.
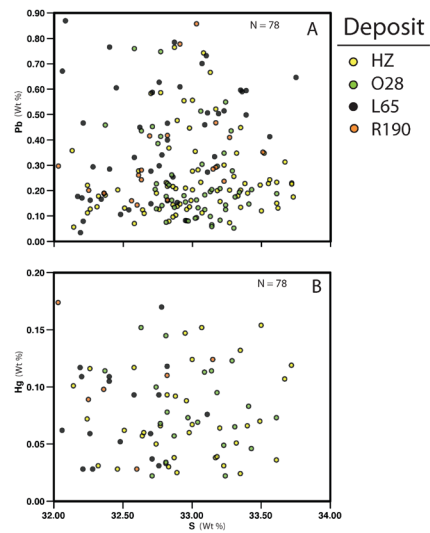
Fig. 4: Concentrations of Pb vs S and Hg vs S content in sphalerite grains from bedrock from four different deposits determined by EMP analysis.
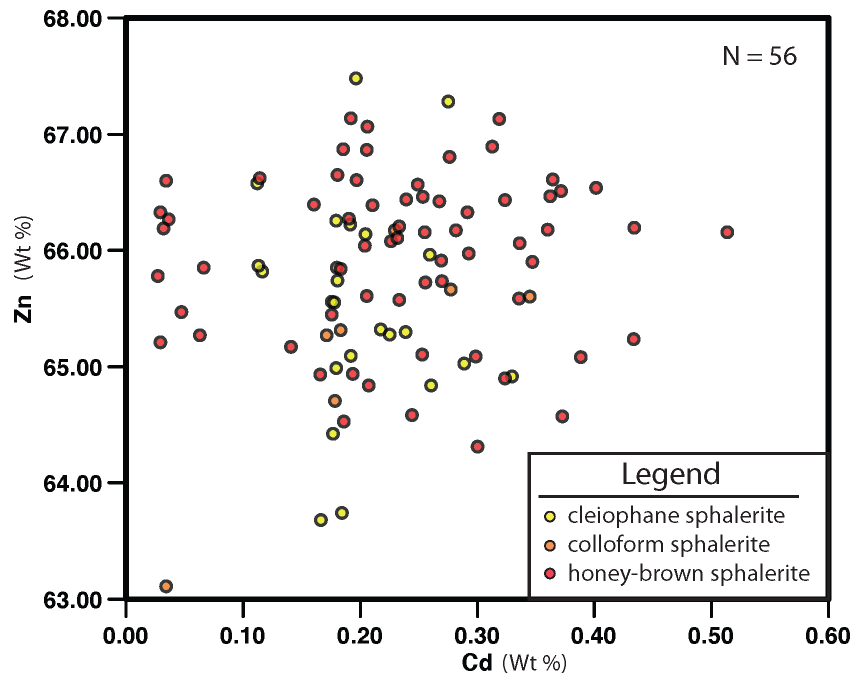
Fig. 5: Concentrations of Zn and Cd in sphalerite grain varieties from bedrock samples determined by EMP analysis. Blackjack sphalerite is absent from these graphs because Cd contents are not within 3 standard deviations of the detection limit of 0.18 wt. %.
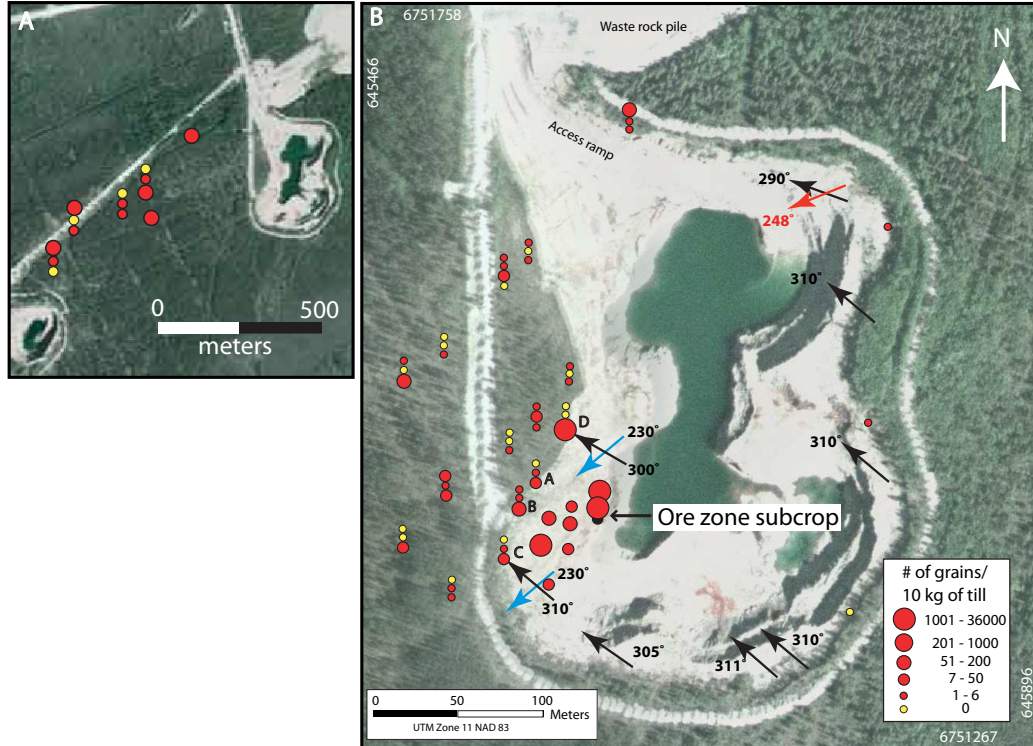
Fig. 6: Distribution of sphalerite grains in the 0.25 to 0.5 mm fraction of till at deposit O28: A) area down ice (west) of the deposit, and B) area immediately around the deposit. Three vertical samples were collected at some sites for which the data are plotted as vertically stacked symbols. Yellow dots indicate barren till samples. Blue arrows indicate the oldest ice flow trajectory, black are intermediate and red are youngest.

average in comparison to sphalerite grains recovered from bedrock samples.

Secondary electron images of the 0.25-0.5 mm grains reveal that the grain morphology for sphalerite in till ranges from sub-rounded to angular (Fig. 7). Table 5 compares indicator mineral grain counts recovered from till and sample distance from the ore body at O28. Most grains recovered from till samples proximal to the deposit are angular to sub-angular while some grains from samples 250 m down-ice in the SW direction are sub-rounded to rounded.

128

7.3.2. Sphalerite in till

Raw abundances of the indicator minerals recovered from till are listed in Open File 7267 (McClenaghan et al., 2012). The majority of sphalerite grains recovered from till range from 0.25 to 1.0 mm. The most abundant size is 0.25 to 0.5 mm. The pan and 1.0-2.0 mm fraction do contain some sphalerite grains, but these are limited to till samples closest to the deposit (Table 6). Till samples collected on the bedrock bench (not including samples 10-MPB-004 and 10-MPB-005 which overlie the deposit) contain 38 to 114 grains in the 0.25 to 0.5 mm fraction. Figure 6 shows the distribution of sphalerite grains in till around deposit O28. Background concentration in till is 0 to 1 grain. Background values are determined by taking the average of till samples 10-MPB-023, -024, -025 and 11-MPB-058 which are all located up-ice of the O28 deposit. Till sample 10-MPB-004, which overlies the deposit, contains 35,398 grains and till samples 10-MPB-005 and -028 have 4839 and 3226 grains. These till samples are all down-ice (to the SW) of the ore zone in the direction of the first ice flow trajectory.

Till samples from the Buffalo River (11-MPB-059, -060 and 085B-2010-1008) contain between 0 and 6 grains of sphalerite. Till samples from deposit P24 contain 288462 to 980392 sphalerite grains and samples from deposit N32 contain between 15789 and 42105 sphalerite grains. Regional till sample 11-MPB-061, collected at deposit K77, contains 459 grains and sample 11-MPB-062, collected at deposit S65, contains no sphalerite grains.

EPMA of sphalerite grains from till samples indicate that these grains have similar concentrations to those recovered from bedrock samples. Zinc concentration ranges from 64.06 to 67.27 wt % while S concentration ranges from 32.24 to 34.13 wt %. The concentrations for Mn, Fe, Ge and Se are similar to sphalerite grains recovered from bedrock. Sphalerite grains recovered from till samples have lower concentrations of As, Ag, Cd, In, Sb, Pb, Cu, and Hg on
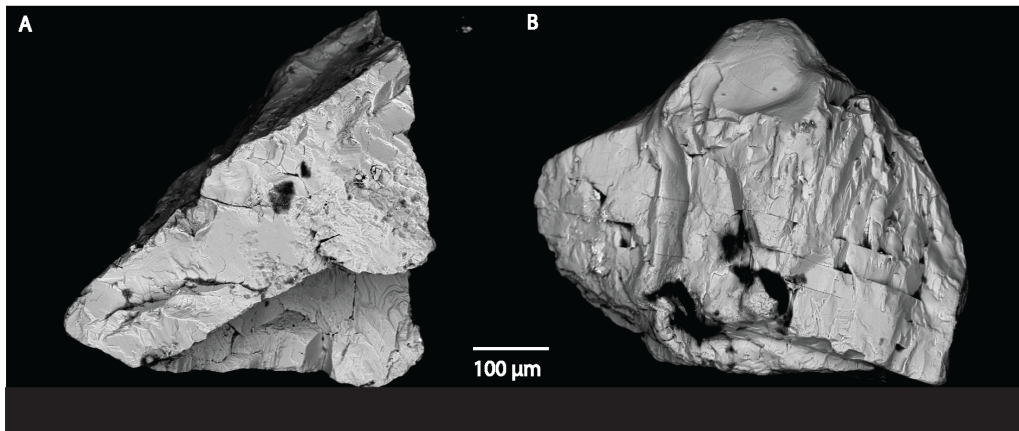
Fig. 7: Secondary electron images showing the morphology of sphalerite grains from till samples: A) an angular grain from 10-MPB-004 and B) a sub-angular grain from 11-MPB-029.

7.4. Galena

7.4.1. Galena in bedrock

Cubic and skeletal galena are the two main varieties that occur in PTS. Different textures of galena identified in PTS are dendritic, fracture filling (late galena), and banded galena (Plate 6). Cubic grains range from 50 to 5000 μm and dimensions for skeletal grains range from 50 to 1500 μm. As with sphalerite grains, fragments of each of these types of galena occur in brecciated samples.

Galena grains were recovered from heavy mineral concentrates of bedrock samples from pan concentrate to 2 mm, though most grains were recovered from the pan concentrate fraction (Table 1). More galena was recovered from the pan concentrates than sphalerite was. The highest concentration was recovered from sample 10-MPB-R58 which is a sample that consists of approximately 80% galena.

EPMA was conducted on 58 grains of both varieties as well as each texture of galena in PTS. The concentration of Pb ranges from 83.87 to 89.27 wt %. Sulphur concentrations in galena range from 12.53 to 13.93 wt % and appear to have a bimodal distribution (Fig. 8a). Low S concentrations range from 12.5 to

Table 4: Indicator mineral data for bedrock samples. These data have been normalized to 1 kg processing weight.

Sample	Processed weight (g) of < 2 mm fraction	Sphalerite		Galena		Pyrite	
		Raw counts for < 2mm fraction	No. Sphalerite grains/1 kg	Raw counts for < 2mm fraction	No. galena grains/1 kg	Raw counts for < 2mm fraction	No. of pyrite grains/1 kg
10-MPB-R25	36.5	10000	273973	15	411	0	0
10-MPB-R32	34.6	20000	578035	150	4335	2	58
10-MPB-R37	47.9	0	0	0	0	35000	730689
10-MPB-R38	56.9	0	0	0	0	30000	527241
10-MPB-R43	81.4	60000	737101	1200	14742	1	12
10-MPB-R21	55.0	70000	1272727	8000	145455	0	0
10-MPB-R30	98.2	120000	1221996	400	4073	0	0
10-MPB-R17	29.8	20000	671141	1500	50336	30000	1006711
10-MPB-R59	90.9	70000	770077	12000	132013	35000	385039
10-MPB-R12	82.6	7000	84746	5000	60533	0	0
10-MPB-R15	67.9	55000	810015	60000	883652	6000	88365
10-MPB-R05	114.9	35000	304613	100000	870322	35000	304613
10-MPB-R58	157.9	200000	1266624	200000	1266624	0	0
10-MPB-R34	129.9	150000	1154734	180000	1385681	0	0
10-MPB-R57	227.3	100000	439947	300000	1319842	0	0

Table 5: Listing of the sulphide minerals in till samples and relative distances from the O28 ore zone on the west side of the open pit.

Sample	Distance from ore zone (m)	Sample depth top (m)	Sample depth bottom (m)	Relative to ore zone	No. sphalerite grains/10 kg	No. galena grains/10 kg	No. smithsonite grains/10 kg	No. pyrite grains/10 kg	Pb (ppm)	Zn (ppm)	Cd (ppm)	Fe (%)	Tl (ppm)	S (%)	Se (ppm)
11-MPB-058	-15000	1.3	1.6	up ice	0	0	0	8	10.55	36.5	0.07	1.71	0.046	0.01	0.1
11-MPB-055	-280	7.8	8.0	up ice	152	76	0	2273	33.22	88.3	0.16	0.93	0.027	0.10	0.2
11-MPB-056	-280	3.5	3.7	up ice	15	0	0	48	25.86	88.9	0.24	0.73	0.019	0.01	0.1
11-MPB-057	-280	1.0	1.3	up ice	6	17	0	61	23.45	66.0	0.17	0.88	0.025	0.01	0.1
10-MPB-023	-250	4.0	5.0	up ice	2	0	0	205	37.40	109.1	0.28	0.77	0.020	0.01	0.2
10-MPB-024	-200	4.0	4.5	up ice	4	0	0	4	35.30	97.6	0.26	0.80	0.024	0.01	0.1
10-MPB-025	-200	2.5	3.0	up ice	0	0	0	0	29.97	84.5	0.21	0.86	0.024	0.01	0.2
10-MPB-004	7	5.4	5.9	overlying	35398	53097	133	26549	2015.41	3497.4	11.37	1.15	0.016	0.27	0.3
10-MPB-005	19	5.4	5.9	overlying	4839	2419	65	3226	383.43	911.0	2.08	0.78	0.020	0.08	0.2
10-MPB-030	20	5.8	5.9	overlying	114	45	0	7576	877.72	2215.5	3.18	1.67	0.018	0.06	0.3
10-MPB-026	23	5.8	5.9	overlying	159	397	0	952	1018.36	1620.4	5.91	1.11	0.017	0.10	0.2
10-MPB-031	24	5.8	5.9	down ice	38	30	0	1136	410.96	1772.2	2.07	1.00	0.020	0.05	0.3
10-MPB-039	40	3.5	4.0	down ice	63	236	0	1181	145.22	322.7	0.72	0.95	0.017	0.01	0.2
10-MPB-040	40	2.0	2.5	down ice	2	0	0	9	30.79	86.3	0.19	1.08	0.028	0.01	0.3
10-MPB-041	40	0.8	1.0	down ice	4	3	0	58	26.87	82.1	0.21	0.95	0.024	0.01	0.3
11-MPB-008	50	5.8	5.9	down ice	42	15	0	1681	33.90	92.4	0.22	0.80	0.017	0.01	0.1
10-MPB-027	50	3.8	3.9	down ice	38	11	0	152	64.67	122.9	0.25	0.86	0.022	0.02	0.2
10-MPB-028	51	3.7	3.9	down ice	3226	8065	40	1613	610.97	679.5	2.98	0.96	0.019	0.03	0.2
10-MPB-032	54	5.0	5.5	down ice	40	28	0	462	128.50	291.1	0.47	0.86	0.018	0.01	0.2
10-MPB-033	54	2.0	2.5	down ice	3	3	0	19	53.60	183.6	0.35	1.03	0.027	0.01	0.1
10-MPB-034	54	1.0	1.5	down ice	0	0	0	29	130.87	332.1	0.72	0.92	0.023	0.01	0.1
10-MPB-036	60	2.5	3.0	down ice	47	16	0	379	85.95	255.1	0.46	0.78	0.018	0.02	0.2
10-MPB-037	60	1.5	2.0	down ice	3	75	0	113	48.40	113.3	0.27	0.72	0.021	0.01	0.1
10-MPB-038	60	0.9	1.1	down ice	0	0	0	192	35.94	74.5	0.16	0.82	0.022	0.01	0.1

Sample															
11-MPB-009	65	5.0	5.3	down ice	2308	62	0	615	15.41	41.4	0.11	0.80	0.022	0.01	0.1
11-MPB-010	65	3.0	3.3	down ice	0	0	0	3	29.99	114.7	0.26	0.86	0.024	0.01	0.1
11-MPB-011	65	0.8	1.2	down ice	0	0	0	21	594.62	589.1	1.39	1.35	0.022	0.01	0.1
11-MPB-002	75	2.5	2.7	down ice	0	0	0	18	21.40	64.0	0.14	0.84	0.024	0.01	0.1
11-MPB-003	75	1.2	1.3	down ice	0	0	0	1	16.52	47.4	0.16	0.88	0.028	0.01	0.1
11-MPB-004	75	0.5	0.6	down ice	5	0	0	9	35.21	118.6	0.33	0.81	0.023	0.01	0.2
11-MPB-005	80	0.8	1.0	down ice	9	23	0	130	206.55	603.5	1.19	1.07	0.024	0.01	0.2
11-MPB-006	80	1.5	1.6	down ice	63	15	0	2	136.29	404.2	0.88	1.03	0.025	0.01	0.2
11-MPB-007	80	2.8	2.9	down ice	7	102	0	4	25.82	86.3	0.27	0.86	0.027	0.01	0.2
11-MPB-012	90	1.1	1.2	down ice	6	0	0	172	33.42	155.0	0.48	0.84	0.024	0.01	0.1
11-MPB-013	90	2.5	2.7	down ice	2	63	0	8	66.03	233.7	0.56	0.86	0.027	0.01	0.1
11-MPB-014	90	1.9	2.1	down ice	0	0	0	3	32.78	137.2	0.39	0.85	0.027	0.01	0.2
11-MPB-030	90	1.3	1.5	down ice	31	31	0	12	117.11	310.2	0.63	0.84	0.021	0.01	0.2
11-MPB-031	90	2.2	2.4	down ice	2	1	0	2	20.23	70.2	0.20	0.78	0.025	0.01	0.3
11-MPB-032	90	2.7	2.9	down ice	22	13	0	22	26.26	83.8	0.22	0.78	0.025	0.01	0.1
11-MPB-024	100	0.6	0.9	down ice	0	0	0	15	15.36	50.3	0.14	0.78	0.021	0.01	0.1
11-MPB-025	100	1.7	1.8	down ice	1	0	0	2	23.08	68.6	0.19	0.81	0.028	0.01	0.1
11-MPB-026	100	2.5	2.8	down ice	5	0	0	4	28.91	75.4	0.21	0.83	0.025	0.01	0.2
11-MPB-027	120	1.0	1.4	down ice	0	0	0	8	17.03	54.4	0.12	0.80	0.021	0.01	0.1
11-MPB-028	120	2.4	2.6	down ice	0	8	0	5	25.16	90.1	0.24	0.83	0.027	0.01	0.2
11-MPB-029	120	2.9	3.1	down ice	7	6	0	5	20.02	80.7	0.17	0.82	0.027	0.01	0.2
11-MPB-037	140	0.8	1.0	down ice	0	2	0	6	85.10	272.1	0.65	0.92	0.023	0.01	0.1
11-MPB-038	140	2.0	2.2	down ice	0	6	0	8	77.43	280.4	0.63	0.83	0.021	0.01	0.1
11-MPB-039	140	2.6	2.8	down ice	2	0	0	8	87.70	363.6	0.68	0.88	0.024	0.01	0.2
11-MPB-033	150	1.2	1.4	down ice	3	0	0	41	59.10	228.6	0.55	0.95	0.025	0.01	0.1
11-MPB-035	150	1.6	1.8	down ice	0	0	0	4	60.24	224.7	0.55	0.88	0.023	0.01	0.1
11-MPB-036	150	2.7	2.8	down ice	81	242	0	8	185.00	475.2	1.13	0.94	0.027	0.01	0.2
11-MPB-017	160	0.7	0.9	down ice	3	0	0	6	65.68	234.0	0.55	0.78	0.020	0.01	0.2

Sample															
11-MPB-018	160	1.6	1.7	down ice	2	13	0	8	91.12	311.4	0.67	0.89	0.022	0.01	0.1
11-MPB-019	160	2.2	2.3	down ice	13	7	0	7	97.03	360.7	0.73	0.67	0.016	0.01	0.2
11-MPB-020	160	3.1	3.3	down ice	0	0	0	4	74.67	282.4	0.66	0.80	0.022	0.01	0.1
11-MPB-021	160	0.8	1.0	down ice	1	0	0	8	80.95	241.4	0.70	0.84	0.026	0.01	0.1
11-MPB-022	170	1.6	1.9	down ice	0	26	0	8	77.26	278.1	0.62	0.86	0.022	0.01	0.2
11-MPB-023	170	2.7	2.9	down ice	3	68	0	254	82.91	414.3	0.85	0.89	0.022	0.01	0.1
11-MPB-043	350	0.9	1.0	down ice	31	0	0	2	36.10	115.6	0.38	0.75	0.023	0.01	0.2
11-MPB-048	400	0.8	0.9	down ice	9	0	0	15	46.11	142.0	0.40	0.73	0.023	0.01	0.2
11-MPB-052	400	1.0	1.2	down ice	0	8	0	4	46.62	153.5	0.42	0.75	0.024	0.01	0.2
11-MPB-053	400	2.0	2.1	down ice	2	31	0	9	48.63	189.1	0.53	0.80	0.026	0.01	0.3
11-MPB-054	400	2.9	3.0	down ice	20	5	0	31	31.05	108.2	0.32	0.82	0.027	0.01	0.3
11-MPB-049	450	0.8	1.0	down ice	0	1	0	1	64.28	211.9	0.60	0.85	0.026	0.01	0.3
11-MPB-050	450	1.8	2.0	down ice	1	78	0	1	79.34	250.1	0.62	0.86	0.027	0.01	0.2
11-MPB-051	450	2.5	2.6	down ice	2	1	0	0	56.63	218.6	0.65	0.81	0.026	0.01	0.2
11-MPB-045	600	2.0	2.1	down ice	7	31	0	8	70.64	214.3	0.60	0.76	0.023	0.01	0.1
11-MPB-046	600	1.0	1.2	down ice	0	2	0	0	95.50	248.8	0.72	0.80	0.023	0.01	0.2
11-MPB-047	600	2.9	3.0	down ice	2	0	0	4	67.71	235.1	0.62	0.80	0.025	0.01	0.2
11-MPB-040	700	1.2	1.3	down ice	36	1	0	3	38.45	166.8	0.52	0.80	0.025	0.01	0.2
11-MPB-041	700	1.8	2.0	down ice	3	23	0	2	41.30	166.5	0.56	0.82	0.026	0.01	0.2
11-MPB-042	700	2.4	2.6	down ice	0	2	0	5	19.36	59.8	0.13	0.87	0.026	0.01	0.1

13.25 wt % and high S concentrations range from 13.75 to 14.00 wt %. Galena grains with lower S concentrations have higher As (Fig. 8b) and Mn contents (Fig. 8c) than grains with higher S concentrations. Galena grains with high concentrations of S have low concentrations of Fe (Fig. 8d). Deposits R190 (86.69-89.18 wt %) and HZ (83.87-89.27 wt %) have the highest Pb concentrations in galena. All five deposits have similar concentrations of S, As, Ag, Cd, Pb and Se in galena. The differences in composition of bedrock galena grains occur in elements Mn, Fe, Zn, Ge, In, Sb, and Hg. Deposit O28 has the highest concentration of Mn (0.01-0.05 wt %) and the lowest concentration of Zn (0.02-2.12 wt %). Deposit O28 also has an elevated concentration of In (0.02-0.07 wt %) and Sb (0.02-0.04 wt). Deposit R190 and M67 have concentrations of In, Sb and Hg that are below detection limit. Deposit M67 has concentrations of Ge, As, Ag, Cd, In, Sb, Cu and Hg that are below detection limit, and has a low concentration of Fe (0.04-0.05 wt %). Deposits O28 and HZ have the highest concentrations of Ge (0.01-0.12 wt % and 0.02-0.12 wt %, Fig. 9). Cubic and skeletal galena have similar geochemistry but vary in Zn, In, Sb, and Hg concentrations. Skeletal galena has a higher concentration of Zn (0.02-0.91 wt %) and lower concentrations of In (0.02-0.04 wt %), Sb and Hg (below detection limit) than cubic galena. Iron concentration in dendritic galena is below detection limit while banded galena has a concentration range from 0.043 to 0.47 wt % Fe. Banded galena has below a detection limit concentration of In while dendritic galena contains from 0.026 to 0.043 wt % In. Fracture-filling galena is very similar to skeletal galena.

7.4.2. Galena in till

Galena grains were recovered from all size fractions (pan concentrate, 0.25-0.5, 0.5-1.0 and 1.0-2.0 mm) in 27% of the till samples (Table 4). The coarsest grains (1.0-2.0 mm) were recovered from samples closest to the deposit. Most grains were recovered from the pan concentrate of till. Till sample 10-MPB-004 contains 53097 grains in the 0.25 to 0.5 mm fraction, while till sample 10-MPB-005 contains 2419 grains followed by till sample 10-MPB-028, which
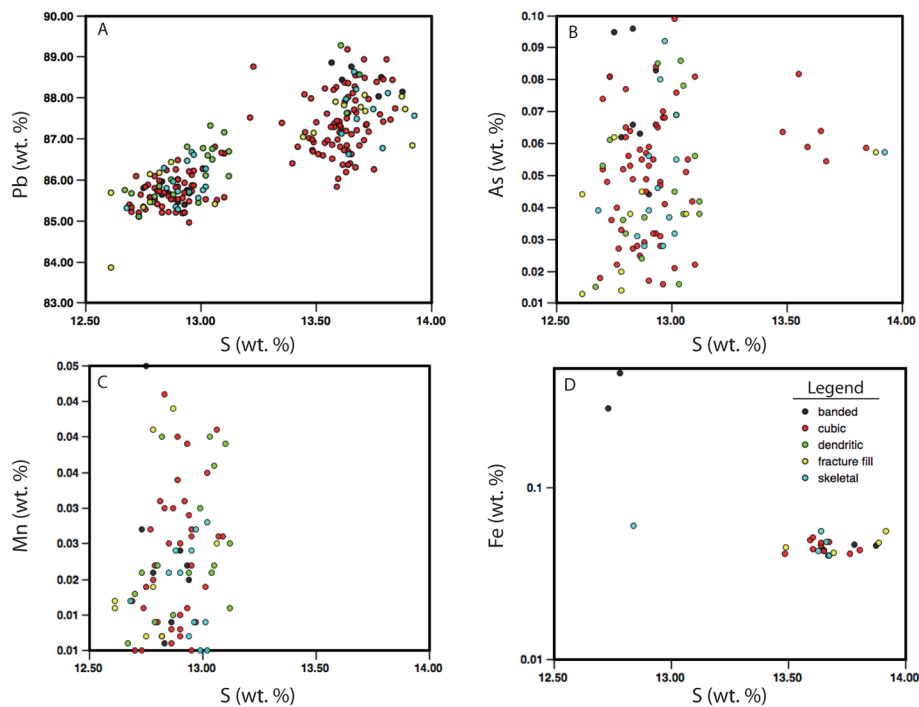
Fig. 8: Concentrations of Pb, As, Mn and Fe versus S in different varieties of galena grains from bedrock samples determined by EMP analysis.
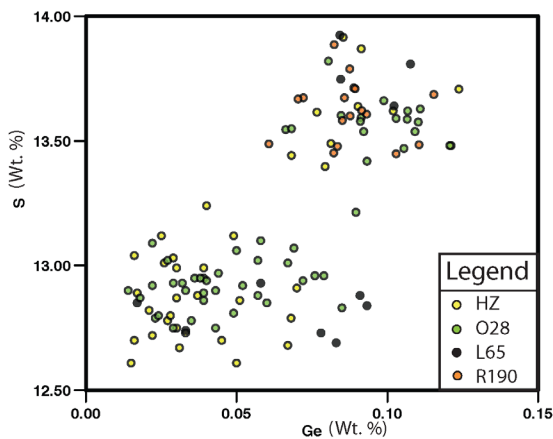
Fig. 9: Concentrations of S versus Ge in galena grains in bedrock from different deposits determined by EMP analysis. Grains from deposit M67 are absent because their Ge values were reported as less than detection limit (109 ppm).

contains 8065 grains (Fig. 10). These till samples are all immediately down-ice of the ore zone of deposit O28. Background concentration for galena is 0 grains which is defined in the same manner as sphalerite grains. Metal-rich till samples from deposit P24 (10-MPB-013 and -014) each contain 192308 and 196078 grains while samples 10-MPB-020, and -021 from deposit N42 contain 4211 and 3158 galena grains, respectively. Buffalo River samples (11-MPB-059, -060 and 085B-

2010-1008) contain between 0 and 6 grains of galena. Regional till sample 11-MPB-061, collected at deposit K77, contains 28 grains and sample 11-MPB-062, collected at deposit S65, contains 0 grains of galena.

Grain morphology for galena in till is typically cubic, though some grains have a coating of anglesite which makes grains appear subcubic to rounded (Fig. 11).

EMPA conducted on galena grains recovered from till samples indicate that grains in till contain similar concentrations of Pb, S and Se to those recovered from bedrock samples. Concentrations of Fe, Zn, Ge, As, In, Sb, Cu and Hg are much lower in grains recovered from till samples than those recovered from bedrock samples. Cadmium concentration ranges from 0.008 to 0.093 wt % in galena grains recovered from till samples.
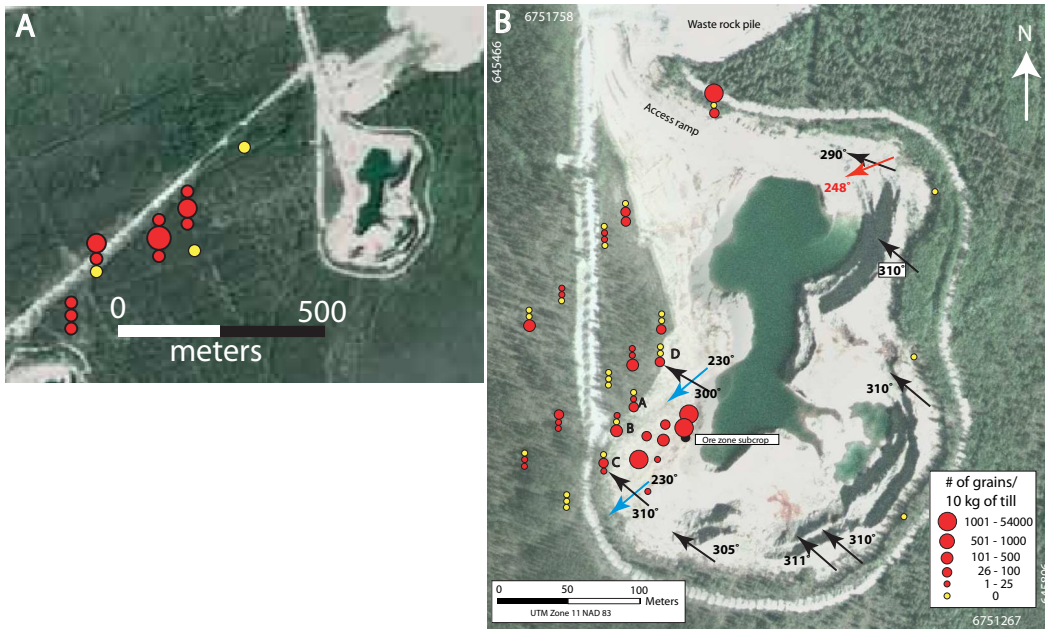
Fig. 10: Distribution of galena grains in the 0.25-0.5 mm fraction of till at deposit O28: A) area down ice (west) of the deposit, and B) area immediately around the deposit. Three vertical samples were collected at some sites for which the data are plotted as vertically stacked symbols. Yellow dots indicate barren till samples. Blue arrows indicate the oldest ice flow trajectory, black are intermediate and red are youngest.

7.5. Pyrite

7.5.1. Pyrite in bedrock

Pyrite in PTS occurs as cubic crystals, botryoidal fans, or needles as well as fine-grained masses. Disseminated particles of anhedral grains also occur throughout most samples. Pyrite grains typically range in size from <50 to 500 µm, though some larger grains (~2500 µm) do occur. In hand sample, pyrite cubes were observed to be 2 cm across (Plate 7).

Pyrite grains in HMC were observed in the pan concentrate and the
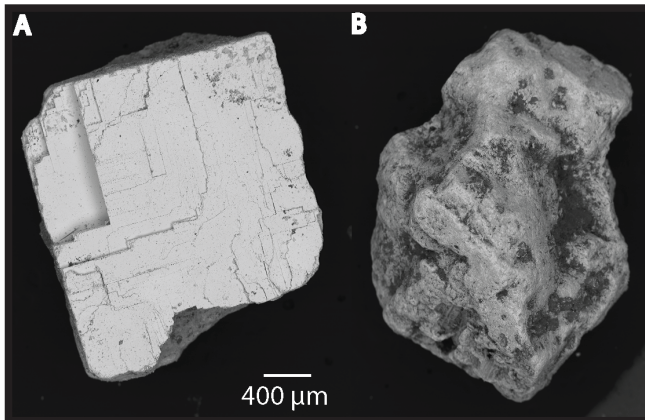
Fig. 11: Secondary electron images of galena grains from till sample 11-MPB-029 showing grain morphology: A) cubic grain with sharp crystal edges and, B) galena grain coated with anglesite producing rounded edges.

0.25 to 0.5 mm. The majority of grains were recovered from the 0.25 to 0.5 mm fraction of till. Samples 1-MPB-R37 and –R38 contained 100% pyrite with 730689 and 527241 grains/1 kg, respectively. Sample 10-MPB-R17 contains 1006711 grains/1 kg.

EPMA data indicate that the concentration of major elements Fe and S range from 41.98 to 47.25 wt % and 51.70 to 54.37 wt %, respectively. Minor elements include Zn (0.012-7.03 wt %), As (less than detection to 0.22 wt. %), and Pb (less than detection to 0.29 wt. %). Selenium (0.012-0.07 wt %) occurs in all five deposits excluding R190. Deposit O28 shows an enrichment in Ge, In, Sb, Pb (Fig. 12a) and Hg (Fig. 12b) in pyrite while pyrite in the other four deposits contain below detection limits of these elements. In Deposit O28, Ge and Hg concentrations range from less than detection to 0.05 wt % and 0.20 wt %,

respectively. Indium concentration ranges from less than detection to 0.04 wt % and Sb concentration ranges from less than detection to 0.03 wt %. Deposit L65 contains more Mn (0.03-0.24 wt %) and As (0.05-0.22 wt %) than other deposits. Deposits HZ contains the highest concentration of Zn (0.48-7.03 wt %) in pyrite, and deposit R190 contains a higher concentration of Cu (0.06-0.70 wt %) in pyrite than the other deposits. Inclusion pyrite and botryoidal pyrite have near identical concentrations of all elements analyzed using EMPA except that botryoidal pyrite contains 0.03-0.24 wt % Mn and inclusion pyrite contains 0.05-0.22 wt % As. Massive pyrite contains the highest concentration of Zn (0.02-7.03 wt %) as well as Cu (0.01-0.46 wt %).

7.5.2. Pyrite in till

Pyrite grains were recovered from the pan concentrate and 0.25-0.5 mm fractions of till. Till sample 10-MPB-004 contains 26549 grains, 10-MPB-030 contains 7576 grains, and till sample 10-MPB-005 contains 3226 grains (Fig. 13). These till samples are overlying and immediately down-ice in the direction
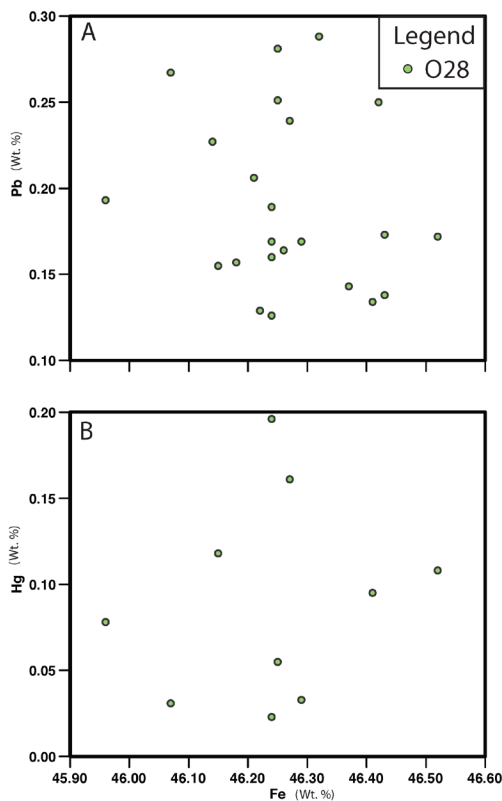
Fig. 12: Concentrations of Pb (A) and Hg (B) versus Fe in pyrite grains from bedrock samples from deposit O28 determined by EMP analysis. Deposit O28 is the only deposit for which Pb and Hg values were reported as greater than the lower detection limits.

of the first known ice-flow direction of the ore body. Till samples 10-MPB-020 and 10-MPB-021, collected from deposit N32 contain 15789 and 8421 grains respectively. Till samples collected from deposit P24 (10-MPB-013 and -014) contain 5882 and 57692 grains. Buffalo River till samples (11-MPB-059, -060 and 085B-2010-1008) contain between 6 and 33 grains of pyrite. Regional till sample 11-MPB-061, collected at deposit K77, contains 2752 grains and sample 11-MPB-062, collected at deposit S65, contains 31 grains.

7.6.   Smithsonite (ZnCO$_3$)

7.6.1. Smithsonite in bedrock

No smithsonite grains were identified in PTS and bedrock HMC.

7.6.2. Smithsonite in till

Smithsonite was identified in till heavy mineral concentrates by its white color and botryoidal habit. Smithsonite was recovered from till samples 10-MPB-004, -005, -20, -021, -026 and -028. All of these till samples excluding 10-MPB-020 and -021 were collected from the shoulder pit O28 (Fig. 14). Till samples 10-MPB-020 and -021 were collected on the west shoulder of pit N32. Smithsonite
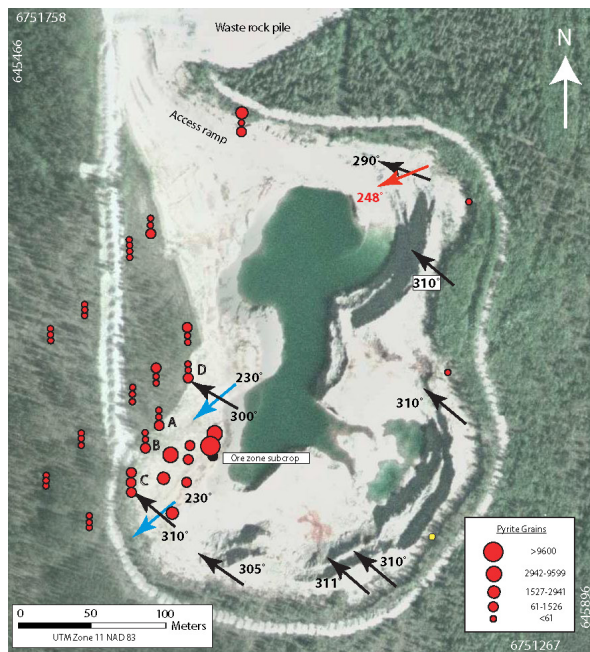
Fig. 13: Distribution of pyrite grains in the 0.25-0.5 mm fraction of till around deposit O28. Three vertical samples were collected at some sites which are shown as vertically stacked symbols. Yellow dots indicate barren samples. Blue arrows indicate the oldest ice flow trajectory, black are intermediate and red are youngest.

concentrations range from 0 to 133 grains and the background concentration is 0 grains. Most smithsonite grains were recovered from the 0.25 to 0.5 mm fraction of till.

Till samples 10-MPB-013 and -014 (from deposit P24) contain 58824 and 57692 smithsonite grains, respectively.
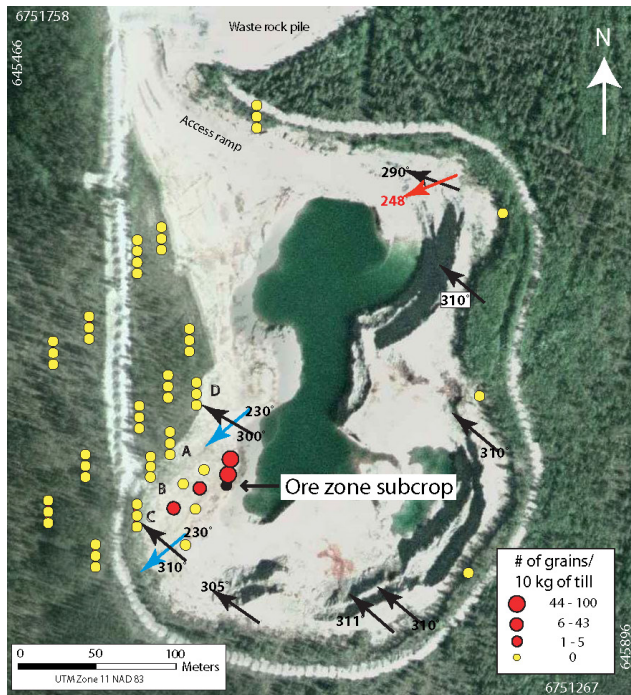
Fig. 14: Distribution of smithsonite grains grains in the 0.25-0.5 mm fraction of till around deposit O28. Three vertical samples were collected at some sites which are shown as vertically stacked symbols. Yellow dots indicate barren samples. Blue arrows indicate the oldest ice flow trajectory, black are intermediate and red are youngest.

7.7.   Cerussite (PbCO$_3$)

7.7.1. Cerussite in bedrock

No cerussite grains were identified in PTS or bedrock HMC.

7.7.2. Cerussite in till

Cerussite was recovered from the 0.25 to 1 mm fraction of till samples 11-MPB-036 and 11-MPB-021 down ice of pit O28. Till sample 11-MPB-036 contains 27 grains and till sample 11-MPB-021 contains 1 grain.

Table 6: Listing of indicator minerals recovered from the pan concentrate, 0.25 – 0.5 mm, 0.5 – 1.0 mm and 1.0 – 2.0 mm size fractions of till samples. These indicator mineral counts have been normalized to 10 kg.

Sample	Sphalerite				Galena				Pyrite				Smithsonite			
	No. grains pan	No. grains 0.25-0.5 mm	No. grains 0.5-1.0 mm	No. grains 1.0-2.0 mm	No. grains pan	No. grains 0.25-0.5 mm	No. grains 0.5-1.0 mm	No. grains 1.0-2.0 mm	No. grains pan	No. grains 0.25-0.5 mm	No. grains 0.5-1.0 mm	No. grains 1.0-2.0 mm	No. grains pan	No. grains 0.25-0.5 mm	No. grains 0.5-1.0 mm	No. grains 1.0-2.0 mm
085B-2010-1001BT	0	0	0	0	1	0	0	0	2	0	0	0	0	0	0	0
085B-2010-1008BT	0	0	0	0	0	0	0	0	465	6	0	0	0	0	0	0
10-MPB-002	0	0	0	0	0	0	0	0	0	0	0	0	0	0	0	0
10-MPB-004	88	35398	265	16	60%	53097	8850	708	0	26549	0	0	0	133	0	0
10-MPB-005	81	4839	121	3	30%	2419	121	12	0	3226	0	0	0	65	0	0
10-MPB-009	0	889	59	21	5%	37	10	4	0	2222	0	0	0	0	0	0
10-MPB-013	0	980392	39216	1961	95%	196078	49020	15686	392	5882	0	0	0	58824	0	0
10-MPB-014	0	288462	19231	58	10%	192308	4808	769	0	57692	0	0	0	57692	0	0
10-MPB-018	0	0	0	0	75	0	0	0	980	2	0	0	0	0	0	0
10-MPB-020	105	15789	263	3	20%	4211	158	26	0	8421	0	0	0	5	0	0
10-MPB-021	105	42105	105	14	20%	3158	632	27	40%	15789	0	0	0	21	0	0
10-MPB-022	0	3	2	0	100	2	0	1	0	0	0	0	0	0	0	0
10-MPB-023	0	0	0	0	6	0	0	0	164	0	0	0	0	0	0	0
10-MPB-024	0	4	0	0	0	0	0	0	25	4	0	0	0	0	0	0
10-MPB-025	0	0	0	0	2	0	0	0	48	0	0	0	0	0	0	0
10-MPB-026	40	159	198	7	40%	397	952	0	20%	952	0	0	0	6	0	0
10-MPB-027	0	38	5	0	75	11	1	0	189	152	0	0	0	0	0	0
10-MPB-028	40	3226	32	0	50%	8065	242	23	0	1613	0	0	0	40	0	0
10-MPB-029	0	19	13	1	200	13	8	6	0	1	0	0	0	0	0	0
10-MPB-030	0	114	5	1	5%	45	38	11	0	7576	0	0	0	0	0	0
10-MPB-031	0	38	0	0	500	30	30	12	152	1136	0	0	0	0	0	0

Sample	Sphalerite				Galena				Pyrite				Smithsonite			
	No. grains pan	No. grains 0.25-0.5 mm	No. grains 0.5-1.0 mm	No. grains 1.0-2.0 mm	No. grains pan	No. grains 0.25-0.5 mm	No. grains 0.5-1.0 mm	No. grains 1.0-2.0 mm	No. grains pan	No. grains 0.25-0.5 mm	No. grains 0.5-1.0 mm	No. grains 1.0-2.0 mm	No. grains pan	No. grains 0.25-0.5 mm	No. grains 0.5-1.0 mm	No. grains 1.0-2.0 mm
10-MPB-032	0	40	2	0	2000	28	5	0	77	462	0	0	0	0	0	0
10-MPB-033	0	3	0	0	50	3	1	0	2	19	0	0	0	0	0	0
10-MPB-034	0	0	0	0	1	0	0	0	10	29	0	0	0	0	0	0
10-MPB-036	0	47	4	0	1000	16	1	0	76	379	0	0	0	0	0	0
10-MPB-037	0	3	0	0	10000	75	8	0	0	113	0	0	0	0	0	0
10-MPB-038	0	0	0	0	3	0	0	0	10	192	0	0	0	0	0	0
10-MPB-039	0	63	3	0	1000	236	43	2	39	1181	0	0	0	0	0	0
10-MPB-040	0	2	0	0	0	0	0	0	0	9	0	0	0	0	0	0
10-MPB-041	0	4	0	0	5	3	0	0	96	58	0	0	0	0	0	0
11-MPB-001	0	0	0	0	0	0	0	0	0		0	0	0	0	0	0
11-MPB-002	0	0	0	0	0	0	0	0	223	18	0	0	0	0	0	0
11-MPB-003	0	0	0	0	9	0	0	0	89	1	0	0	0	0	0	0
11-MPB-004	0	5	0	0	0	0	0	0	1	9	0	0	0	0	0	0
11-MPB-005	0	9	0	0	304	23	8	2	174	130	0	0	0	0	0	0
11-MPB-006	0	63	13	0	394	15	2	1	31	2	0	0	0	0	0	0
11-MPB-007	0	7	0	0	1695	102	8	1	169	4	0	0	0	0	0	0
11-MPB-008	0	42	1	0	840	15	3	1	42	1681	0	0	0	0	0	0
11-MPB-009	0	2308	46	1	76923	62	15	0	385	615	0	0	0	0	0	0
11-MPB-010	0	0	0	0	1	0	0	0	132	3	0	0	0	0	0	0
11-MPB-011	0	0	0	0	2	0	0	0	83	21	0	0	0	0	0	0
11-MPB-012	0	6	0	0	9	0	0	0	172	172	0	0	0	0	0	0
11-MPB-013	0	2	0	0	3968	63	5	2	40	8	0	0	0	0	0	0

Sample	Sphalerite No. grains pan	Sphalerite No. grains 0.25-0.5 mm	Sphalerite No. grains 0.5-1.0 mm	Sphalerite No. grains 1.0-2.0 mm	Galena No. grains pan	Galena No. grains 0.25-0.5 mm	Galena No. grains 0.5-1.0 mm	Galena No. grains 1.0-2.0 mm	Pyrite No. grains pan	Pyrite No. grains 0.25-0.5 mm	Pyrite No. grains 0.5-1.0 mm	Pyrite No. grains 1.0-2.0 mm	Smithsonite No. grains pan	Smithsonite No. grains 0.25-0.5 mm	Smithsonite No. grains 0.5-1.0 mm	Smithsonite No. grains 1.0-2.0 mm
11-MPB-013	0	2	0	0	3968	63	5	2	40	8	0	0	0	0	0	0
11-MPB-014	0	0	0	0	16	0	0	0	4	3	0	0	0	0	0	0
11-MPB-015	0	0	0	0	0	0	0	0	0	0	0	0	0	0	0	0
11-MPB-016	0	2	0	0	23	1	0	0	153	2	0	0	0	0	0	0
11-MPB-017	0	3	1	0	80	0	0	0	0	6	0	0	0	0	0	0
11-MPB-018	0	2	0	1	403	13	4	0	16	8	0	0	0	0	0	0
11-MPB-019	0	13	4	0	74	7	5	0	7	7	0	0	0	0	0	0
11-MPB-020	0	0	0	0	4	0	0	0	16	4	0	0	0	0	0	0
11-MPB-021	0	1	0	0	0	0	1	0	16	8	0	0	0	0	0	0
11-MPB-022	0	0	0	0	407	26	6	0	16	8	0	0	0	0	0	0
11-MPB-023	0	3	0	0	1695	68	11	5	169	254	0	0	0	0	0	0
11-MPB-024	0	0	0	0	11	0	0	0	15	15	0	0	0	0	0	0
11-MPB-025	0	1	0	0	0	0	0	0	156	2	0	0	0	0	0	0
11-MPB-026	0	5	1	0	0	0	0	0	77	4	0	0	0	0	0	0
11-MPB-027	0	0	0	0	0	0	0	0	23	8	0	0	0	0	0	0
11-MPB-028	0	0	0	0	75	8	1	1	376	5	0	0	0	0	0	0
11-MPB-029	0	7	0	0	153	6	2	0	76	5	0	0	0	0	0	0
11-MPB-030	0	31	5	0	233	31	2	0	78	12	0	0	0	0	0	0
11-MPB-031	0	2	0	0	0	1	0	0	152	2	0	0	0	0	0	0
11-MPB-032	0	22	1	0	3704	13	7	1	148	22	0	0	0	0	0	0
11-MPB-033	0	3	2	0	41	0	0	0	25	41	0	0	0	0	0	0
11-MPB-034	0	0	0	0	159	4	3	0	16	1	0	0	0	0	0	0

Sample	Sphalerite				Galena				Pyrite				Smithsonite			
	No. grains pan	No. grains 0.25-0.5 mm	No. grains 0.5-1.0 mm	No. grains 1.0-2.0 mm	No. grains pan	No. grains 0.25-0.5 mm	No. grains 0.5-1.0 mm	No. grains 1.0-2.0 mm	No. grains pan	No. grains 0.25-0.5 mm	No. grains 0.5-1.0 mm	No. grains 1.0-2.0 mm	No. grains pan	No. grains 0.25-0.5 mm	No. grains 0.5-1.0 mm	No. grains 1.0-2.0 mm
11-MPB-035	0	0	0	0	0	0	0	0	4	4	0	0	0	0	0	0
11-MPB-036	0	81	10	0	2823	242	40	11	0	8	0	0	0	0	0	0
11-MPB-037	0	0	0	0	0	2	0	0	122	6	0	0	0	0	0	0
11-MPB-038	0	0	0	0	16	6	2	1	16	8	0	0	0	0	0	0
11-MPB-039	0	2	0	0	8	0	0	0	0	8	0	0	0	0	0	0
11-MPB-040	0	36	5	0	39	1	1	2	78	3	0	0	0	0	0	0
11-MPB-041	0	3	0	0	388	23	4	2	39	2	0	0	0	0	0	0
11-MPB-042	0	0	0	0	0	2	0	0	21	5	0	0	0	0	0	0
11-MPB-043	0	31	1	0	0	0	0	0	16	2	0	0	0	0	0	0
11-MPB-044	0	0	0	0	0	0	0	0	0	0	0	0	0	0	0	0
11-MPB-045	0	7	2	1	787	31	9	2	24	8	0	0	0	0	0	0
11-MPB-046	0	0	0	0	0	2	5	0	0	0	0	0	0	0	0	0
11-MPB-047	0	2	0	0	2	0	0	0	8	4	0	0	0	0	0	0
11-MPB-048	0	9	1	0	12	0	0	0	62	15	0	0	0	0	0	0
11-MPB-049	0	0	0	0	0	1	0	0	39	1	0	0	0	0	0	0
11-MPB-050	0	1	0	0	1563	78	23	6	16	1	0	0	0	0	0	0
11-MPB-051	0	2	0	0	4	1	1	0	16	0	0	0	0	0	0	0
11-MPB-052	0	0	0	0	7692	8	2	0	38	4	0	0	0	0	0	0
11-MPB-053	0	2	0	1	385	31	5	0	115	9	0	0	0	0	0	0
11-MPB-054	0	20	3	0	8	5	0	0	197	31	0	0	0	0	0	0
11-MPB-055	0	152	38	8	379	76	9	2	0	2273	0	0	0	0	0	0
11-MPB-056	0	15	0	0	40	0	0	0	81	48	0	0	0	0	0	0

Sample	Sphalerite				Galena				Pyrite				Smithsonite			
	No. grains pan	No. grains 0.25-0.5 mm	No. grains 0.5-1.0 mm	No. grains 1.0-2.0 mm	No. grains pan	No. grains 0.25-0.5 mm	No. grains 0.5-1.0 mm	No. grains 1.0-2.0 mm	No. grains pan	No. grains 0.25-0.5 mm	No. grains 0.5-1.0 mm	No. grains 1.0-2.0 mm	No. grains pan	No. grains 0.25-0.5 mm	No. grains 0.5-1.0 mm	No. grains 1.0-2.0 mm
11-MPB-057	0	6	0	0	379	17	0	0	152	61	0	0	0	0	0	0
11-MPB-058	0	0	0	0	3	0	0	0	38	8	0	0	0	0	0	0
11-MPB-059	0	0	0	0	0	1	1	1	20	5	0	0	0	0	0	0
11-MPB-060	0	6	0	0	2	6	1	0	125	33	0	0	0	0	0	0
11-MPB-061	0	459	46	5	18349	28	7	0	4587	2752	0	0	0	0	0	0
11-MPB-062	0	0	0	0	0	0	0	0	15	31	0	0	0	0	0	0
11-MPB-063	0	0	0	0	0	0	0	0	0	0	0	0	0	0	0	0
11-PTA-037	0	4	0	0	84	6	0	0	168	8	0	0	0	0	0	0
11-PTA-042	0	0	0	0	5	0	0	0	13	18	0	0	0	0	0	0

Plate 1: Galena textures: A) Cubic galena grains in polished thin section of sample 10-MPB-R76 from deposit HZ. Field of view is 4 mm, B) Massive galena with colloform sphalerite in a bedrock grab sample from a waste rock pile beside deposit O42. Canadian one dollar coin for scale, and, C) Skeletal galena in polished thin section from bedrock sample 10-MPB-R67 from deposit HZ. Field of view is 4 mm.
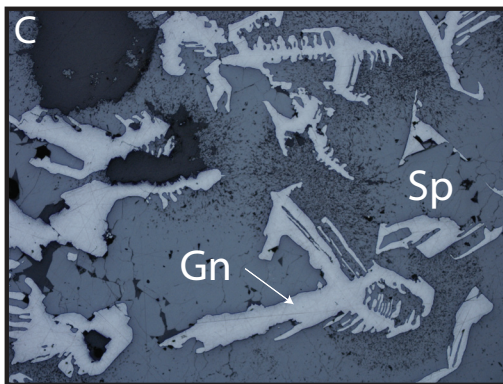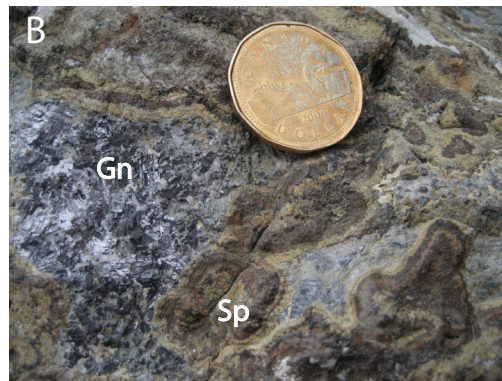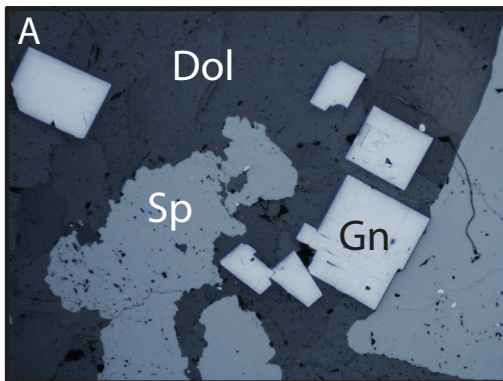
Plate 2: Sphalerite textures and features: A) Polished thin section scan of sample 10-MPB-R46A from deposit O28 showing colloform sphalerite and galena. Field of view is 10 cm, B) Subhedral, honey-brown sphalerite grains in polished thin section from drill core sample 10-MPB-R63 from deposit R190. Interstitial space is filled with native sulphur. Field of view is 4 mm and, C) Brecciated grains of galena, pyrite and sphalerite from drill core sample 10-MPB-R17 from deposit R190. Some brecciated sphalerite grains contain fragments of galena and pyrite. Field of view is 4 mm.
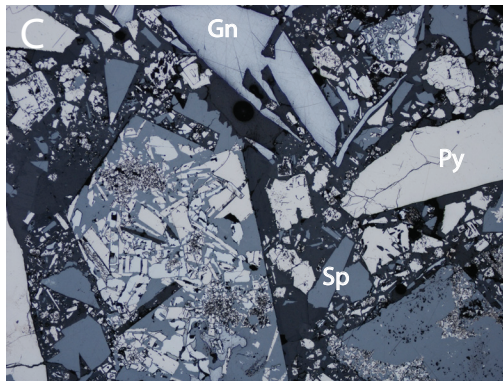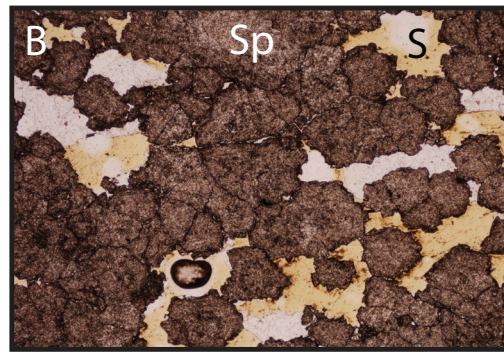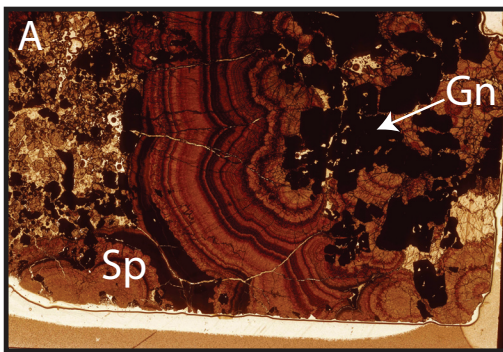
Plate 3: Section A (Fig. 2) consisting of 3 till samples collected around deposit O28. Till section is approximately 6 m high, and till samples were collected at ~1, 3, and 5 m below the natural land surface.
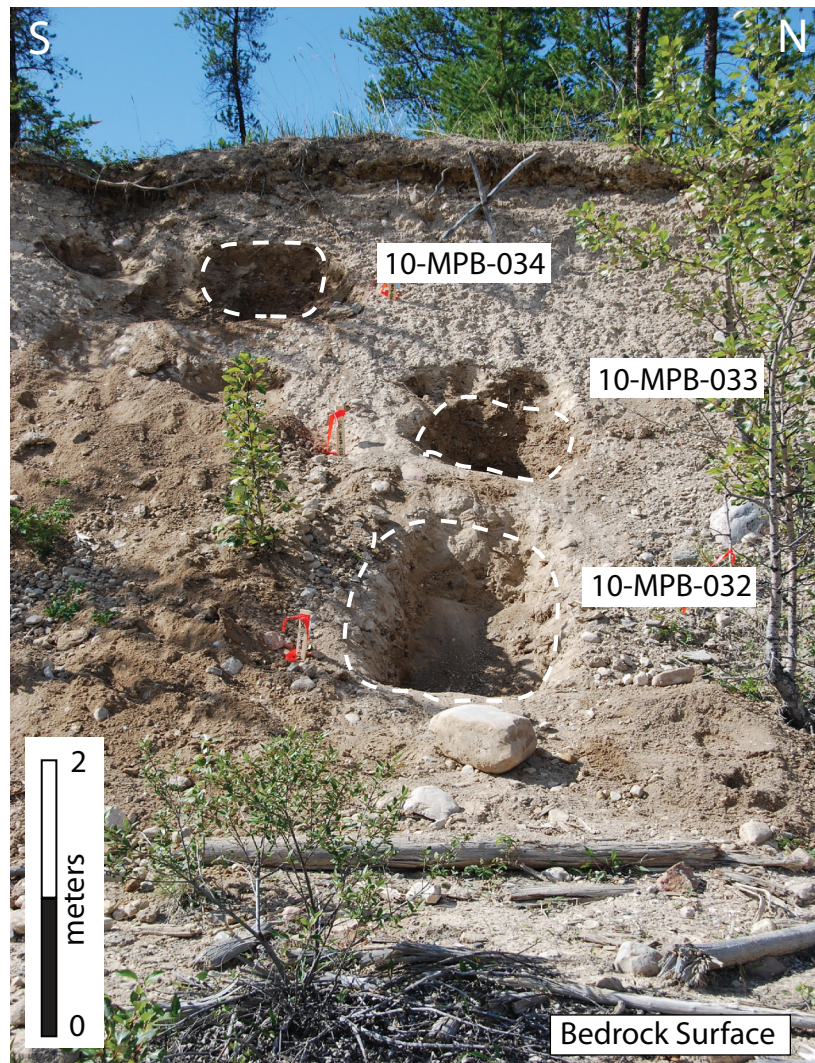
Plate 4: Trench for samples taken away from the pit walls. A trench was excavated to approximately 3 m, with samples being collected every meter.

11-MPB-012

11-MPB-014

1m

11-MPB-013
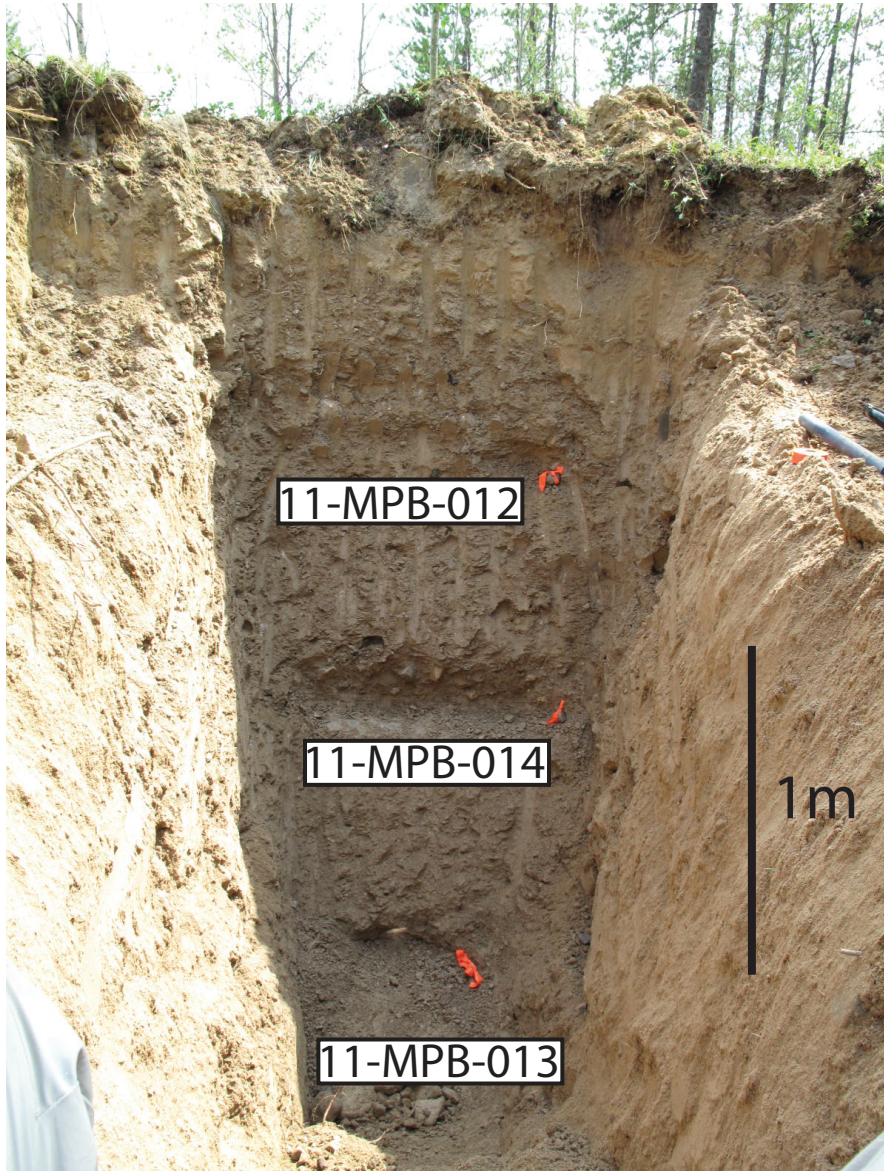
Plate 5: Sphalerite grain types and textures in bedrock sample polished thin sections: A) Honey-brown sphalerite in sample 10-MPB-R02, B) banded honey-brown sphalerite in sample 10-MPB-R41, C) snow-on-roof honey-brown sphalerite in sample 10-MPB-R67, and D) dendritic, blackjack sphalerite in sample 10-MPB-R75.
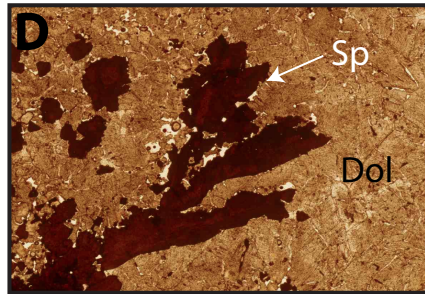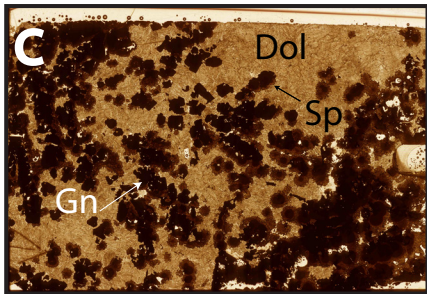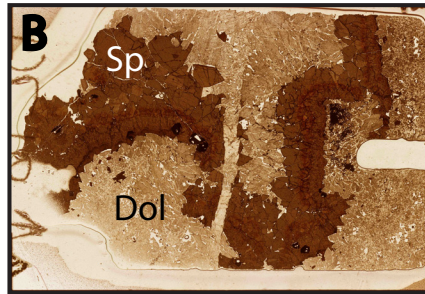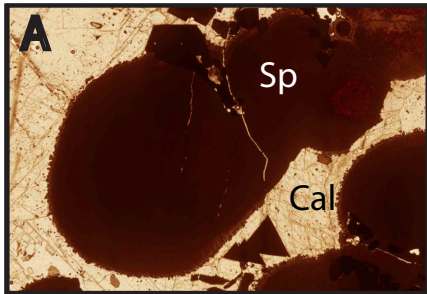
Plate 6: Galena grain types and textures in bedrock sample polished thin sections: A) Galena crystal with curved crystal faces indicating diagenesis in bedrock sample 10-MPB-R63, B) skeletal galena in bedrock sample 10-MPB-R35, C) banded galena and sphalerite in bedrock sample 10-MPB-R55, D) banded galena in bedrock sample 10-MPB-R50.
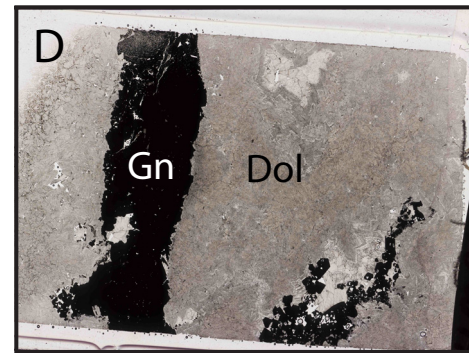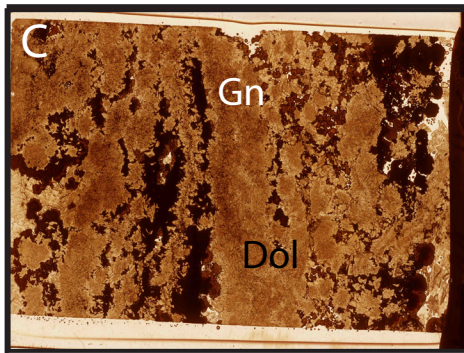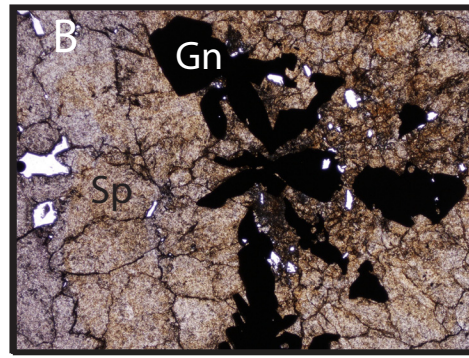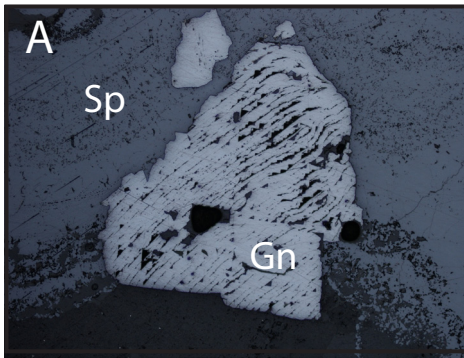
Plate 7: Pyrite textures in bedrock sample polished thin sections: A) botryoidal pyrite in sample 10-MPB-64, and B) massive pyrite in sample 10-MPB-R38, C) Cubic pyrite grain encased in honey-brown sphalerite grain from bedrock sample 10-MPB-R69. Sphalerite grain also contains fragments of galena and, D) Cubic pyrite in bedrock grab sample from deposit S65.
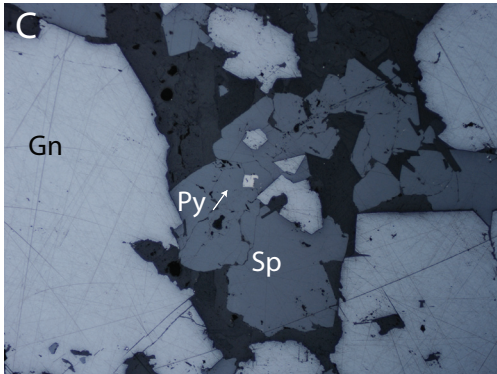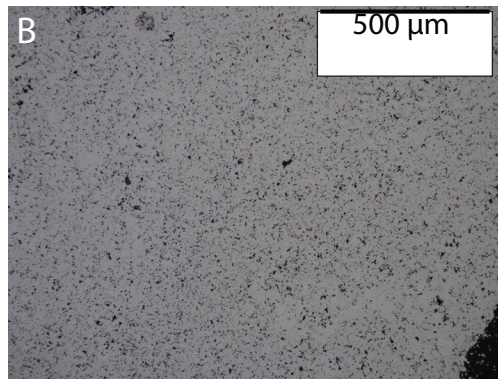
8.   DISCUSSION

8.1.   Indicator mineral compositions

Cleiophane and colloform sphalerite in bedrock contain higher concentrations of Pb than the other varieties. These two sphalerite varieties commonly occur with skeletal galena which could account for the high concentrations of Pb. Deposit M67 contains lower concentrations of Ge, Ag, In, Sb, Pb, Cu, and Hg in bedrock samples than other deposits. Ascicular sphalerite in bedrock also has lower concentrations of these elements which could indicate that the sphalerite in deposit M67 may contain more of this texture of sphalerite. Deposits R190 and O28 have the highest Zn concentrations in sphalerite grains in bedrock which could indicate the presence of more cleiophane and colloform sphalerite than in the other deposits. Cadmium and Fe both substitute for Zn in sphalerite crystal structure which could account for the decreased concentrations of Cd in blackjack sphalerite.

The bimodal distribution of S (low and high) in galena grains in bedrock as determined by EPMA could be due the differences in geochemistry between the different varieties of galena. The majority of skeletal grains fall within the low S group, this could be due to the presence of more Zn in the crystal structure than in cubic galena. Deposits R190 and M67 have lower concentrations of In, Sb, and Hg in bedrock which could indicate that these deposits contain more of the fracture-filling and skeletal galena than the other deposits.

Data from EPMA shows some differences within trace elements of pyrite in bedrock by deposit as well as by variety. Botryoidal pyrite and inclusions of pyrite in other minerals have essentially the same geochemical signature. This could indicate that the botryoidal pyrite is early-stage mineralization or that the mineralizing fluids for each of these varieties of pyrite were the same. Deposit L65 has higher concentrations of As and Mn than the other deposits which could indicate the presence of more botryoidal pyrite in this deposit. Deposits R190

154

and HZ contain the highest concentrations of Zn and Cu in pyrite grains from bedrock indicating that these deposits may contain more massive pyrite than the other deposits

8.2.   Comparison of Pine Point grains with other deposits

Table 6 lists EPMA data for select elements from other MVT deposits in Canada. Data for sphalerite grains in this study are similar to data from previous studies at Pine Point (Kyle, 1981) with the exception of Cd concentrations. This study has, on average, a higher Cd concentration (0.17 wt % higher) than previously reported at Pine Point. This could be due to the larger sample set of this study (n=418) compared to the previous study (n=69) capturing a larger range in compositions of Cd in sphalerite. Pine Point sphalerite has higher Zn and lower Fe, Mn and Cu concentrations on average when compared to the Nanisivik MVT deposit on Baffin Island. This MVT deposit has different general characteristics such as a higher Ag content and higher formation temperatures than Pine Point (Arne et al., 1990). Nanisivik also has three vertical and four horizontal ore zones that are texturally and mineralogically distinct (Arne et al., 1990). Wurtzite ((Zn, Fe)S) is also documented to occur at Nanisivik (Olson, 1977) which could account for the higher Fe concentrations sphalerite than at Pine Point. Concentrations of Pb and Fe are lower in sphalerite grains in anomalous till samples collected in northwestern Alberta (Plouffe et al., 2006; Paulen et al., 2011) ~330 km to the SW, and higher in Cd (on average) than at Pine Point.

Concentrations of selected elements in galena grains from this study are similar to those previously studied at Pine Point (Kyle, 1981), with the exception of Fe and Cu concentrations. On average, Fe concentrations are higher and Cu concentrations are lower in galena grains than those determined by Kyle (1981).

Concentrations of elements in pyrite grains from this study are similar to those determined by previous studies (Kyle, 1981).

8.3. Indicator mineral abundances

Table 7: Comparison of EPMA data for other studies conducted at Pine Point as well as for Nanisivik (Nunavut) and northwestern Alberta

Sphalerite		Zn wt. %	S wt. %	Pb wt. %	Fe wt. %	Mn wt. %	Cu wt. %	Cd wt. %
This study								
	Mean (n=418)	64.15	33.10	0.29	2.04	0.02	0.02	0.23
	Minimum	43.95	32.03	0.03	0.04	0.01	0.01	0.03
	Maximum	67.48	39.19	0.87	16.94	0.04	0.12	0.51
Pine Point								
(Kyle, 1981)								
	Mean (n=69)	64.16	33.38	0.21	2.23	0.01	0.02	0.05
	Minimum	55.47	31.48	0.00	0.15	0.00	0.00	0.00
	Maximum	66.64	33.61	1.05	10.30	0.02	0.16	0.32
Nanisivik								
(Arne et al., 1991)								
	Mean (n=52)	63.87	33.19	N/A	4.54	0.41	0.24	0.30
	Minimum	59.53	32.80	N/A	0.12	0.12	0.18	0.27
	Maximum	68.73	34.02	N/A	15.00	1.15	0.53	0.32
Northwestern Alberta								
(Plouffe et al., 2007)								
	Mean (n=180)	65.45	33.39	0.00	0.71	0.00	0.01	0.43
	Minimum	63.30	32.47	0.00	0.10	0.00	0.00	0.00
	Maximum	66.67	34.22	0.11	3.13	0.02	0.08	1.56
Galena								
This study								
	Mean (n=232)	0.27	13.25	86.66	0.12	0.02	0.02	N/A
	Minimum	0.01	12.59	83.87	0.04	0.01	0.01	N/A
	Maximum	3.32	13.92	89.27	1.33	0.05	0.03	N/A
Pine Point								
(Kyle, 1981)								
	Mean (n=24)	0.23	13.34	85.76	0.01	N/A	0.08	N/A
	Minimum	0.00	13.09	84.47	0.00	N/A	0.00	N/A
	Maximum	1.30	13.66	86.60	0.15	N/A	0.24	N/A
Pyrite								
This study								
	Mean (n=87)	1.96	53.06	0.19	45.95	0.04	0.22	0.00
	Minimum	0.01	51.70	0.13	41.98	0.01	0.01	0.00
	Maximum	7.03	54.37	0.29	47.25	0.24	0.70	0.00
Pine Point								
(Kyle, 1981)								
	Mean (n=31)	N/A	53.26	N/A	46.10	N/A	0.16	N/A
	Minimum	N/A	51.95	N/A	45.00	N/A	0.00	N/A
	Maximum	N/A	53.95	N/A	46.82	N/A	1.27	N/A

Sphalerite, galena and pyrite were detectable in surface till down-ice

to the west and northwest of the O28 deposit at least 500 m from the deposit. Smithsonite was detectable immediately down-ice (to the SW) from the deposit for approximately 40 m. Smithsonite is likely not as abundant as sphalerite at deposit O28 which is why it is difficult to detect at the surface in this area. Smithsonite is a secondary mineral that forms from the oxidation of Zn ores (ie. sphalerite), which could also explain its presence in only a few samples. Smithsonite has a hardness of 4.5 (moh's) and would likely survive glacial transport. May reflect incorporation of preglacial oxidized zone containing smithsonite

Cerussite is a secondary mineral that forms from the oxidation of Pb ores. It was detected in two till samples down ice of the O28 ore zone. There was no cerussite observed in bedrock samples from deposit O28 or any other deposit in this study. Cerussite has a hardness of 3 to 3.5 (mohs) and would likely behave similar to galena and sphalerite during glacial transport. It may be soft enough to be crushed into <25 µm grains.

Till samples that had high concentrations of Zn in the silt + clay fraction (<0.063 mm) did not necessarily have large quantities of sphalerite grains in the sand sized fraction of till. For example, till sample 11-MPB-009 had 2308 sphalerite grains and only 41.4 ppm Zn. This till sample was collected approximately 30 m down ice from the ore zone. The sphalerite grains in the till remained in the sand sized fraction. They were not glacially crushed to the <0.063 mm size fraction. Conversely, some till samples (10-MPB-034, 11-MPB-011, and 11-MPB-005) contain high concentrations of Zn (332-604 ppm) in the till matrix and contain little to no visible sphalerite grains. These till three samples are located at the tops of 3 m vertical till sections. Till in these locations would have been subjected to all three phases of ice-flow and thus the grains were likely communited to the silt size fraction, resulting in the high Zn content in the <0.063 mm fraction and the relatively barren sand-sized fraction.

Abundance of galena grains recovered from the 0.25 to 0.5 mm fraction

of till have a stronger correlation with Pb concentrations in the silt + clay fraction of till. This correlation due to the fact that galena is a softer mineral (Hardness: 2.5) than sphalerite (Hardness: 3.5-4) and therefore would be more susceptible to glacial comminution than sphalerite. Coarse (1.0 to 2.0 mm) sphalerite grains were mainly detected in till samples on the bedrock bench surrounding deposit O28 while galena grains of this size were detected at larger distances from the ore body. This could be due to the larger initial grain size of galena crystals and patches compared to the smaller sphalerite grain size.

Galena grains coated in anglesite ($PbSO_4$) were recovered from till samples 10-MPB-021, -026, -030, -032, 11-MPB-005, -007, -008, -013, -016, -019, -021, -033, -036, -038, -045, and -046. The anglesite coating on galena grains usually only covers a small area likely indicating only minor weathering of galena grains or that the anglesite coating has been scoured off during glacial transport. Galena grains coated with anglesite were recovered from till samples that were considered to be low to moderately oxidized. SEM images (Figure 14) indicate that the majority of anglesite occurs in depressions within the grain, which would be protected from glacial scouring. Anglesite has a hardness of 2-2.5 and could easily be scoured off during glacial transport. There was no anglesite identified in PTS or recovered from bedrock samples.

Till samples 10-MPB-020 and -021 had some of the highest concentrations of sphalerite, galena and pyrite grains of the samples in this study, as well as high concentrations of Zn, Pb, Fe, and Se in the till matrix. These till samples were collected from deposit N32, which had a total tonnage of 2.1 Mt and an average grade for Pb of 3.4 % and for Zn of 8.4 %. These values are nearly double the recorded grades for deposit O28 (Holroyd et al., 1988) which could account for the higher concentrations in these samples than those collected at deposit O28.

Till samples collected along the banks of the Buffalo River do not contain any sphalerite grains, and only slightly elevated concentrations of galena and

158

pyrite. These till sample sites are located approximately 9 km west from the western most known ore body in the district. It is not known if this orebody subcrops or where the nearest subcropping orebody is to Buffalo River so these values may be a reflection of the region or they could indicate that the transport distance of these grains are possibly upwards of 9 km. Further work would be required to establish the dispersal train associated with the Pine Point deposits.

8.4. Indicator minerals recovered from till samples compared to bedrock grains

Sphalerite and galena grains recovered from till have a similar composition as the grains recovered from bedrock. Sphalerite grains recovered from till samples have lower concentrations of As, Ag, Cd, In, Sb, Pb, Cu and Hg than those in bedrock samples. Galena grains recovered from till samples were depleted in Fe, Zn, Ge, As, In, Sb, Cu, Hg, and enriched in Cd in comparison to galena grains in bedrock. Some of these elements show an enrichment in the till matrix geochemistry possibly from matrix/grain interaction.

9.   CONCLUSIONS

Minerals indicative of the presence of Pb-Zn mineralization in the Pine Point mining district are sphalerite, galena, pyrite, cerussite and smithsonite. These indicators, with the exception of cerussite and smithsonite, are detectable in surface till samples at least 500 m down-ice, to the west and northwest, of the O28 deposit.

EPMA data from bedrock grains suggests a difference in trace element geochemistry across the five deposits in this study. Further investigation using LA-ICPMS would be recommended to quantify these differences and to determine their validity.

The relationship between till matrix geochemistry and indicator minerals recovered from till is less obvious between Zn content and sphalerite grains than that of Pb content and galena grains. This is likely due to the differences

159

in mineral properties between these two minerals. The softness of galena (H=2.5), as compared to sphalerite (H=3.5-4), means galena is more susceptible to crushing by glaciers allowing for larger galena grains to contribute to both indicator mineral counts (sand sized grains) and till geochemistry (silt + clay fraction). Sphalerite grains are more physically robust than galena grains, therefore grain morphology of sphalerite grains may be useful for indicating relative glacial transport distances.

Till matrix geochemistry and indicator mineral concentrates recovered from till are both useful tools when exploring for MVT deposits in glaciated terrain. Indicator minerals were detectable in regional till samples that had above background concentrations of pathfinder elements indicating that both indicator minerals and till geochemistry are detectable at a regional scale.

Indicator mineral and till geochemical methods used to explore for MVT each have their strengths and weaknesses. Using either one in conjunction with the other will yield the best results.

10.   ACKNOWLEDGEMENTS

11. REFERENCES

Brabec, D. 1983. Evaluation of soil anomalies by discriminant analysis in geochemical exploration for carbonate-hosted lead-zinc deposits. Economic Geology, v. 78, p. 333-339.

Campbell, N., 1966. The lead-zinc deposits of Pine Point: Canadian Mining and Metallurgical Bulletin, v. 59, p. 953-960.

Dreimanis, A. 1960. Geochemical prospecting for Cu, Pb and Zn in glaciated areas, Eastern Canada. International Geological Congress 21, Session Part 2, p. 7-19.

Dyke, A.S. 2004. An outline of North American deglaciation with emphasis on central and northern Canada. *In*: J. Ehlers and P.L. Gibbard (eds.), Quaternary Glaciations - Extent and Chronology, Part II. North America. Elsevier B.V., Amsterdam, Development in Quaternary Science Series, Vol. 2: 373-424.

Dyke, A.S., and Prest, V.K., 1987. Late Wisconsin and Holocene history of the Laurentide Ice Sheet. Geographie physique et Quaternaire, v. 41, p. 237-263.

Eaton, D.W. and Hope, J. 2003. Structure of the crust and upper mantle of the Great Slave Lake shear zone, northwestern Canada, from teleseismic analysis and gravity modelling. Canadian Journal of Earth Sciences, v. 40, p. 1203-1218.

Hannigan, P.K., 2006. Introduction. *In:* Hannigan, P.K. (ed) *Potential for Carbonate-hosted Lead-zinc Mississippi Valley-type Mineralization in Northern Alberta and Southern Northwest Territories.* Geoscience Contributions, Targeted Geoscience Initiative, Geological Survey of Canada, Bulletin 591, p. 9-39.

Hannigan, P., 2007. Metallogeny of the Pine Point Mississippi Valley-Type zinc-lead district, southern Northwest Territories. *In:* Goodfellow, W.D. (ed) *Mineral Deposits of Canada: A Synthesis of Major Deposit-Types, District Metallogeny, the Evolution of Geological Provinces, and Exploration Methods*. Geological Association of Canada, Mineral Deposits Division, Special Publication No. 5, p. 609-632.

Hannon, P.J., Roy, W.D., Flint, I.M. and Ernst, B.E. 2012. Technical report on the R-190, X-25, P-499, O-556, Z-155 and G-03 deposits of the Pine Point project for Tamerlane Ventures Incorporated. MineTech International Limited, Halifax, 160 p.

Holroyd, R.W., Hodson, T.W., and Carter, K.M., 1988. Unpublished termination report, Pine Point Mines Ltd., June 28, 1988.

Kyle, J.R., 1977. Development of sulphide hosting structures and mineralization,

Pine Point, Northwest Territories. Ph.D. thesis, University of Western Ontario, 226 p.

Kyle, J.R., 1981. Geology of the Pine Point lead-zinc district. *In:* Wolf, K.H., (ed) *Handbook of strata-bound and stratiform ore deposits.* Elsevier Publishing Company, New York, v. 9, p 643-741.

Lemmen, D.S., 1990. Surficial materials associated with glacial Lake McConnell, southern District of Mackenzie. *In*: Current Research, Part D, Geological Survey of Canada, Paper 90-1D, p. 79-83.

Lemmen, D.S., 1998a. Surficial geology, Klewi River, District of Mackenzie; Northwest Territories. Geological Survey of Canada, "A" Series Map 1905, scale 1: 250 000.

Lemmen, D.S., 1998b. Surficial geology, Buffalo Lake, District of Mackenzie; Northwest Territories. Geological Survey of Canada, "A" Series Map 1906, scale 1:250 000.

Lemmen, D.S., Duk-Rodkin, A., and Bednarski, J.M., 1994. Late glacial drainage systems along the northwestern margin of the Laurentide Ice Sheet. Quaternary Science Reviews, v. 13, p. 805-828.

Macqueen, R.W. and Ghent, E.D., 1975. Occurrence of zinc in Devonian metalliferous shales, Pine Point region, District of Mackenzie. Geological Survey of Canada Paper 75-1B, p. 53-57.

McClenaghan, M.B., 2005. Indicator mineral methods in mineral exploration. Geochemistry: Exploration, Environment, Analysis v. 5, p. 233-245.

McClenaghan, M.B., Oviatt, N.M., Averill, S.A., Paulen, R.C., Gleeson, S.A., McNeil, R.J., McCurdy, M.W., Paradis, S., and Rice, J.M., 2012. Indicator mineral abundance data for bedrock, till and stream sediment samples from the Pine Point Mississippi Valley-Type Zn-Pb deposits, Northwest Territories. Geological Survey of Canada Open File 7267.

Morrow, D.W., MacLean, B.C., Miles, W.F., Tzeng, P., and Pana, D., 2006. Subsurface structures in southern Northwest Territories and northern Alberta: implications for mineral and petroleum potential. *In:* Hannigan, P.K. (ed) *Potential for Carbonate-hosted Lead-zinc Mississippi Valley-type Mineralization in Northern Alberta and Southern Northwest Territories.* Geoscience Contributions, Targeted Geoscience Initiative, Geological Survey of Canada, Bulletin 591 p. 41-59.

Nelson, J., Paradis, S., Christensen, J., and Gabites, J., 2002. Canadian Cordilleran Mississippi Valley-type deposits: A case for Devonian-Mississippian back-arc hydrothermal origin. Economic Geology, 97: 1013-1036.

Okulitch, A.V. (compiler) 2006. Phanerozoic bedrock geology, Slave River, District

of Mackenzie, Northwest Territories. Geological Survey of Canada, Open File 5281, scale 1:1,000,000.

Oviatt, N.M., McClenaghan, M.B., Paulen, R.C., and Gleeson, S.A., 2013. Till geochemical signatures of the Pine Point Pb-Zn Mississippi Valley-Type district, Northwest Territories. Geological Survey of Canada Open File 7320.

Paradis, S., Turner, W.A., Coniglio, M., Wilson, N., and Nelson, J.L., 2006. Stable and Radiogenic isotopic signatures of mineralized Devonian carbonate rocks of the northern Rocky Mountain and WCSB. *In:* Hannigan, P.K. (ed) *Potential for Carbonate-hosted Lead-zinc Mississippi Valley-type Mineralization in Northern Alberta and Southern Northwest Territories.* Geoscience Contributions, Targeted Geoscience Initiative, Geological Survey of Canada, Bulletin 591, p. 75-103.

Paulen, R.C., Plouffe, A., and Smith, I.R. 2008. Diamond and base metal indicator minerals in glacial sediments of northern Alberta, Canada. EXPLORE, 138: 1-7.

Paulen, R.C., Paradis, S., Plouffe, A., and Smith, I.R., 2009. Base metal exploration with indicator minerals in glacial sediments of northwest Alberta, Canada. *In*: Lentz, D.R., Thorne, K.G. and Beal, K.L. (eds) *Proceedings of the 24th International Applied Geochemistry Symposium (IAGS), Fredricton, New Brunswick*, v.2, p 557-560.

Plouffe, A., Paulen, R.C., and Smith, I.R., 2006. Indicator mineral content and geochemistry of glacial sediments from northwest Alberta (NTS 84L, M): new opportunities for mineral exploration. Geological Survey of Canada, Open File 5121.

Prest, V.K., Grant, D.R., and Rampton, V.N., 1968. Glacial map of Canada. Geological Survey of Canada, "A" Series Map 1253, scale 1: 5 000 000.

Rhodes, D., Lantos, E.A., Lantos, J.A., Webb, R.J., Owens, D.C., 1984. Pine Point orebodies and their relationship to the stratigraphy, structure, dolomitization, and karstification of the middle Devonian Barrier complex. Economic Geology, v. 79, p. 991-1055.

Sangster, D.F., 2002. MVT deposits of the world; database documentation of the World Minerals Geoscience Database Project, http://www.nrcan.gc.ca/gsc/mrd/wmgdb/index_e.php

Shilts, W.W., 1976. Glacial till and mineral exploration, *In:* Legget, R.F. (ed) Royal Society of Canada Special Publication No. 12, p. 205-224.

Skall, H., 1975. The paleoenvironment of the Pine Point lead-zinc district. Economic Geology, v. 70, p. 22-47.

Skall, H., 1977. The geology of the Pine Point barrier reef complex. *In:* McIlreath, I.A., and Harrison, R.D. (eds) *The geology of selected carbonate oil, gas and lead-*

zinc reservoirs in western Canada. Canadian Society of Petroleum Geologists, Core Conference, no. 5, p 19-38.

Smith, D.G. 1994. Glacial Lake McConnell: paleogeography, age, duration and associated river deltas, Mackenzie River basin, western Canada. Quaternary Science Reviews, v. 13, p. 829-843.

Stothart, Paul. "The Mining Association of Canada." *2011 Facts and Figures*, accessed 14 October 2012.

Appendix B2. Geological Survey of Canada Open File 7320

TILL GEOCHEMICAL SIGNATURES OF THE PINE POINT Pb-Zn MISSISSIPPI VALLEY-TYPE DISTRICT, NORTHWEST TERRITORIES

Natasha M. Oviatt[1], M. Beth McClenaghan[2], Roger C. Paulen[2], and Sarah A. Gleeson[1]

(1) University of Alberta, Department of Earth and Atmospheric Sciences, Edmonton, Alberta, oviatt@ualberta.ca

(2) Geological Survey of Canada, 601 Booth Street, Ottawa, Ontario, K1A 0E8

TABLE OF CONTENTS

LIST OF TABLES

LIST OF FIGURES

1. ABSTRACT

Exploration for base metal deposits using till geochemistry and indicator mineral methods have been the focus of many studies initiated in recent years. The University of Alberta, Geological Survey of Canada, Tamerlane Ventures Incorporated and Teck Resources Limited are examining the indicator minerals and till geochemistry that characterize glacial dispersal from the Pine Point Mississippi Valley-Type (MVT) district, Northwest Territories. This case study documents the clastic glacial dispersal down-ice from the O-28 former open pit mine.

Aqua regia digestion/ICP-MS of the <0.063 mm fraction of till identify Zn, Pb, Cd, Fe, Tl, S and Se as the pathfinder elements associated with Pit O-28 at the Pine Point MVT district. Concentrations of Zn, Pb and Cd are highest directly down-ice of the sub-cropping mineralization in the direction of the earliest recorded ice flow trajectory (~230°). This geochemical signature does not appear detectable at the surface. This may be due to extensive till cover and dilution by multiple ice-flow trajectories, or due to the extensive winnowing and reworking of the till surface by glacial Lake McConnell that inundated the region during deglaciation.

2. INTRODUCTION

Indicator mineral and till geochemical methods have proven to be very successful exploration tools in glaciated terrains (e.g., Dreimanis, 1960; Shilts, 1996; McClenaghan, 2005; Paulen et al., 2009), however, there are few published studies of these methodologies applied to Mississippi Valley-Type (MVT) base metal deposits. To improve exploration in glaciated terrain, the Geological Survey of Canada (GSC), University of Alberta, Tamerlane Ventures Incorporated, and Teck Cominco Limited initiated a collaborative study in 2010 to document till geochemical and indicator mineral signatures of the Pb-Zn deposits in the Pine Point MVT district, Northwest Territories. This research is part of the GSC's Geo-Mapping for Energy & Minerals (GEM) Program (2008-2013) Tri-Territorial

171

Indicator Mineral Project.

2.1. Location and physiography

The Pine Point mining district is located on the south shore of Great Slave Lake, Northwest Territories, in the Great Slave Plain physiographic region of the Western Interior Plains (Bostock, 1970). The former mining district is approximately 180 km due south of Yellowknife, in the Buffalo Lake topographic map sheet (NTS 85B) and approximately 50 km east of the town of Hay River. The Buffalo River flows north into Great Slave Lake on the western side of the study area. Black spruce bogs characterize the area and local relief does not exceed 15 m (Lemmen et al., 1994). The Pine Point mine site and open pits can be accessed via Highways 5 and 6 and mine roads by truck or all-terrain vehicle in the summer.

2.2. Previous work

Surficial mapping was carried out in the Pine Point area by the GSC from 1989 to 1994, mainly to expand the knowledge of Glacial Lake McConnell and associated deposits (Lemmen 1998a, 1998b). Surficial geology maps were published for Buffalo Lake (NTS 85B) and Klewi River (NTS 85A) and a single phase of ice flow to the west was identified (Lemmen, 1990). There is very little published information on the ice flow history of the region and southern Great Slave Lake in general (Prest et al., 1968; Paulen et al., 2009). Additional research on Glacial Lake McConnell was conducted east of the area by Smith (1994).

Soil surveys have been conducted in the area to characterize the Zn-rich shales that occur in the region and whether or not they are a source for the Zn metal at Pine Point. The high concentrations of Zn that still remain in these shales indicate that they were likely not the source for mineralization at Pine Point (Macqueen and Ghent, 1975; Brabec, 1983).

2.3. Exploration history

The Pine Point mining district was discovered by prospectors heading north during the Klondike gold rush (1896-1898) who staked claims on a gossanous outcrop at Sulphur Point on the shore of Great Slave Lake. Little work was conducted on these claims until 1929 when the Northern Lead Zinc Company was formed, which included Cominco Limited (Campbell, 1966). The focus of Northern Lead Zinc Company's 1929-1930 exploration program was to determine if the known ore bodies were connected beneath the surface and to define the ore grade of the sub-cropping mineralization. The occurrence of the Great Depression in the early 1930s halted all exploration in the area. Between 1940 and 1947, Cominco Limited directed a drilling program to delineate ore bodies associated with basement faulting (Campbell, 1966). In 1963, an induced polarization geophysical survey was conducted in the area, which led to the discovery of ore bodies that did not subcrop (Hannigan, 2006). The Pine Point mines opened in 1964 and were one of Canada's most profitable Pb-Zn mining districts until 1987 when they were shut down. Between 1975 and 1981, Westmin Resources conducted drilling programs approximately 25 km west of Cominco's open pits and discovered nine additional deposits (Hannigan, 2007). None of these western deposits have been mined.

Figure 1: Bedrock geology map of the Pine Point area (modified from Hannigan, 2007) showing three trends of the orebodies. Deposits labelled in red are locations of till samples. Regional till samples are marked with green dots. Red dots are stream sediment samples.

Tamerlane Ventures Incorporated picked up the unmined Westmin Resources deposits at Pine Point in 2008 and are currently exploring and assessing the feasibility of several deposits (Hannon et al., 2012).

3. BEDROCK GEOLOGY

The Pine Point region is underlain by rocks of the eastern margin of the Western Canada Sedimentary Basin. The bedrock of the Pine Point area is consists of 350 to 600 m thick Ordovician to Devonian rocks that overlie crystalline basement rocks of the Archean and Proterozoic (Skall, 1975; Kyle, 1981; Rhodes et al., 1984; Okulitch, 2006; Hannigan, 2007). More specifically, the deposits are hosted by, or proximal to, the Presqu'ile barrier which is a reef-like complex (200 m at its thickest point) that separates the deep marine rocks to the north from the shallow marine rocks to the south (Rhodes et al., 1984; Hannigan, 2007). The Presqu'ile barrier consists of the Upper Keg River and Sulphur Point formations. The Upper Keg River Formation includes the lower two-thirds of the barrier and consists of flat, lensoidal beds of carbonate sandstones and mudstones and fine, dense, grey-brown to buff brown dolomite with abundant carbonaceous fossils (Skall, 1975; Hannigan, 2007). The overlying Sulphur Point Formation consists of a build-up of bioherms, bioclastic limestones and carbonate sandstones (Rhodes et al., 1984; Hannigan, 2007) and has undergone alteration into a coarse crystalline, vuggy dolomite known as Presqu'ile dolomite which is the host of the majority of the ore bodies (Skall, 1975; Hannigan, 2007). Karstification was the primary control for ore deposition in the area (Rhodes et al., 1984; Hannigan, 2007).

The Great Slave Lake Shear Zone (GSLSZ) is an area of highly deformed and sheared rocks that extends for approximately 700 km from Northwest Territories down into northeastern British Columbia (Eaton and Hope, 2003). It is considered to be a boundary between the Churchill and Slave cratonic provinces (Morrow et al., 2006). Lead isotopic studies (Nelson et al., 2002; Paradis et al., 2006) indicate that mineralizing fluids likely originated in the basement using faults using the

174

Figure 2: Thick deposit of till within a karst collapse structure, at Pit K-62.

GSLSZ as a conduit. This event would likely have occurred in the Phanerozoic when the fault zone was reactivated during the Laramide orogeny (Morrow et al., 2006). The orebodies are concentrated within 3 NE-SW trending zones referred to as the North trend, Main trend and South trend (Figure 1). The McDonald Fault, a component of the GSLSZ, cuts through the basement rocks immediately below and sub-parallel to these three trends (Skall, 1975; and Kyle, 1981). It has been interpreted that tectonic activity associated with the MacDonald fault may have had a part in creating these trends (Skall, 1977).

The ore field consists of 100 drill-defined orebodies (Hannigan, 2007) that span an area of approximately 1600 km2. The orebodies range from 100,000 to 17.5 million tonnes and have an average grade of 2% Pb and 6.2% Zn (Hannigan, 2007). The total geological resource (produced and remaining proven resource) is estimated to be 95.4 Mt (Hannigan, 2007). The mine site closed in 1988 due to dropping market prices for Pb and Zn and due to rising mining costs.

The deposits consist of galena and sphalerite with minor pyrite and marcasite

Figure 3: Locations of regional till and bedrock samples; striation sites are shown in pink. Digital colour airphoto mosaic provided by Tamerlane Ventures Incorporated.
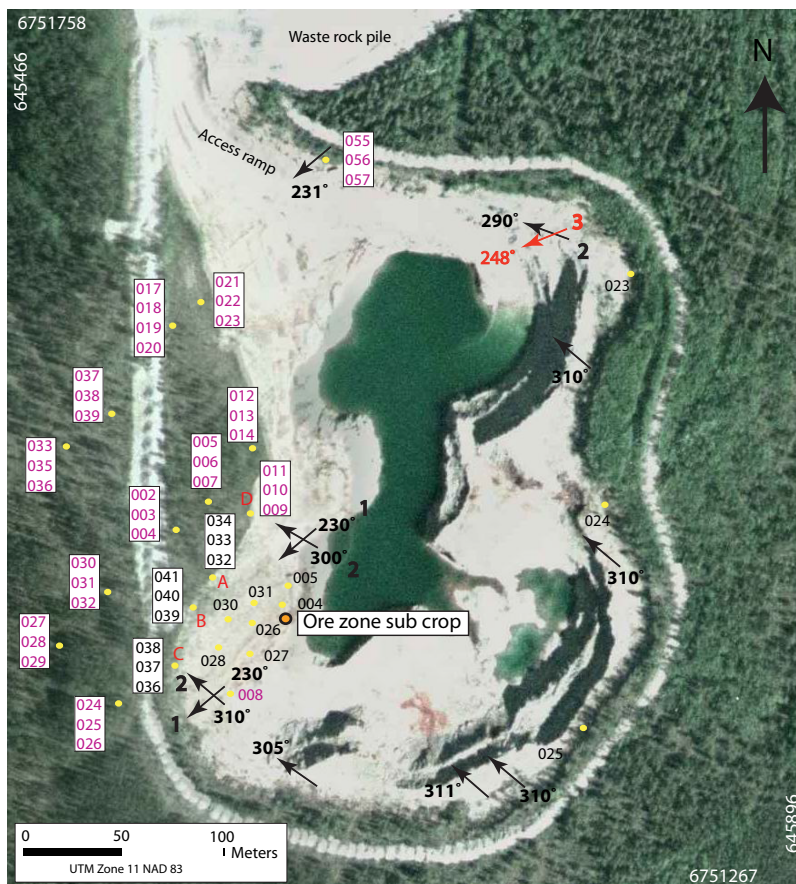
Figure 4: Locations of till samples collected at Pit O-28. Samples collected in 2010 are shown in black while samples collected in 2011 are shown in pink. Digital colour aerial photo provided by Tamerlane Ventures Incorporated.
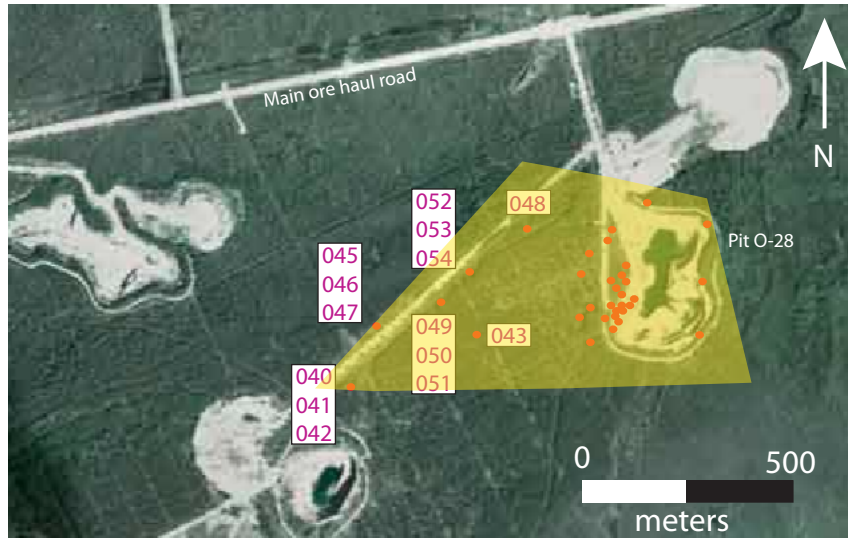
Figure 5: Locations of samples collected along the haul road around Pit O-28. Digital colour aerial photo provided by Tamerlane Ventures Incorporated.
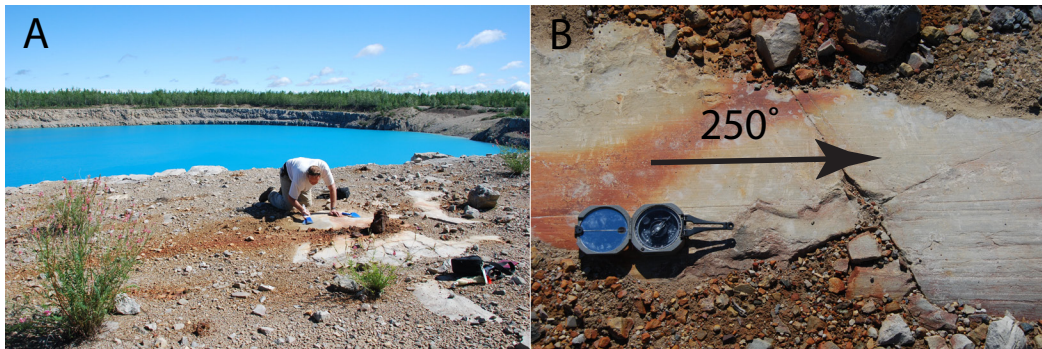
Figure 6: A) Striation site on bedrock exposure on shoulder of Pit W-19 and, B) measurement taken from a striated bedrock surface, trending in the direction of the youngest ice flow trajectory.

(Hannigan, 2007). Galena occurs as isolated crystals or as massive patches and, as the skeletal variety within colloform sphalerite. Sphalerite is present as very fine-crystalline colloform textures or occurs as isolated crystals (from 1 mm to 5 mm). Sphalerite crystals range from a dark Fe-rich variety to a light honey-brown type. Sphalerite, galena, and pyrite also occur as brecciated clasts in some instances. Minor hydrothermal minerals associated with the Pine Point deposits include marcasite, pyrite, sulphur, pyrrhotite, celestite, barite, gypsum, anhydrite, and fluorite (Hannigan, 2007). Bitumen is also present in the host Paleozoic carbonate rocks.

4. SURFICIAL GEOLOGY

The low-relief geomorphology of the Pine Point area is the result of the relatively flat bedrock topography overlain by glacial sediments formed and deposited by the Keewatin sector of the Laurentide Ice Sheet. Till cover occurs as a continuous blanket that generally increases in thickness from east to west across the Pine Point mine district. Till deposits at the eastern margin of the former mine district range from <1 m to 3 m thick, and gradually thicken westward to >25 m at the western pits. Till is locally thicker where karst collapse structures have created depressions in the bedrock surface (Figure 2). Historic drill hole data indicates that till is up 100 m thick in places (Lemmen, 1990). Commonly, till in the area has a silt to fine sand matrix with very little clay (Lemmen, 1998b). The landscape surrounding the Pine Point mine site has glacially streamlined features such as flutings that mostly reflect the last ice flow trajectory. The

The Pine Point region was deglaciated sometime between 10.0 and 9.6 14C ka BP (Dyke, 2004) and was inundated by Glacial Lake McConnell (Smith, 1994). Most of the till surfaces are winnowed, and there was extensive reworking of the till into glaciolacustrine littoral sediments over much of the area (Lemmen, 1990). Glaciolacustrine deposits occur as shorelines and beach ridges, some of which have been reworked into eolian dunes. At approximately 7.8 14C ka BP, it

Figure 7: Sample of cemented, ore-rich till collected at Pit P-24. Note the large pebble of galena (Canadian two-dollar coin, 28 mm diameter, for scale).

was speculated that basin uplift in the region had restored Great Slave Lake to its current position (Dyke and Prest, 1987; Dyke, 2004).

5. METHODS

Geologists from the GSC, Tamerlane Ventures Incorporated and the University of Alberta worked together to collect the till and rock samples from open pits and Tamerlane Ventures Incorporated diamond drillcore. Till sampling and observations of ice flow indicators were conducted following a reconnaissance of 30 open pits on the Pine Point property. A total of 96 till and 54 bedrock samples were collected and striae were mapped at 12 sites (Figures 3 to 5), over the course of two field seasons (summers of 2010 and 2011). Bulk (15-22 kg) till samples were collected for heavy mineral analysis and approximately 2 kg was collected for till matrix geochemistry. Samples 11-PTA-004, -006, -008, -010, -011, -023A, -023B, -030, -035, -037 and -042 are part of a separate till micromorphology study and will not be discussed in this report.

5.1. Ice flow patterns

Assessment of glacial history within the study area included the observation

179

of the orientation of large-scale glacially streamlined landforms to small-scale erosional ice-flow indicators on bedrock such as glacial striae, grooves and outcrop sculpting. Landform mapping encompasses the examination of large subglacial bedforms such as drumlins and flutings from aerial photographs.

Natural exposures of outcrop in the region are scarce, and are usually weathered to the point that glacial striations are not preserved. Striation measurements were recorded from the bedrock surfaces exposed on the shoulders of the former open pits at 12 sites throughout the mine property (Figure 6). Striations were measured on relatively flat outcrop surfaces. Relative ages of striated surfaces are determined (where possible) by evaluating their relative positions on an outcrop according to the criteria defined by Lundqvist (1990) and McMartin and Paulen (2009). Striation site locations and measurements are given in Appendix H.

5.2.   Field sampling

Metal-rich, cemented till (Figure 7) was sampled in Pit P-24 (10-MPB-013, -014). Two till samples (10-MPB-020, -021) were collected from the bedrock surface overlying Pit N-32 as well as three till samples (10-MPB-009, -017 and -018) from Pit P-41 to document any variance in the geochemistry and indicator mineral size and morphology from different ore bodies. Sample 11-MPB-058 was collected from Paulette Creek 15 km up-ice of the eastern most Pb-Zn deposit to determine "background" concentrations. Seven till samples were collected from pits K-62 (11-PTA-037, -042), S-65 (11-MPB-062), K-77 (11-MPB-061). Three samples collected from sections along the Buffalo River (11-MPB-059, -060, 085B101008BT) were collected to establish the overall down-ice concentrations from the Pine Point mining district.

Pit O-28 was chosen for a detailed dispersal study because: a) mineralization sub-cropped and thus was directly eroded and entrained by the Laurentide Ice Sheet, b) multiple striated outcrops on the bedrock surface of the open pit

Table 1: Transport distance of pathfinder elements in the Pit O-28 area

Sample	Distance from ore zone (m)	Sample depth top (m)	Sample depth bottom (m)	Relative to ore zone	Pb (ppm)	Zn (ppm)	Cd (ppm)	Fe (%)	Tl (ppm)	S (%)	Se (ppm)
11-MPB-058	-15000	1.3	1.6	up ice	10.55	36.5	0.07	1.71	0.046	0.01	0.1
11-MPB-055	-280	7.8	8	up ice	33.22	88.3	0.16	0.93	0.027	0.10	0.2
11-MPB-056	-280	3.5	3.7	up ice	25.86	88.9	0.24	0.73	0.019	0.01	0.1
11-MPB-057	-280	1	1.25	up ice	23.45	66.0	0.17	0.88	0.025	0.01	0.1
10-MPB-023	-250	4	5	up ice	37.40	109.1	0.28	0.77	0.020	0.01	0.2
10-MPB-024	-200	4	4.5	up ice	35.30	97.6	0.26	0.80	0.024	0.01	0.1
10-MPB-025	-200	2.5	3	up ice	29.97	84.5	0.21	0.86	0.024	0.01	0.2
10-MPB-004	7	5.4	5.9	overlying	2015.41	3497.4	11.37	1.15	0.016	0.27	0.3
10-MPB-005	19	5.4	5.9	overlying	383.43	911.0	2.08	0.78	0.020	0.08	0.2
10-MPB-030	20	5.8	5.9	overlying	877.72	2215.5	3.18	1.67	0.018	0.06	0.3
10-MPB-026	23	5.8	5.9	overlying	1018.36	1620.4	5.91	1.11	0.017	0.10	0.2
10-MPB-031	24	5.75	5.9	down ice	410.96	1772.2	2.07	1.00	0.020	0.05	0.3
10-MPB-039	40	3.5	4	down ice	145.22	322.7	0.72	0.95	0.017	0.01	0.2
10-MPB-040	40	2	2.5	down ice	30.79	86.3	0.19	1.08	0.028	0.01	0.3
10-MPB-041	40	0.8	1	down ice	26.87	82.1	0.21	0.95	0.024	0.01	0.3
11-MPB-008	50	5.8	5.9	down ice	33.90	92.4	0.22	0.80	0.017	0.01	0.1
10-MPB-027	50	3.8	3.9	down ice	64.67	122.9	0.25	0.86	0.022	0.02	0.2
10-MPB-028	51	3.7	3.9	down ice	610.97	679.5	2.98	0.96	0.019	0.03	0.2
10-MPB-032	54	5	5.5	down ice	128.50	291.1	0.47	0.86	0.018	0.01	0.2
10-MPB-033	54	2	2.5	down ice	53.60	183.6	0.35	1.03	0.027	0.01	0.1
10-MPB-034	54	1	1.5	down ice	130.87	332.1	0.72	0.92	0.023	0.01	0.1
10-MPB-036	60	2.5	3	down ice	85.95	255.1	0.46	0.78	0.018	0.02	0.2
10-MPB-037	60	1.5	2	down ice	48.40	113.3	0.27	0.72	0.021	0.01	0.1
10-MPB-038	60	0.9	1.1	down ice	35.94	74.5	0.16	0.82	0.022	0.01	0.1
11-MPB-009	65	5	5.3	down ice	15.41	41.4	0.11	0.80	0.022	0.01	0.1

11-MPB-010	65	3	3.3	down ice	29.99	114.7	0.26	0.86	0.024	0.01	0.1
11-MPB-011	65	0.8	1.2	down ice	594.62	589.1	1.39	1.35	0.022	0.01	0.1
11-MPB-002	75	2.5	2.7	down ice	21.40	64.0	0.14	0.84	0.024	0.01	0.1
11-MPB-003	75	1.2	1.3	down ice	16.52	47.4	0.16	0.88	0.028	0.01	0.1
11-MPB-004	75	0.5	0.6	down ice	35.21	118.6	0.33	0.81	0.023	0.01	0.2
11-MPB-005	80	0.8	1	down ice	206.55	603.5	1.19	1.07	0.024	0.01	0.2
11-MPB-006	80	1.5	1.6	down ice	136.29	404.2	0.88	1.03	0.025	0.01	0.2
11-MPB-007	80	2.8	2.9	down ice	25.82	86.3	0.27	0.86	0.027	0.01	0.2
11-MPB-012	90	1.1	1.2	down ice	33.42	155.0	0.48	0.84	0.024	0.01	0.1
11-MPB-013	90	2.5	2.7	down ice	66.03	233.7	0.56	0.86	0.027	0.01	0.1
11-MPB-014	90	1.9	2.1	down ice	32.78	137.2	0.39	0.85	0.027	0.01	0.2
11-MPB-030	90	1.3	1.45	down ice	117.11	310.2	0.63	0.84	0.021	0.01	0.2
11-MPB-031	90	2.2	2.35	down ice	20.23	70.2	0.20	0.78	0.025	0.01	0.3
11-MPB-032	90	2.7	2.9	down ice	26.26	83.8	0.22	0.78	0.025	0.01	0.1
11-MPB-024	100	0.6	0.9	down ice	15.36	50.3	0.14	0.78	0.021	0.01	0.1
11-MPB-025	100	1.7	1.8	down ice	23.08	68.6	0.19	0.81	0.028	0.01	0.1
11-MPB-026	100	2.5	2.8	down ice	28.91	75.4	0.21	0.83	0.025	0.01	0.2
11-MPB-027	120	1	1.4	down ice	17.03	54.4	0.12	0.80	0.021	0.01	0.1
11-MPB-028	120	2.4	2.6	down ice	25.16	90.1	0.24	0.83	0.027	0.01	0.2
11-MPB-029	120	2.9	3.1	down ice	20.02	80.7	0.17	0.82	0.027	0.01	0.2
11-MPB-037	140	0.8	1	down ice	85.10	272.1	0.65	0.92	0.023	0.01	0.1
11-MPB-038	140	2	2.2	down ice	77.43	280.4	0.63	0.83	0.021	0.01	0.1
11-MPB-039	140	2.6	2.8	down ice	87.70	363.6	0.68	0.88	0.024	0.01	0.2
11-MPB-033	150	1.2	1.4	down ice	59.10	228.6	0.55	0.95	0.025	0.01	0.1
11-MPB-035	150	1.6	1.8	down ice	60.24	224.7	0.55	0.88	0.023	0.01	0.1
11-MPB-036	150	2.7	2.8	down ice	185.00	475.2	1.13	0.94	0.027	0.01	0.2
11-MPB-017	160	0.7	0.9	down ice	65.68	234.0	0.55	0.78	0.020	0.01	0.2
11-MPB-018	160	1.6	1.7	down ice	91.12	311.4	0.67	0.89	0.022	0.01	0.1

11-MPB-019	160	2.2	2.3	down ice	97.03	360.7	0.73	0.67	0.016	0.01	0.2
11-MPB-020	160	3.1	3.3	down ice	74.67	282.4	0.66	0.80	0.022	0.01	0.1
11-MPB-021	160	0.8	0.95	down ice	80.95	241.4	0.70	0.84	0.026	0.01	0.1
11-MPB-022	170	1.6	1.9	down ice	77.26	278.1	0.62	0.86	0.022	0.01	0.2
11-MPB-023	170	2.65	2.85	down ice	82.91	414.3	0.85	0.89	0.022	0.01	0.1
11-MPB-043	350	0.85	0.95	down ice	36.10	115.6	0.38	0.75	0.023	0.01	0.2
11-MPB-048	400	0.8	0.9	down ice	46.11	142.0	0.40	0.73	0.023	0.01	0.2
11-MPB-052	400	1	1.2	down ice	46.62	153.5	0.42	0.75	0.024	0.01	0.2
11-MPB-053	400	2	2.1	down ice	48.63	189.1	0.53	0.80	0.026	0.01	0.3
11-MPB-054	400	2.85	3	down ice	31.05	108.2	0.32	0.82	0.027	0.01	0.3
11-MPB-049	450	0.8	1	down ice	64.28	211.9	0.60	0.85	0.026	0.01	0.3
11-MPB-050	450	1.8	2	down ice	79.34	250.1	0.62	0.86	0.027	0.01	0.2
11-MPB-051	450	2.5	2.6	down ice	56.63	218.6	0.65	0.81	0.026	0.01	0.2
11-MPB-045	600			down ice	70.64	214.3	0.60	0.76	0.023	0.01	0.1
11-MPB-046	600		1.2	down ice	95.50	248.8	0.72	0.80	0.023	0.01	0.2
11-MPB-047	600	2.9	3	down ice	67.71	235.1	0.62	0.80	0.025	0.01	0.2
11-MPB-040	700		1.3	down ice	38.45	166.8	0.52	0.80	0.025	0.01	0.2
11-MPB-041	700	1.8	2	down ice	41.30	166.5	0.56	0.82	0.026	0.01	0.2
11-MPB-042	700	2.4	2.6	down ice	19.36	59.8	0.13	0.87	0.026	0.01	0.1

shoulders provide detailed ice flow information, c) till was of moderate thickness (<6 m) providing the opportunity to sample vertical sections, d) the land surface is relatively undisturbed for sampling both up and down ice, e) no known sub-
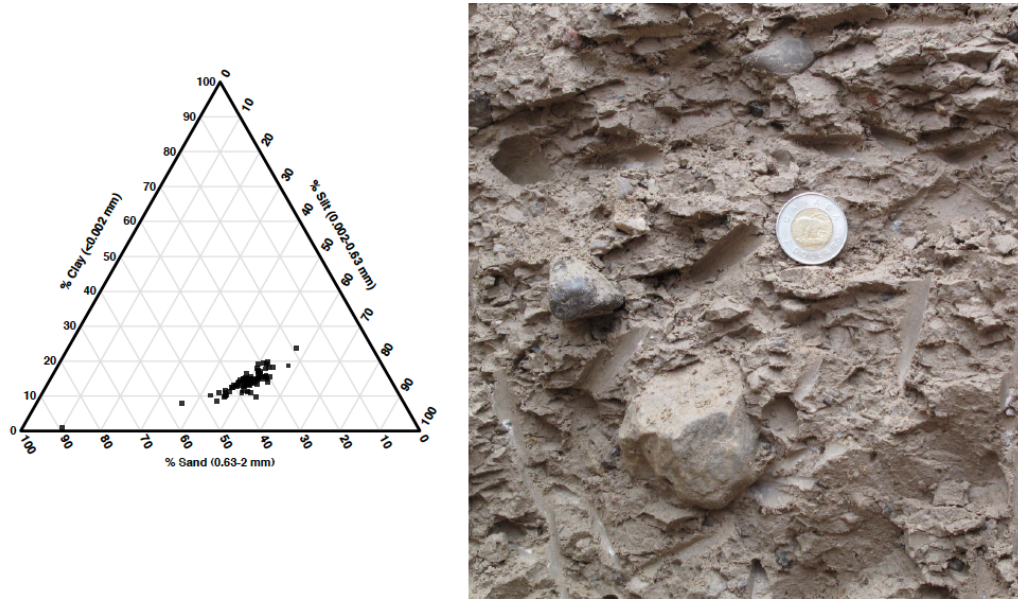
Figure 8: A) Ternary plot of the percentage of clay, silt and sand in the till matrix (n=85) and, B) Till collected from sample 11-MPB-013, with subangular faceted clasts and fissile nature (Canadian two-dollar coin, 28 mm diameter, for scale).

cropping ore bodies occur directly up-ice (east) of Pit O-28, and, f) it is one of the few pits in the region where till is exposed at surface, and was not extensively reworked by Glacial Lake McConnell.

Till samples were collected up-ice, overlying and down-ice of the ore zone at Pit O-28 with respect to the three prominent ice-flow trajectories determined by striae measurements preserved in the bedrock on the shoulder of Pit O-28 (Figure 4). Up-ice samples (10-MPB-023, -024, -025) were collected at the till/ bedrock interface and were used to establish background concentrations. Eight till samples (10-MPB-004, -005, -026 to -028, -030, -031, 11-MPB-008), were collected overlying and just down-ice of the O-28 ore zone on the stripped bedrock surface on the west side of the pit.

Three vertical sections (A, B, and C, in Figure 4) were sampled down-ice from the
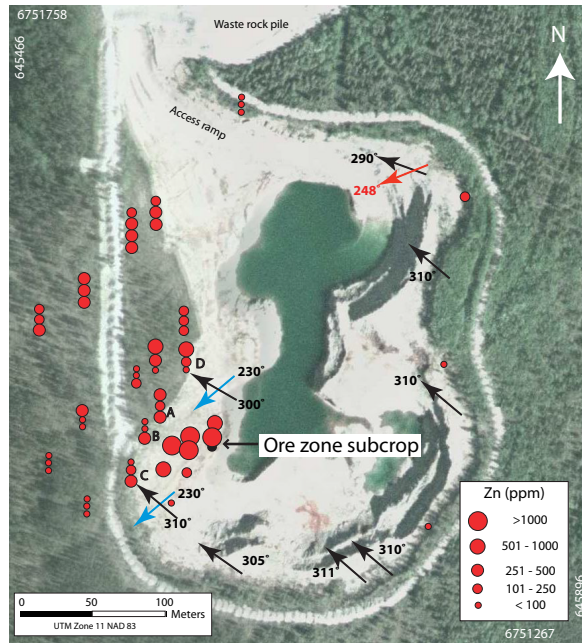
Figure 9: Proportional dots for Zn concentrations (ppm) for samples collected at Pit O-28. Three stacking dots indicate a vertical section where samples were collected from 1, 2 and 3 m below the natural land surface.
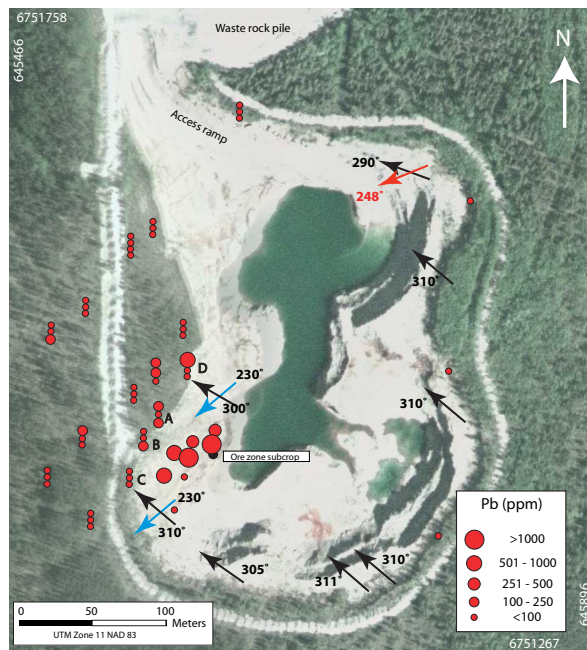
Figure 10: Proportional dots for Pb concentrations (ppm) for samples collected at Pit O-28. Three stacking dots indicate a vertical section where samples were collected from 1, 2 and 3 m below the natural land surface.
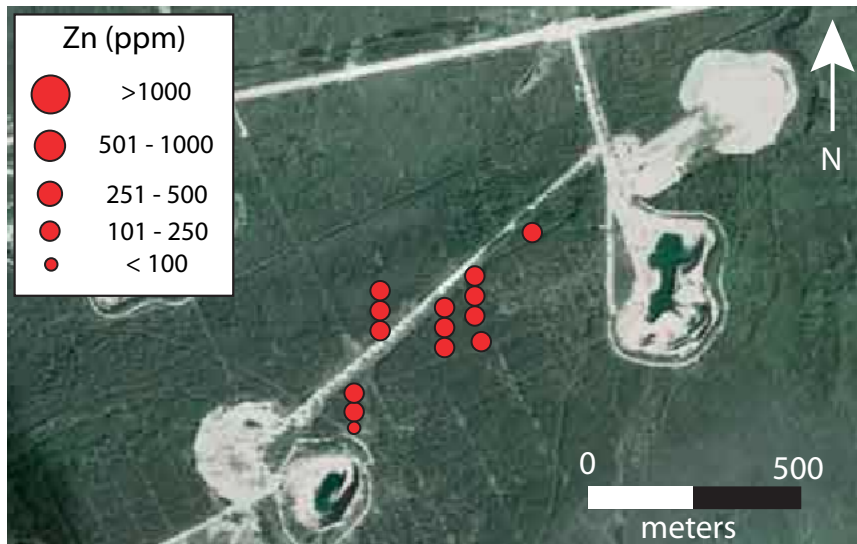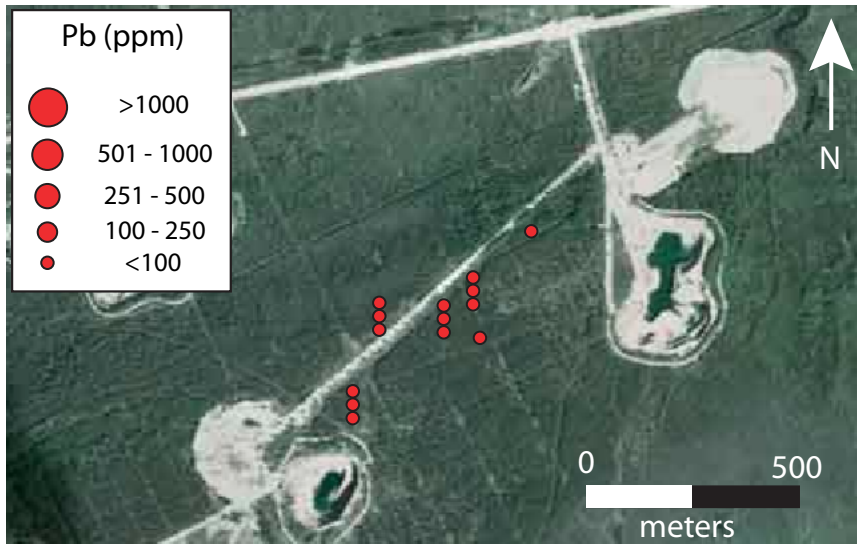
Figure 11: Proportional dots for Pb and Zn concentrations (ppm) for samples collected along the haul road in the Pit O-28 area.

ore zone in the upper west wall of Pit O-28. Three samples were collected from each section at 1, 3 and 5 m depth from the original, natural land surface (Figure 9). Based on the results for these 2010 samples (10-MPB-032 to 034, -036 to 041), additional samples were collected in 2011 fanning outward from the ore zone (11-MPB-002 to 007, -009 to 014, -017 to 033, -035 to 044, -046 to 054). These samples were collected from excavated pits to document vertical patterns in the till composition. An additional section (D, in Figure 4) was sampled in the upper west wall of the pit. This section was sampled in the same manner as sections A, B, and C. Two field duplicates were collected at sites 11-MPB-033 (11-MPB-034) and 11-MPB-009 (11-MPB-016) and submitted with the batch. Field data for sample collection are listed in Appendix E3.

Fifty-four bedrock samples were collected from diamond drill core, pit walls and waste rock piles adjacent to open pits. These samples were collected to determine the nature of sulphide minerals present at Pine Point, and to provide an understanding of the host rocks. The intent is to document the variety of colour, texture and size range of each ore and accessory mineral.

5.3.   Grain size and matrix carbonate analysis

Samples were submitted to the GSC Sedimentology Lab, Ottawa for archiving, sample preparation, grain size analysis and Munsell Color determination. A 800 g split is archived at the GSC before sample preparation. The classes of sizes >0.063 mm material were determined using wet seiving in a stack of sieves and the classes of sizes smaller than <0.063 mm were determined using a Lecotrac LT-100 Particle Size Analyser. Data are listed in Appendix I1. Carbonate content was also determined using the LECO Cr 412 Method. These processes are described in detail by Girard et al. (2004) and Spirito et al. (2011). Data are listed in Appendix I2.

5.4.   Geochemical analysis

Table 2: Correlation matrix for aqua-regia digestion method

	Mo	Cu	Pb	Zn	Ag	Ni	Co	Mn	Fe	As	U	Au	Th	Sr	Cd	Sb	Bi	V	Ca	Mg	Ba	Tl	S	Hg	Se	Te	Ga	Ge	In
Mo	1.00																												
Cu	0.47	1.00																											
Pb	0.42	0.09	1.00																										
Zn	0.38	0.12	0.92	1.00																									
Ag	0.56	0.73	0.03	-0.01	1.00																								
Ni	0.54	0.94	0.03	0.04	0.78	1.00																							
Co	0.50	0.91	0.05	0.05	0.77	0.95	1.00																						
Mn	0.60	0.88	0.18	0.25	0.66	0.91	0.88	1.00																					
Fe	0.61	0.94	0.28	0.25	0.73	0.92	0.91	0.89	1.00																				
As	0.55	0.68	0.07	0.09	0.50	0.68	0.69	0.71	0.74	1.00																			
U	0.71	0.81	0.16	0.20	0.75	0.86	0.81	0.91	0.82	0.57	1.00																		
Au	-0.03	0.11	-0.13	-0.15	0.11	0.03	-0.03	-0.01	-0.01	-0.16	0.09	1.00																	
Th	0.44	0.96	0.04	0.08	0.70	0.95	0.90	0.88	0.91	0.63	0.80	0.11	1.00																
Sr	0.57	0.72	-0.02	0.01	0.60	0.80	0.72	0.85	0.71	0.59	0.81	0.08	0.72	1.00															
Cd	0.38	0.14	0.91	0.99	-0.03	0.06	0.06	0.30	0.27	0.11	0.23	-0.13	0.10	0.04	1.00														
Sb	0.56	0.74	0.01	0.01	0.58	0.74	0.67	0.72	0.69	0.59	0.68	0.29	0.73	0.84	0.04	1.00													
Bi	0.13	0.51	-0.06	0.00	0.47	0.48	0.51	0.44	0.49	0.42	0.40	0.09	0.54	0.28	0.00	0.34	1.00												
V	0.47	0.93	0.06	0.08	0.73	0.95	0.93	0.87	0.93	0.67	0.80	-0.01	0.96	0.70	0.09	0.65	0.53	1.00											
Ca	0.67	0.63	0.13	0.21	0.53	0.71	0.68	0.88	0.70	0.71	0.80	-0.10	0.62	0.88	0.25	0.67	0.28	0.66	1.00										
Mg	0.60	0.56	0.20	0.31	0.39	0.60	0.58	0.83	0.63	0.71	0.70	-0.15	0.53	0.77	0.36	0.57	0.25	0.56	0.96	1.00									
Ba	0.58	0.73	0.29	0.28	0.72	0.75	0.68	0.67	0.69	0.31	0.76	0.11	0.75	0.60	0.26	0.58	0.32	0.72	0.47	0.32	1.00								
Tl	0.44	0.48	0.47	0.36	0.25	0.42	0.49	0.52	0.67	0.61	0.40	-0.15	0.38	0.28	0.41	0.28	0.29	0.47	0.46	0.52	0.10	1.00							
S	0.17	0.11	0.03	0.00	0.34	0.18	0.18	0.15	0.11	-0.16	0.36	0.08	0.09	0.10	-0.02	-0.13	0.01	0.11	0.03	-0.06	0.33	-0.08	1.00						
Hg	0.36	0.17	0.05	0.02	0.50	0.18	0.20	0.15	0.18	0.12	0.33	0.10	0.11	0.17	-0.01	0.15	0.12	0.12	0.20	0.09	0.34	-0.02	0.32	1.00					
Se	0.25	0.15	0.33	0.41	0.10	0.20	0.08	0.33	0.15	-0.02	0.31	-0.07	0.14	0.33	0.44	0.17	-0.18	0.06	0.30	0.35	0.25	0.00	0.18	0.00	1.00				
Te	0.04	0.05	-0.04	-0.04	-0.01	0.01	-0.01	0.04	0.02	0.12	0.01	0.07	0.05	0.12	-0.01	0.15	-0.01	0.01	0.06	0.08	0.01	0.04	-0.06	-0.13	0.07	1.00			
Ga	0.49	0.96	0.08	0.11	0.75	0.96	0.92	0.91	0.93	0.65	0.84	0.09	0.97	0.80	0.13	0.78	0.50	0.95	0.70	0.59	0.76	0.41	0.10	0.18	0.20	0.05	1.00		
Ge	0.00	0.00	0.00	0.00	0.00	0.00	0.00	0.00	0.00	0.00	0.00	0.00	0.00	0.00	0.00	0.00	0.00	0.00	0.00	0.00	0.00	0.00	0.00	0.00	0.00	0.00	0.00	1.00	
In	-0.11	0.27	-0.09	-0.12	0.24	0.17	0.17	0.03	0.15	-0.03	0.08	0.79	0.26	-0.02	-0.14	0.24	0.24	0.18	-0.19	-0.25	0.20	-0.06	0.13	0.13	-0.15	-0.06	0.21	0.00	1.00
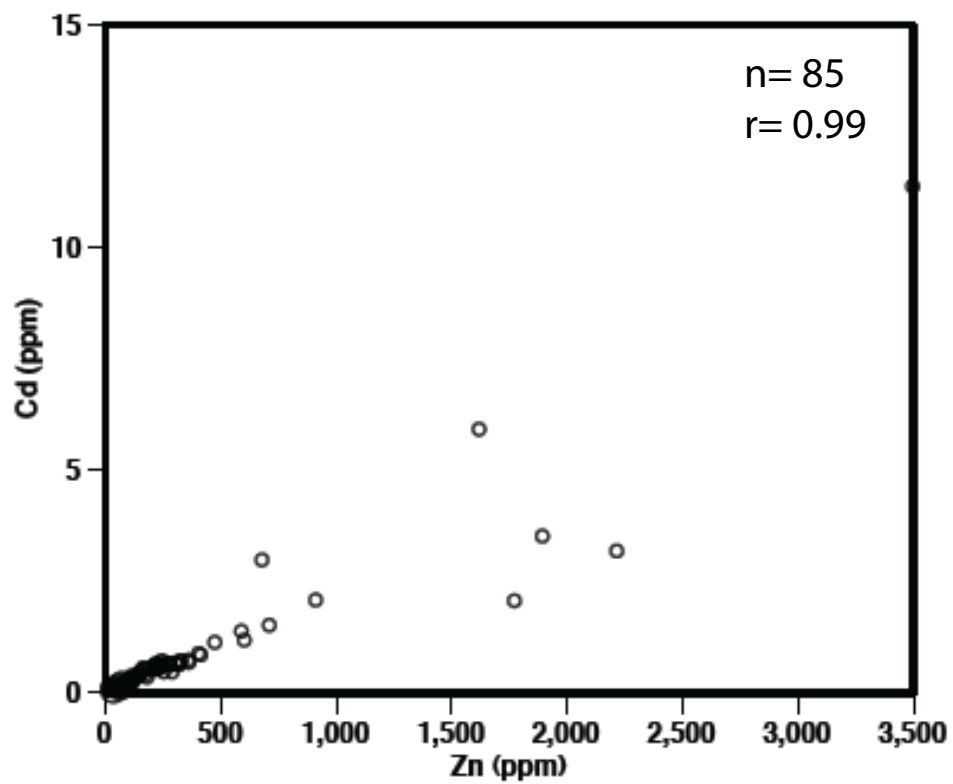
Figure 12: Scatterplot showing correlation between Zn and Cd concentrations in the <0.063 mm fraction of till as determined by aqua regia/ICP-MS.

The <0.063 mm till fraction was sent to ACME Analytical Laboratories, Vancouver, after being dried and sieved at the GSC Sedimentology Laboratory. A 30 g split was digested in aqua regia and analyzed using ICP-MS for base and precious metals (ACME Group 1F method). In addition, major oxides and several minor elements (Ba, Ni, Sr, Zr, Y, Nb, and Sc) were determined on a 0.2 g split by lithium metaborate fusion/ICP-MS followed by nitric acid digestion (ACME Group 4A and 4B method). Data for Group 1F method are listed in Appendix D1 and data for Groups 4A and 4B are listed in Appendix D2.

Accuracy and precision were monitored using CANMET standards Till 2, Till 4 and Fer-1 (http://www.nrcan.gc.ca/minerals-metals/technology/certified-reference-materials/certificate-price-list/4261) throughout the analytical batch. The GSC Sedimentology Laboratory prepared blind duplicates from samples 10-MPB-032 (10-MPB-043), 11-MPB-004 (11-MPB-065), 11-MPB-014 (11-MPB-066) and 11-MPB-047 (11-MPB-064). Data for blind duplicates and CANMET standards are listed in Appendix I3.

5.5.   Data plotting

Prior to plotting data or calculating statistics, all geochemical values reported as less than detection limit were reassigned values of one half the lower detection limit. Field duplicate samples 11-MPB-016 and 11-MPB-034 as well as the cemented ore-rich samples 10-MPB-013 and -014 were removed from the data set prior to data plotting. Correlation coefficients (r) were calculated for 81 till samples using Microsoft® Excel® 2008 for Mac v.12.3.3. Scatter plots were constructed for these samples using the Macintosh® program Aabel® v.3.0.6.

Elemental concentrations were plotted on maps using a combination of ArcGIS® v.9.3 and Adobe® Illustrator® v. 14.0 using proportional dots. Till samples 10-MPB-023 to 025 collected up-ice (east side of Pit O-28) and sample 11-MPB-058, collected 15 km up-ice of the eastern most orebody in the Pine Point mine district were used to establish background concentrations (Table 1). Values

greater than the threshold between background and anomalous concentrations were cut off points based on frequency histograms.

6.   RESULTS

Striation trends in the area reveal an ice flow history with a minimum of three known trajectories. Cross-cutting relationships of striations at various open pits documented in this study indicate that the earliest ice flow direction was to the southwest (~230°), an intermediate phase flowed to the northwest (~300°), followed by the last phase to the west southwest (~250°). Streamlined glacial landforms also reflect this last trajectory of ice flow. The bedrock surface at Pit X-15 has cross-cutting striae that indicate an additional, short-lived, intermediate phase in the northwest direction (~330°). Cross-cutting relationships of striations indicate the timing of this phase to be before the northwest (~300°) intermediate phase and after the oldest the southwest (~250°) phase.

Till in the Pine Point area has a sandy-silt matrix containing an average of 14% clay, 50% silt and 36% sand (Figure 8). The till matrix contains an average of 8 % inorganic carbon and 0.3 % organic carbon as determined by the LECO method.

Proportional dot maps of elemental concentrations of the <0.063 mm fraction of till determined by aqua regia ICP-MS have been plotted for Zn and Pb (Figures
Table 3: Comparison of other till and soil sample surveys for carbonate hosted Pb and Zn.

Deposit	Location	Size fraction	Method	Pathfinder elements	Dispersal	Reference
Pine Point (this study)	Canada	<0.063 mm	aqua regia	Pb, Zn, Fe, Cd, Tl, S, Se	1+ km	this study
Keel	Ireland	<0.190 mm		Pb, Zn, Cd, Sb, Ag	1 km	Hale and Moon, 1982
Tynagh	Ireland	<0.177 mm		Pb, Zn	500+ m	Donovan and James, 1967
Newfoundland Zinc	Canada	<0.063 mm	AAS	Zn, Cu	1 km	Hornbrook et al., 1975

9 and 10, respectively), and at a local scale around Pit O-28 (Figure 11). A

correlation matrix for elements determined by aqua regia ICP-MS (Group 1F method) is shown in Table 2.

6.1. Zn in the <0.063 mm fraction of till

Aqua regia digestion contents of Zn in till range from 1 to 3497 ppm. The highest values are in samples 10-MPB-004, which directly overlies the Pit O-28 ore zone, and 10-MPB-030, -031, which are located on the bedrock bench surrounding Pit O-28. Sample 10-MPB-021 also has high values of Zn. This sample is a regional sample from Pit N-32, approximately 6 km down-ice from Pit O-28. Background values for Zn is <85 ppm. Zinc has strong (r>0.8) positive correlations with Pb and Cd and significant correlation (r>0.6) with S (Table 2).

6.2. Pb in the <0.063 mm fraction of till

Lead values in till samples range from 15 and 2015 ppm as determined by aqua-regia digestion. The highest values are in samples 10-MPB-004 from Pit O-28, and 10-MPB-026, on the bedrock bench directly down-ice of the first phase of ice flow (230°) from sample 10-MPB-004 (Figure 10). Background values for Pb is <30 ppm. Lead has strong (r>0.8) positive correlations with Zn and Cd and significant correlation (r>0.6) with S (Table 2).

6.3. Cd in the <0.063 mm fraction

Cadmium concentrations determined by aqua-regia digestion of till samples vary between 0.11 and 11.37 ppm. The highest concentration occurs in sample 10-MPB-004, which directly overlies the subcropping ore zone. Elevated values also occur in samples 10-MPB-005, -026, -028, -030 and -031, all located on the bedrock bench surrounding Pit O-28. Cadmium background concentrations are <0.21 ppm. Cadmium has strong positive correlations with Zn and Pb (Figure 12).

6.4. Fe in the <0.063 mm fraction

Concentrations of Fe determined by aqua regia in till vary between 0.70 to 1.71 %. The highest value is in sample 11-MPB-058, which is located up ice of the district at Paulette Creek. Other elevated values occur in samples 10-MPB-004, -026, -030, and -031, which all occur on the bedrock bench surrounding Pit O-28. Samples 10-MPB-033 and 10-MPB-040 also have elevated concentrations of Fe. These two samples were collected from sections A and B exposed in the western wall of Pit O-28. Iron has a background concentration of <1.04 % and has significant (r=0.6-0.8) correlations with Cu and Mn.

6.5.   S in the <0.063 mm fraction

Aqua regia digestion sulphur concentrations in the till matrix range from 0.2 to 0.33 %. Sulphur contents are highest in sample 10-MPB-021, which was collected at Pit N-32. Other elevated concentrations of S occur in samples 10-MPB-004, -005, and -026, which are located on the bedrock bench surrounding the pit. Background concentrations for S are <0.01%.

6.6.   Tl and Se in the <0.063 mm fraction

Thallium and Se concentrations determined by aqua-regia digestion vary from 0.01 to 0.42 and 0.05 to 6.2 ppm, respectively. The highest concentration of Tl is in sample 11-MPB-011, which is located 1m below the natural land surface in section D on the west side of Pit O-28 (Figure 4). Other elevated concentrations of Tl are in samples collected 1 m below the surface mainly in the direction of the second ice flow trajectory on the west side of Pit O-28. Background concentrations for Tl are <0.13 ppm. Thallium has a significant correlation with As (r=0.61).

The highest concentration of Se occurs in till sample 10-MPB-009 which was collected at Pit P-41. Other elevated concentrations occur in samples 10-MPB-004, -030, -031 on the bedrock surface surrounding Pit O-28 as well as in samples (10-MPB-040, -041) from the upper wall of the west side of Pit O-28. Samples

(11-MPB-031, -049, -053, -054) collected from trenches 100 to 400 m from the ore zone at Pit O-28 have elevated concentrations as does sample 10-MPB-021, collected at Pit N-42. Background concentrations for Se are <0.14%. Selenium has no strong or significant correlations with any other elements.

7.   DISCUSSION

7.1.   Till texture and carbonate contents

Till in the Pine Point area is a sandy-silt till containing on average 14% clay, 50% silt and 36% sand. These values are somewhat similar to those found in northwestern Alberta (Plouffe et al., 2006), the closest study with grain size data. The sand content of the Pine Point till is moderate but the till is still useful for indicator mineral studies. The high inorganic carbon content of the till matrix is a reflection of the underlying Paleozoic carbonate rocks.

7.2.   Till geochemistry

The Pine Point MVT deposits are dominated by sphalerite, galena, pyrite and marcasite. Zinc and Pb concentrations show a distinct trend associated with Pit O-28, with the highest values overlying the mineralized zone and decreasing with increasing down-ice from the first ice flow event (230°). Cadmium, Fe and Se concentrations are also the highest in till immediately overlying the ore zone, however, these elements are near background concentrations within 40 m down-ice of the ore zone. Sulphur concentrations are near background values within 24 m of the ore zone.

Samples at the bottom of vertical sections within 100m of the Pit O-28 ore zone have higher concentrations of Pb and Zn than those at the top of the sections. Of these samples, Pb and Zn concentrations are highest in sections A and D, which is likely the result of net dispersal from the first two ice flow trajectories. Till samples collected >250 m from the orezone have elevated concentrations at the top of vertical sections, however, these concentrations were not nearly as

high as those collected on the pit shoulder. This is likely because the geochemical signature has been masked or diluted by glacial transport and re-entrainment during multiple ice-flows. These results also indicate a relatively low angle of climb of the dispersal of mineral-rich debris in the till down-ice from the orebody. Lead, Zn and Cd have higher concentrations in samples that are as far as 500 m from the orezone at Pit O-28 as opposed to Fe, Tl, S and Se whose concentrations are near background in samples 10 m from the orezone (Table 1). The absence of striae from the last known ice flow trajectory (250°) on the south side of Pit O-28 likely indicates that this area was till-covered and therefore the glacier at this time, and its deforming bed (e.g., Alley et al., 1986; van der Meer et al., 2003), did not have access to bedrock or the ore zone. This would account for the most of the glacial dispersal of metal-rich till being in the direction of the first two ice flow trajectories.

Samples (10-MPB-013, -014) of metal-rich cemented till collected at Pit P-24 contain the highest concentrations of all pathfinder elements. Concentrations of Pb and Zn were above the upper detection limit of aqua-regia digestion/ICP-MS (>10,000 ppm) and these two samples were very enriched in Cd, Fe, S, Tl and Se. This signature could be due to Pit P-24 having either a larger area of sub-cropping ore that the glaciers eroded than Pit O-28 or a richer (i.e., higher grade) ore zone.

Samples 10-MPB-020 and -021 were collected at Pit N-42 and have high concentrations of all the pathfinder elements excluding Tl and Se. These samples are down-ice of Pit O-28 as well as two other pits. The Pb and Zn concentrations are similar to those found approximately 150-200 m down-ice from Pit O-28.

Down-ice regional samples (11-MPB-059 to -062, 085B101008BT and 11-PTA-037, -042), with the exception of 11-MPB-061, all have above background concentrations for all pathfinder elements. Samples 11-MPB-059, -060 and 085B101008BT collected along the Buffalo River all have well above background concentrations for Pb, Zn and Cd indicating that the signature is detectable at a

regional scale.

7.3. Glacial transport

Three ice flow trajectories were recorded on the bedrock shoulders of pit O-28 indicating that glaciers were in contact with the surface and therefore eroded the orezone. Till sample locations were chosen to determine if the signature of the O-28 deposit could be detected at varying distances down-ice of the sub-cropping ore zone. The metal rich till occurs mostly on the bedrock surface on the west side of the open pit as well as in those samples that are located down-ice of the first recorded ice flow (~230°). Some samples located in sections of till surrounding the pit also had some elevated concentrations.

Table 3 compares the results of this study with other till and soil studies conducted on carbonate hosted Pb-Zn deposits. The results of this study were able to detect a larger suite of pathfinder elements. This is likely due to the increasing accuracy and precision of analytical techniques and methods.

8. CONCLUSIONS

Three, possibly four, phases of ice flow are now known in the Pine Point district. Ice flow trajectories were recorded in this area in the form of striations, flutings and cross-cutting relationships on bedrock surfaces. The first ice flow trajectory was to the southwest (230°) followed by an intermediate ice-flow direction to the northwest (300°) with the youngest trajectory to the west-southwest (250°). One single striation site has evidence of a short-lived intermediate ice flow trajectory to the north-northwest (330°).

Metal rich till has been dispersed to the west and northwest of Pit O-28 indicating that the oldest recorded ice flow trajectory had direct contact with mineralization. The elements Zn, Pb, Fe, Cd, S, Tl and Se are pathfinder elements in the <0.063 mm fraction of till around the Pine Point MVT deposits and are detectable at the surface near a known ore body.

196

9. ACKNOWLEDGEMENTS

10. REFERENCES

Alley, R.B., Blankenship, D.D., Bentley, C.R. and Rooney, S.T. 1986. Deformation of till beneath ice stream B, West Antarctica. Nature, v. 322, p. 57-59.

Bostock, H.S. 1970. Physiographic regions of Canada. Geological Survey of Canada, Map 1254A, scale 1:5,000,000.

Brabec, D. 1983. Evaluation of soil anomalies by discriminant analysis in geochemical exploration for carbonate-hosted lead-zinc deposits. Economic Geology, v. 78, p. 333-339.

Campbell, N., 1966. The lead-zinc deposits of Pine Point: Canadian Mining and Metallurgical Bulletin, v. 59, p. 953-960.

Donovan, P.R. and James, C.H. 1967. Geochemical dispersion in glacial overburden over the Tynagh (Northgate) base metal deposit, west-central Eire. *In*: E.M. Cameron (ed.), *Proceedings, Symposium on Geochemical Prospecting*, Geological Survey of Canada, Paper 66-54, p. 89-110.

Dreimanis, A., 1960. Geochemical prospecting for Cu, Pb, and Zn in glaciated areas, eastern Canada. *In*: Marmo, V., Puranen, M. (eds.), *Geological Results of Applied Geochemistry and Geophysics,* p. 7-19. Report of the 21st International Geological Congress, Part 2, Det Berlingske Bogtrykkeri, Copenhagen.

Dyke, A.S. 2004. An outline of North American deglaciation with emphasis on central and northern Canada. *In*: J. Ehlers and P.L. Gibbard (eds.), *Quaternary Glaciations - Extent and Chronology, Part II. North America*. Elsevier B.V., Amsterdam, Development in Quaternary Science Series, Vol. 2: 373-424.

Dyke, A.S., and Prest, V.K., 1987. Late Wisconsin and Holocene history of the Laurentide Ice Sheet. Geographie physique et Quaternaire, v. 41, p. 237-263.

Eaton, D.W. and Hope, J. 2003. Structure of the crust and upper mantle of the Great Slave Lake shear zone, northwestern Canada, from teleseismic analysis and gravity modelling. Canadian Journal of Earth Sciences, v. 40, p. 1203-1218.

Hale, M. and Moon, C.J. 1982. Geochemical expressions at surface of mineralization concealed beneath glacial till at Keel, Eire. *In*: P.H. Davenport (ed.), Prospecting in Areas of Glaciated Terrain - 1982. Canadian Institute of Mining and Metallurgy, p. 228- 239.

Hannigan, P.K., 2006. Introduction. *In:* Hannigan, P.K. (ed) *Potential for Carbonate-hosted Lead-zinc Mississippi Valley-type Mineralization in Northern Alberta and Southern Northwest Territories.* Geoscience Contributions, Targeted Geoscience Initiative, Geological Survey of Canada, Bulletin 591, p. 9-39.

Hannigan, P., 2007. Metallogeny of the Pine Point Mississippi Valley-Type zinc-lead district, southern Northwest Territories. *In:* Goodfellow, W.D. (ed) *Mineral Deposits of Canada: A Synthesis of Major Deposit-Types, District Metallogeny, the Evolution of Geological Provinces, and Exploration Methods.* Geological Association of Canada, Mineral Deposits Division, Special Publication No. 5, p. 609-632.

Hannon, P.J., Roy, W.D., Flint, I.M. and Ernst, B.E. 2012. Technical report on the R-190, X-25, P-499, O-556, Z-155 and G-03 deposits of the Pine Point project for Tamerlane Ventures Incorporated. MineTech International Limited, Halifax, 160 p.

Hornbrook, E.H.W., Davenport, P.H. and Grant, D.R. 1975. Regional and detailed geochemical exploration studies in glaciated terrain in Newfoundland. Newfoundland Department of Mines and Energy, Mineral Development Division, Report 75-2, 116 p.

Girard, I., Klassen, R.A., and Laframboise. 2004. Sedimentology laboratory manual, Terrain Sciences Division. Open file 4823, Geological Survey of Canada.

Kyle, J.R., 1981. Geology of the Pine Point lead-zinc district. *In*: Wolf, K.H., (ed) Handbook of strata-bound and stratiform ore deposits. Elsevier Publishing Company, New York, v. 9, p 643-741.

Lemmen, D.S., 1990. Surficial materials associated with glacial Lake McConnell, southern District of Mackenzie. Current Research, Part D, Geological Survey of Canada, Paper 90-1D, p. 79-83.

Lemmen, D.S., 1998a. Surficial geology, Klewi River, District of Mackenzie; Northwest Territories. Geological Survey of Canada, "A" Series Map 1905, scale 1: 250 000.

Lemmen, D.S., 1998b. Surficial geology, Buffalo Lake, District of Mackenzie; Northwest Territories. Geological Survey of Canada, "A" Series Map 1906, scale 1:250 000.

Lemmen, D.S., Duk-Rodkin, A., and Bednarski, J.M., 1994. Late glacial drainage systems along the northwestern margin of the Laurentide Ice Sheet. Quaternary Science Reviews, v. 13, p. 805-828.

Macqueen, R.W. and Ghent, E.D., 1975. Occurrence of zinc in Devonian metalliferous shales, Pine Point region, District of Mackenzie. Geological Survey

of Canada Paper 75-1B, p. 53-57.

McClenaghan, M.B. 2005. Indicator mineral methods in exploration. Geochemistry: Exploration, Environment, Analysis, vol. 5, p. 233–245.

McClenaghan, M.B, Plouffe, A., McMartin, I., Campbell, J.E., Spirito, W.A., Paulen, R.C., Garrett, R.G. and Hall, G.E.M. In Press. Till sampling and geochemical analytical protocols for Geological Survey of Canada projects. Geochemistry: Exploration, Environment, Analysis.

Morrow, D.W., MacLean, B.C., Miles, W.F., Tzeng, P. and Pana, D. 2006. Subsurface structures in southern Northwest Territories and northern Alberta: implications for mineral and petroleum potential. *In*: Hannigan, P.K. (ed.) *Potential for Carbonate-hosted Lead-zinc Mississippi Valley-type Mineralization in Northern Alberta and Southern Northwest Territories*: Geoscience Contributions, Targeted Geoscience Initiative. Geological Survey of Canada, Bulletin 591, p. 41-59.

Nelson, J., Paradis, S., Christensen, J. and Gabites, J. 2002. Canadian Cordilleran Mississippi Valley-type deposits: A case for Devonian-Mississippian back-arc hydrothermal origin; Economic Geology, v. 97, p. 1013–1036.

Okulitch, A.V. (compiler) 2006. Phanerozoic bedrock geology, Slave River, District of Mackenzie, Northwest Territories. Geological Survey of Canada, Open File 5281, scale 1:1,000,000.

Paradis, S., Turner, W.A., Coniglio, M., Wilson, N. and Nelson, J.L. 2006. Stable and radiogenic isotopic signatures of mineralized Devonian carbonate rocks of the northern Rocky Mountains and the Western Canada Sedimentary Basin. *In*: P.K. Hannigan (ed.), *Potential for Carbonate-hosted Lead-zinc Mississippi Valley-type Mineralization in Northern Alberta and Southern Northwest Territories:* Geoscience Contributions, Targeted Geoscience Initiative, Geological Survey of Canada, Bulletin 591, p. 75-103.

Paulen, R.C., Plouffe, A., and Smith, I.R. 2008. Diamond and base metal indicator minerals in glacial sediments of northern Alberta, Canada. EXPLORE, 138: 1-7.

Paulen, R.C., Paradis, S., Plouffe, A., and Smith, I.R., 2009. Base metal exploration with indicator minerals in glacial sediments of northwest Alberta, Canada. *In*: Lentz, D.R., Thorne, K.G. and Beal, K.L. (eds) *Proceedings of the 24th International Applied Geochemistry Symposium (IAGS*), Fredricton, New Brunswick, v.2, p 557-560.

Plouffe, A., Paulen, R.C., and Smith, I.R., 2006. Indicator mineral content and geochemistry of glacial sediments from northwest Alberta (NTS 84L, M): new opportunities for mineral exploration. Geological Survey of Canada, Open File

5121.

Prest, V.K., Grant, D.R., and Rampton, V.N., 1968. Glacial map of Canada. Geological Survey of Canada, "A" Series Map 1253, scale 1: 5 000 000.

Rhodes, D., Lantos, E.A., Lantos, J.A., Webb, R.J., Owens, D.C., 1984. Pine Point orebodies and their relationship to the stratigraphy, structure, dolomitization, and karstification of the middle Devonian Barrier complex. Economic Geology, v. 79, p. 991-1055.

Shilts, W.W. 1996. Chapter 15, Drift exploration. *In*: MENZIES, J. (ed.) Past Glacial Environments, Sediments, Forms and Techniques, Butterworth Heinemann, Toronto, p. 411-439.

Skall, H., 1975. The paleoenvironment of the Pine Point lead-zinc district. Economic Geology, v. 70, p. 22-47.

Skall, H., 1977. The geology of the Pine Point barrier reef complex. *In:* McIlreath, I.A., and Harrison, R.D. (eds) The geology of selected carbonate oil, gas and lead-zinc reservoirs in western Canada. Canadian Society of Petroleum Geologists, Core Conference, no. 5, p 19-38.

Smith, D.G. 1994. Glacial Lake McConnell: paleogeography, age, duration and associated river deltas, Mackenzie River basin, western Canada. Quaternary Science Reviews, v. 13, p. 829-843.

Spirito, W.A., McClenaghan, M.B., Plouffe, A., McMartin, I., Campbell, J.E., Paulen, R.C., Garrett, R.G. and Hall, G.E.M. 2011. Till sampling and analytical protocols for GEM projects: from field to archive. Geological Survey of Canada, Open File 6850, 1 CD-ROM.

van der Meer, J.J.M., Menzies, J. and Rose, J. 2003. Subglacial till: the deforming glacier bed. Quaternary Science Reviews, v. 22, p. 1659-1685.